US Army Corps of Engineers

U.S. Army Corps of Engineers
Walla Walla District

Lower Snake River Programmatic Sediment Management Plan, Final Environmental Impact Statement

Appendix M - Sediment Transport in the Lower Snake and Clearwater River Basins, Idaho and Washington

August 2014

Contents

Lower Snake River Programmatic Sediment Management Plan Environmental Impact Statement

Appendix M

Sediment Transport in the Lower Snake and Clearwater River Basins, Idaho and Washington

Section 1. Grain-Size Distribution and Selected Major and Trace Element Concentrations in Bed-Sediment Cores from the Lower Granite Reservoir and Snake and Clearwater Rivers, Eastern Washington and Northern Idaho, 2010

U.S. Geological Survey

Prepared in Cooperation with the U.S. Army Corps of Engineers

USGS
science for a changing world

Prepared in cooperation with the U.S. Army Corps of Engineers

Grain-Size Distribution and Selected Major and Trace Element Concentrations in Bed-Sediment Cores from the Lower Granite Reservoir and Snake and Clearwater Rivers, Eastern Washington and Northern Idaho, 2010

Scientific Investigations Report 2012–5219

U.S. Department of the Interior
U.S. Geological Survey

August 2014

Front cover:

Top left, The vibracorer (laying on boat deck) and its stabilizing frame on Lower Granite Reservoir, Washington, May 13, 2010. Photograph by Candice B. Adkins, U.S. Geological Survey.

Top middle, Draining overlying water from a sediment core collected at Lower Granite Reservoir, Washington, May 11, 2010. Photograph by Candice B. Adkins, U.S. Geological Survey.

Top right, Hydrologic technician K. Craig Weiss on Snake River upstream from U.S. Highway 12, Washington, May 19, 2010. Photograph by Jennifer T. Wilson, U.S. Geological Survey.

Bottom left, Hydrologist Ryan L. Fosness (left) and Research Hydrologist Peter C. Van Metre (right) preparing a core liner for the vibracorer on Lower Granite Reservoir, Washington, May 12, 2010. Photograph by Candice B. Adkins, U.S. Geological Survey.

Bottom middle, Section of sediment core number 50 collected from Lower Granite Reservoir, Washington, at river mile 136.29, May 14, 2010. Photograph by Jennifer T. Wilson, U.S. Geological Survey.

Bottom right, Hydrologists Rhonda J. Weakland (left) and Ryan L. Fosness (right) removing sediment core liner from core barrel at Lower Granite Reservoir, Washington, May 11, 2010. Photograph by Candice B. Adkins, U.S. Geological Survey.

Back cover: Lower Granite Reservoir near Nisqually John Landing, Washington, April, 6, 2010. Photograph by Jennifer T. Wilson, U.S. Geological Survey.

Grain-Size Distribution and Selected Major and Trace Element Concentrations in Bed-Sediment Cores from the Lower Granite Reservoir and Snake and Clearwater Rivers, Eastern Washington and Northern Idaho, 2010

By Christopher L. Braun, Jennifer T. Wilson, Peter C. Van Metre, Rhonda J. Weakland, Ryan L. Fosness, and Marshall L. Williams

Prepared in cooperation with the U.S. Army Corps of Engineers

Scientific Investigations Report 2012–5219

U.S. Department of the Interior
U.S. Geological Survey

U.S. Department of the Interior
KEN SALAZAR, Secretary

U.S. Geological Survey
Marcia K. McNutt, Director

U.S. Geological Survey, Reston, Virginia: 2012

This and other USGS information products are available at http://store.usgs.gov/

U.S. Geological Survey
Box 25286, Denver Federal Center
Denver, CO 80225

To learn about the USGS and its information products visit http://www.usgs.gov/
1-888-ASK-USGS

Suggested citation:
Braun, C.L., Wilson, J.T., Van Metre, P.C., Weakland, R.J., Fosness, R.L., and Williams, M.L., 2012, Grain-size distribution and selected major and trace element concentrations in bed-sediment cores from the Lower Granite Reservoir and Snake and Clearwater Rivers, eastern Washington and northern Idaho, 2010: U.S. Geological Survey Scientific Investigations Report 2012–5219, 81 p.

Contents

Figures

Table

Conversion Factors

SI to Inch/Pound

Multiply	By	To obtain
	Length	
centimeter (cm)	0.3937	inch (in.)
millimeter (mm)	0.03937	inch (in.)
meter (m)	3.281	foot (ft)
kilometer (km)	0.6214	mile (mi)
meter (m)	1.094	yard (yd)

Inch/Pound to SI

Multiply	By	To obtain
	Length	
inch (in.)	2.54	centimeter (cm)
inch (in.)	25.4	millimeter (mm)
foot (ft)	0.3048	meter (m)
mile (mi)	1.609	kilometer (km)
	Volume	
cubic yard (yd^3)	0.7646	cubic meter (m^3)
	Flow rate	
cubic foot per second (ft^3/s)	0.02832	cubic meter per second (m^3/s)

Vertical coordinate information is referenced to the North American Vertical Datum of 1988 (NAVD 88).

Horizontal coordinate information is referenced to North American Datum of 1983 (NAD 83).

Grain-Size Distribution and Selected Major and Trace Element Concentrations in Bed-Sediment Cores from the Lower Granite Reservoir and Snake and Clearwater Rivers, Eastern Washington and Northern Idaho, 2010

By Christopher L. Braun, Jennifer T. Wilson, Peter C. Van Metre, Rhonda J. Weakland, Ryan L. Fosness, and Marshall L. Williams

Abstract

Lower Granite Dam impounds the Snake and Clearwater Rivers in eastern Washington and northern Idaho, forming Lower Granite Reservoir. Since 1975, the U.S. Army Corps of Engineers has dredged sediment from the Lower Granite Reservoir and the Snake and Clearwater Rivers in eastern Washington and northern Idaho to keep navigation channels clear and to maintain the flow capacity. In recent years, other Federal agencies, Native American governments, and special interest groups have questioned the negative effects that dredging might have on threatened or endangered species. To help address these concerns, the U.S. Geological Survey, in cooperation with the U.S. Army Corps of Engineers, collected and analyzed bed-sediment core samples (hereinafter cores) in Lower Granite Reservoir and impounded or backwater affected parts of the Snake and Clearwater Rivers. Cores were collected during the spring and fall of 2010 from submerged sampling locations in the Lower Granite Reservoir, and Snake and Clearwater Rivers. A total of 69 cores were collected by using one or more of the following corers: piston, gravity, vibrating, or box. From these 69 cores, 185 subsamples were removed and submitted for grain size analyses, 50 of which were surficial-sediment subsamples. Fifty subsamples were also submitted for major and trace elemental analyses. Surficial-sediment subsamples from cores collected from sites at the lower end of the reservoir near the dam, where stream velocities are lower, generally had the largest percentages of silt and clay (more than 80 percent). Conversely, all of the surficial-sediment subsamples collected from sites in the Snake River had less than 20 percent silt and clay. Most of the surficial-sediment subsamples collected from sites in the Clearwater River contained less than 40 percent silt and clay. Surficial-sediment subsamples collected near midchannel at the confluence generally had more silt and clay than most surficial-sediment subsamples collected from sites on the Snake and Clearwater Rivers or even sites further downstream in Lower Granite Reservoir. Two cores collected at the confluence and all three cores collected on the Clearwater River immediately upstream from the confluence were extracted from a thick sediment deposit as shown by the cross section generated from the bathymetric surveys. The thick sediment deposits at the confluence and on the Clearwater River may be associated with floods in 1996 and 1997 on the Clearwater River.

Fifty subsamples from 15 cores were analyzed for major and trace elements. Concentrations of trace elements were low, with respect to sediment quality guidelines, in most cores. Typically, major and trace element concentrations were lower in the subsamples collected from the Snake River compared to those collected from the Clearwater River, the confluence of the Snake and Clearwater Rivers, and Lower Granite Reservoir. Generally, lower concentrations of major and trace elements were associated with coarser sediments (larger than 0.0625 millimeter) and higher concentrations of major and trace elements were associated with finer sediments (smaller than 0.0625 millimeter).

Introduction

The Lower Granite Dam impounds the Snake and Clearwater Rivers in eastern Washington and northern Idaho. Backwater from Lower Granite Reservoir extends to just upstream from the confluence of the Snake and Clearwater Rivers. The Snake and Clearwater Rivers transition at their confluence from free-flowing water to backwater caused by the Lower Granite Dam, and backwater marks the upstream extent of the reservoir pool. Delta deposits of bed-sediment material form as velocity and transport capacity diminish where streams enter the reservoir pool. In addition to deltaic deposition of primarily coarse sediments, processes in reservoirs include deposition of fine sediments from homogeneous flow, and transport and deposition of sediment from stratified flow (Fan and Morris, 1992, p. 355). Since its impoundment in 1975, 2.6 million cubic yards (2.0 million cubic meters) of sediment have been deposited annually into Lower Granite Reservoir and the Snake and Clearwater Rivers that flow into the reservoir (U.S. Army Corps of Engineers, 2003). The Snake River continues downstream from Lower Granite Dam; upstream from the confluence of the Snake and Columbia Rivers, the USACE operates three additional dams on the Snake River as part of the Snake River System (U.S. Army Corps of Engineers, 2002) (fig. 1). Historically, the USACE dredged sediment from the Snake River System, including Lower Granite Reservoir, to keep navigation channels clear and to maintain the flow capacity. Increases in reservoir stage in Lower Granite Reservoir caused by sedimentation also reduce the effectiveness of the levees protecting Clarkston, Wash., and Lewiston, Idaho, from flooding (Greg Teasdale, U.S. Army Corps of Engineers, written commun., 2011). In recent years, other Federal agencies, Native American governments, and special interest groups have questioned the negative effects that dredging might have on threatened or endangered species. The negative effects of dredging might include biological effects (on distribution, behavior, migration, feeding, spawning, development, and fish injury), physical effects (on disturbance, displacement, avoidance, entrainment, burial, noise, sedimentation, turbidity, suspended sediments, and habitat and food source modification), and water-quality effects (on acute toxicity, bioavailability, bioaccumulation, and exposure pathways) (U.S. Army Corps of Engineers, 2004).

To address these concerns, the USACE initiated a multiyear project to assess the current status of sediment deposition in the reservoir and to explore alternative sediment control measures. The multiyear project included surveys of the sedimentary structures (bedforms) of Lower Granite Reservoir. Bed-sediment core samples (hereinafter cores) were collected by the U.S. Geological Survey in cooperation with the USACE during the spring and fall of 2010. A multibeam echosounding (MBES) bathymetric survey during fall 2009 and winter 2010 and an underwater video map (UVM) survey of sediment facies during fall 2009 and winter 2010, also part of the multiyear study (Williams and others, 2012), were used to help interpret surficial sedimentary structures (bedforms) in the study area. The MBES and UVM surveys are described in detail by Williams and others (2012). The data from all three surveys will be used to model flood hydraulics and sediment transport and to make biological assessments in support of the USACE Programmatic Sediment Management Plan (U.S. Army Corps of Engineers, 2003).

Purpose and Scope

This report describes the results from cores collected in the Lower Granite Reservoir and the Snake and Clearwater Rivers impounded by the reservoir during spring 2010 and fall 2010. Specifically, the grain-size distribution of surficial-sediment subsamples from cores collected underwater in Lower Granite Reservoir, the Snake and Clearwater Rivers, and the confluence of these two rivers are described, along with the down-core grain-size distribution in cores collected at or near the confluence of the Snake and Clearwater Rivers. Grain-size analyzes are compared with results from previous surveys to assess the predominant surficial sediment grain-size classes and how they relate to bed-sediment accumulation history, surficial sedimentary structures (bedforms), and embeddedness (degree to which gravel, cobble, boulders, or snags are sunken into the silt, sand or clay of a river or lake bottom) in Lower Granite Reservoir, the Snake and Clearwater Rivers, and the confluence of these two rivers. Results from the grain-size analyses were used to provide a quantitative mechanism for verification of the facies map generated from the UVM surveys done by Williams and others (2012). Selected major and trace element concentrations measured in subsamples of cores also are discussed.

Previous Studies

Multibeam Echosounding Bathymetric Survey

During fall 2009 and winter 2010, the U.S. Geological Survey (USGS), in cooperation with the USACE, conducted a hydrographic survey using a MBES to develop a digital elevation dataset on 12 river miles (RM) of Lower Granite Reservoir and the Snake River, and 2 RM of the Clearwater River upstream from the confluence with the Snake River (figs. 1 and 2) (Williams and others, 2012). The confluence of the Snake and Clearwater Rivers is upstream from the Lower Granite Dam and is where the rivers transition from free-flowing to backwater. Data from the survey will be used by the USACE to better understand and predict sediment transport and deposition in the reservoir as part of its Programmatic Sediment Management Plan (U.S. Army Corps of Engineers, 2003). The digital elevation dataset also can be used to display river-bed elevation and geomorphology such as scour holes, rock outcrops, and bedforms like ripples and dunes. This survey represents a snapshot-in-time of benthic geomorphology that can rapidly change because of fluctuations in reservoir stage, river discharge, and boat traffic.

The MBES bathymetric survey was conducted from RM 130 to RM 142 on the Lower Granite Reservoir and Snake River and from RM 0 to RM 2 on the Clearwater River (fig. 2*A*). The survey mapped the full width of the river except areas along banks that were inaccessible to the boat or too shallow (less than 10 meters) to be measured with echosounding equipment. The survey was conducted in 1-mile segments, and the resulting datasets were composited to provide a continuous digital elevation dataset of the reservoir and rivers. The primary purpose for these data is to support the USACE's sediment transport modeling effort. However, these data also can provide a visual representation of bed geomorphology, which may be used for habitat assessments and other purposes. Figure 2*B* shows a two-dimensional overhead view of part of the surveyed area, which includes areas of sand dunes, a scour hole, basalt outcrop, and areas where bed material was removed for levee construction.

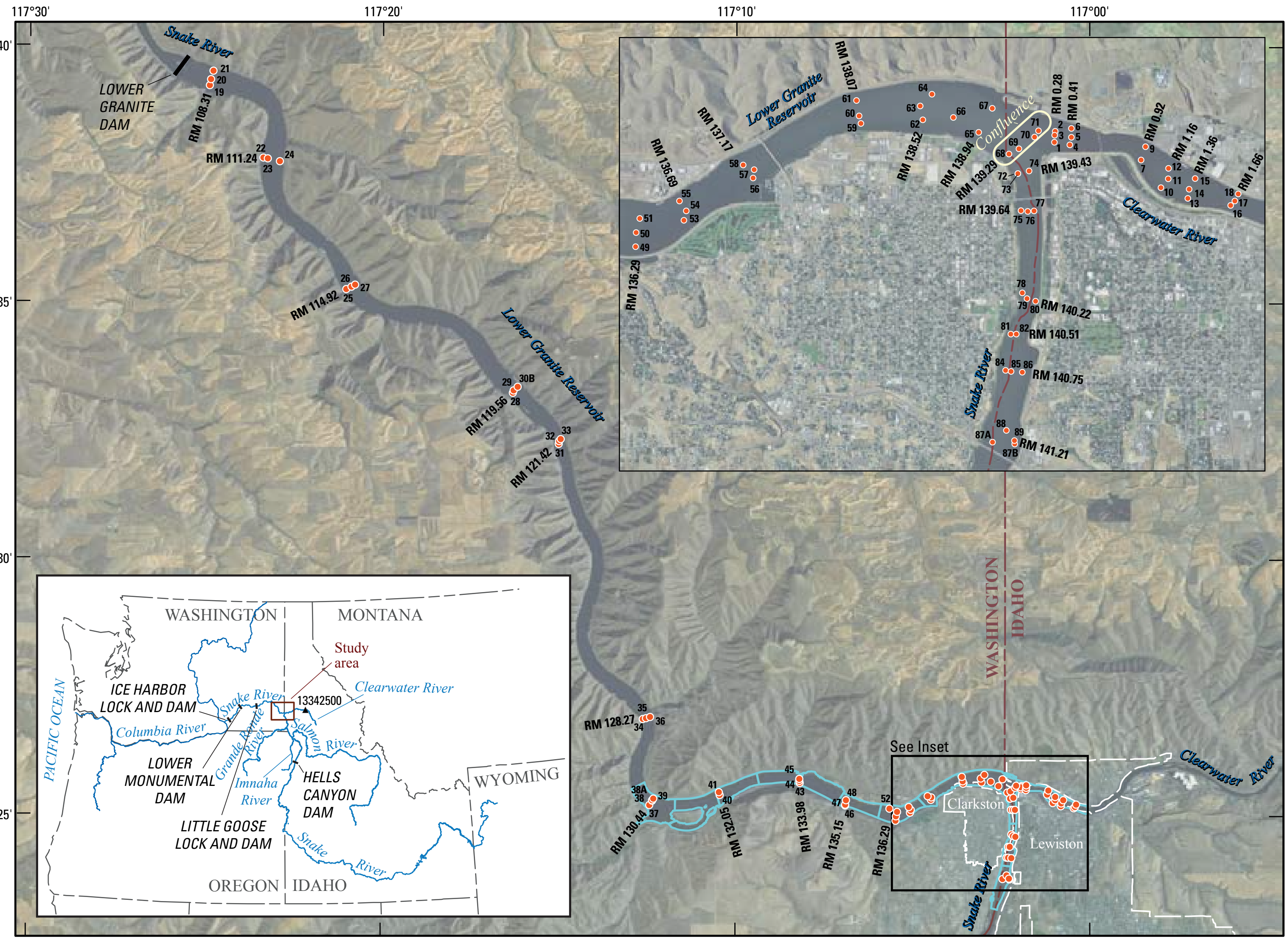

Base from U.S. Geological Survey 1:100,000-scale digital data
Aerial imagery from National Agriculture Imagery Program, 2009
Universe Transverse Mercator projection, zone 11
North American Datum of 1983

EXPLANATION

- **Multibeam echo sounding survey (MBES) extent**
- 77 **Bed-sediment core sample site and identifier (table 1)**
- RM 139.64 **River mile designation**
- 13342500 **U.S. Geological Survey streamflow-gaging station and station number**

Figure 1. Study area and sediment coring locations in Lower Granite Reservoir and the Snake and Clearwater Rivers, eastern Washington and northern Idaho, 2010.

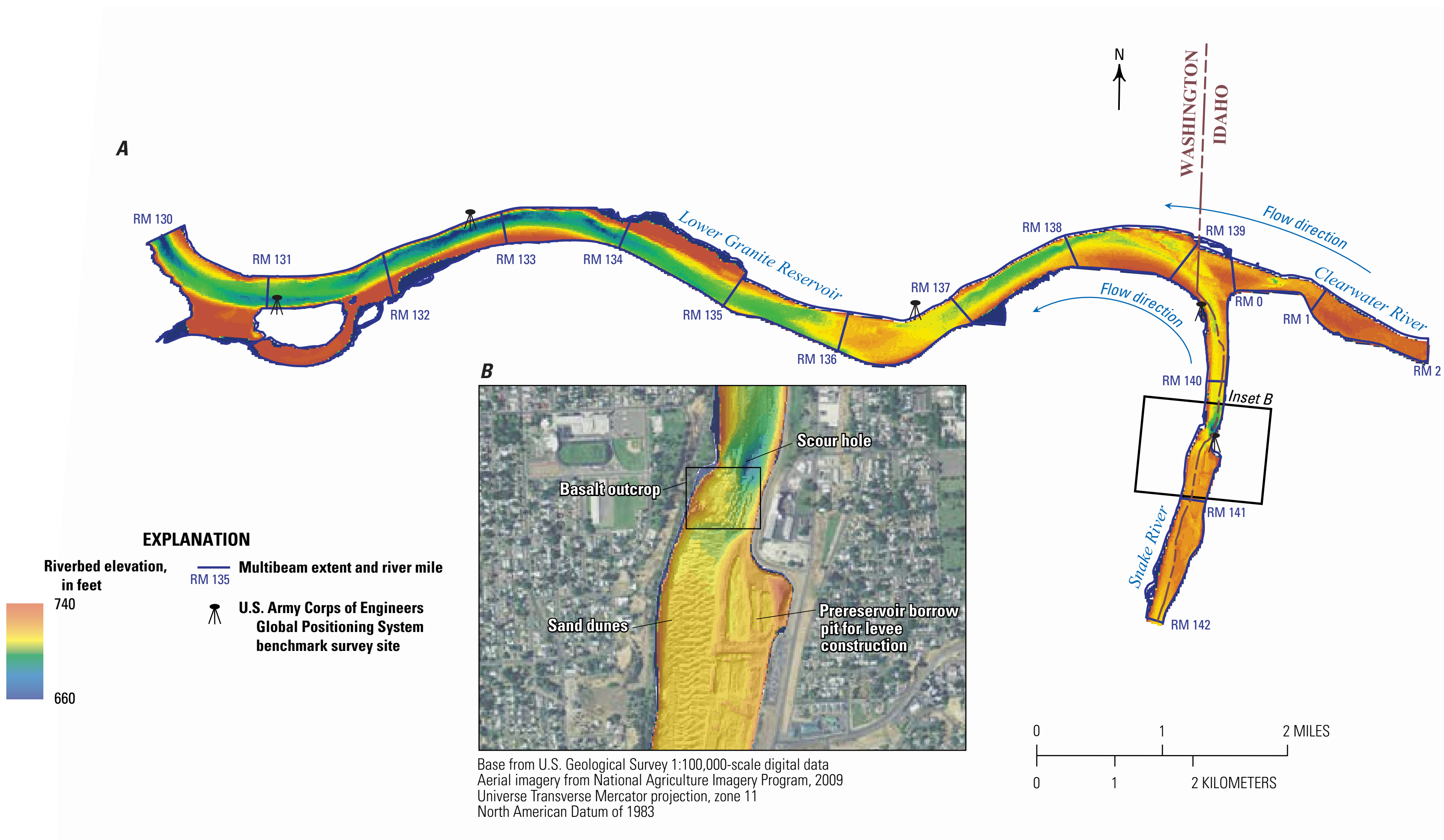

Figure 2. *A*, Bathymetry from river mile 130 to river mile 142 of Lower Granite Reservoir and the Snake River and from river mile 0 to river mile 2 of the Clearwater River, eastern Washington and northern Idaho, and *B*, multibeam bathymetry overlying imagery showing geomorphologic features such as sand dunes, a scour hole, and rock outcrop between river miles 140 and 142 (modified from Williams and others, 2012, p. 6).

Underwater Video Map Survey

UVM surveys were done by the USGS in cooperation with the USACE during fall 2009 and winter 2010 (Williams and others, 2012) to visually identify the surface substrate type and percent embeddedness by determining particle size and the extent to which coarse substrate is surrounded or covered by silt and clay particles less than 0.0625 mm in diameter (commonly referred to as "fines" [Guy, 1969]). UVM surveys provide georeferenced information about the type and size of sediment on the surface of the bed. This information was used to enhance the bathymetric data and create a surficial sediment facies map of the current sediment distribution within the study area. The sediment facies map provides information on benthic habitat characteristics, variability of surface substrate, sediment transition zones, and unrealized areas of preferred species-specific habitat.

The UVM surveys were done between RM 107.73 and RM 141.78 on Lower Granite Reservoir and the Snake River and between RM 0.28 and RM 1.66 on the Clearwater River and at RM 139.29 at the confluence of the Snake and Clearwater Rivers. More than 900 video clips were recorded at discrete, equal-width increments (video points, fig. 3*A*) along 61 historic USACE survey lines and 5 existing longitudinal dredge-material deposit sites established by the USACE (fig. 3*B*). Video clips were recorded using a high-resolution, color-video camera outfitted with two high-power laser pointers that had a constant 4-inch (102 millimeter) separation as a scale of reference to determine sediment grain size (fig. 3*A*). The camera was lowered through the water column until it was close to the sediment-bed surface; sediment size and percent embeddedness were estimated based on a visual inspection of the video by an experienced hydrologist.

Sediment sizes and categories were defined as bedrock, boulder, cobble, gravel, sand, rip-rap, and fines (silt and clay). Coarse substrates (boulder, cobble, and gravel) were combined into one category for the purposes of this study because the occurrence of these types of substrates can vary greatly over a small area (fig. 3*D*).

Historically, facies maps were created by collecting sediment samples from the bed of the water body and analyzing the samples for grain size and sediment type. The level of effort and cost for such an endeavor limits the number of samples that can be collected, resulting in the creation of a facies map with a large amount of interpolation. Coupling results from the UVM survey with results from the MBES bathymetric survey enables the creation of a high resolution facies map (fig. 3) superior to a map created using traditional methods. The video record captures the primary attributes of the substrate, such as bottom type, texture, small bedforms, disturbance indicators, unusual features, and embeddedness; it also provides verification of the sediment type identified from the MBES data. For bedforms that are greater than the camera's field of view, especially in limited light conditions, the MBES bed-elevation data provide the fidelity to define larger geomorphological features. The bathymetric survey results can be used to identify bedform features that might otherwise be misinterpreted, on the basis of video analysis alone, such as a featureless bottom (Williams and others, 2012).

Methods

Core samples were collected at 67 locations (at each of two locations, 2 core samples were collected) in Lower Granite Reservoir, the Snake and Clearwater Rivers, and the confluence of these two rivers using one or more of the following corers: piston, gravity, vibrating (also called a vibracore), or box. From these 69 cores, 185 subsamples were removed and submitted for grain size analyses, 50 of which were surficial-sediment subsamples. Surficial samples were not submitted for grain-size analysis from cores that had surficial layers made up of predominantly organic matter and detritus that were unsuitable for grain-size analysis. A total of 50 subsamples were also submitted for major and trace elemental analyses. The cores were collected in April, May, and October 2010 between RM 0.28 and 1.66 on the Clearwater River, between RM 108.31 and 138.94 on Lower Granite Reservoir, at RM 139.29 at the confluence of the Snake and Clearwater Rivers, and between RM 139.43 and 141.21 on the Snake River (table 1). The collection of cores was attempted at 86 locations using a piston, gravity, box, or vibrating core sampler.

Collection of Cores

All cores were collected from submerged sediment deposits using a 7.5-meter (m) long pontoon boat with a 4.5-m A-frame (fig. 4). This boat has the advantages of (1) accommodating the use of a hydraulic winch to deploy box, gravity, and piston corers or a vibracorer; (2) providing sufficient height for recovery of long cores (up to 3.5 m); (3) providing plenty of workspace; and (4) providing a stable work environment that is minimally affected by high winds typical of the study area.

Site Selection

Locations for the collection of cores (fig. 1) included cross sections that were measured as part of the 1995 and 2008 bed-sediment surveys done by the USACE (Greg Teasdale, U.S. Army Corps of Engineers, written commun., 2010) (appendix 1). Core sampling locations were grouped closely together (2.9 cross sections per river mile) near the confluence of the Snake and Clearwater Rivers (RM 139.29). To investigate the relative sediment contributions from the Snake and Clearwater Rivers, cores samples were collected in the reach of the Snake River immediately downstream from the confluence of the Snake and Clearwater Rivers and in both rivers upstream from the confluence (fig. 1 inset). Farther downstream from the confluence, extending through the Lower Granite Reservoir to Lower Granite Dam, sampling locations were more widely distributed (10 sections of Lower Granite Reservoir were sampled from RM 135.15 to 108.31).

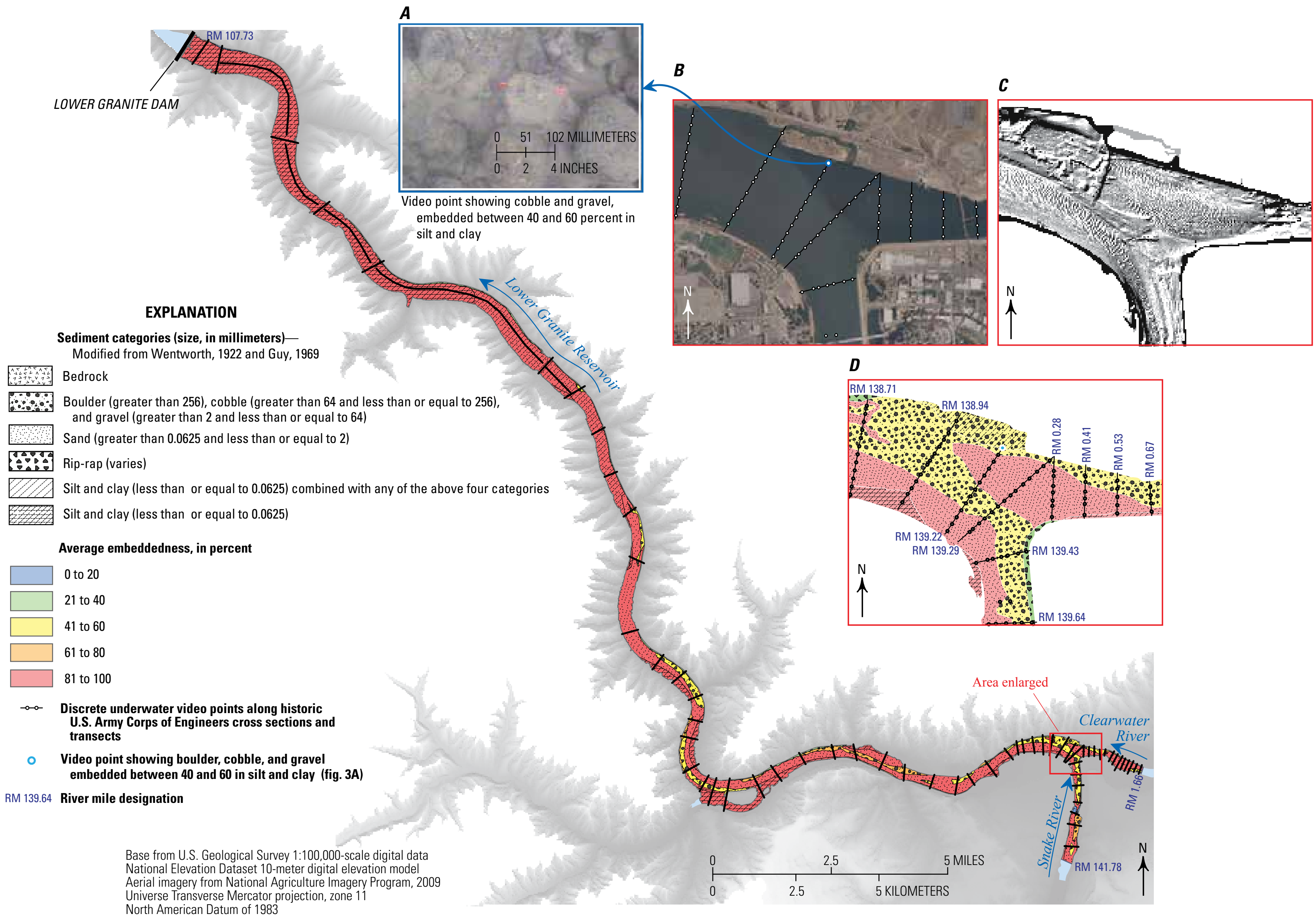

Figure 3. Facies of Lower Granite Reservoir and the Snake and Clearwater Rivers in eastern Washington and northern Idaho derived from *A*, video points (to determine sediment size and embeddedness) from the underwater video mapping (UVM) survey recorded at *B*, discrete increments along sections and dredge-material deposit areas used in conjunction with *C*, a bathymetric map created using multibeam echosounding (MBES) survey results, and composite UVM and MBES results shown enlarged as inset *D* (modified from Williams and others, 2012).

Table 1. Bed-sediment core samples collected from the Lower Granite Reservoir and Snake and Clearwater Rivers in eastern Washington and northern Idaho, 2010.

[NAVD 88, North American Vertical Datum of 1988; m, meters; cm, centimeters; --, no USGS station number established because it was not possible to collect a core sample or the core sample was not submitted for analyses]

USGS station number	Bed-sediment core sample site and core identifier	River mile	Collection date	Latitude (decimal degrees)	Longitude (decimal degrees)	Bottom elevation NAVD 88 (m)	Type of core sampler	Core sample length (cm)	Water depth (m)	Number of grain size subsamples	Number of major and trace element subsamples
Clearwater River											
462534117015500	1	0.28	5/14/2010	46.4258	117.03242	219	vibracore	21	4.5	2	0
462537117015600	2	0.28	5/13/2010	46.4269	117.03233	220	vibracore	172	4.1	3	0
462535117015700	3	0.28	5/14/2010	46.4265	117.03240	216	vibracore	134	3.8	6	0
462532117014900	4	0.41	5/13/2010	46.4256	117.03026	218	vibracore	52	5.8	2	0
462535117014800	5	0.41	5/14/2010	46.4263	117.03005	219	vibracore	55	4.5	4	0
--	6	0.41	5/11/2010	46.4272	117.03004	217	vibracore and box	0	6.7	0	0
462527117011300	7	0.92	5/18/2010	46.4241	117.02025	220	box	2	4.9	1	0
462532117011101	9	0.92	5/13/2010	46.4254	117.01963	218	vibracore	55	6.4	3	3
462517117010300	10	1.16	5/13/2010	46.4214	117.01745	220	vibracore	110	4.4	4	0
462520117005900	11	1.16	5/18/2010	46.4223	117.01643	222	box[1]	3	2.7	1	0
462524117005900	12	1.16	5/13/2010	46.4233	117.01637	219	vibracore	37	4.6	2	0
462513117004900	13	1.36	5/18/2010	46.4204	117.01368	220	box[1]	4	4.2	1	0
462517117004900	14	1.36	5/18/2010	46.4213	117.01348	221	vibracore	57	3.4	3	0
462520117004700	15	1.36	5/18/2010	46.4223	117.01263	219	vibracore	61	4.2	5	0
462511117002800	16	1.66	5/18/2010	46.4197	117.00767	219	box[1]	3	5.3	1	0
462512117002500	17	1.66	5/18/2010	46.4201	117.00705	219	box[1]	3	5.0	1	0
462515117002400	18	1.66	5/18/2010	46.4208	117.00658	219	box[1]	3	4.4	1	0
Lower Granite Reservoir											
463914117245400	19	108.31	4/7/2010	46.6538	117.41492	202	piston	213	22.9	3	0
463921117245200	20	108.31	4/7/2010	46.6558	117.41440	191	piston	308	33.5	3	0
463930117244800	21	108.31	4/7/2010	46.6585	117.41330	198	piston	49	26.2	3	0
463749117232500	22	111.24	4/7/2010	46.6304	117.39038	188	piston	172	36.0	3	0
463748117231500	23	111.24	4/7/2010	46.6301	117.38758	191	piston	169	33.5	3	0
463745117225500	24	111.24	4/6/2010	46.6292	117.38183	211	piston	32	11.3	2	0
463516117210100	25	114.92	4/7/2010	46.5877	117.35022	193	piston	49	31.7	3	0
463519117205200	26	114.92	4/7/2010	46.5886	117.34780	196	piston	179	29.0	3	0
463521117204600	27	114.92	4/7/2010	46.5892	117.34603	202	piston	264	21.9	4	0
463316117161800	28	119.56	4/6/2010	46.5543	117.27168	214	gravity	102	12.8	3	0
463318117161600	29	119.56	4/6/2010	46.5551	117.27120	202	gravity	96	21.0	3	0
463322117161000	30B	119.56	4/6/2010	46.5563	117.26935	197	gravity	19	27.1	2	0
463216117150001	31	121.42	4/6/2010	46.5378	117.24992	199	piston	167	25.9	3	13
463219117145900	32	121.42	4/6/2010	46.5387	117.24982	198	piston	91	27.7	3	0
463221117145700	33	121.42	4/6/2010	46.5393	117.24910	200	gravity	27	23.2	2	0

Table 1. Bed-sediment core samples collected from the Lower Granite Reservoir and Snake and Clearwater Rivers in eastern Washington and northern Idaho, 2010. —Continued

[NAVD 88, North American Vertical Datum of 1988; m, meters; cm, centimeters; --, no USGS station number established because it was not possible to collect a core sample or the core sample was not submitted for analyses]

USGS station number	Bed-sediment core sample site and core identifier	River mile	Collection date	Latitude (decimal degrees)	Longitude (decimal degrees)	Bottom elevation NAVD 88 (m)	Type of core sampler	Core sample length (cm)	Water depth (m)	Number of grain size subsamples	Number of major and trace element subsamples
Lower Granite Reservoir—Continued											
462655117123600	34	128.27	4/9/2010	46.4485	117.21002	214	piston	266	9.1	5	0
--	35	128.27	4/9/2010	46.4488	117.20862	206	box	2	18.6	0	0
--	36	128.27	4/9/2010	46.4492	117.20662	201	box	3	22.9	0	0
--	37	130.44	4/9/2010	46.4206	117.20688	211	box	4	12.5	0	0
462520117122001	38	130.44	5/12/2010	46.4220	117.20573	210	vibracore	178	14.6	6	6
462520117122001	38A	130.44	4/9/2010	46.4221	117.20558	210	gravity	65	14.3	3	0
462522117121800	39	130.44	5/12/2010	46.4227	117.20501	215	vibracore	164	10.1	4	0
462525117102600	40	132.05	5/12/2010	46.4238	117.1739	209	vibracore	173	12.5	4	0
462529117102800	41	132.05	5/12/2010	46.4247	117.1744	205	vibracore	8	19.1	1	0
462540117081100	43	133.98	5/12/2010	46.4278	117.13626	208	vibracore	140	16.8	4	0
462542117081100	44	133.98	5/12/2010	46.4284	117.13651	205	vibracore	4	19.1	1	0
--	45	133.98	5/12/2010	46.4291	117.13659	206	box	0	16.2	0	0
462514117065400	46	135.15	5/13/2010	46.4205	117.11497	214	vibracore	124	9.8	4	0
462515117065401	47	135.15	5/13/2010	46.4208	117.11497	211	vibracore	124	12.8	3	3
462520117065300	48	135.15	5/12/2010	46.4223	117.11466	211	box	2	12.5	1	0
462456117052900	49	136.29	5/14/2010	46.4156	117.09128	217	vibracore	135	7.5	5	0
462501117052800	50	136.29	5/14/2010	46.4170	117.09121	216	vibracore	151	7.9	3	0
--	51	136.29	5/14/2010	46.4184	117.09071	217	box	0	6.9	0	0
462510117053900	52	136.29	5/14/2010	46.4196	117.09420	215	vibracore	115	10.1	4	0
462506117050400	53	136.69	5/12/2010	46.4182	117.08449	215	vibracore	66	9.6	3	0
462509117050300	54	136.69	5/15/2010	46.4191	117.08418	214	vibracore	123	10.1	3	0
--	55	136.69	5/15/2010	46.4201	117.08514	213	box	0	10.8	0	0
462520117042900	56	137.17	5/15/2010	46.4223	117.07477	217	gravity	20	7.8	1	0
462523117042900	57	137.17	5/15/2010	46.4232	117.07463	213	box	1	12.2	1	0
--	58	137.17	5/15/2010	46.4236	117.07618	210	box	0	14.6	0	0
462540117033500	59	138.07	5/15/2010	46.4277	117.05961	218	box[1]	3	6.7	1	0
462542117033601	60	138.07	5/15/2010	46.4284	117.05988	217	vibracore	70	7.2	3	3
--	61	138.07	5/11/2010	46.4299	117.06026	210	box	0	11.8	0	0
462541117030300	62	138.52	5/12/2010	46.4280	117.05092	220	vibracore	136	3.9	2	0
462546117030500	63	138.52	5/20/2010	46.4294	117.05130	216	piston	147	8.3	2	0
--	64	138.52	5/11/2010	46.4305	117.04965	213	box	0	8.9	0	0
462536117023500	65	138.94	5/11/2010	46.4268	117.04306	220	vibracore	121	4.6	3	0
462542117024801	66	138.94	5/20/2010	46.4282	117.04665	215	piston	76	10.1	2	1
--	67	138.94	5/11/2010	46.4291	117.04117	216	box	0	9.4	0	0

Table 1. Bed-sediment core samples collected from the Lower Granite Reservoir and Snake and Clearwater Rivers in eastern Washington and northern Idaho, 2010. —Continued

[NAVD 88, North American Vertical Datum of 1988; m, meters; cm, centimeters; --, no USGS station number established because it was not possible to collect a core sample or the core sample was not submitted for analyses]

USGS station number	Bed-sediment core sample site and core identifier	River mile	Collection date	Latitude (decimal degrees)	Longitude (decimal degrees)	Bottom elevation NAVD 88 (m)	Type of core sampler	Core sample length (cm)	Water depth (m)	Number of grain size subsamples	Number of major and trace element subsamples
Confluence											
--	68	139.29	5/19/2010	46.4247	117.03882	216	box	0	8.3	0	0
--	69	139.29	5/11/2010	46.4252	117.03742	215	box	0	9.1	0	0
462535117020701	70	139.29	5/14/2010	46.4263	117.03522	220	vibracore	62	3.8	6	6
462537117020500	71	139.29	5/14/2010	46.4269	117.03468	220	vibracore	162	3.8	5	0
Snake River											
462522117021500	72	139.43	5/19/2010	46.4228	117.03755	214	box	0.5	10.1	1	0
462522117021501	73	139.43	5/19/2010	46.4228	117.03757	213	box	2	11.3	1	1
--	74	139.43	5/11/2010	46.4230	117.03597	216	box	0	9.3	0	0
--	75	139.64	5/19/2010	46.4192	117.03712	218	box	0	5.9	0	0
--	76	139.64	5/19/2010	46.4191	117.03618	214	vibracore	0	10.5	0	0
--	77	139.64	5/19/2010	46.4192	117.03530	217	box	0	7.9	0	0
462440117021300	78	140.22	5/19/2010	46.4112	117.03693	218	box	0.5	4.4	1	0
--	79	140.22	5/19/2010	46.4106	117.03628	212	box	0	11.4	0	0
462437117020601	80	140.22	5/19/2010	46.4104	117.03505	209	box	1	15.2	1	1
462426117021901	81	140.51	5/19/2010	46.4072	117.03855	215	box	3	9.9	1	1
462426117021600	82	140.51	10/13/2010	46.4072	117.03777	213	box[1]	3	11.9	1	0
462413117022101	84	140.75	10/13/2010	46.4037	117.03927	217	vibracore	110	7.3	5	5
462412117021801	85	140.75	10/13/2010	46.4036	117.03850	218	vibracore	75	7.9	4	4
--	86	140.75	5/19/2010	46.4035	117.03692	218	box	0	6.7	0	0
462348117022801	87A	141.21	5/19/2010	46.3967	117.04110	218	vibracore	19	6.1	1	1
462348117022801	87B	141.21	10/13/2010	46.3965	117.0380	218	vibracore	84	7.3	4	0
462352117022101	88	141.21	5/19/2010	46.3978	117.03917	218	box	3	6.1	1	1
462348117021701	89	141.21	5/19/2010	46.3968	117.03803	217	box[1]	3	7.6	1	1

[1]Box core sampler used after attempts to collect a vibracore or gravity core were unsuccessful.

Three coring sites were sampled at most of the preselected sampling locations (table 1). Coring sites were positioned along each section of river or reservoir where samples were collected to maximize the following selection criteria: thickness of lacustrine sediment (based on bathymetric survey data), sampling of differing depositional environments, and spacing between coring locations. One of the coring locations typically was selected at or near the deepest point within the channel along each section sampled.

Tool Selection

The advantages and disadvantages of each coring tool were taken into account when determining the most appropriate tool for a given sample. One consideration is the thickness of sediment. In reservoirs with thick sediment deposits, such as Lower Granite Reservoir, gravity and piston corers as well as a vibracorer are used because they are able to collect a much longer core compared to a box corer. Gravity

Figure 4. Pontoon boat with A-frame at Lower Granite Reservoir, 2010.

and piston corers are capable of collecting a 3-m core that is 6.7 cm in diameter, whereas the vibracorer is capable of collecting a 3.2-m core that is 7.6 cm in diameter. The box corer, which is 14 (length) × 14 (width) × 20 (height) cm, provides a shorter core but collects more material for a given interval compared to the tubular gravity and piston corers, and also has the advantage of collecting a less-disturbed sample (figs. 5*A* and 5*B*). Box corers were used predominantly for reconnaissance purposes (particularly at sites that were not expected to have thick sediment deposits) because of the relative ease of use compared to the tubular samplers. However, in some cases, box cores were subsampled for grain size and major and trace elements on the boat at the coring location.

The choice between using a gravity or piston corer is influenced by multiple factors. Gravity corers likely collect a less disturbed core and are easier to use. As a result, gravity corers were used often, especially for reconnaissance purposes. However, gravity corers have one important limitation—core shortening. Core shortening refers to the thinning of sediment layers recovered relative to undisturbed sediment; it has been attributed to friction on the walls of the liner (Emery and Hulsemann, 1964). In addition to friction, the sediment in the gravity corer barrel must push water out the top through a check valve, which generates back pressure inside the liner. In 1998, a piston and a gravity core were collected side by side in White Rock Lake, Tex. (Van Metre and others, 2004). Both encountered prereservoir sediment and appeared to represent the complete sediment sequence on the basis of color banding in the cores. The thickness of lacustrine sediment in the gravity core was 122 cm compared to 206 cm in the piston core, a core shortening of 41 percent. Therefore, if quantifying total lacustrine thickness is a primary objective, as it was in this study, an alternative coring method to gravity coring should be used, or an accounting of core shortening should be done (Juracek, 1998).

Vibrating core samplers (vibracorers) have an advantage over coring devices that sink (box corers), drop (gravity corers), or propel (piston corers) (Van Metre and others, 2004); unlike these other samplers, the vibracorer generates a high frequency vibration that transfers more energy to the sediment—greatly reducing wall friction inside and outside of the tube used to collect the core. This results in longer, more representative cores. One disadvantage of vibracoring occurs when wall friction inside the tube (as the tube penetrates sediment) exceeds the bearing strength of the sediment causing the sediment inside the tube to stop moving even though the tube continues to penetrate the sediment. This can lead to intermediate layers of sediment being bypassed unbeknownst to the investigator; this effect is referred to as plugging or rodding. Additional drawbacks associated with vibracoring include the potential for resuspension of the top few centimeters of water-rich sediment and possible compaction of sand and organic-rich layers by the associated vibrations (Vibracoring Concepts, 2011).

Coring

One or more cores were collected at selected core sampling sites for grain size distribution analysis and for trace element analysis following procedures described by Shelton (1994). In most cases, only one core was collected unless the sediment thickness was less than expected based on the river-bed elevation and geomorphology from the bathymetric survey. In these instances, a second or even third core would often be collected, frequently using an alternative coring method. Latitude and longitude of the coring site were obtained from a global positioning system to ensure that the location being sampled was at or near the predetermined sampling location. The depth of water at each site was obtained using a fathometer, and the approximate thickness of sediment obtained in each core was measured (fig. 5*C*) and recorded.

The gravity corers used in this study had a steel barrel with a polybuterate liner or an aluminum core barrel with lead weight attached and a polybuterate liner held in place by a polyvinyl chloride flange and hose clamps (fig. 5*D*). Each liner had a check-valve attached to the top, which allowed water to escape during penetration and then closed to help retain sediment during recovery. A cutting head was attached to the bottom of the steel barrel to help protect the liner and penetrate firmer sediments. A core catcher was inserted at the bottom of the liner to help retain sediment during recovery. The corer typically was allowed to free fall during sample collection to maximize sediment recovery. During retrieval, the bottom of the core was immediately capped as it approached the water surface. The cap was taped on while the core was suspended vertically from the A-frame, and the core was removed from the barrel and stored upright until subsampling. Core liners were cut about 1 cm above the top of the sediment to drain any water overlying the sediment (fig. 5*E*) and then capped and taped to minimize disturbance during transport to the subsampling location. A small gravity corer with an aluminum core barrel (fig. 5*D*) was used as a reconnaissance tool to estimate sediment thickness and determine the predominant sediment type. Reconnaissance was particularly important in areas where little sediment thickness was expected.

The piston corer works like a syringe with the bottom cut off to create an open cylinder—the piston acts as the plunger and the core barrel acts as the outside of the syringe. The plunger (piston) is held in place just above the sediment and the outside of the syringe is pushed past the piston into the sediment. The piston corer used in this study was the same weight with the same barrel as the gravity corer. However, it contained a piston inside the liner connected to a trigger arm located above the corer and attached to the winch on the boat (figs. 6*A* and 6*B*). When the trigger weight suspended from the trigger arm reaches the bottom, the arm releases the corer allowing it to fall past the piston into the sediment. The piston should stop just above the top of the sediment by the cable

Figure 5. Different bed-sediment coring tools and procedures, including: *A*, a box corer, *B*, a box core, *C*, measurement of sediment-core thickness, *D*, components of a short aluminum gravity corer, and *E*, draining water overlying a bed-sediment core by cutting the liner with a tubing cutter.

Figure 6. U.S. Geological Survey personnel *A*, lowering piston corer into the water and *B*, preparing to remove a bed-sediment core from the steel core barrel.

attached to the winch if the length of cable between the trigger arm and piston and the length of rope between the trigger arm and trigger weight were properly measured and the winch operator stopped lowering as soon as the trigger arm released the corer. As the barrel falls past the piston into the sediment, a strong vacuum is created below the piston, which enhances the recovery of sediment. The winch pulls the piston to the top of the corer, if it was not already there, and lifts the corer. Once out of water, the trigger arm and weight are disconnected from the cable. The methods associated with piston core retrieval and storage were comparable to those associated with gravity core retrieval and storage.

The vibracorer was used to collect cores from substrates with predominantly sand or larger particle sizes. The vibrating mechanism of the vibracorer, referred to as the vibrahead (fig. 7A), is powered by an external electrical source and generates 3,000 to 11,000 vibrations per minute. These vibrations cause a thin layer of material to mobilize along the inner and outer walls of the core barrel or liner, reducing friction and easing penetration into the substrate. Metal tubes conduct vibration energy best, with hard steel performing better than aluminum. Plastic tubes are poorer conductors than metals, but this disadvantage is partially offset by the reduced mass requiring vibration (Vibracoring

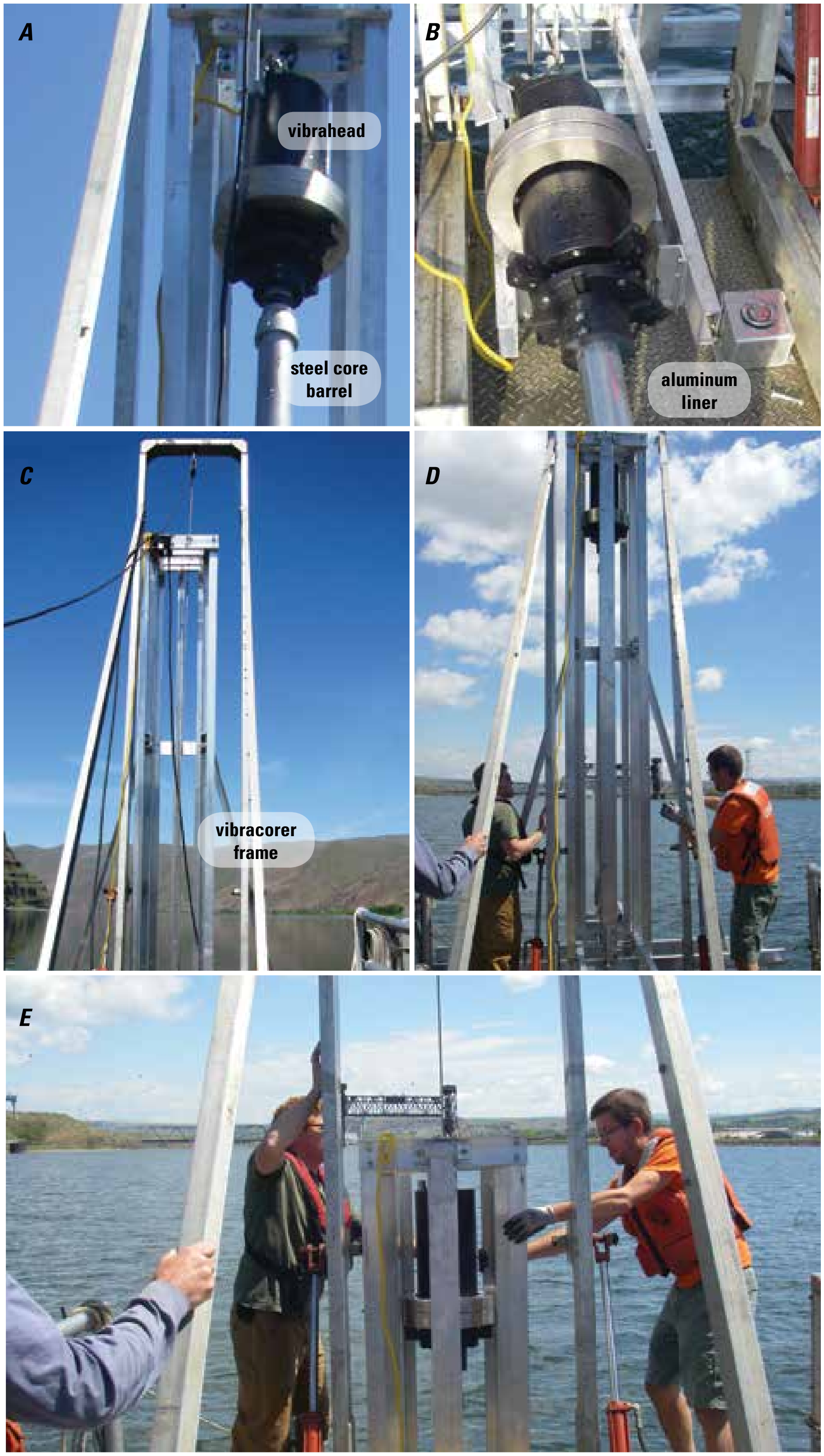

Figure 7. Use of vibracoring system *A*, use of vibracorer with steel core barrel and polybuterate liner, *B*, use of vibracorer with aluminum liner and no barrel, *C*, vibracoring frame resting on the deck of the boat, *D*, preparation for deployment of vibracorer, and *E*, lowering of vibracorer inside frame.

Concepts, 2011). For this study, the same steel barrels and polybuterate liners used to collect the gravity and piston cores were used initially to collect the vibracores (fig. 7*A*). However, the vibracorer did not appear to be penetrating the sediment to the expected depth. This was likely due to a loss in vibration efficiency because of the small gap between the liner and the barrel. Therefore, a transition was made to using aluminum liners without a core barrel (fig. 7*B*). In order to keep the vibracorer from penetrating the sediment at an angle, a frame was constructed to house the vibracorer and ensure penetration perpendicular to the sediment surface (figs. 7*A*, 7*B*, and 7*C* (Vibracoring Concepts, 2011). The vibracorer frame was lowered from the front end of the pontoon boat using an onboard winch until the base of the frame was resting on the bottom sediment of the reservoir or river being sampled (figs. 7*D* and 7*E*). Once a vibracore was collected (using an aluminum liner), a handsaw was used to remove most of the unused liner above the uppermost sediment layer in the core; any water that was collected above the top of the sediment in the core also escaped at this time. Because the aluminum core liner is opaque, locating the top of the sediment core was problematic. Therefore, using a handsaw, the liner was cut several centimeters above where the top of the sediment core was anticipated. The last few centimeters of liner above the top of the core were then removed using a tubing cutter (fig. 5*E*).

Subsampling and Description of Cores

Piston cores, gravity cores, and vibracores were held vertically during removal from the samplers and transported to the river bank or reservoir shore, where they were split lengthwise, photographed, described, and subsampled. Core extraction from bottom sediments is referred to as sampling, whereas the subdivision of each core into discrete intervals is referred to as subsampling. The cores were laid on the ground and split lengthwise using a circular saw to cut through most of the liner, cutting the rest of the liner with a utility knife, and then slicing the sediment with a stainless steel or Teflon spatula. The core was then split open next to a tape measure, photographed, and described. Descriptions included color, texture, odor, and the presence or absence of organic detritus and biota or other visible debris. Surficial sediment samples were designated as any sample that included some part of the top 5 cm of the core. Identification of the prereservoir land surface (if penetrated) was an important part of the description. Lacustrine sediments typically have a high water content (porosity of 70 to 90 percent) and are usually silt and clay, whereas prereservoir soils are drier or stickier compared to the overlying lacustrine sediment, and often have root hairs and gravel (sediment larger than 2.0 mm in diameter). The top of the prereservoir surface may also have a layer of decaying leaves and sticks.

After a core was described and photographed, one-half of the core was cut into sections and placed into a plastic core archival box. The sediment depths of each core section were noted on the core archival box. Archived cores were provided to the USACE in Walla Walla, Wash., for long-term storage. Samples for laboratory analyses were collected from the remaining one-half of the core. Samples were collected from each section of the core with a distinct grain size. For example, the sediment in core sample 38 collected on May 12, 2010, changed at a depth of 101.4 cm from a gray colored, medium to fine–sized sand (0.25 to 0.125 mm in diameter) to dark brown silt and clay (fig. 8). Two to five samples were collected from most gravity cores, piston cores, and vibracores for grain-size analysis. One sample was collected from most box cores for grain-size analysis. The samples were collected by scooping the sediment out of the core liner at a selected depth interval with a Teflon spatula and transferring it to a sample container. Samples for grain-size analysis were placed in precleaned polypropylene jars. Samples for analysis of major and trace elements were placed in separate precleaned polypropylene jars. Each sample was labeled with the river mile, core identification, and depth interval of the core, in centimeters. Sampling tools were rinsed in tap water, soaked and washed with a brush in phosphate-free detergent, and rinsed again in tap water between samples.

Analytical Methods

Sediment samples were analyzed for grain size and selected major and trace elements. All samples selected for grain-size analysis were sent to the USGS Cascades Volcano Observatory Laboratory in Vancouver, Wash. Samples for major and trace element analyses were sent to the USGS Mineral Resources Program Analytical Laboratories in Denver, Colorado.

Grain Size

Two methods were used for grain-size analysis. For coarse material (sand-sized particle larger than 0.0625 mm in diameter), the wet sieve method was used (Pope and Ward, 1998). For silt and clay sized particles, a Micromeritics SediGraph 5120 was used to perform a sedimentation technique (referred to hereinafter as the Meyer-Fisher sedimentation technique), which measures the gravity-induced settling rates of different size particles in a liquid with known properties as a means to provide grain-size information (Meyer and Fisher, 1997). Sand-fine separation and scale of size classes defined in Wentworth (1922) and Guy (1969) for gravel, sand, silt, and clay particles were followed.

A sand-fine separation was initially done to determine which grain-size classification method would be used. If less than 5 percent of the sample by weight was sand, then a total sand weight was reported, and the Meyer-Fisher sedimentation technique was used to analyze the silt and clay (fines). If the sample had less than 5 percent silt and clay by weight, then a total weight for the fines was reported, and the wet sieve

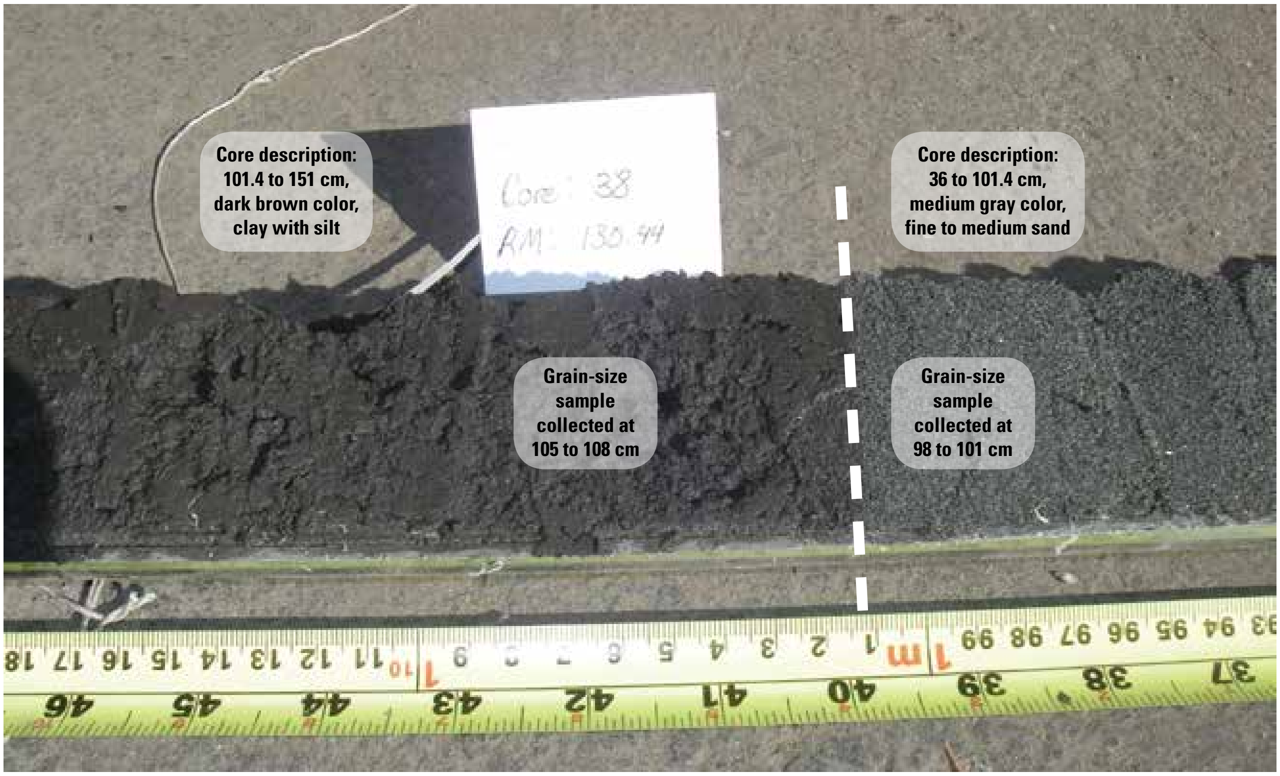

Figure 8. Bed-sediment core 38 collected at river mile (RM) 130.44 showing two sections of the core with distinct grain sizes for core intervals above and below a depth of 101.4 centimeters (cm) and intervals where grain-size samples were collected.

method was used to analyze the coarse sediment. If the sample had enough material from both size classes, then a complete size analysis was performed. Because it was necessary to keep the material wet throughout the analysis, the decision for a complete size analysis was based on a visual determination by the technician performing the analysis. If the amount of silt and clay material was less than 5 percent, then generally there was not enough material to perform the Meyer-Fisher sedimentation technique (appendix 2).

Major and Trace Elements

Freeze-dried sediment samples were analyzed for major and trace elements by the USGS Mineral Resources Program Analytical Laboratories in Denver, Colo., for the USGS National Water Quality Laboratory. Samples for major and trace element analyses were digested completely using a mixture of hydrochloric, nitric, perchloric, and hydrofluoric acids and analyzed by inductively coupled plasma–mass spectrometry (ICP–MS) (Briggs and Meier, 2002). Concentrations of mercury were determined by continuous flow-cold vapor-atomic fluorescence spectrometry (CVAFS) (Hageman, 2007) (appendix 3).

Quality Assurance and Quality Control

Quality-control (QC) samples for the major and trace elements were analyzed to ensure the quality, precision, accuracy, and completeness of the dataset; no QC samples were analyzed for grain size. The QC samples for major and trace elements consisted of laboratory reagent blank samples, standard reference materials (SRMs), and replicate samples analyzed with each set of environmental samples (appendix 4). The Lower Granite Reservoir samples were analyzed for major and trace elements in two different sets. A "lower reporting limit" described by Taggart (2002, p. viii) as greater than or equal to "five times the standard deviation determined from the method blank" was used for major and trace elements. Major and trace element concentrations less than the respective lower reporting limits are hereinafter referred to as nondetections, and concentrations equal to or greater than the respective lower reporting limits are hereinafter referred to as detections.

At least one major or trace element was detected in 13 percent of the blank analyses; cesium, niobium, and antimony were the most frequently detected trace elements. There were no detections in the blank analyses for 21 of the 38 elements. The laboratory analyzed SRMs, compared the values to published or standard results, computed the percent recoveries, and noted unacceptable SRM recoveries that were 10 percent more or less than 100 percent recovery. The SRM results are used to assess bias for each analysis. Titanium recoveries were less than 90 percent in 13 of 16 SRM analyses, whereas gallium recoveries were greater than 110 percent in 11 of 16 SRM analyses. Other elements with 50 percent or more unacceptable SRM recoveries included bismuth, cerium, and yttrium.

The laboratory analyzed two laboratory replicates in which the sample was split at the laboratory (appendix 4). Replicates provide information about variability in the analytical process, but results can be affected by sample heterogeneity, particularly when sediments are the sample media (Pirkey and Glodt, 1998). The relative percent difference (RPD) was computed between each pair of replicate analyses to provide a measure of precision using the equation:

$$RPD = |C_1 - C_2|/((C_1 + C_2)/2) \times 100, \qquad (1)$$

where

C_1 is the constituent concentration, in micrograms per gram, of one observed value; and

C_2 is the constituent concentration, in micrograms per gram, of a second observed value.

The overall average RPD for the major and trace element replicate analyses was 3.7 percent. The highest RPDs were for replicate analyses of antimony (88.8, 84.7, and 33.8 percent), followed by silver (29.4 percent).

Grain-Size Distribution

Results from the three data collection techniques used in the multiyear study (MBES bathymetric survey map, facies map based on UVM survey results, and grain-size analyses of sediment cores) were consolidated to better understand the grain-size distribution. This data consolidation also provided information on variations in substrate type relative to embeddedness throughout the reach as well as the predominance of fines (silt and clay) in the backwater-affected area downstream from the confluence. It also provides an opportunity to interpret surficial sedimentary structures (bedforms) of Lower Granite Reservoir, the Snake and Clearwater Rivers, and the confluence of these two rivers (fig. 9).

Results from the grain-size analyses of sediment cores also provided a quantitative mechanism for verifying the facies map generated from the UVM surveys (Williams and others, 2012) (fig. 10). None of the 25 surficial sediment samples with less than 20.1 percent silt and clay (based on grain-size analysis) were located in areas that the facies map identified as having silt and clay size particles. Of the 12 surficial sediment samples with greater than 80 percent silt and clay (based on grain-size analysis), 10 were located in areas that were identified as having silt and clay size particles based on the facies map; the two remaining samples were located in areas classified as sand on the facies map.

Percent silt and clay in surficial sediment samples obtained from bed-sediment cores collected in the Snake and Clearwater Rivers and Lower Granite Reservoir are shown in figure 10. Sites at the lower end of the reservoir, closest to the dam (sites 19–30) where stream velocities are lower, tended to have larger volumes of silt and clay compared to the other sites that were surveyed. All of the surficial sediment samples collected in the Snake River upstream from the confluence had less than 20 percent silt and clay. This is most likely because velocities in this reach of the Snake River are high enough to keep fine-grained (silt and clay) sediment particles entrained. Most of the surficial sediment samples collected in the Clearwater River (9 out of 13) contained less than 40 percent silt and clay; only one site (site 16) had more than 60 percent silt and clay, and this site was located in a near-bank, lower-velocity margin environment. Surficial sediment samples collected near midchannel at the confluence (site 70) tended to have more silt and clay than most surficial sediment sample collection sites on the Snake and Clearwater Rivers or even sites further downstream in Lower Granite Reservoir (sites 59, 60, and 63). The turbulence and reduction in velocity induced by the confluence of the Snake and Clearwater Rivers likely caused these two rivers to drop much of their sediment load in this area. Of the remaining surficial sediment samples (those located downstream from site 70 and upstream from site 30), all but two (site 52, which is located in a low-velocity, near-shore environment and site 66, which is located on the inside of a bend in Lower Granite Reservoir) had less than 40 percent silt and clay.

Downcore grain-size data from cores collected near the confluence of the Snake and Clearwater Rivers were plotted (fig. 11) to explore grain-size variations in this transitional area from free flowing to backwater conditions. Of the four proposed coring locations at the confluence, cores could only be collected at two locations, sites 70 and 71. Attempts at collecting box cores at the two remaining confluence sites, 68 and 69, resulted in nothing more than a trace amount of sand at site 69. Site 68 was located in an area identified as sand on the facies map and had visible dunes in the images generated from the MBES survey (Williams and others, 2012), so the inability to collect a core at this location was unexpected; rivers are dynamic systems and locations of dunes can change gradually over time or rapidly in response to storm events (Germanoski and Schumm, 1993). Site 69 was located in an area defined as boulder, cobble, and gravel on the facies map, so the inability to collect a core at this location was expected.

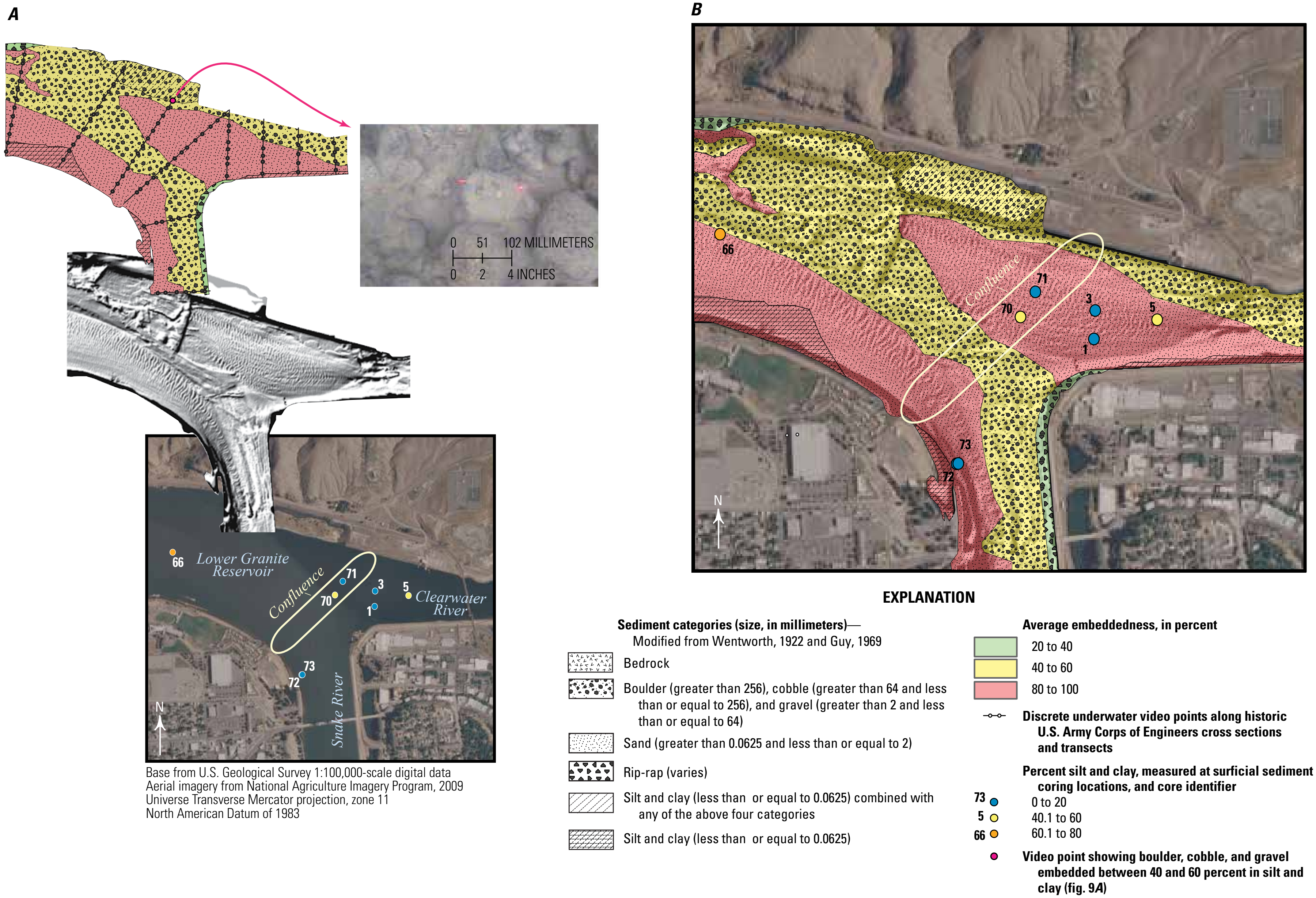

Figure 9. *A*, Consolidation of data from various data-collection methods, including: facies map (derived from underwater video map survey results), bathymetry (derived from multibeam echosounding survey results), and grain-size data from surficial sediment coring and laser projection to generate *B*, a composite map of these data layers.

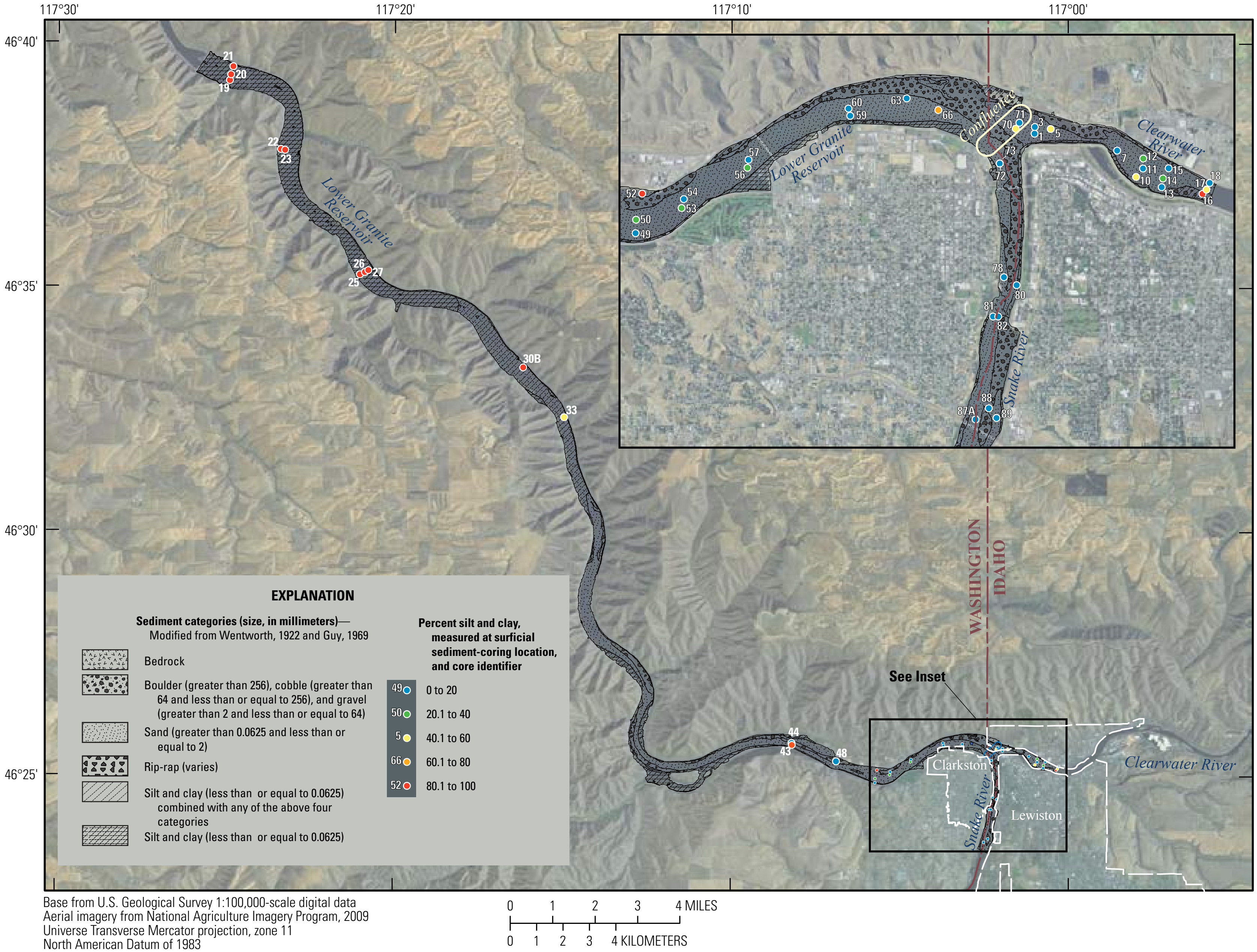

Figure 10. Percent silt and clay in surficial-sediment samples obtained from bed-sediment cores collected in Lower Granite Reservoir and the Snake and Clearwater Rivers, eastern Washington and northern Idaho, 2010.

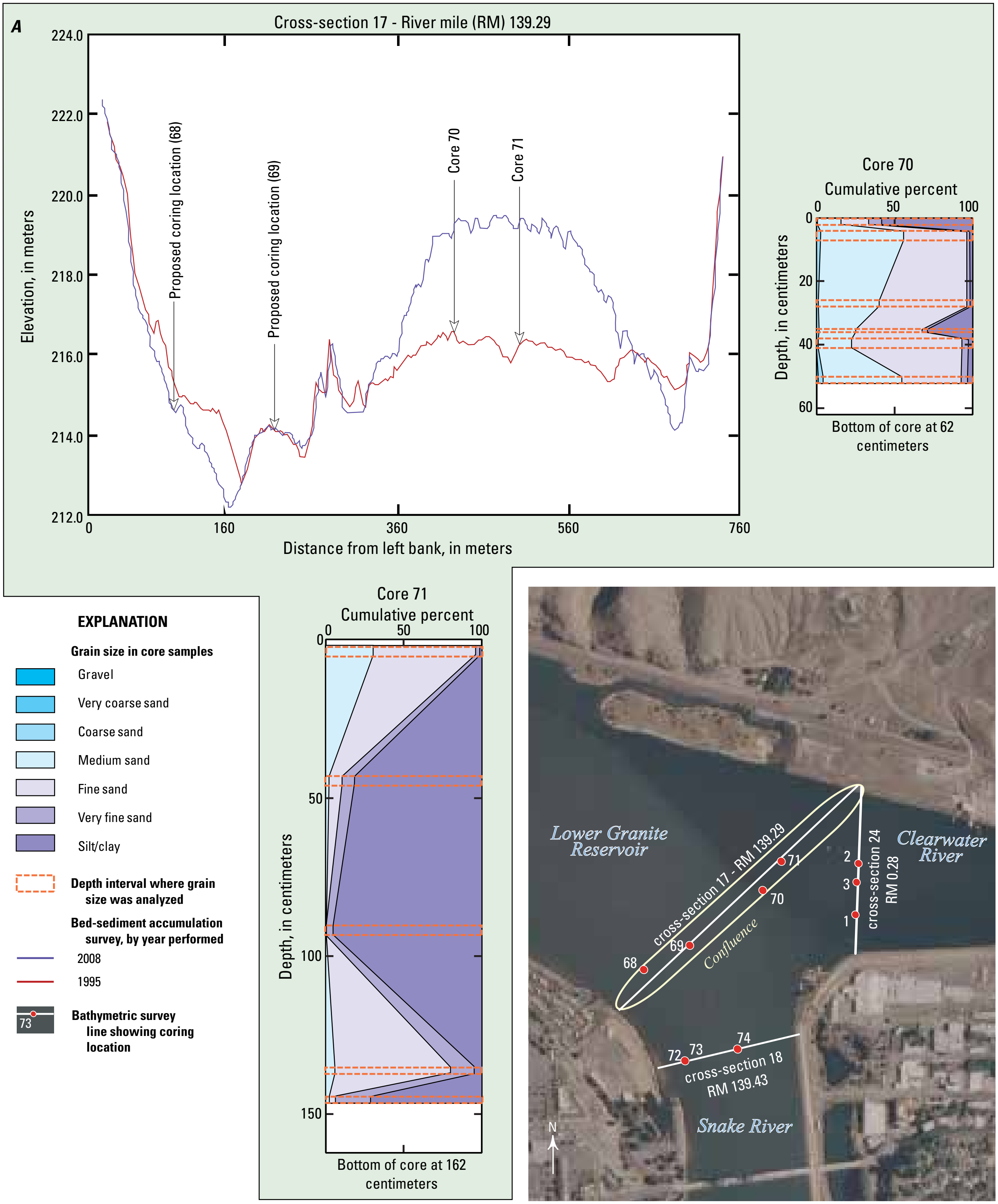

Figure 11. Comparison of grain-size distribution (as it relates to results from bed-sediment accumulation surveys done by the U.S. Army Corps of Engineers in 1995 and 2008) in bed-sediment cores collected near the confluence of the Snake and Clearwater Rivers at *A*, cross-section 17, *B*, cross-section 18, and *C*, cross-section 24, eastern Washington and northern Idaho, 2010.

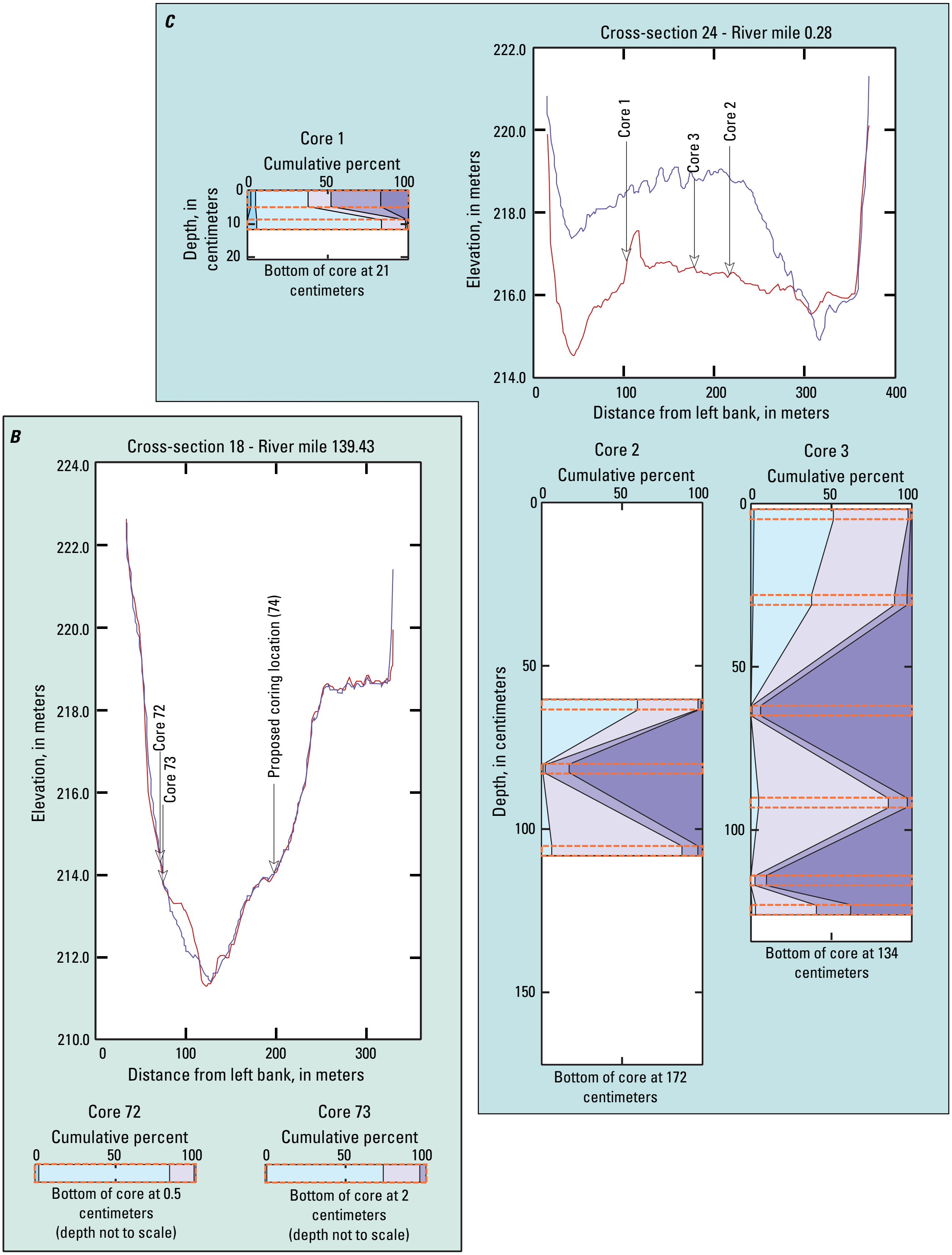

Figure 11. Comparison of grain-size distribution (as it relates to results from bed-sediment accumulation surveys done by the U.S. Army Corps of Engineers in 1995 and 2008) in bed-sediment cores collected near the confluence of the Snake and Clearwater Rivers at *A*, cross-section 17, *B*, cross-section 18, and *C*, cross-section 24, eastern Washington and northern Idaho, 2010.—Continued

The cores collected at sites 70 and 71 were collected from a thick sediment deposit along cross-section 17 just downstream from the confluence. Following the bed-sediment survey in 1995, floods with peak discharges of more than 80,000 ft^3/s occurred in both 1996 and 1997 on the Clearwater River. Streamflow records from U.S. Geological Survey streamflow-gaging station 13342500 Clearwater River at Spalding, Idaho, document peak streamflows of more than 85,000 ft^3/s during 1996 and 1997 (U.S. Geological Survey, 2011); this gaging station is about 16 miles upstream from the confluence of the Snake and Clearwater Rivers (fig. 1). The large peak streamflows likely deposited large amounts of sediment and substantially changed the channel geometry of the Clearwater River; 2008 channel-geometry surveys at cross-sections 17 and 24 document appreciable changes compared to 1995 (figs. 11*A* and11*C*, respectively). Channel-geometry surveys done at cross-section 18 on the Snake River upstream from the confluence with Clearwater River were essentially unchanged in 2008 compared to 1995 (fig. 11*B*). The core sample collected at site 71 (core 71), which was collected near the middle part of the sediment deposit at the confluence of the Clearwater River and Snake Rivers, consisted predominantly of silt and clay with some fine to very fine (0.25 to 0.0625 mm in diameter) sand, whereas the core sample collected at site 70 (core 70), which was collected closer to the margin of the sediment deposit, consisted predominantly of medium to fine sand (0.50 to 0.125 mm in diameter) (fig. 11*A*). Based on the results of the bed-sediment accumulation survey, approximately 2.6 m of bed sediment accumulated where core 70 was collected between 1995 and 2008, and approximately 3.1 m of bed sediment accumulated at site 71 during that same period. Core shortening effects associated with vibracorer use likely resulted in sediment-core thicknesses that were approximately one-half of the measured sediment accumulation at these two locations. This would mean that core 71 penetrated to approximately the same bed-surface elevation that was observed in 1995, whereas core 70 only penetrated about one-half of the distance to the 1995 bed surface. This may be because of the more coarse-grained material encountered in core 70 (very coarse sand from 1 to 2 mm in diameter) towards the bottom of the core. The thick sediment deposits at the confluence and on the Clearwater River may be flood-related deposits associated with large peak streamflows in 1996 and 1997 on the Clearwater River.

Neither of the cores collected on the Snake River just upstream from the confluence (cross-section 18, river mile 139.43) contained silt and clay (fig. 11*B*). Both cores were very short (the core sample collected at site 72 was 0.5 cm long; the core sample collected at site 73 was 2 cm long) and made up predominantly of medium sand. An attempt also was made to collect a box core at site 74, but no core could be collected at this location because of minimal sediment accumulation at this location since the 1995 bathymetric survey (fig. 11*B*). The bottom material in the Snake River upstream from the confluence, in general, is composed predominantly of gravel, cobble, and boulders as a result of upstream reservoir trapping of fine-grained sediment by Hells Canyon Dam (fig. 1) (Parkinson and others, 2003) and the delivery of coarser grained materials from the Salmon River (King and others, 2004). As a result, scant silt and clay were found in the cores collected at sites 72 and 73.

All of the cores collected on the Clearwater River just upstream from the confluence (cross-section 24, river mile 0.28) contain some silt- and clay-sized particles (fig. 11*C*). No grain-size analyses were performed on the top 60 cm of the bed-sediment sample collected at site 2 (core 2), but based on field notes, this interval was predominantly fine to medium sand with lenses of woody debris and clay. Cores 2 and 3 contained an interval with a high percentage of silt and clay at approximately the same depth. Based on the core descriptions in the field notes, an interval in core 2 from 76 to 99 cm was classified as clay (the interval from 80 to 83 cm in this core was analyzed for grain size). An interval in the bed-sediment sample collected at site 3 (core 3) from 56 to 87 cm was classified as silt and clay (the interval from 62 to 65 cm in this core was analyzed for grain size). Based on bathymetric survey images (fig. 2) (Williams and others, 2012), it appears as though these silt and clay deposits may be flood-related deposits associated with large peak streamflows in 1996 and 1997 on the Clearwater River.

Major and Trace Element Concentrations

Of the 69 cores collected, 50 subsamples from 15 cores were analyzed for major and trace elements (appendix 3). Concentrations of trace elements were low, with respect to sediment-quality guidelines (SQGs), in most cores. There are typically two SQGs—a lower level, below which adverse effects to aquatic biota are not expected, and a higher level, above which adverse effects are expected to occur. The threshold effect concentration (TEC), or lower level, and probable effect concentration (PEC), or higher level (MacDonald and others, 2000), were used to evaluate the concentrations of trace elements in the cores. Of the trace elements with TECs (arsenic, cadmium, chromium, copper, mercury, nickel, lead, and zinc), concentrations were greater than TECs in 43 percent of the analyses in the core sample collected at site 31 from the reservoir and 29 percent of the analyses in the core sample collected at site 9 from the Clearwater River (fig. 12). Chromium and copper concentrations most frequently exceeded the respective TECs. Two concentrations, 740 µg/g of copper in the bed-sediment sample collected at site 9 (core 9) at 34 to 37 cm and 2.32 µg/g of mercury in the bed-sediment sample collected at site 81 (core 81) at 0 to 3 cm, exceeded their respective PECs (150 µg/g for copper and 1.1 µg/g for mercury). The outlier trace element concentrations that were greater than the PECs were verified by the analytical laboratory (LaDonna Choate, U.S. Geological Survey, National Water Quality Laboratory, written commun., May 10, 2011).

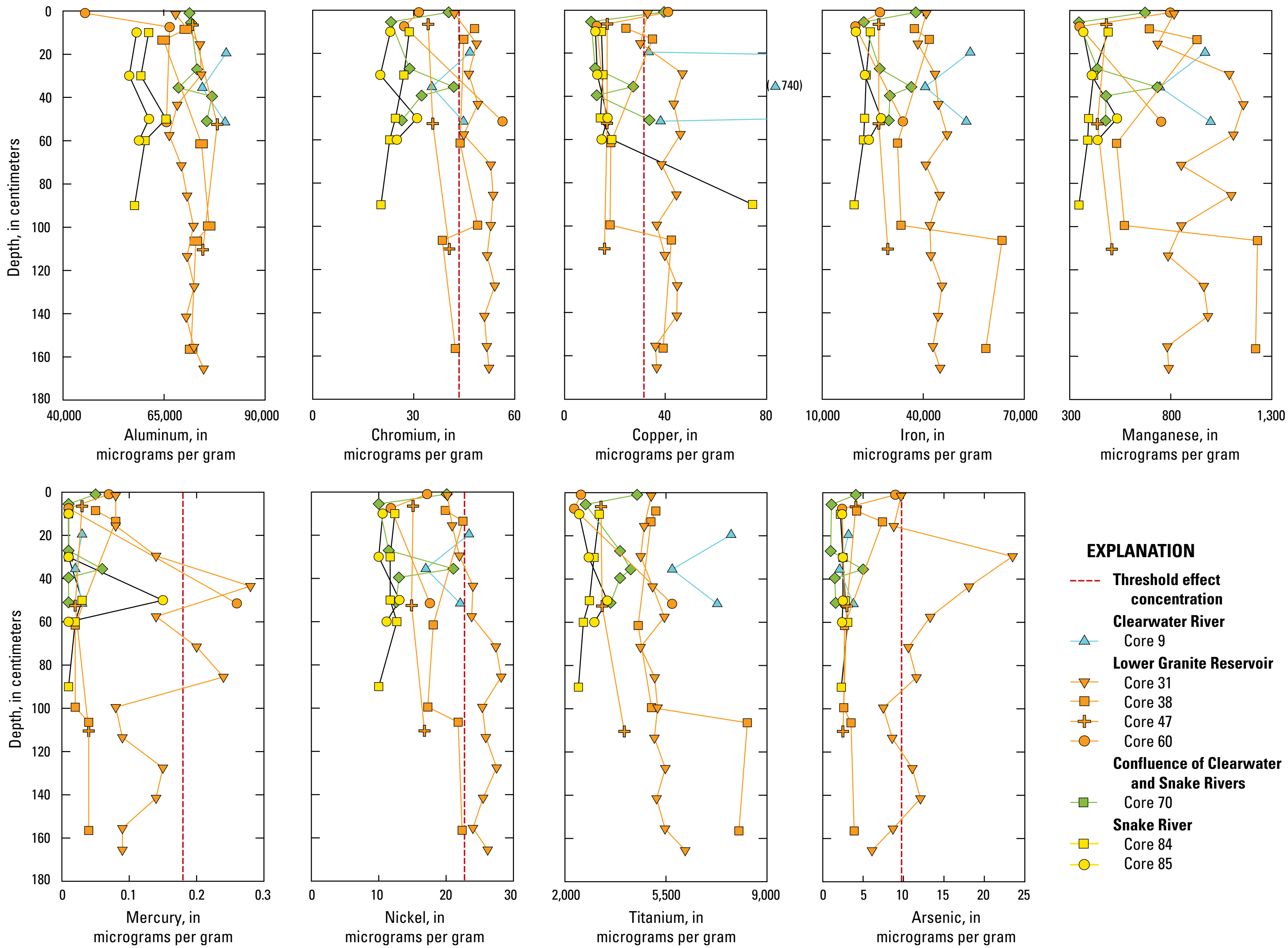

Figure 12. Concentrations of selected major and trace elements with depth (where a depth of 0 centimeters is the top of the core) in selected bed-sediment cores collected in Lower Granite Reservoir, the Snake and Clearwater Rivers, and the confluence of the Snake and Clearwater Rivers, eastern Washington and northern Idaho, 2010.

Major and trace element concentrations varied substantially at different coring locations and with depth in a single core (fig. 12). Typically, concentrations were lower in the samples collected from the Snake River compared to those collected from the Clearwater River, the confluence of the Snake and Clearwater Rivers, or Lower Granite Reservoir. Large variations in grain size occurred with depth in the sediment cores. The percentage of silt and clay-sized particles varied from 0.2 to 96.1 percent in the cores that were analyzed for major and trace elements. Because of the large grain-size variability, it is not possible to describe patterns in major and trace element concentrations with depth in the cores.

Major elements in sediment generally indicate the minerals present. For example, high aluminum and iron concentrations are typically associated with clay minerals that, because of their finer grain size, can preferentially sorb trace elements (Horowitz and Elrick, 1987). All of the samples in the cores, except core 31, that were analyzed for major and trace elements were also analyzed for grain size. Generally, lower concentrations of major and trace elements were associated with coarser sediments (larger than 0.0625 mm in diameter) and higher concentrations of major and trace elements were associated with finer sediments (smaller than 0.0625 mm in diameter) (fig. 13). Samples from the Clearwater River and Lower Granite Reservoir typically had the largest percentage of fine-grained sediments and the highest major and trace element concentrations. Conversely, the samples from the Snake River upstream from the confluence typically had the smallest percentage of fine-grained sediments and the lowest major and trace element concentrations.

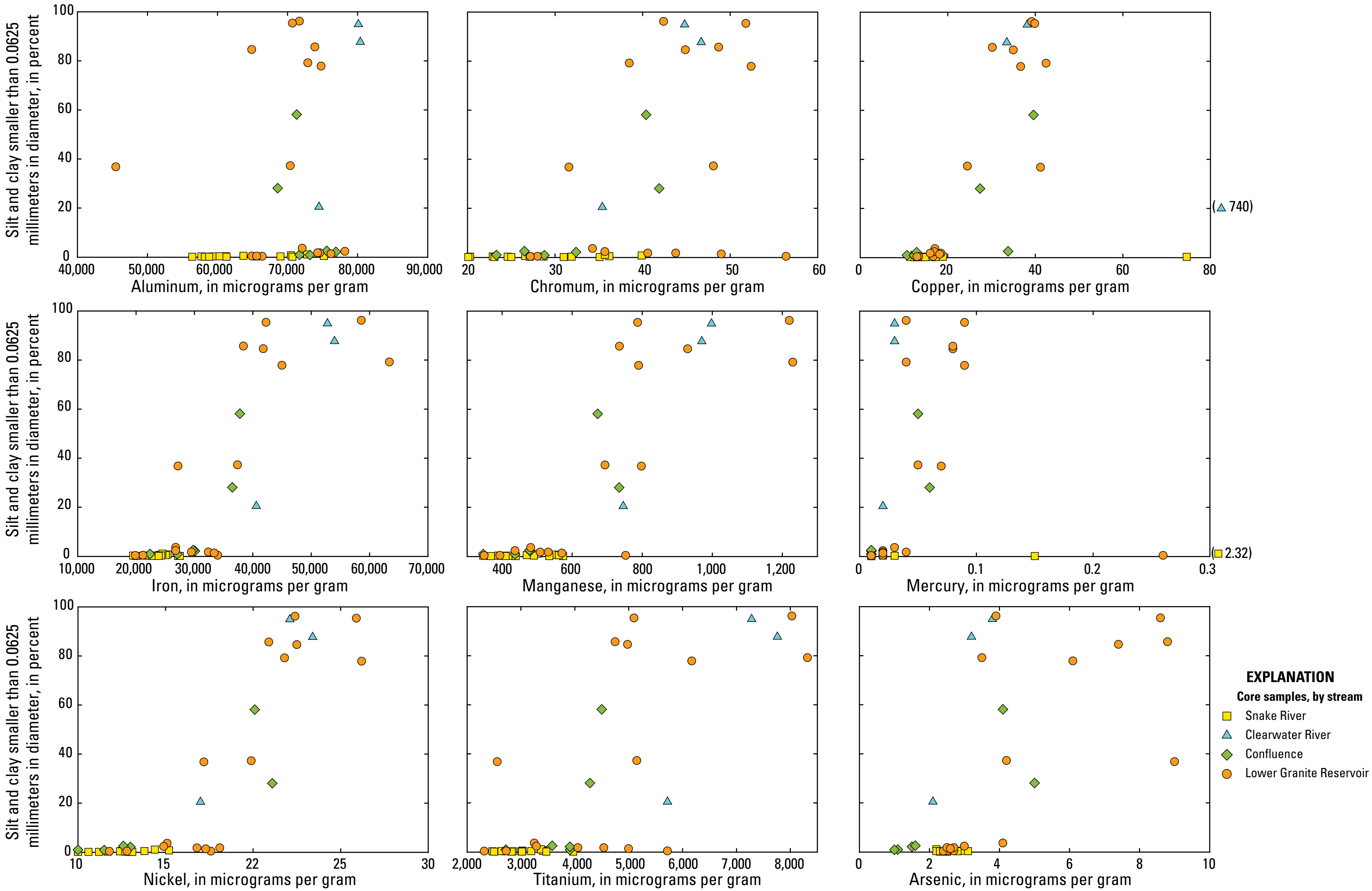

Figure 13. Comparison of percent silt and clay to selected major and trace element concentrations from bed-sediment core samples collected in Lower Granite Reservoir, the Snake and Clearwater Rivers, and the confluence of the Snake and Clearwater Rivers, eastern Washington and northern Idaho, 2010.

Summary

Lower Granite Reservoir is immediately downstream from the confluence of the Snake and Clearwater Rivers in eastern Washington and northern Idaho. According to U.S. Army Corps of Engineers (USACE), 2.6 million cubic yards (2.0 million cubic meters) of sediment have been deposited annually into Lower Granite Reservoir since its impoundment in 1975. Historically, the USACE dredged sediment to keep navigation channels clear and to maintain the flow capacity because increases in reservoir stage near the confluence reduce the effectiveness of the levees protecting the cities of Clarkston, Wash., and Lewiston, Idaho, against flooding. However, in recent years, other Federal agencies, Native American governments, and special interest groups have questioned the negative effects that dredging might have on threatened or endangered species. To help address these concerns, the U.S. Geological Survey (USGS), in cooperation with the USACE, collected bed-sediment core samples upstream from the Lower Granite Dam in the Lower Granite Reservoir and Snake and Clearwater Rivers. A total of 69 bed-sediment cores were collected at 67 locations in the study area, which includes Lower Granite Reservoir, the Snake and Clearwater Rivers, and the confluence of these two rivers, using one or more of the following corers: piston, gravity, vibrating (also called a vibracore), or box. From these 69 cores, 185 subsamples were removed and submitted for grain size analyses, 50 of which were surficial-sediment subsamples. A total of 50 subsamples were also submitted for major and trace element analyses. The multiyear project included surveys of the sedimentary structures (bedforms) of Lower Granite Reservoir using different methods. This report describes the results of a bed-sediment core samples (hereinafter cores) collected by the USGS in cooperation with the USACE during the spring and fall of 2010. A multibeam echosounding (MBES) bathymetric survey during fall 2009 and winter 2010 and an underwater video map (UVM) survey of sediment facies during fall 2009 and winter 2010, also part of the multiyear study, are briefly described and referred to in the context of core sample analyses, and used to help interpret surficial sedimentary structures (bedforms) in the study area. The grain-size distribution of surficial-sediment subsamples from cores collected underwater in Lower Granite Reservoir, the Snake and Clearwater Rivers, and the confluence of these two rivers are described, along with the down-core grain-size distribution in cores collected at or near the confluence of the Snake and Clearwater Rivers. In addition, grain-size analyses of cores are used to provide a quantitative mechanism for verifying the facies map generated from previous UVM surveys. Percent silt and clay in surficial sediment samples collected from sites at the lower end of the reservoir near the dam, where stream velocities are lower, tended to have the largest proportions (more than 80 percent) of silt and clay. Conversely, all of the surficial sediment samples collected in the Snake River upstream from the confluence had less than 20 percent silt and clay, probably a result of velocities in the Snake River high enough to keep fine-grained sediment particles entrained. Most of the surficial sediment samples collected in the Clearwater River (9 out of 13) contained less than 40 percent silt and clay. Only one site had more than 60 percent silt and clay, and this site was located in a near-shore, lower-velocity margin environment. Surficial sediment samples collected near midchannel at the confluence tended to have more silt and clay than most surficial sediment sample collection sites on the Snake and Clearwater Rivers or even sites further downstream in Lower Granite Reservoir. The turbulence and reduction in velocity induced by the confluence of the Snake and Clearwater Rivers likely caused these two rivers to drop much of their sediment load in this area.

Two core samples collected at the confluence were extracted from a thick sediment deposit that likely accumulated predominantly between 1995 and 1997; large peak streamflows occurred on the Clearwater River in both 1996 and 1997. The core collected near the middle of this sediment deposit consisted predominantly of silt and clay with some fine to very fine sand, whereas the core collected closer to the margin of this sediment deposit consisted predominantly of fine to medium sand. Cores collected on the Clearwater River just upstream from the confluence included intervals with a high percentage of silt and clay at approximately the same depths. Based on the cross section generated from the bathymetric surveys, it appears as though these silt and clay deposits may be flood-related deposits associated with large peak streamflows in 1996 and 1997 on the Clearwater River. Both of the cores collected on the Snake River just upstream from the confluence were 2 cm or less in length and neither contained silt or clay.

Fifty samples from 15 cores were analyzed for major and trace elements. Concentrations of trace elements in most of the cores were low with respect to sediment-quality guidelines. Concentrations were greater than threshold effect concentrations in 43 percent of the analyses in core 31 collected from the reservoir and 29 percent of the analyses in core 9 collected from the Clearwater River. Copper and chromium concentrations most frequently exceeded their threshold effect concentrations. Typically, major and trace element concentrations were lower in the samples collected from the Snake River upstream from the confluence as compared to those collected from the Clearwater River, the confluence of the Snake and Clearwater Rivers, and Lower Granite Reservoir. Large variations in grain size occurred with depth in the sediment cores. The percent of silt and clay-sized particles (smaller than 0.0625 millimeter [mm] in diameter) varied from 0.2 to 96.1 percent in the cores analyzed for major and trace elements. Because of the large grain size variability, it is not possible to describe trends with depth in the cores. Generally, lower concentrations of major and trace elements were associated with coarser sediments (larger than 0.0625 mm in diameter) and higher concentrations of major and trace elements were associated with finer sediments (smaller than 0.0625 mm in diameter). Samples from the Clearwater River

and Lower Granite Reservoir typically had higher proportions of fine-grained sediments and higher concentrations of major and trace elements as compared to samples collected from the Snake River upstream from the confluence.

References Cited

Briggs, P.H., and Meier, A.L., 2002, The determination of forty-two elements in geological materials by inductively coupled plasma-mass spectrometry for NAWQA, *in* Taggart, J.E., Jr., ed., Analytical methods for chemical analysis of geologic and other materials: U.S. Geological Survey Open-File Report 02–223–J, p. J1–J14. (Also available at http://pubs.usgs.gov/of/2002/ofr-02-0223/J22NAWQAMethod_M.pdf.)

Emery, K.O., and Hulsemann, J., 1964, Shortening of sediment cores collected in open barrel gravity corers: Sedimentology, v. 3, p. 144–154.

Fan, Jiahua, and Morris, G.L., 1992, Reservoir sedimentation—Delta and density current deposits: Journal of Hydraulic Engineering, v. 118, no. 3, p. 354–369.

Germanoski, D., and Schumm, S.A., 1993, Changes in braided river morphology resulting from aggradation and degradation: The Journal of Geology, v. 101, no. 4, p. 451–466.

Guy, H.P., 1969, Laboratory theory and methods for sediment analysis: U.S. Geological Survey Techniques of Water-Resources Investigations, chap. Cl, book 5, 58 p.

Hageman, P.L., 2007, Determination of mercury in aqueous and geologic materials by continuous flow-cold vapor-atomic fluorescence spectrometry (CVAFS): U.S. Geological Survey Techniques and Methods, book 5, chap. D2, 6 p.

Horowitz, A.J., and Elrick, K.A., 1987, The relation of stream sediment surface area, grain size and composition to trace element chemistry: Applied Geochemistry, v. 2, p. 437–451.

Juracek, K.E., 1998, Analysis of lake-bottom sediment to estimate historical nonpoint-source phosphorous loads: Journal of the American Water Resources Association, v. 34, no. 6, p. 1449–1463.

King, J.G., Emmett, W.W., Whiting, P.J., Kenworthy, R.P., and Barry, J.J., 2004, Sediment transport data and related information for selected coarse-bed streams and rivers in Idaho: U.S. Department of Agriculture Forest Service, Rocky Mountain Research Station General Technical Report RMRS–GTR–131, 26 p., accessed July 9, 2012, at http://www.fs.fed.us/rm/boise/publications/watershed/rmrs_gtr131.pdf.

MacDonald, D.D., Ingersoll, C.G., and Berger, T.A., 2000, Development and evaluation of consensus-based sediment quality guidelines for freshwater ecosystems: Archives of Environmental Contamination and Toxicology, v. 39, p. 20–31.

Meyer, A., and Fisher, A., 1997, Data report: Grain-size analysis of sediments from the northern Barbados accretionary prism, *in* Shipley, T.H., Ogawa, Y., Blum, P., and Bahr, J.M., eds., Proceedings of the Ocean Drilling Program, Scientific Results, College Station, Tex., Ocean Drilling Program, p. 337–341.

National Agriculture Imagery Program, 2009, 1-Meter compressed county mosaic map: U.S. Department of Agriculture Farm Service Agency, Aerial Photography Field Office, scale 1:3,780.

National Institute of Standards and Technology, 2003a, Certificate of analysis, standard reference material 2709, San Joaquin soil—Baseline trace element concentrations: National Institute of Standards and Technology, accessed February 3, 2011, at https://www-s.nist.gov/srmors/certificates/2709.pdf.

National Institute of Standards and Technology, 2003b, Certificate of analysis, standard reference material 2711, Montana soil—Moderately elevated trace element concentrations: National Institute of Standards and Technology, accessed June 15, 2011, at https://www-s.nist.gov/srmors/certificates/view_certPDF.cfm?certificate=2711.

National Institute of Standards and Technology, 2008, Report of investigation, reference material 8704, Buffalo River sediment: National Institute of Standards and Technology, accessed February 3, 2011, at https://www-s.nist.gov/srmors/reports/8704.pdf.

Parkinson, S., Anderson, K., Conner, J., and Milligan J., 2003, Sediment transport, supply and stability in the Hells Canyon Reach of the Snake River: Idaho Power Technical Report for FERC No. 1971, 140 p.

Pirkey, K.D., and Glodt, S.R., 1998, Quality control at the U.S. Geological Survey National Water Quality Laboratory: U.S. Geological Survey Fact Sheet FS–026–98, 4 p.

Pope, L.R., and Ward, C.W., eds., 1998, Manual on test sieving methods—Guidelines for establishing sieve analysis procedures (4th ed.): West Conshohocken, Pa., American Society for Testing and Materials, 43 p.

Potts, P.J., Tindle, A.G., and Webb, P.C., 1992, Geochemical reference material compositions—Rocks, minerals, sediments, soils, carbonates, refractories, and ores used in research and industry: Boca Raton, Fla., CRC Press, 313 p.

Shelton, L.R., 1994, Guidelines for collecting and processing samples of bed sediment for analysis of trace elements and organic contaminants for the National Water Quality Assessment Program: U.S. Geological Survey Open-File Report 94–458, 20 p.

Taggart, J.E., Jr., ed., 2002, Analytical methods for chemical analysis of geologic and other materials: U.S. Geological Survey Open-File Report 02–223 [variously paged].

U.S. Army Corps of Engineers, 2002, Lower Snake River juvenile salmon migration feasibility report/environmental impact statement—Appendix T: US Army Corps of Engineers, Walla Walla District, accessed September 19, 2012, at http://www.nww.usace.army.mil/portals/28/docs/environmental/lsrstudy/Appendix_T.pdf.

U.S. Army Corps of Engineers, 2003, Supplemental environmental analysis for the purposes of 2003-2004 dredging (Lower Snake and Clearwater Rivers, Washington and Idaho): U.S. Army Corps of Engineers, Walla Walla District, Washington.

U.S. Army Corps of Engineers, 2004, Framework for assessment of potential effects of dredging on sensitive fish species in San Francisco Bay: U.S. Army Corps of Engineers Final Report, August 5, 2004, 001-09170-00, San Francisco District, California.

U.S. Geological Survey, 2011, USGS water data for Idaho: National Water Information System: Web interface, accessed on September 14, 2011, at http://waterdata.usgs.gov/id/nwis.

Van Metre, P.C., Wilson, J.T., Fuller, C.C., Callender, Edward, and Mahler, B.J., 2004, Collection, analysis, and age-dating of sediment cores from 56 U.S. lakes and reservoirs sampled by the U.S. Geological Survey, 1992–2001: U.S. Geological Survey Scientific Investigations Report 2004–5184, 180 p.

Vibracoring Concepts, 2011, Core sampling basics, *in* Vibracoring a practical guide: Vibracoring Concepts, accessed on February 15, 2011, at http://www.vibracoring.com/VCconcepts.html.

Wentworth, C.K., 1922, A scale of grade and class terms for clastic sediments: The Journal of Geology, v. 30, p. 377–392.

Williams, M.L., Fosness, R.L., and Weakland, R.J., 2012, Bathymetric and underwater video survey of Lower Granite Reservoir and vicinity, Washington and Idaho, 2009–10: U.S. Geological Survey Scientific Investigations Report 2012–5089, 22 p.

Appendix 1—Distance from Bank and Elevation Data for Cross Sections 17, 18, and 24

Appendix 1. Distance from bank and elevation data for cross sections 17, 18, and 24 measured near the confluence of the Clearwater and Snake Rivers in eastern Washington and and northern Idaho, 1995 and 2008.

[dist., distance; left bank, as viewed by looking downstream; m, meters; elevation above the North American Vertical Datum of 1988; NA, not applicable; 1995 data were digitized from cross sections measured by the U.S. Army Corps of Engineers during 1995; 2008 data were from cross sections measured during 2008; data provided by the U.S. Army Corps of Engineers [Gregg Teasdale, U.S. Army Corps of Engineers, written commun., 2010])

Cross section 17				Cross section 18				Cross section 24			
1995		2008		1995		2008		1995		2008	
Dist. from left bank (m)	Elevation (m)	Dist. from left bank (m)	Elevation (m)	Dist. from left bank (m)	Elevation (m)	Dist. from left bank (m)	Elevation (m)	Dist. from left bank (m)	Elevation (m)	Dist. from left bank (m)	Elevation (m)
22.2	221.819	17.3	222.332	34.2	222.627	35.1	222.452	15.6	219.902	15.1	220.456
25.6	221.471	17.3	222.277	34.2	222.151	35.1	222.324	16.9	219.210	15.1	220.456
26.8	221.415	18.3	222.228	38.2	221.200	35.1	222.059	17.9	218.400	16.9	219.999
30.4	221.200	18.3	222.171	40.9	220.808	35.1	221.693	18.9	217.258	18.8	219.755
30.9	221.083	19.5	222.100	42.0	220.728	39.3	221.327	23.5	216.480	18.8	219.755
32.4	220.871	20.8	221.975	42.7	220.725	39.3	220.961	24.9	216.100	20.9	219.450
36.8	220.700	22.3	221.854	44.2	220.522	41.6	220.715	25.7	215.854	23.1	219.054
40.0	220.500	23.9	221.762	46.0	220.222	41.6	220.471	27.0	215.805	23.1	219.054
45.6	220.090	25.7	221.637	48.2	220.034	43.9	220.288	27.8	215.805	25.3	218.688
48.4	219.183	25.7	221.515	49.2	219.852	43.9	220.105	29.5	215.711	25.3	218.688
49.8	218.861	27.6	221.393	49.3	219.709	46.3	220.041	30.4	215.606	27.6	218.383
52.5	218.400	29.6	221.241	50.5	219.376	46.3	219.889	32.5	215.222	29.9	218.139
54.2	218.330	29.6	221.116	52.6	218.663	48.8	219.706	32.9	215.100	29.9	218.139
66.6	217.121	31.7	221.055	53.4	218.400	48.8	219.553	35.0	215.019	32.3	217.865
70.3	217.004	33.8	220.964	54.9	217.600	51.4	219.218	37.4	214.794	32.3	217.865
70.6	216.789	33.8	220.903	55.4	217.300	51.4	218.913	40.6	214.628	34.6	217.865
76.4	216.539	36.0	220.781	55.6	217.176	54.0	218.547	42.6	214.562	34.6	217.865
78.9	216.829	36.0	220.686	56.8	216.753	54.0	218.212	44.3	214.539	37.0	217.743
81.3	216.856	38.2	220.564	58.2	216.000	56.5	217.813	45.3	214.546	39.4	217.621
83.9	216.533	40.4	220.442	61.5	215.520	56.5	217.356	47.6	214.669	39.4	217.621
86.7	216.340	40.4	220.287	68.3	214.800	59.1	216.716	48.5	214.686	41.8	217.591
90.0	216.238	42.7	220.074	72.5	214.200	61.7	216.350	49.4	214.712	41.8	217.591
93.3	215.691	42.7	219.860	73.5	214.008	61.7	215.981	53.8	214.948	44.3	217.499
97.1	215.595	45.0	219.555	74.8	213.832	64.3	215.737	54.1	214.959	46.8	217.499
97.5	215.470	47.3	219.129	75.9	213.720	64.3	215.524	56.4	215.111	46.8	217.499
99.1	215.341	47.3	218.821	77.5	213.616	66.9	215.310	59.6	215.381	49.2	217.499
105.5	214.953	49.6	218.607	79.0	213.582	66.9	215.036	61.7	215.504	51.7	217.530
108.8	214.948	49.6	218.333	80.4	213.493	69.4	214.850	64.2	215.591	51.7	217.530
109.7	214.981	52.0	218.059	85.7	213.316	69.4	214.667	65.9	215.680	54.2	217.652
112.0	214.975	54.4	217.876	86.8	213.293	71.9	214.515	67.0	215.716	54.2	217.652
118.8	214.779	54.4	217.724	95.1	213.302	71.9	214.362	68.0	215.721	56.7	217.743
122.5	214.771	56.8	217.632	97.9	213.141	74.5	214.149	68.6	215.711	59.2	217.774
123.7	214.813	56.8	217.477	99.3	213.133	74.5	213.783	70.1	215.711	59.2	217.774
125.7	214.809	59.3	217.294	100.9	213.055	77.1	213.661	71.2	215.749	61.7	217.865
130.8	214.660	59.3	217.172	107.0	212.700	77.1	213.722	72.9	215.733	61.7	217.865

Appendix 1. Distance from bank and elevation data for cross sections 17, 18, and 24 measured near the confluence of the Clearwater and Snake Rivers in eastern Washington and and northern Idaho, 1995 and 2008.—Continued

[dist., distance; left bank, as viewed by looking downstream; m, meters; elevation above the North American Vertical Datum of 1988; NA, not applicable; 1995 data were digitized from cross sections measured by the U.S. Army Corps of Engineers during 1995; 2008 data were from cross sections measured during 2008; data provided by the U.S. Army Corps of Engineers [Gregg Teasdale, U.S. Army Corps of Engineers, written commun., 2010])

Cross section 17				Cross section 18				Cross section 24			
1995		2008		1995		2008		1995		2008	
Dist. from left bank (m)	Elevation (m)	Dist. from left bank (m)	Elevation (m)	Dist. from left bank (m)	Elevation (m)	Dist. from left bank (m)	Elevation (m)	Dist. from left bank (m)	Elevation (m)	Dist. from left bank (m)	Elevation (m)
133.4	214.619	61.7	217.050	109.6	212.389	79.7	213.661	74.0	215.706	64.2	217.926
140.3	214.619	64.2	216.958	113.3	212.114	82.3	213.201	75.0	215.717	66.7	218.017
142.2	214.583	64.2	216.898	114.4	211.980	82.3	213.140	76.9	215.840	66.7	218.017
144.5	214.659	66.7	216.837	117.3	211.436	84.9	213.110	78.2	215.874	69.1	218.109
148.9	214.537	69.1	216.715	118.7	211.366	84.9	213.049	79.5	215.904	69.1	218.109
151.6	214.616	69.1	216.623	122.3	211.288	87.6	212.988	80.6	215.904	71.6	218.078
156.0	214.340	71.6	216.471	123.1	211.288	90.3	212.896	81.2	215.878	74.1	217.956
160.3	214.440	71.6	216.349	124.8	211.352	90.3	212.835	82.1	215.883	74.1	217.956
176.9	212.911	74.1	216.318	127.3	211.348	92.8	212.741	83.3	215.904	76.6	218.170
178.1	212.773	74.1	216.227	130.0	211.463	95.3	212.619	85.0	215.971	79.0	218.200
185.0	213.148	76.6	216.166	132.5	211.544	95.3	212.558	86.4	216.048	79.0	218.200
193.2	213.914	79.0	216.075	135.3	211.964	97.8	212.436	87.3	216.059	81.5	218.170
198.8	214.042	79.0	215.953	138.2	212.033	97.8	212.345	90.3	216.075	81.5	218.170
200.5	214.159	81.5	215.861	142.4	212.038	100.3	212.284	91.9	216.091	84.0	218.200
202.5	214.151	83.9	215.831	144.8	211.978	100.3	212.192	96.7	216.279	86.4	218.292
202.9	214.074	83.9	215.770	147.4	211.980	102.8	212.162	99.2	216.284	86.4	218.292
205.0	214.081	86.4	215.648	150.4	212.307	105.3	212.101	100.0	216.330	88.9	218.292
210.4	214.253	86.4	215.556	153.1	212.301	105.3	212.070	101.9	216.564	91.4	218.292
217.6	214.081	88.9	215.465	160.8	212.932	107.8	212.040	103.8	216.883	91.4	218.292
221.4	214.081	88.9	215.374	163.1	213.078	107.8	212.009	110.9	217.461	93.8	218.353
223.2	214.102	91.3	215.282	163.8	213.157	110.3	212.101	114.4	217.562	93.8	218.353
226.1	214.061	91.3	215.221	165.8	213.292	110.3	212.101	116.5	217.562	96.3	218.353
226.9	214.000	93.8	215.069	167.5	213.369	112.8	212.040	116.7	217.483	98.7	218.292
231.2	214.010	93.8	214.886	170.4	213.378	115.2	211.948	117.7	217.239	98.7	218.292
238.4	213.761	96.2	214.886	170.6	213.414	115.2	211.888	118.5	216.931	101.2	218.475
241.6	213.756	96.2	214.825	172.5	213.500	117.7	211.827	120.8	216.868	101.2	218.475
244.6	213.609	98.7	214.733	176.4	213.707	117.7	211.766	122.7	216.776	103.6	218.536
245.9	213.454	98.7	214.703	178.0	213.739	120.2	211.644	123.7	216.707	106.1	218.566
251.7	213.441	101.1	214.612	180.8	213.773	122.6	211.583	126.5	216.707	106.1	218.566
257.0	213.868	103.5	214.581	183.5	213.867	122.6	211.552	128.4	216.648	108.5	218.627
260.5	214.230	103.5	214.551	185.1	213.901	125.1	211.552	130.4	216.685	108.5	218.627
261.7	214.730	106.0	214.672	187.6	213.899	125.1	211.522	131.7	216.700	111.0	218.657
264.7	215.300	108.4	214.733	190.6	213.838	127.6	211.461	133.7	216.700	111.0	218.657
267.8	215.141	108.4	214.733	192.0	213.822	130.1	211.552	135.4	216.777	113.4	218.596
272.1	215.059	110.8	214.672	193.7	213.850	130.1	211.613	136.1	216.787	115.9	218.627

Appendix 1. Distance from bank and elevation data for cross sections 17, 18, and 24 measured near the confluence of the Clearwater and Snake Rivers in eastern Washington and and northern Idaho, 1995 and 2008.—Continued

[dist., distance; left bank, as viewed by looking downstream; m, meters; elevation above the North American Vertical Datum of 1988; NA, not applicable; 1995 data were digitized from cross sections measured by the U.S. Army Corps of Engineers during 1995; 2008 data were from cross sections measured during 2008; data provided by the U.S. Army Corps of Engineers [Gregg Teasdale, U.S. Army Corps of Engineers, written commun., 2010])

Cross section 17				Cross section 18				Cross section 24			
1995		2008		1995		2008		1995		2008	
Dist. from left bank (m)	Elevation (m)	Dist. from left bank (m)	Elevation (m)	Dist. from left bank (m)	Elevation (m)	Dist. from left bank (m)	Elevation (m)	Dist. from left bank (m)	Elevation (m)	Dist. from left bank (m)	Elevation (m)
275.9	215.051	110.8	214.551	196.1	213.939	132.6	211.647	137.7	216.787	115.9	218.627
277.2	215.500	115.6	214.429	198.2	214.037	135.1	211.677	138.4	216.777	118.4	218.657
280.3	216.371	115.6	214.337	199.9	214.045	135.1	211.677	139.5	216.780	118.4	218.657
285.1	215.487	115.6	214.218	201.3	214.092	137.6	211.769	141.0	216.797	120.8	218.627
289.3	215.414	118.0	214.127	202.9	214.249	137.6	211.830	143.6	216.776	120.8	218.627
290.9	215.114	118.0	214.035	204.8	214.341	140.1	211.921	147.9	216.809	123.3	218.657
303.9	214.702	120.4	214.005	205.8	214.372	142.7	211.982	150.4	216.819	125.8	218.657
308.4	214.841	122.8	213.914	208.8	214.534	142.7	212.043	152.3	216.781	125.8	218.657
310.0	215.041	122.8	213.822	216.1	214.821	145.2	212.073	153.7	216.728	128.3	218.779
310.6	215.181	125.3	213.761	217.7	215.028	145.2	212.101	154.6	216.718	128.3	218.779
313.6	215.341	127.7	213.667	218.5	215.094	147.7	212.131	158.2	216.707	130.7	218.688
319.4	214.758	127.7	213.667	219.1	215.231	147.7	212.314	160.3	216.562	130.7	218.688
322.3	214.692	130.2	213.697	221.9	215.331	150.2	212.375	161.6	216.562	133.2	218.779
323.8	214.969	130.2	213.728	222.3	215.420	152.7	212.467	164.0	216.589	135.7	218.871
326.3	215.231	132.7	213.728	224.1	215.628	152.7	212.558	166.3	216.599	135.7	218.871
329.0	215.295	135.0	213.757	227.9	215.845	155.2	212.619	168.4	216.648	138.2	218.962
331.0	215.295	135.0	213.787	231.2	216.119	155.2	212.710	171.5	216.652	138.2	218.962
333.3	215.253	137.4	213.726	232.0	216.147	157.7	212.802	175.0	216.672	140.6	218.901
336.9	215.253	137.4	213.604	233.9	216.518	157.7	212.893	177.2	216.690	140.6	218.901
345.4	215.399	139.8	213.513	237.5	217.081	160.2	213.015	179.3	216.620	143.1	218.718
347.9	215.351	142.1	213.422	239.5	217.755	160.2	213.107	180.4	216.510	143.1	218.718
351.2	215.454	142.1	213.361	242.1	217.913	162.7	213.198	183.7	216.561	145.5	218.779
354.4	215.429	144.5	213.300	243.4	217.948	165.2	213.320	185.2	216.582	148.0	218.779
355.4	215.697	144.5	213.208	246.3	217.956	165.2	213.351	187.2	216.545	150.5	218.810
358.7	215.611	146.9	213.147	247.8	218.020	167.7	213.442	188.2	216.530	150.5	218.810
371.6	215.989	146.9	213.086	250.0	218.330	167.7	213.472	192.5	216.530	153.0	218.840
375.2	215.930	149.2	213.056	252.3	218.532	170.2	213.533	194.2	216.498	153.0	218.840
377.4	215.989	151.6	212.995	254.0	218.583	172.7	213.503	195.3	216.481	155.4	218.871
380.4	215.989	151.6	212.873	255.7	218.620	172.7	213.533	196.8	216.514	155.4	218.871
386.5	216.223	153.9	212.781	257.2	218.628	175.2	213.747	199.0	216.529	157.9	218.871
392.7	216.243	153.9	212.751	259.0	218.583	175.2	213.686	202.1	216.546	160.4	218.901
393.3	216.326	156.2	212.721	260.6	218.563	177.7	213.744	204.6	216.535	160.4	218.901
398.5	216.243	158.6	212.660	262.5	218.557	180.3	213.744	208.7	216.557	162.9	218.962
405.3	216.410	158.6	212.446	264.5	218.479	180.3	213.805	211.4	216.529	162.9	218.962
406.6	216.485	160.9	212.355	268.6	218.471	182.8	213.896	212.9	216.487	165.4	218.901

Appendix 1. Distance from bank and elevation data for cross sections 17, 18, and 24 measured near the confluence of the Clearwater and Snake Rivers in eastern Washington and and northern Idaho, 1995 and 2008.—Continued

[dist., distance; left bank, as viewed by looking downstream; m, meters; elevation above the North American Vertical Datum of 1988; NA, not applicable; 1995 data were digitized from cross sections measured by the U.S. Army Corps of Engineers during 1995; 2008 data were from cross sections measured during 2008; data provided by the U.S. Army Corps of Engineers [Gregg Teasdale, U.S. Army Corps of Engineers, written commun., 2010])

Cross section 17				Cross section 18				Cross section 24			
1995		2008		1995		2008		1995		2008	
Dist. from left bank (m)	Elevation (m)	Dist. from left bank (m)	Elevation (m)	Dist. from left bank (m)	Elevation (m)	Dist. from left bank (m)	Elevation (m)	Dist. from left bank (m)	Elevation (m)	Dist. from left bank (m)	Elevation (m)
409.2	216.432	160.9	212.355	270.7	218.515	185.4	213.927	214.2	216.439	167.8	218.962
412.1	216.557	163.2	212.324	273.0	218.500	185.4	213.957	214.9	216.439	167.8	218.962
416.0	216.458	165.5	212.294	275.0	218.468	187.9	213.927	216.7	216.503	170.3	219.023
417.6	216.362	165.5	212.233	276.9	218.483	187.9	213.927	218.5	216.541	172.4	218.871
422.1	216.578	167.8	212.233	278.8	218.675	190.5	213.927	221.3	216.556	172.4	218.871
424.4	216.583	170.3	212.263	281.0	218.779	190.5	213.866	223.9	216.504	175.3	218.993
427.3	216.452	170.3	212.324	283.9	218.604	193.0	213.957	224.8	216.476	175.3	218.993
428.3	216.361	172.9	212.416	285.4	218.567	193.0	213.927	226.5	216.467	177.7	218.932
431.2	216.286	172.9	212.480	286.2	218.571	195.5	213.988	228.1	216.423	180.2	218.993
435.4	216.340	175.5	212.571	288.7	218.687	198.1	214.018	229.3	216.358	180.2	218.993
441.5	216.251	178.1	212.663	294.0	218.687	198.1	214.110	231.5	216.343	182.7	218.932
448.5	216.258	178.1	212.693	296.5	218.584	200.7	214.170	233.7	216.283	182.7	218.932
453.5	216.369	180.6	212.845	298.5	218.727	203.2	214.231	240.3	216.280	185.2	218.901
456.8	216.369	180.6	212.967	300.2	218.828	203.2	214.292	241.6	216.262	187.7	218.932
462.0	216.452	183.2	213.059	302.2	218.831	205.8	214.353	242.8	216.252	187.7	218.932
465.9	216.452	183.2	213.211	304.7	218.692	205.8	214.414	248.0	216.241	189.6	218.932
471.4	216.353	185.8	213.333	305.7	218.651	208.4	214.536	249.0	216.182	192.0	219.023
474.3	216.257	185.8	213.394	308.5	218.651	208.4	214.597	250.2	216.123	192.0	219.023
477.2	216.216	188.4	213.547	309.6	218.699	213.6	214.628	255.6	216.129	194.5	219.115
481.7	215.951	188.4	213.638	314.2	218.695	213.6	214.719	257.5	216.042	194.5	219.115
487.3	215.943	190.9	213.760	316.8	218.629	213.6	214.814	260.8	216.480	196.9	219.084
490.8	215.798	190.9	213.821	318.0	218.661	216.2	214.966	263.6	216.124	199.4	218.962
496.6	216.052	193.5	213.943	320.7	218.652	218.9	215.057	266.2	216.188	199.4	218.962
500.3	216.230	196.1	213.973	322.0	218.748	218.9	215.179	268.6	216.232	201.8	218.871
505.5	216.342	196.1	213.973	322.8	218.748	221.4	215.301	270.2	216.267	204.3	218.932
509.0	216.389	198.7	214.004	324.2	218.689	221.4	215.393	271.7	216.200	204.3	218.932
511.2	216.348	201.4	214.004	325.5	218.695	224.0	215.515	272.5	216.129	206.8	219.084
516.1	216.334	201.4	214.034	326.0	218.716	224.0	215.758	273.4	216.123	209.2	219.237
518.4	216.278	204.0	214.065	326.4	218.800	226.5	215.789	274.8	216.149	209.2	219.237
520.6	216.238	204.0	214.034	327.7	219.032	226.5	215.880	276.3	216.161	211.7	219.298
525.5	216.292	206.6	214.126	328.9	219.071	229.0	216.002	276.9	216.129	211.7	219.298
530.4	216.300	206.6	214.126	329.3	219.940	229.0	216.094	278.0	216.129	214.1	219.267
533.8	216.188	209.3	214.187	NA	NA	231.6	216.216	280.3	216.194	214.1	219.267
538.5	216.188	209.3	214.187	NA	NA	231.6	216.246	282.0	216.213	216.6	219.176
543.0	216.111	211.9	214.217	NA	NA	234.2	216.460	283.9	216.230	219.1	219.054

Appendix 1. Distance from bank and elevation data for cross sections 17, 18, and 24 measured near the confluence of the Clearwater and Snake Rivers in eastern Washington and and northern Idaho, 1995 and 2008.—Continued

[dist., distance; left bank, as viewed by looking downstream; m, meters; elevation above the North American Vertical Datum of 1988; NA, not applicable; 1995 data were digitized from cross sections measured by the U.S. Army Corps of Engineers during 1995; 2008 data were from cross sections measured during 2008; data provided by the U.S. Army Corps of Engineers [Gregg Teasdale, U.S. Army Corps of Engineers, written commun., 2010])

Cross section 17				Cross section 18				Cross section 24			
1995		2008		1995		2008		1995		2008	
Dist. from left bank (m)	Elevation (m)	Dist. from left bank (m)	Elevation (m)	Dist. from left bank (m)	Elevation (m)	Dist. from left bank (m)	Elevation (m)	Dist. from left bank (m)	Elevation (m)	Dist. from left bank (m)	Elevation (m)
548.5	216.145	214.6	214.187	NA	NA	234.2	216.764	285.9	216.210	219.1	219.054
552.4	216.082	214.6	214.156	NA	NA	236.7	217.069	287.3	216.161	223.9	218.962
555.6	215.944	214.6	214.126	NA	NA	239.2	217.465	290.0	215.931	223.9	218.962
562.1	215.938	217.3	214.156	NA	NA	239.2	217.648	291.7	215.889	226.3	218.932
566.0	215.881	219.9	214.156	NA	NA	241.8	217.801	294.9	215.889	226.3	218.932
572.9	215.881	219.9	214.156	NA	NA	241.8	217.743	296.3	215.844	228.7	218.901
576.7	215.805	222.5	214.095	NA	NA	244.4	217.804	297.2	215.829	228.7	218.901
579.0	215.811	225.2	214.065	NA	NA	247.0	217.926	299.0	215.774	231.1	218.901
581.3	215.839	225.2	214.034	NA	NA	247.0	218.044	301.1	215.722	233.5	218.871
583.5	215.749	227.9	214.004	NA	NA	249.6	218.166	302.2	215.708	235.0	218.718
589.2	215.728	227.9	214.004	NA	NA	249.6	218.258	304.4	215.582	235.0	218.718
591.3	215.651	230.6	214.034	NA	NA	252.1	218.380	306.6	215.541	237.4	218.657
595.5	215.740	230.6	214.034	NA	NA	252.1	218.471	308.2	215.556	237.4	218.657
600.6	215.423	233.3	214.037	NA	NA	254.6	218.532	309.9	215.582	239.9	218.596
603.3	215.330	235.9	214.068	NA	NA	257.2	218.563	312.4	215.641	242.4	218.505
606.3	215.330	235.9	214.037	NA	NA	257.2	218.593	314.5	215.716	242.4	218.505
609.1	215.380	238.6	214.007	NA	NA	259.9	218.502	316.3	215.797	244.8	218.383
611.1	215.392	238.6	213.946	NA	NA	262.5	218.471	316.9	215.846	244.8	218.383
612.1	215.545	241.3	213.854	NA	NA	262.5	218.471	318.1	215.846	247.4	218.261
613.0	215.671	241.3	213.824	NA	NA	265.1	218.441	319.3	215.835	247.4	218.261
615.9	215.733	243.9	213.824	NA	NA	267.7	218.471	321.0	215.931	249.9	217.865
616.8	215.837	246.6	213.854	NA	NA	267.7	218.410	322.6	216.007	252.4	217.713
617.9	215.902	246.6	213.748	NA	NA	270.3	218.410	323.9	216.059	252.4	217.713
622.4	215.937	249.2	213.656	NA	NA	272.9	218.410	325.6	216.080	254.9	217.621
630.5	216.118	249.2	213.717	NA	NA	272.9	218.471	327.9	216.059	257.3	217.499
632.9	216.113	251.9	213.748	NA	NA	275.6	218.529	331.0	216.006	257.3	217.499
635.7	216.053	254.6	213.778	NA	NA	278.2	218.590	334.5	215.990	259.9	217.408
638.2	216.042	254.6	213.870	NA	NA	278.2	218.651	339.7	215.941	259.9	217.408
642.0	215.925	257.3	213.900	NA	NA	280.7	218.651	343.8	215.931	262.4	217.255
645.4	215.867	257.3	213.900	NA	NA	280.7	218.590	347.8	215.931	264.9	217.316
646.7	215.811	259.9	213.839	NA	NA	283.3	218.560	349.3	215.963	264.9	217.316
650.1	215.924	259.9	213.839	NA	NA	285.9	218.529	351.8	216.032	267.4	217.225
654.5	215.810	262.6	213.992	NA	NA	285.9	218.499	355.1	216.032	269.8	217.194
659.3	215.742	262.6	214.053	NA	NA	288.5	218.590	358.2	216.589	269.8	217.194
664.8	215.602	265.3	214.174	NA	NA	288.5	218.590	359.9	217.177	272.3	216.951

Appendix 1. Distance from bank and elevation data for cross sections 17, 18, and 24 measured near the confluence of the Clearwater and Snake Rivers in eastern Washington and and northern Idaho, 1995 and 2008.—Continued

[dist., distance; left bank, as viewed by looking downstream; m, meters; elevation above the North American Vertical Datum of 1988; NA, not applicable; 1995 data were digitized from cross sections measured by the U.S. Army Corps of Engineers during 1995; 2008 data were from cross sections measured during 2008; data provided by the U.S. Army Corps of Engineers [Gregg Teasdale, U.S. Army Corps of Engineers, written commun., 2010])

Cross section 17				Cross section 18				Cross section 24			
1995		2008		1995		2008		1995		2008	
Dist. from left bank (m)	Elevation (m)	Dist. from left bank (m)	Elevation (m)	Dist. from left bank (m)	Elevation (m)	Dist. from left bank (m)	Elevation (m)	Dist. from left bank (m)	Elevation (m)	Dist. from left bank (m)	Elevation (m)
665.8	215.502	265.3	214.296	NA	NA	291.1	218.621	361.7	217.960	272.3	216.951
668.7	215.436	268.1	214.662	NA	NA	293.6	218.560	363.0	218.360	274.8	216.951
672.3	215.461	268.1	214.936	NA	NA	293.6	218.560	365.0	218.860	274.8	216.951
676.2	215.288	270.7	215.089	NA	NA	296.2	218.529	367.0	219.300	277.3	216.890
681.4	215.129	270.7	215.363	NA	NA	298.8	218.590	368.5	219.600	277.3	216.890
686.4	215.169	273.4	215.455	NA	NA	298.8	218.682	369.7	219.954	279.8	216.676
693.4	215.280	273.4	215.607	NA	NA	301.3	218.755	370.8	220.112	279.8	216.676
695.8	215.495	276.1	215.272	NA	NA	301.3	218.697	NA	NA	282.2	216.341
695.4	215.742	276.1	215.512	NA	NA	303.9	218.666	NA	NA	284.7	216.250
698.4	215.797	278.8	215.025	NA	NA	303.9	218.636	NA	NA	284.7	216.250
698.6	216.051	278.8	214.964	NA	NA	306.4	218.636	NA	NA	287.2	215.975
705.0	215.950	281.5	215.177	NA	NA	308.9	218.636	NA	NA	287.2	215.975
708.8	215.882	281.5	215.604	NA	NA	311.4	218.636	NA	NA	289.6	215.792
711.2	215.812	284.3	215.848	NA	NA	311.4	218.636	NA	NA	292.0	215.609
714.7	215.865	284.3	216.214	NA	NA	313.9	218.639	NA	NA	292.0	215.609
718.3	216.051	287.0	216.274	NA	NA	316.2	218.608	NA	NA	294.4	215.457
721.4	216.284	287.0	216.122	NA	NA	316.2	218.547	NA	NA	296.8	215.274
726.4	217.900	289.7	215.970	NA	NA	318.4	218.608	NA	NA	296.8	215.274
730.6	219.318	289.7	215.787	NA	NA	320.4	218.669	NA	NA	299.2	215.183
730.6	219.577	292.4	215.573	NA	NA	322.3	218.642	NA	NA	299.2	215.183
734.2	220.089	292.4	215.540	NA	NA	324.1	218.672	NA	NA	301.6	215.061
737.4	220.952	295.2	215.357	NA	NA	325.7	219.160	NA	NA	304.0	214.939
NA	NA	295.2	215.205	NA	NA	327.1	219.831	NA	NA	304.0	214.939
NA	NA	297.9	215.051	NA	NA	328.3	220.775	NA	NA	306.4	214.908
NA	NA	297.9	214.716	NA	NA	329.2	221.388	NA	NA	306.4	214.908
NA	NA	300.7	214.625	NA	NA	NA	NA	NA	NA	309.9	214.939
NA	NA	303.4	214.594	NA	NA	NA	NA	NA	NA	309.9	214.939
NA	NA	303.4	214.533	NA	NA	NA	NA	NA	NA	312.3	214.969
NA	NA	309.0	214.533	NA	NA	NA	NA	NA	NA	312.3	214.969
NA	NA	309.0	214.503	NA	NA	NA	NA	NA	NA	314.6	214.939
NA	NA	309.0	214.533	NA	NA	NA	NA	NA	NA	316.9	215.030
NA	NA	311.7	214.533	NA	NA	NA	NA	NA	NA	316.9	215.030
NA	NA	314.5	214.533	NA	NA	NA	NA	NA	NA	319.3	215.183
NA	NA	314.5	214.533	NA	NA	NA	NA	NA	NA	321.6	215.366
NA	NA	317.2	214.564	NA	NA	NA	NA	NA	NA	321.6	215.366

Appendix 1. Distance from bank and elevation data for cross sections 17, 18, and 24 measured near the confluence of the Clearwater and Snake Rivers in eastern Washington and and northern Idaho, 1995 and 2008.—Continued

[dist., distance; left bank, as viewed by looking downstream; m, meters; elevation above the North American Vertical Datum of 1988; NA, not applicable; 1995 data were digitized from cross sections measured by the U.S. Army Corps of Engineers during 1995; 2008 data were from cross sections measured during 2008; data provided by the U.S. Army Corps of Engineers [Gregg Teasdale, U.S. Army Corps of Engineers, written commun., 2010])

Cross section 17				Cross section 18				Cross section 24			
1995		2008		1995		2008		1995		2008	
Dist. from left bank (m)	Elevation (m)	Dist. from left bank (m)	Elevation (m)	Dist. from left bank (m)	Elevation (m)	Dist. from left bank (m)	Elevation (m)	Dist. from left bank (m)	Elevation (m)	Dist. from left bank (m)	Elevation (m)
NA	NA	320.0	214.533	NA	NA	NA	NA	NA	NA	324.0	215.701
NA	NA	320.0	214.533	NA	NA	NA	NA	NA	NA	326.3	215.670
NA	NA	322.7	214.533	NA	NA	NA	NA	NA	NA	326.3	215.670
NA	NA	322.7	214.564	NA	NA	NA	NA	NA	NA	328.7	215.548
NA	NA	325.4	214.777	NA	NA	NA	NA	NA	NA	331.0	215.609
NA	NA	325.4	214.990	NA	NA	NA	NA	NA	NA	333.3	215.640
NA	NA	328.1	215.143	NA	NA	NA	NA	NA	NA	335.7	215.731
NA	NA	328.1	215.234	NA	NA	NA	NA	NA	NA	335.7	215.731
NA	NA	330.8	215.292	NA	NA	NA	NA	NA	NA	338.1	215.823
NA	NA	333.5	215.353	NA	NA	NA	NA	NA	NA	340.4	215.853
NA	NA	333.5	215.505	NA	NA	NA	NA	NA	NA	342.7	215.853
NA	NA	336.1	215.627	NA	NA	NA	NA	NA	NA	342.7	215.853
NA	NA	336.1	215.688	NA	NA	NA	NA	NA	NA	345.0	215.823
NA	NA	336.1	215.780	NA	NA	NA	NA	NA	NA	347.3	215.884
NA	NA	338.8	215.841	NA	NA	NA	NA	NA	NA	349.6	215.914
NA	NA	341.5	215.841	NA	NA	NA	NA	NA	NA	351.9	215.975
NA	NA	341.5	215.902	NA	NA	NA	NA	NA	NA	354.2	216.006
NA	NA	344.1	215.902	NA	NA	NA	NA	NA	NA	354.2	216.006
NA	NA	346.8	215.932	NA	NA	NA	NA	NA	NA	356.5	216.341
NA	NA	346.8	215.932	NA	NA	NA	NA	NA	NA	358.7	217.012
NA	NA	349.4	215.932	NA	NA	NA	NA	NA	NA	358.7	217.012
NA	NA	352.1	215.902	NA	NA	NA	NA	NA	NA	361.0	217.987
NA	NA	352.1	215.902	NA	NA	NA	NA	NA	NA	363.1	218.475
NA	NA	354.8	215.932	NA	NA	NA	NA	NA	NA	363.1	218.475
NA	NA	354.8	215.993	NA	NA	NA	NA	NA	NA	365.1	219.480
NA	NA	357.4	215.993	NA	NA	NA	NA	NA	NA	366.9	219.755
NA	NA	357.4	216.024	NA	NA	NA	NA	NA	NA	366.9	219.755
NA	NA	360.1	215.963	NA	NA	NA	NA	NA	NA	368.5	220.456
NA	NA	360.1	215.993	NA	NA	NA	NA	NA	NA	369.8	220.700
NA	NA	362.8	216.115	NA	NA	NA	NA	NA	NA	370.7	221.279
NA	NA	362.8	216.420	NA	NA	NA	NA	NA	NA	370.7	221.279
NA	NA	365.5	216.511	NA	NA	NA	NA	NA	NA	NA	NA
NA	NA	365.5	216.511	NA	NA	NA	NA	NA	NA	NA	NA
NA	NA	368.2	216.542	NA	NA	NA	NA	NA	NA	NA	NA
NA	NA	368.2	216.755	NA	NA	NA	NA	NA	NA	NA	NA

Appendix 1. Distance from bank and elevation data for cross sections 17, 18, and 24 measured near the confluence of the Clearwater and Snake Rivers in eastern Washington and and northern Idaho, 1995 and 2008.—Continued

[dist., distance; left bank, as viewed by looking downstream; m, meters; elevation above the North American Vertical Datum of 1988; NA, not applicable; 1995 data were digitized from cross sections measured by the U.S. Army Corps of Engineers during 1995; 2008 data were from cross sections measured during 2008; data provided by the U.S. Army Corps of Engineers [Gregg Teasdale, U.S. Army Corps of Engineers, written commun., 2010])

Cross section 17				Cross section 18				Cross section 24			
1995		2008		1995		2008		1995		2008	
Dist. from left bank (m)	Elevation (m)	Dist. from left bank (m)	Elevation (m)	Dist. from left bank (m)	Elevation (m)	Dist. from left bank (m)	Elevation (m)	Dist. from left bank (m)	Elevation (m)	Dist. from left bank (m)	Elevation (m)
NA	NA	370.8	216.908	NA	NA	NA	NA	NA	NA	NA	NA
NA	NA	370.8	216.969	NA	NA	NA	NA	NA	NA	NA	NA
NA	NA	373.6	216.999	NA	NA	NA	NA	NA	NA	NA	NA
NA	NA	373.6	217.029	NA	NA	NA	NA	NA	NA	NA	NA
NA	NA	376.3	217.090	NA	NA	NA	NA	NA	NA	NA	NA
NA	NA	376.3	217.182	NA	NA	NA	NA	NA	NA	NA	NA
NA	NA	379.0	217.273	NA	NA	NA	NA	NA	NA	NA	NA
NA	NA	379.0	217.395	NA	NA	NA	NA	NA	NA	NA	NA
NA	NA	381.7	217.517	NA	NA	NA	NA	NA	NA	NA	NA
NA	NA	381.7	217.639	NA	NA	NA	NA	NA	NA	NA	NA
NA	NA	384.4	217.731	NA	NA	NA	NA	NA	NA	NA	NA
NA	NA	384.4	217.700	NA	NA	NA	NA	NA	NA	NA	NA
NA	NA	387.2	217.761	NA	NA	NA	NA	NA	NA	NA	NA
NA	NA	387.2	217.761	NA	NA	NA	NA	NA	NA	NA	NA
NA	NA	389.9	217.700	NA	NA	NA	NA	NA	NA	NA	NA
NA	NA	389.9	217.700	NA	NA	NA	NA	NA	NA	NA	NA
NA	NA	392.5	217.883	NA	NA	NA	NA	NA	NA	NA	NA
NA	NA	395.2	218.340	NA	NA	NA	NA	NA	NA	NA	NA
NA	NA	395.2	218.401	NA	NA	NA	NA	NA	NA	NA	NA
NA	NA	397.9	218.371	NA	NA	NA	NA	NA	NA	NA	NA
NA	NA	397.9	218.310	NA	NA	NA	NA	NA	NA	NA	NA
NA	NA	400.6	218.432	NA	NA	NA	NA	NA	NA	NA	NA
NA	NA	403.3	218.767	NA	NA	NA	NA	NA	NA	NA	NA
NA	NA	403.3	218.950	NA	NA	NA	NA	NA	NA	NA	NA
NA	NA	406.0	218.950	NA	NA	NA	NA	NA	NA	NA	NA
NA	NA	406.0	218.950	NA	NA	NA	NA	NA	NA	NA	NA
NA	NA	408.6	218.950	NA	NA	NA	NA	NA	NA	NA	NA
NA	NA	408.6	218.950	NA	NA	NA	NA	NA	NA	NA	NA
NA	NA	411.3	218.950	NA	NA	NA	NA	NA	NA	NA	NA
NA	NA	414.0	219.011	NA	NA	NA	NA	NA	NA	NA	NA
NA	NA	414.0	219.011	NA	NA	NA	NA	NA	NA	NA	NA
NA	NA	416.7	219.041	NA	NA	NA	NA	NA	NA	NA	NA
NA	NA	416.7	219.041	NA	NA	NA	NA	NA	NA	NA	NA
NA	NA	419.4	219.041	NA	NA	NA	NA	NA	NA	NA	NA
NA	NA	422.1	219.011	NA	NA	NA	NA	NA	NA	NA	NA

Appendix 1. Distance from bank and elevation data for cross sections 17, 18, and 24 measured near the confluence of the Clearwater and Snake Rivers in eastern Washington and and northern Idaho, 1995 and 2008.—Continued

[dist., distance; left bank, as viewed by looking downstream; m, meters; elevation above the North American Vertical Datum of 1988; NA, not applicable; 1995 data were digitized from cross sections measured by the U.S. Army Corps of Engineers during 1995; 2008 data were from cross sections measured during 2008; data provided by the U.S. Army Corps of Engineers [Gregg Teasdale, U.S. Army Corps of Engineers, written commun., 2010])

Cross section 17				Cross section 18				Cross section 24			
1995		2008		1995		2008		1995		2008	
Dist. from left bank (m)	Elevation (m)	Dist. from left bank (m)	Elevation (m)	Dist. from left bank (m)	Elevation (m)	Dist. from left bank (m)	Elevation (m)	Dist. from left bank (m)	Elevation (m)	Dist. from left bank (m)	Elevation (m)
NA	NA	422.1	218.922	NA	NA	NA	NA	NA	NA	NA	NA
NA	NA	424.7	218.861	NA	NA	NA	NA	NA	NA	NA	NA
NA	NA	424.7	218.922	NA	NA	NA	NA	NA	NA	NA	NA
NA	NA	427.4	219.044	NA	NA	NA	NA	NA	NA	NA	NA
NA	NA	427.4	219.288	NA	NA	NA	NA	NA	NA	NA	NA
NA	NA	430.1	219.349	NA	NA	NA	NA	NA	NA	NA	NA
NA	NA	432.8	219.349	NA	NA	NA	NA	NA	NA	NA	NA
NA	NA	432.8	219.379	NA	NA	NA	NA	NA	NA	NA	NA
NA	NA	435.5	219.349	NA	NA	NA	NA	NA	NA	NA	NA
NA	NA	435.5	219.319	NA	NA	NA	NA	NA	NA	NA	NA
NA	NA	438.2	219.319	NA	NA	NA	NA	NA	NA	NA	NA
NA	NA	440.9	219.319	NA	NA	NA	NA	NA	NA	NA	NA
NA	NA	440.9	219.352	NA	NA	NA	NA	NA	NA	NA	NA
NA	NA	443.6	219.291	NA	NA	NA	NA	NA	NA	NA	NA
NA	NA	446.3	219.047	NA	NA	NA	NA	NA	NA	NA	NA
NA	NA	446.3	218.986	NA	NA	NA	NA	NA	NA	NA	NA
NA	NA	446.3	219.047	NA	NA	NA	NA	NA	NA	NA	NA
NA	NA	449.0	219.108	NA	NA	NA	NA	NA	NA	NA	NA
NA	NA	451.7	219.352	NA	NA	NA	NA	NA	NA	NA	NA
NA	NA	451.7	219.413	NA	NA	NA	NA	NA	NA	NA	NA
NA	NA	454.4	219.383	NA	NA	NA	NA	NA	NA	NA	NA
NA	NA	454.4	219.352	NA	NA	NA	NA	NA	NA	NA	NA
NA	NA	457.1	219.230	NA	NA	NA	NA	NA	NA	NA	NA
NA	NA	457.1	219.108	NA	NA	NA	NA	NA	NA	NA	NA
NA	NA	459.8	219.108	NA	NA	NA	NA	NA	NA	NA	NA
NA	NA	459.8	219.108	NA	NA	NA	NA	NA	NA	NA	NA
NA	NA	462.5	219.107	NA	NA	NA	NA	NA	NA	NA	NA
NA	NA	465.2	219.107	NA	NA	NA	NA	NA	NA	NA	NA
NA	NA	465.2	219.168	NA	NA	NA	NA	NA	NA	NA	NA
NA	NA	467.9	219.168	NA	NA	NA	NA	NA	NA	NA	NA
NA	NA	470.6	219.229	NA	NA	NA	NA	NA	NA	NA	NA
NA	NA	470.6	219.290	NA	NA	NA	NA	NA	NA	NA	NA
NA	NA	473.3	219.412	NA	NA	NA	NA	NA	NA	NA	NA
NA	NA	476.0	219.476	NA	NA	NA	NA	NA	NA	NA	NA
NA	NA	476.0	219.476	NA	NA	NA	NA	NA	NA	NA	NA

Appendix 1. Distance from bank and elevation data for cross sections 17, 18, and 24 measured near the confluence of the Clearwater and Snake Rivers in eastern Washington and and northern Idaho, 1995 and 2008.—Continued

[dist., distance; left bank, as viewed by looking downstream; m, meters; elevation above the North American Vertical Datum of 1988; NA, not applicable; 1995 data were digitized from cross sections measured by the U.S. Army Corps of Engineers during 1995; 2008 data were from cross sections measured during 2008; data provided by the U.S. Army Corps of Engineers [Gregg Teasdale, U.S. Army Corps of Engineers, written commun., 2010])

Cross section 17				Cross section 18				Cross section 24			
1995		2008		1995		2008		1995		2008	
Dist. from left bank (m)	Elevation (m)	Dist. from left bank (m)	Elevation (m)	Dist. from left bank (m)	Elevation (m)	Dist. from left bank (m)	Elevation (m)	Dist. from left bank (m)	Elevation (m)	Dist. from left bank (m)	Elevation (m)
NA	NA	478.6	219.446	NA	NA	NA	NA	NA	NA	NA	NA
NA	NA	478.6	219.415	NA	NA	NA	NA	NA	NA	NA	NA
NA	NA	481.3	219.415	NA	NA	NA	NA	NA	NA	NA	NA
NA	NA	481.3	219.415	NA	NA	NA	NA	NA	NA	NA	NA
NA	NA	484.0	219.415	NA	NA	NA	NA	NA	NA	NA	NA
NA	NA	486.7	219.415	NA	NA	NA	NA	NA	NA	NA	NA
NA	NA	486.7	219.446	NA	NA	NA	NA	NA	NA	NA	NA
NA	NA	489.4	219.446	NA	NA	NA	NA	NA	NA	NA	NA
NA	NA	489.4	219.415	NA	NA	NA	NA	NA	NA	NA	NA
NA	NA	492.0	219.415	NA	NA	NA	NA	NA	NA	NA	NA
NA	NA	492.0	219.354	NA	NA	NA	NA	NA	NA	NA	NA
NA	NA	494.7	219.293	NA	NA	NA	NA	NA	NA	NA	NA
NA	NA	497.4	219.232	NA	NA	NA	NA	NA	NA	NA	NA
NA	NA	497.4	219.141	NA	NA	NA	NA	NA	NA	NA	NA
NA	NA	500.1	219.110	NA	NA	NA	NA	NA	NA	NA	NA
NA	NA	502.8	219.141	NA	NA	NA	NA	NA	NA	NA	NA
NA	NA	502.8	219.232	NA	NA	NA	NA	NA	NA	NA	NA
NA	NA	505.4	219.385	NA	NA	NA	NA	NA	NA	NA	NA
NA	NA	505.4	219.385	NA	NA	NA	NA	NA	NA	NA	NA
NA	NA	508.1	219.385	NA	NA	NA	NA	NA	NA	NA	NA
NA	NA	510.8	219.324	NA	NA	NA	NA	NA	NA	NA	NA
NA	NA	510.8	219.263	NA	NA	NA	NA	NA	NA	NA	NA
NA	NA	513.5	219.171	NA	NA	NA	NA	NA	NA	NA	NA
NA	NA	513.5	219.110	NA	NA	NA	NA	NA	NA	NA	NA
NA	NA	516.2	219.049	NA	NA	NA	NA	NA	NA	NA	NA
NA	NA	516.2	219.202	NA	NA	NA	NA	NA	NA	NA	NA
NA	NA	518.9	219.293	NA	NA	NA	NA	NA	NA	NA	NA
NA	NA	518.9	219.232	NA	NA	NA	NA	NA	NA	NA	NA
NA	NA	521.6	219.171	NA	NA	NA	NA	NA	NA	NA	NA
NA	NA	524.3	219.141	NA	NA	NA	NA	NA	NA	NA	NA
NA	NA	524.3	219.049	NA	NA	NA	NA	NA	NA	NA	NA
NA	NA	527.0	219.019	NA	NA	NA	NA	NA	NA	NA	NA
NA	NA	529.7	219.229	NA	NA	NA	NA	NA	NA	NA	NA
NA	NA	529.7	219.412	NA	NA	NA	NA	NA	NA	NA	NA
NA	NA	529.7	219.412	NA	NA	NA	NA	NA	NA	NA	NA

Appendix 1. Distance from bank and elevation data for cross sections 17, 18, and 24 measured near the confluence of the Clearwater and Snake Rivers in eastern Washington and and northern Idaho, 1995 and 2008.—Continued

[dist., distance; left bank, as viewed by looking downstream; m, meters; elevation above the North American Vertical Datum of 1988; NA, not applicable; 1995 data were digitized from cross sections measured by the U.S. Army Corps of Engineers during 1995; 2008 data were from cross sections measured during 2008; data provided by the U.S. Army Corps of Engineers [Gregg Teasdale, U.S. Army Corps of Engineers, written commun., 2010])

Cross section 17				Cross section 18				Cross section 24			
1995		2008		1995		2008		1995		2008	
Dist. from left bank (m)	Elevation (m)	Dist. from left bank (m)	Elevation (m)	Dist. from left bank (m)	Elevation (m)	Dist. from left bank (m)	Elevation (m)	Dist. from left bank (m)	Elevation (m)	Dist. from left bank (m)	Elevation (m)
NA	NA	532.4	219.351	NA	NA	NA	NA	NA	NA	NA	NA
NA	NA	535.1	219.260	NA	NA	NA	NA	NA	NA	NA	NA
NA	NA	535.1	219.229	NA	NA	NA	NA	NA	NA	NA	NA
NA	NA	537.8	219.168	NA	NA	NA	NA	NA	NA	NA	NA
NA	NA	537.8	219.077	NA	NA	NA	NA	NA	NA	NA	NA
NA	NA	540.5	219.016	NA	NA	NA	NA	NA	NA	NA	NA
NA	NA	540.5	218.894	NA	NA	NA	NA	NA	NA	NA	NA
NA	NA	543.2	219.138	NA	NA	NA	NA	NA	NA	NA	NA
NA	NA	545.8	219.199	NA	NA	NA	NA	NA	NA	NA	NA
NA	NA	545.8	219.168	NA	NA	NA	NA	NA	NA	NA	NA
NA	NA	548.5	219.229	NA	NA	NA	NA	NA	NA	NA	NA
NA	NA	548.5	219.199	NA	NA	NA	NA	NA	NA	NA	NA
NA	NA	551.2	219.168	NA	NA	NA	NA	NA	NA	NA	NA
NA	NA	551.2	219.077	NA	NA	NA	NA	NA	NA	NA	NA
NA	NA	553.9	218.955	NA	NA	NA	NA	NA	NA	NA	NA
NA	NA	556.5	218.803	NA	NA	NA	NA	NA	NA	NA	NA
NA	NA	556.5	218.711	NA	NA	NA	NA	NA	NA	NA	NA
NA	NA	559.1	218.650	NA	NA	NA	NA	NA	NA	NA	NA
NA	NA	561.8	218.955	NA	NA	NA	NA	NA	NA	NA	NA
NA	NA	561.8	219.077	NA	NA	NA	NA	NA	NA	NA	NA
NA	NA	564.4	219.046	NA	NA	NA	NA	NA	NA	NA	NA
NA	NA	564.4	218.985	NA	NA	NA	NA	NA	NA	NA	NA
NA	NA	567.1	218.894	NA	NA	NA	NA	NA	NA	NA	NA
NA	NA	567.1	218.891	NA	NA	NA	NA	NA	NA	NA	NA
NA	NA	569.7	218.830	NA	NA	NA	NA	NA	NA	NA	NA
NA	NA	572.3	218.739	NA	NA	NA	NA	NA	NA	NA	NA
NA	NA	572.3	218.708	NA	NA	NA	NA	NA	NA	NA	NA
NA	NA	574.9	218.708	NA	NA	NA	NA	NA	NA	NA	NA
NA	NA	577.5	218.647	NA	NA	NA	NA	NA	NA	NA	NA
NA	NA	577.5	218.525	NA	NA	NA	NA	NA	NA	NA	NA
NA	NA	580.1	218.373	NA	NA	NA	NA	NA	NA	NA	NA
NA	NA	580.1	218.251	NA	NA	NA	NA	NA	NA	NA	NA
NA	NA	582.7	218.159	NA	NA	NA	NA	NA	NA	NA	NA
NA	NA	585.2	218.129	NA	NA	NA	NA	NA	NA	NA	NA
NA	NA	585.2	218.068	NA	NA	NA	NA	NA	NA	NA	NA

Appendix 1. Distance from bank and elevation data for cross sections 17, 18, and 24 measured near the confluence of the Clearwater and Snake Rivers in eastern Washington and and northern Idaho, 1995 and 2008.—Continued

[dist., distance; left bank, as viewed by looking downstream; m, meters; elevation above the North American Vertical Datum of 1988; NA, not applicable; 1995 data were digitized from cross sections measured by the U.S. Army Corps of Engineers during 1995; 2008 data were from cross sections measured during 2008; data provided by the U.S. Army Corps of Engineers [Gregg Teasdale, U.S. Army Corps of Engineers, written commun., 2010])

Cross section 17				Cross section 18				Cross section 24			
1995		2008		1995		2008		1995		2008	
Dist. from left bank (m)	Elevation (m)	Dist. from left bank (m)	Elevation (m)	Dist. from left bank (m)	Elevation (m)	Dist. from left bank (m)	Elevation (m)	Dist. from left bank (m)	Elevation (m)	Dist. from left bank (m)	Elevation (m)
NA	NA	587.8	218.037	NA	NA	NA	NA	NA	NA	NA	NA
NA	NA	590.3	217.977	NA	NA	NA	NA	NA	NA	NA	NA
NA	NA	590.3	217.885	NA	NA	NA	NA	NA	NA	NA	NA
NA	NA	592.8	217.824	NA	NA	NA	NA	NA	NA	NA	NA
NA	NA	592.8	217.733	NA	NA	NA	NA	NA	NA	NA	NA
NA	NA	595.3	217.702	NA	NA	NA	NA	NA	NA	NA	NA
NA	NA	595.3	217.611	NA	NA	NA	NA	NA	NA	NA	NA
NA	NA	597.8	217.550	NA	NA	NA	NA	NA	NA	NA	NA
NA	NA	600.3	217.611	NA	NA	NA	NA	NA	NA	NA	NA
NA	NA	600.3	217.580	NA	NA	NA	NA	NA	NA	NA	NA
NA	NA	602.8	217.489	NA	NA	NA	NA	NA	NA	NA	NA
NA	NA	602.8	217.367	NA	NA	NA	NA	NA	NA	NA	NA
NA	NA	605.3	217.275	NA	NA	NA	NA	NA	NA	NA	NA
NA	NA	605.3	217.275	NA	NA	NA	NA	NA	NA	NA	NA
NA	NA	607.8	217.489	NA	NA	NA	NA	NA	NA	NA	NA
NA	NA	607.8	217.489	NA	NA	NA	NA	NA	NA	NA	NA
NA	NA	610.3	217.397	NA	NA	NA	NA	NA	NA	NA	NA
NA	NA	612.8	217.306	NA	NA	NA	NA	NA	NA	NA	NA
NA	NA	612.8	217.154	NA	NA	NA	NA	NA	NA	NA	NA
NA	NA	615.3	217.001	NA	NA	NA	NA	NA	NA	NA	NA
NA	NA	615.3	216.757	NA	NA	NA	NA	NA	NA	NA	NA
NA	NA	617.8	216.574	NA	NA	NA	NA	NA	NA	NA	NA
NA	NA	620.3	216.544	NA	NA	NA	NA	NA	NA	NA	NA
NA	NA	620.3	216.513	NA	NA	NA	NA	NA	NA	NA	NA
NA	NA	622.7	216.178	NA	NA	NA	NA	NA	NA	NA	NA
NA	NA	625.2	216.453	NA	NA	NA	NA	NA	NA	NA	NA
NA	NA	625.2	216.574	NA	NA	NA	NA	NA	NA	NA	NA
NA	NA	630.1	216.574	NA	NA	NA	NA	NA	NA	NA	NA
NA	NA	630.1	216.482	NA	NA	NA	NA	NA	NA	NA	NA
NA	NA	632.6	216.330	NA	NA	NA	NA	NA	NA	NA	NA
NA	NA	635.0	216.208	NA	NA	NA	NA	NA	NA	NA	NA
NA	NA	635.0	216.086	NA	NA	NA	NA	NA	NA	NA	NA
NA	NA	637.4	215.933	NA	NA	NA	NA	NA	NA	NA	NA
NA	NA	637.4	215.842	NA	NA	NA	NA	NA	NA	NA	NA
NA	NA	639.9	215.781	NA	NA	NA	NA	NA	NA	NA	NA

Appendix 1. Distance from bank and elevation data for cross sections 17, 18, and 24 measured near the confluence of the Clearwater and Snake Rivers in eastern Washington and and northern Idaho, 1995 and 2008.—Continued

[dist., distance; left bank, as viewed by looking downstream; m, meters; elevation above the North American Vertical Datum of 1988; NA, not applicable; 1995 data were digitized from cross sections measured by the U.S. Army Corps of Engineers during 1995; 2008 data were from cross sections measured during 2008; data provided by the U.S. Army Corps of Engineers [Gregg Teasdale, U.S. Army Corps of Engineers, written commun., 2010])

Cross section 17				Cross section 18				Cross section 24			
1995		2008		1995		2008		1995		2008	
Dist. from left bank (m)	Elevation (m)	Dist. from left bank (m)	Elevation (m)	Dist. from left bank (m)	Elevation (m)	Dist. from left bank (m)	Elevation (m)	Dist. from left bank (m)	Elevation (m)	Dist. from left bank (m)	Elevation (m)
NA	NA	642.3	215.933	NA	NA	NA	NA	NA	NA	NA	NA
NA	NA	642.3	215.994	NA	NA	NA	NA	NA	NA	NA	NA
NA	NA	644.7	215.964	NA	NA	NA	NA	NA	NA	NA	NA
NA	NA	647.1	215.994	NA	NA	NA	NA	NA	NA	NA	NA
NA	NA	647.1	216.025	NA	NA	NA	NA	NA	NA	NA	NA
NA	NA	649.6	215.994	NA	NA	NA	NA	NA	NA	NA	NA
NA	NA	649.6	215.964	NA	NA	NA	NA	NA	NA	NA	NA
NA	NA	652.0	215.872	NA	NA	NA	NA	NA	NA	NA	NA
NA	NA	652.0	215.751	NA	NA	NA	NA	NA	NA	NA	NA
NA	NA	654.4	215.598	NA	NA	NA	NA	NA	NA	NA	NA
NA	NA	656.9	215.385	NA	NA	NA	NA	NA	NA	NA	NA
NA	NA	656.9	215.415	NA	NA	NA	NA	NA	NA	NA	NA
NA	NA	656.9	215.415	NA	NA	NA	NA	NA	NA	NA	NA
NA	NA	661.9	215.537	NA	NA	NA	NA	NA	NA	NA	NA
NA	NA	661.9	215.659	NA	NA	NA	NA	NA	NA	NA	NA
NA	NA	661.9	215.629	NA	NA	NA	NA	NA	NA	NA	NA
NA	NA	664.3	215.537	NA	NA	NA	NA	NA	NA	NA	NA
NA	NA	666.8	215.443	NA	NA	NA	NA	NA	NA	NA	NA
NA	NA	666.8	215.321	NA	NA	NA	NA	NA	NA	NA	NA
NA	NA	669.3	215.229	NA	NA	NA	NA	NA	NA	NA	NA
NA	NA	669.3	215.138	NA	NA	NA	NA	NA	NA	NA	NA
NA	NA	671.7	214.985	NA	NA	NA	NA	NA	NA	NA	NA
NA	NA	674.2	214.894	NA	NA	NA	NA	NA	NA	NA	NA
NA	NA	674.2	214.772	NA	NA	NA	NA	NA	NA	NA	NA
NA	NA	676.6	214.711	NA	NA	NA	NA	NA	NA	NA	NA
NA	NA	676.6	214.589	NA	NA	NA	NA	NA	NA	NA	NA
NA	NA	679.1	214.498	NA	NA	NA	NA	NA	NA	NA	NA
NA	NA	681.6	214.437	NA	NA	NA	NA	NA	NA	NA	NA
NA	NA	681.6	214.315	NA	NA	NA	NA	NA	NA	NA	NA
NA	NA	684.1	214.196	NA	NA	NA	NA	NA	NA	NA	NA
NA	NA	686.6	214.105	NA	NA	NA	NA	NA	NA	NA	NA
NA	NA	686.6	214.074	NA	NA	NA	NA	NA	NA	NA	NA
NA	NA	689.1	214.196	NA	NA	NA	NA	NA	NA	NA	NA
NA	NA	691.6	214.288	NA	NA	NA	NA	NA	NA	NA	NA
NA	NA	691.6	214.288	NA	NA	NA	NA	NA	NA	NA	NA

Appendix 1. Distance from bank and elevation data for cross sections 17, 18, and 24 measured near the confluence of the Clearwater and Snake Rivers in eastern Washington and and northern Idaho, 1995 and 2008.—Continued

[dist., distance; left bank, as viewed by looking downstream; m, meters; elevation above the North American Vertical Datum of 1988; NA, not applicable; 1995 data were digitized from cross sections measured by the U.S. Army Corps of Engineers during 1995; 2008 data were from cross sections measured during 2008; data provided by the U.S. Army Corps of Engineers [Gregg Teasdale, U.S. Army Corps of Engineers, written commun., 2010])

Cross section 17				Cross section 18				Cross section 24			
1995		2008		1995		2008		1995		2008	
Dist. from left bank (m)	Elevation (m)	Dist. from left bank (m)	Elevation (m)	Dist. from left bank (m)	Elevation (m)	Dist. from left bank (m)	Elevation (m)	Dist. from left bank (m)	Elevation (m)	Dist. from left bank (m)	Elevation (m)
NA	NA	694.1	214.288	NA	NA	NA	NA	NA	NA	NA	NA
NA	NA	696.5	214.653	NA	NA	NA	NA	NA	NA	NA	NA
NA	NA	696.5	214.958	NA	NA	NA	NA	NA	NA	NA	NA
NA	NA	699.0	215.354	NA	NA	NA	NA	NA	NA	NA	NA
NA	NA	699.0	215.507	NA	NA	NA	NA	NA	NA	NA	NA
NA	NA	701.5	215.751	NA	NA	NA	NA	NA	NA	NA	NA
NA	NA	701.5	215.933	NA	NA	NA	NA	NA	NA	NA	NA
NA	NA	704.0	215.903	NA	NA	NA	NA	NA	NA	NA	NA
NA	NA	706.5	215.872	NA	NA	NA	NA	NA	NA	NA	NA
NA	NA	706.5	215.812	NA	NA	NA	NA	NA	NA	NA	NA
NA	NA	708.9	215.690	NA	NA	NA	NA	NA	NA	NA	NA
NA	NA	711.4	215.568	NA	NA	NA	NA	NA	NA	NA	NA
NA	NA	713.9	215.568	NA	NA	NA	NA	NA	NA	NA	NA
NA	NA	713.9	215.632	NA	NA	NA	NA	NA	NA	NA	NA
NA	NA	713.9	215.601	NA	NA	NA	NA	NA	NA	NA	NA
NA	NA	718.8	215.601	NA	NA	NA	NA	NA	NA	NA	NA
NA	NA	718.8	215.632	NA	NA	NA	NA	NA	NA	NA	NA
NA	NA	721.2	215.662	NA	NA	NA	NA	NA	NA	NA	NA
NA	NA	723.7	215.754	NA	NA	NA	NA	NA	NA	NA	NA
NA	NA	726.0	216.028	NA	NA	NA	NA	NA	NA	NA	NA
NA	NA	726.0	216.180	NA	NA	NA	NA	NA	NA	NA	NA
NA	NA	728.4	216.485	NA	NA	NA	NA	NA	NA	NA	NA
NA	NA	728.4	216.820	NA	NA	NA	NA	NA	NA	NA	NA
NA	NA	730.6	217.369	NA	NA	NA	NA	NA	NA	NA	NA
NA	NA	732.7	217.704	NA	NA	NA	NA	NA	NA	NA	NA
NA	NA	732.7	218.314	NA	NA	NA	NA	NA	NA	NA	NA
NA	NA	734.7	218.893	NA	NA	NA	NA	NA	NA	NA	NA
NA	NA	736.5	219.106	NA	NA	NA	NA	NA	NA	NA	NA
NA	NA	738.2	219.536	NA	NA	NA	NA	NA	NA	NA	NA
NA	NA	738.2	219.871	NA	NA	NA	NA	NA	NA	NA	NA
NA	NA	739.7	220.329	NA	NA	NA	NA	NA	NA	NA	NA
NA	NA	741.0	220.938	NA	NA	NA	NA	NA	NA	NA	NA

Appendix 2—Grain-Size Data from Bed-Sediment Core Samples

Appendix 2. Grain-size data from bed-sediment core samples collected in Lower Granite Reservoir and the Clearwater and Snake Rivers just above their confluence, 2010.

[# , number; cm, centimeter; mm, millimeter; --, not analyzed]

USGS station number	Core identifier	Core sample interval analyzed (cm)	Sample identifier	Date	Percent finer than 16 mm; coarse/medium pebbles	Percent finer than 8 mm; medium/fine pebbles	Percent finer than 4 mm; fine/very fine pebbles	Percent finer than 2 mm; very fine pebbles/very coarse sand	Percent finer than 1 mm; very coarse sand/coarse sand	Percent finer than 0.50 mm; coarse/medium sand
				Clearwater River						
462534117015500	1	0–5	Core #1 0–5	5/14/10	--	--	--	100.0	97.9	94.9
462534117015500	1	9–12	Core #1 9–12	5/14/10	--	--	--	--	99.7	94.2
462537117015600	2	60–63	Core #2 60–63	5/13/10	--	--	--	--	100.0	98.0
462537117015600	2	80–83	Core #2 80–83	5/13/10	--	--	--	100.0	99.9	99.9
462537117015600	2	105–108	Core #2 105–108	5/13/10	--	--	--	--	100.0	99.7
462535117015700	3	2–5	Core #3 2–5	5/14/10	--	--	--	100.0	99.9	98.2
462535117015700	3	28–31	Core #3 28–31	5/14/10	--	--	--	100.0	99.8	98.5
462535117015700	3	62–65	Core #3 62–65	5/14/10	--	--	--	--	--	100.0
462535117015700	3	90–93	Core #3 90–93	5/14/10	--	--	--	--	100.0	99.9
462535117015700	3	114–117	Core #3 114–117	5/14/10	--	--	--	--	--	100.0
462535117015700	3	123–126	Core #3 123–126	5/14/10	--	--	--	--	100.0	99.5
462532117014900	4	22–25	Core #4 22–25	5/13/10	--	--	--	100.0	99.7	94.8
462532117014900	4	44–47	Core #4 44–47	5/13/10	--	--	--	100.0	99.8	94.4
462535117014800	5	0–2	Core #5 0–2	5/14/10	--	--	--	100.0	99.6	97.8
462535117014800	5	4–6	Core #5 4–6	5/14/10	--	--	--	100.0	99.7	96.6
462535117014800	5	20–22	Core #5 20–22	5/14/10	--	--	--	100.0	99.8	96.0
462535117014800	5	43–45	Core #5 43–45	5/14/10	--	--	--	100.0	99.2	96.7
462527117011300	7	0–2	Core #7 0–2	5/18/10	--	100.0	99.5	98.7	98.3	76.4
462532117011101	9	18–21	Core #9 18–21	5/13/10	--	--	--	--	100.0	99.9
462532117011101	9	34–37	Core #9 34–37	5/13/10	--	--	--	--	100.0	99.7
462532117011101	9	50–53	Core #9 50–53	5/13/10	--	--	--	--	--	100.0
462517117010300	10	0–1	Core #10 0–1	5/13/10	--	--	--	100.0	99.7	90.2
462517117010300	10	20–23	Core #10 20–23	5/13/10	--	--	100.0	99.6	98.5	67.8
462517117010300	10	80–83	Core #10 80–83	5/13/10	--	--	--	--	100.0	99.3
462517117010300	10	108–110	Core #10 108–110	5/13/10	--	100.0	99.6	99.3	97.9	47.8
462520117005900	11	0–3	Core #11 0–3	5/18/10	--	--	--	100.0	99.9	81.8
462524117005900	12	0–2	Core #12 0–2	5/13/10	--	--	--	100.0	99.0	91.7
462524117005900	12	29–32	Core #12 29–32	5/13/10	--	--	--	100.0	99.9	91.3
462513117004900	13	0–4	Core #13 0–4	5/18/10	--	--	100.0	99.6	98.5	50.5
462517117004900	14	0–1	Core #14 0–1	5/18/10	--	--	--	100.0	99.6	84.5
462517117004900	14	2–5	Core #14 2–5	5/18/10	--	--	--	100.0	99.8	68.9
462517117004900	14	54–56	Core #14 54–56	5/18/10	--	--	--	100.0	99.9	98.0
462520117004700	15	2–5	Core #15 2–5	5/18/10	--	--	--	--	100.0	87.8
462520117004700	15	17–20	Core #15 17–20	5/18/10	--	--	--	100.0	99.3	80.5
462520117004700	15	22–25	Core #15 22–25	5/18/10	--	--	--	100.0	99.6	91.5

Appendix 2. Grain-size data from bed-sediment core samples collected in Lower Granite Reservoir and the Clearwater and Snake Rivers just above their confluence, 2010.—Continued

[# , number; cm, centimeter; mm, millimeter; --, not analyzed]

Sample identifier	Date	Percent finer than 0.25 mm; medium/fine sand	Percent finer than 0.125 mm; fine/very fine sand	Percent finer than 0.0625 mm; very fine sand/coarse silt	Percent finer than 0.031 mm; coarse/medium silt	Percent finer than 0.016 mm; medium/fine silt	Percent finer than 0.008 mm; fine/very fine silt	Percent finer than 0.004 mm; very fine silt/clay	Percent finer than 0.002 mm; silt/clay for mineral analysis	Percent finer than 0.001 mm; finer than clay
Clearwater River										
Core #1 0–5	5/14/10	62.2	48.2	17.2	16.1	12.8	9.8	7.6	5.8	3.6
Core #1 9–12	5/14/10	16.9	1.4	0.7	--	--	--	--	--	--
Core #2 60–63	5/13/10	40.5	3.4	1.2	--	--	--	--	--	--
Core #2 80–83	5/13/10	99.2	97.8	83.0	55.1	32.3	24.8	19.3	15.5	11.3
Core #2 105–108	5/13/10	93.8	12.6	3.1	--	--	--	--	--	--
Core #3 2–5	5/14/10	48.7	2.3	0.6	--	--	--	--	--	--
Core #3 28–31	5/14/10	62.2	10.7	3.0	--	--	--	--	--	--
Core #3 62–65	5/14/10	99.9	99.5	94.0	70.7	45.7	34.4	27.0	21.5	17.8
Core #3 90–93	5/14/10	95.1	14.7	2.8	--	--	--	--	--	--
Core #3 114–117	5/14/10	99.8	97.5	90.2	72.0	45.8	34.4	25.8	21.1	20.3
Core #3 123–126	5/14/10	97.1	59.5	38.1	29.4	19.6	14.6	11.2	8.4	7.9
Core #4 22–25	5/13/10	8.9	1.2	0.6	--	--	--	--	--	--
Core #4 44–47	5/13/10	20.0	2.9	1.8	--	--	--	--	--	--
Core #5 0–2	5/14/10	75.4	61.4	53.1	49.6	40.6	30.9	23.8	18.7	11.7
Core #5 4–6	5/14/10	27.0	1.5	0.6	--	--	--	--	--	--
Core #5 20–22	5/14/10	25.1	1.6	0.6	--	--	--	--	--	--
Core #5 43–45	5/14/10	48.9	8.3	2.5	--	--	--	--	--	--
Core #7 0–2	5/18/10	23.2	8.5	5.4	5.0	3.8	2.6	1.9	1.4	0.6
Core #9 18–21	5/13/10	98.8	95.7	87.7	66.4	42.5	32.4	25.5	20.5	14.2
Core #9 34–37	5/13/10	72.5	29.0	20.5	16.2	11.4	9.4	7.5	6.0	4.1
Core #9 50–53	5/13/10	99.8	98.7	94.9	78.9	51.3	36.1	26.9	20.9	14.9
Core #10 0–1	5/13/10	60.5	55.4	49.4	45.4	35.7	27.3	21.9	17.5	15.8
Core #10 20–23	5/13/10	9.9	0.9	0.4	--	--	--	--	--	--
Core #10 80–83	5/13/10	98.0	97.2	93.5	78.0	51.1	38.2	28.9	23.8	18.4
Core #10 108–110	5/13/10	10.5	2.9	0.5	--	--	--	--	--	--
Core #11 0–3	5/18/10	12.7	3.8	1.8	--	--	--	--	--	--
Core #12 0–2	5/13/10	37.5	27.4	20.7	18.9	14.3	10.6	8.2	6.3	5.0
Core #12 29–32	5/13/10	13.0	1.7	0.3	--	--	--	--	--	--
Core #13 0–4	5/18/10	15.0	11.1	7.4	6.7	5.0	4.0	3.1	2.5	2.5
Core #14 0–1	5/18/10	50.5	38.7	29.8	28.0	20.8	14.7	10.9	8.6	6.7
Core #14 2–5	5/18/10	5.1	0.8	0.4	--	--	--	--	--	--
Core #14 54–56	5/18/10	83.0	70.9	66.9	62.9	50.2	35.3	26.5	20.4	17.1
Core #15 2–5	5/18/10	11.5	1.1	0.3	--	--	--	--	--	--
Core #15 17–20	5/18/10	8.5	2.1	0.6	--	--	--	--	--	--
Core #15 22–25	5/18/10	12.2	1.8	0.4	--	--	--	--	--	--

Appendix 2. Grain-size data from bed-sediment core samples collected in Lower Granite Reservoir and the Clearwater and Snake Rivers just above their confluence, 2010.—Continued

[# , number; cm, centimeter; mm, millimeter; --, not analyzed]

USGS station number	Core identifier	Core sample interval analyzed (cm)	Sample identifier	Date	Percent finer than 16 mm; coarse/ medium pebbles	Percent finer than 8 mm; medium/fine pebbles	Percent finer than 4 mm; fine/ very fine pebbles	Percent finer than 2 mm; very fine pebbles/ very coarse sand	Percent finer than 1 mm; very coarse sand/ coarse sand	Percent finer than 0.50 mm; coarse/ medium sand
				Clearwater River—Continued						
462520117004700	15	45–48	Core #15 45–48	5/18/10	--	--	--	100.0	98.4	86.8
462520117004700	15	58–61	Core #15 58–61	5/18/10	--	--	--	100.0	99.9	95.7
462511117002800	16	0–3	Core #16 0–3	5/18/10	--	--	--	--	--	--
462512117002500	17	0–3	Core #17 0–3	5/18/10	--	--	--	--	100.0	90.8
462515117002400	18	0–3	Core #18 0–3	5/18/10	--	--	--	100.0	99.9	90.6
				Lower Granite Reservoir						
463914117245400	19	0–5	Core #19 0–5	4/7/10	--	--	--	--	--	--
463914117245400	19	65–70	Core #19 65–70	4/7/10	--	--	--	--	--	--
463914117245400	19	170–175	Core #19 170–175	4/7/10	--	--	--	--	--	--
463921117245200	20	0–10	Core #20 0–10	4/7/10	--	--	--	--	--	--
463921117245200	20	147–157	Core #20 147–157	4/7/10	--	--	--	--	--	--
463921117245200	20	224–229	Core #20 224–229	4/7/10	--	--	--	--	--	--
463930117244800	21	0–10	Core #21 0–10	4/7/10	--	--	--	--	--	--
463930117244800	21	21–27	Core #21 21–27	4/7/10	--	--	--	--	100.0	99.8
463930117244800	21	30–35	Core #21 30–35	4/7/10	--	--	--	100.0	99.7	98.3
463749117232500	22	0–5	Core #22 0–5	4/7/10	--	--	--	--	--	--
463749117232500	22	92–97	Core #22 92–97	4/7/10	--	--	--	--	--	--
463749117232500	22	158–162	Core #22 158–162	4/7/10	--	--	--	--	--	100.0
463748117231500	23	0–5	Core #23 0–5	4/7/10	--	--	--	--	--	--
463748117231500	23	50–55	Core #23 50–55	4/7/10	--	--	--	--	100.0	99.3
463748117231500	23	161–164	Core #23 161–164	4/7/10	--	--	--	100.0	99.7	95.7
463745117225500	24	sample 1	Core #24 sample 1	4/6/10	100.0	92.8	76.8	73.7	69.7	66.7
463745117225500	24	sample 2	Core #24 sample 2	4/6/10	100.0	61.6	36.7	35.6	33.4	31.7
463516117210100	25	0–5	Core #25 0–5	4/7/10	--	--	--	--	--	--
463516117210100	25	20–25	Core #25 20–25	4/7/10	--	--	--	--	--	--
463516117210100	25	41–46	Core #25 41–46	4/7/10	--	--	--	--	--	--
463519117205200	26	0–5	Core #26 0–5	4/7/10	--	--	--	--	--	--
463519117205200	26	60–65	Core #26 60–65	4/7/10	--	--	--	--	--	--
463519117205200	26	120–125	Core #26 120–125	4/7/10	--	--	--	--	--	--
463521117204600	27	0–5	Core #27 0–5	4/7/10	--	--	--	--	--	--
463521117204600	27	90–95	Core #27 90–95	4/7/10	--	--	--	--	--	--
463521117204600	27	150–155	Core #27 150–155	4/7/10	--	--	--	--	--	--
463521117204600	27	239–244	Core #27 239–244	4/7/10	--	--	--	--	--	--
463316117161800	28	15–20	Core #28 15–20	4/6/10	--	--	--	--	--	--
463316117161800	28	55–60	Core #28 55–60	4/6/10	--	--	--	--	--	--
463316117161800	28	98–102	Core #28 98–102	4/6/10	--	--	--	--	--	--

Appendix 2. Grain-size data from bed-sediment core samples collected in Lower Granite Reservoir and the Clearwater and Snake Rivers just above their confluence, 2010.—Continued

[# , number; cm, centimeter; mm, millimeter; --, not analyzed]

Sample identifier	Date	Percent finer than 0.25 mm; medium/fine sand	Percent finer than 0.125 mm; fine/very fine sand	Percent finer than 0.0625 mm; very fine sand/coarse silt	Percent finer than 0.031 mm; coarse/medium silt	Percent finer than 0.016 mm; medium/fine silt	Percent finer than 0.008 mm; fine/very fine silt	Percent finer than 0.004 mm; very fine silt/clay	Percent finer than 0.002 mm; silt/clay for mineral analysis	Percent finer than 0.001 mm; finer than clay
Clearwater River—Continued										
Core #15 45–48	5/18/10	20.8	2.3	1.0	--	--	--	--	--	--
Core #15 58–61	5/18/10	34.0	13.5	10.4	9.6	7.9	6.2	4.9	3.8	3.2
Core #16 0–3	5/18/10	--	--	97.2	93.3	72.3	59.9	45.4	34.7	21.3
Core #17 0–3	5/18/10	66.6	61.7	59.0	56.8	42.0	31.9	24.5	19.7	17.2
Core #18 0–3	5/18/10	18.3	7.9	4.6	--	--	--	--	--	--
Lower Granite Reservoir										
Core #19 0–5	4/7/10	--	--	98.8	96.8	80.1	52.9	33.3	22.9	16.7
Core #19 65–70	4/7/10	--	--	99.9	97.1	82.6	54.9	36.3	26.8	17.1
Core #19 170–175	4/7/10	--	--	99.7	95.6	77.1	44.9	26.0	17.1	14.1
Core #20 0–10	4/7/10	--	--	99.7	97.9	83.5	56.4	33.3	22.5	13.8
Core #20 147–157	4/7/10	--	--	99.8	97.8	85.0	52.5	28.3	17.8	10.9
Core #20 224–229	4/7/10	--	--	99.7	97.0	79.1	51.8	31.7	22.5	14.1
Core #21 0–10	4/7/10	--	--	96.4	88.8	66.7	42.9	27.2	18.9	13.1
Core #21 21–27	4/7/10	98.6	89.6	62.3	51.1	37.2	24.5	16.0	11.8	8.5
Core #21 30–35	4/7/10	92.9	80.2	55.0	46.6	35.6	23.7	16.0	11.5	7.5
Core #22 0–5	4/7/10	--	--	99.1	95.9	78.2	49.7	31.2	22.8	16.0
Core #22 92–97	4/7/10	--	--	99.7	97.0	83.1	57.4	36.8	24.8	17.3
Core #22 158–162	4/7/10	99.9	99.8	99.2	94.9	77.3	50.1	31.2	21.3	13.2
Core #23 0–5	4/7/10	--	--	98.4	92.1	67.2	40.8	27.0	20.1	14.1
Core #23 50–55	4/7/10	97.1	96.8	96.1	90.5	67.1	44.3	30.2	22.5	16.6
Core #23 161–164	4/7/10	83.8	78.4	71.8	62.8	47.6	31.0	20.2	14.3	9.2
Core #24 sample 1	4/6/10	63.5	60.1	55.0	44.6	30.0	19.9	13.4	8.9	5.8
Core #24 sample 2	4/6/10	29.7	27.8	25.2	19.6	12.6	7.8	4.9	3.2	2.1
Core #25 0–5	4/7/10	--	--	97.4	90.2	67.4	39.5	25.1	17.7	11.1
Core #25 20–25	4/7/10	--	--	97.8	91.7	65.0	41.7	28.7	21.4	14.2
Core #25 41–46	4/7/10	--	--	98.5	91.6	69.6	43.2	27.8	19.9	12.3
Core #26 0–5	4/7/10	--	--	97.4	87.9	60.2	36.5	23.6	17.7	15.2
Core #26 60–65	4/7/10	--	--	98.5	89.2	64.5	39.2	27.5	19.6	17.4
Core #26 120–125	4/7/10	--	--	98.5	88.7	63.0	38.9	25.1	19.6	14.1
Core #27 0–5	4/7/10	--	--	98.9	94.1	71.0	43.5	28.9	20.3	10.9
Core #27 90–95	4/7/10	--	--	98.8	90.5	63.9	37.5	24.7	17.1	12.0
Core #27 150–155	4/7/10	--	--	97.3	81.4	52.5	30.3	22.3	14.1	5.4
Core #27 239–244	4/7/10	--	--	99.1	92.1	70.0	43.3	28.5	21.5	17.2
Core #28 15–20	4/6/10	--	--	98.1	86.9	57.3	36.9	26.8	18.7	15.0
Core #28 55–60	4/6/10	--	--	99.0	93.0	64.7	43.3	31.5	25.4	20.7
Core #28 98–102	4/6/10	--	--	94.5	76.9	48.0	29.4	21.5	16.8	12.2

Appendix 2. Grain-size data from bed-sediment core samples collected in Lower Granite Reservoir and the Clearwater and Snake Rivers just above their confluence, 2010.—Continued

[# , number; cm, centimeter; mm, millimeter; --, not analyzed]

USGS station number	Core identifier	Core sample interval analyzed (cm)	Sample identifier	Date	Percent finer than 16 mm; coarse/medium pebbles	Percent finer than 8 mm; medium/fine pebbles	Percent finer than 4 mm; fine/very fine pebbles	Percent finer than 2 mm; very fine pebbles/very coarse sand	Percent finer than 1 mm; very coarse sand/coarse sand	Percent finer than 0.50 mm; coarse/medium sand
Lower Granite Reservoir—Continued										
463318117161600	29	10–15	Core #29 10–15	4/6/10	--	--	--	--	--	--
463318117161600	29	70–75	Core #29 70–75	4/6/10	--	--	--	--	--	--
463318117161600	29	87–91	Core #29 87–91	4/6/10	--	--	--	--	--	--
463322117161000	30B	0–3	Core #30B 0–3	4/6/10	--	--	--	--	--	--
463322117161000	30B	10–12	Core #30B 10–12	4/6/10	--	--	--	--	--	--
463216117150001	31	10–14	Core #31 10–14	4/6/10	--	--	--	--	100.0	99.9
463216117150001	31	115–119	Core #31 115–119	4/6/10	--	--	--	--	--	--
463216117150001	31	157–161	Core #31 157–161	4/6/10	--	--	--	--	--	100.0
463219117145900	32	5–12	Core #32 5–12	4/6/10	--	--	--	--	100.0	99.5
463219117145900	32	30–35	Core #32 30–35	4/6/10	--	--	--	--	--	--
463219117145900	32	60–64	Core #32 60–64	4/6/10	--	--	--	--	100.0	99.9
463221117145700	33	3–7	Core #33 3–7	4/6/10	--	--	--	--	--	100.0
463221117145700	33	14–18	Core #33 14–18	4/6/10	--	--	--	--	--	100.0
462655117123600	34	8–11	Core #34 8–11	4/9/10	--	--	--	--	100.0	99.8
462655117123600	34	66–69	Core #34 66–69	4/9/10	--	--	--	--	100.0	99.9
462655117123600	34	122–125	Core #34 122–125	4/9/10	--	--	--	--	--	100.0
462655117123600	34	144–147	Core #34 144–147	4/9/10	--	--	--	--	--	--
462655117123600	34	173–176	Core #34 173–176	4/9/10	--	--	--	--	--	100.0
462520117122001	38	7–10	Core #38 7–10	5/12/10	--	--	--	--	100.0	99.9
462520117122001	38	12–15	Core #38 12–15	5/12/10	--	--	--	--	--	100.0
462520117122001	38	60–63	Core #38 60–63	5/12/10	--	--	--	--	100.0	99.8
462520117122001	38	98–101	Core #38 98–101	5/12/10	--	--	--	--	100.0	99.9
462520117122001	38	105–108	Core #38 105–108	5/12/10	--	--	--	--	100.0	99.9
462520117122001	38	155–158	Core #38 155–158	5/12/10	--	--	--	--	--	--
462520117122001	38A	6–8	Core #38A 6–8	4/9/10	--	--	--	100.0	99.9	99.8
462520117122001	38A	34–36	Core #38A 34–36	4/9/10	--	--	--	--	100.0	99.7
462520117122001	38A	41–43	Core #38A 41–43	4/9/10	--	--	--	--	100.0	99.9
462522117121800	39	12–15	Core #39 12–15	5/12/10	--	--	--	--	100.0	99.6
462522117121800	39	20–23	Core #39 20–23	5/12/10	--	--	--	--	100.0	99.9
462522117121800	39	87–90	Core #39 87–90	5/12/10	--	--	--	--	100.0	99.7
462522117121800	39	136–139	Core #39 136–139	5/12/10	--	--	--	--	--	100.0
462526117102600	40	67–70	Core #40 67–70	5/12/10	--	--	--	--	--	100.0
462526117102600	40	116–119	Core #40 116–119	5/12/10	--	--	--	--	--	100.0
462526117102600	40	122–125	Core #40 122–125	5/12/10	--	--	--	--	100.0	99.9
462526117102600	40	140–143	Core #40 140–143	5/12/10	--	--	--	--	100.0	99.9

Appendix 2. Grain-size data from bed-sediment core samples collected in Lower Granite Reservoir and the Clearwater and Snake Rivers just above their confluence, 2010.—Continued

[# , number; cm, centimeter; mm, millimeter; --, not analyzed]

Sample identifier	Date	Percent finer than 0.25 mm; medium/ fine sand	Percent finer than 0.125 mm; fine/very fine sand	Percent finer than 0.0625 mm; very fine sand/ coarse silt	Percent finer than 0.031 mm; coarse/ medium silt	Percent finer than 0.016 mm; medium/ fine silt	Percent finer than 0.008 mm; fine/very fine silt	Percent finer than 0.004 mm; very fine silt/clay	Percent finer than 0.002 mm; silt/clay for mineral analysis	Percent finer than 0.001 mm; finer than clay
Lower Granite Reservoir—Continued										
Core #29 10–15	4/6/10	--	--	96.4	87.0	62.4	43.0	29.9	22.1	14.9
Core #29 70–75	4/6/10	--	--	97.6	87.9	64.6	42.3	30.5	23.2	19.4
Core #29 87–91	4/6/10	--	--	93.5	77.6	47.9	29.7	19.8	14.8	11.4
Core #30B 0–3	4/6/10	--	--	93.1	79.0	58.8	39.8	26.9	20.3	18.8
Core #30B 10–12	4/6/10	--	--	92.3	86.8	42.6	46.0	28.6	20.2	17.2
Core #31 10–14	4/6/10	99.8	99.4	85.6	62.1	38.3	26.8	20.5	15.7	14.7
Core #31 115–119	4/6/10	--	--	95.3	82.4	56.8	38.9	27.4	21.3	19.2
Core #31 157–161	4/6/10	99.8	99.0	77.8	63.4	44.4	31.8	23.2	18.7	11.9
Core #32 5–12	4/6/10	99.2	97.3	83.1	69.7	50.9	36.8	26.5	20.2	11.1
Core #32 30–35	4/6/10	--	--	96.4	90.2	70.7	49.8	34.6	25.3	22.4
Core #32 60–64	4/6/10	99.4	96.3	61.6	47.2	31.6	21.9	15.9	12.6	8.8
Core #33 3–7	4/6/10	99.7	94.7	56.3	36.9	22.5	15.5	11.5	8.5	5.3
Core #33 14–18	4/6/10	99.8	98.2	76.9	54.1	32.2	22.2	15.9	12.5	9.0
Core #34 8–11	4/9/10	99.2	90.7	70.2	56.9	40.5	28.9	19.9	14.9	11.3
Core #34 66–69	4/9/10	99.2	83.5	38.5	29.8	22.8	18.9	10.1	10.5	9.9
Core #34 122–125	4/9/10	99.9	96.0	75.6	--	--	--	--	--	--
Core #34 144–147	4/9/10	--	--	92.4	81.7	57.6	42.3	31.9	23.0	18.4
Core #34 173–176	4/9/10	99.9	97.8	85.1	63.9	41.3	28.8	20.6	15.5	9.6
Core #38 7–10	5/12/10	98.9	51.6	37.2	30.1	22.4	17.7	13.6	11.0	10.1
Core #38 12–15	5/12/10	99.7	91.9	84.5	75.3	58.6	48.7	38.2	31.2	26.8
Core #38 60–63	5/12/10	96.1	11.6	1.7	--	--	--	--	--	--
Core #38 98–101	5/12/10	97.4	12.1	1.3	--	--	--	--	--	--
Core #38 105–108	5/12/10	99.6	88.9	79.1	63.8	42.5	31.1	22.9	17.8	11.7
Core #38 155–158	5/12/10	100.0	99.2	96.1	87.7	62.3	42.6	31.8	25.1	17.2
Core #38A 6–8	4/9/10	98.5	60.5	39.5	28.6	19.8	14.5	10.6	7.8	4.9
Core #38A 34–36	4/9/10	99.2	79.1	55.2	37.4	24.2	17.9	13.1	9.4	6.0
Core #38A 41–43	4/9/10	99.7	92.8	86.1	76.1	56.6	40.0	28.2	21.4	15.2
Core #39 12–15	5/12/10	85.9	24.3	4.8	--	--	--	--	--	--
Core #39 20–23	5/12/10	99.5	96.4	58.0	40.9	29.4	24.5	18.6	15.3	13.4
Core #39 87–90	5/12/10	89.2	9.2	2.7	--	--	--	--	--	--
Core #39 136–139	5/12/10	99.9	99.2	90.0	63.3	45.7	35.5	25.4	20.2	16.2
Core #40 67–70	5/12/10	99.4	22.9	1.7	--	--	--	--	--	--
Core #40 116–119	5/12/10	99.9	92.3	86.7	78.0	60.0	44.3	32.8	25.3	21.4
Core #40 122–125	5/12/10	98.4	11.8	3.3	--	--	--	--	--	--
Core #40 140–143	5/12/10	99.7	97.3	75.3	59.3	41.4	30.3	23.3	18.4	14.3

Appendix 2. Grain-size data from bed-sediment core samples collected in Lower Granite Reservoir and the Clearwater and Snake Rivers just above their confluence, 2010.—Continued

[# , number; cm, centimeter; mm, millimeter; --, not analyzed]

USGS station number	Core identifier	Core sample interval analyzed (cm)	Sample identifier	Date	Percent finer than 16 mm; coarse/medium pebbles	Percent finer than 8 mm; medium/fine pebbles	Percent finer than 4 mm; fine/very fine pebbles	Percent finer than 2 mm; very fine pebbles/very coarse sand	Percent finer than 1 mm; very coarse sand/coarse sand	Percent finer than 0.50 mm; coarse/medium sand
				Lower Granite Reservoir—Continued						
462529117102800	41	6–8	Core #41 6–8	5/12/10	--	--	100.0	99.9	99.5	97.2
462540117081100	43	3–5	Core #43 3–5	5/12/10	--	--	--	100.0	99.9	99.7
462540117081100	43	15–18	Core #43 15–18	5/12/10	--	--	--	--	100.0	99.7
462540117081100	43	53–56	Core #43 53–56	5/12/10	--	--	--	--	100.0	100.0
462540117081100	43	120–123	Core #43 120–123	5/12/10	--	--	--	100.0	99.4	99.0
462542117081100	44	0–4	Core #44 0–4	5/12/10	--	--	--	100.0	99.0	96.6
462514117065400	46	50–53	Core #46 50–53	5/13/10	--	--	--	--	100.0	99.9
462514117065400	46	55–58	Core #46 55–58	5/13/10	--	--	--	--	--	100.0
462514117065400	46	80–83	Core #46 80–83	5/13/10	--	--	--	--	100.0	99.8
462514117065400	46	97–100	Core #46 97–100	5/13/10	--	--	--	--	100.0	99.9
462515117065401	47	5–8	Core #47 5–8	5/13/10	--	--	--	--	100.0	96.9
462515117065401	47	51–54	Core #47 51–54	5/13/10	--	--	--	100.0	99.3	98.3
462515117065401	47	109–112	Core #47 109–112	5/13/10	--	--	--	--	100.0	99.8
462520117065300	48	0–2	Core #48 0–2	5/12/10	--	--	--	100.0	99.7	95.7
462456117052900	49	2–5	Core #49 2–5	5/14/10	--	--	--	--	100.0	99.9
462456117052900	49	30–33	Core #49 30–33	5/14/10	--	--	--	--	--	100.0
462456117052900	49	86–89	Core #49 86–89	5/14/10	--	--	--	--	100.0	99.6
462456117052900	49	98–101	Core #49 98–101	5/14/10	--	--	--	--	--	100.0
462456117052900	49	128–131	Core #49 128–131	5/14/10	--	--	--	--	100.0	99.9
462501117052800	50	0–2	Core #50 0–2	5/14/10	--	--	--	--	100.0	99.2
462501117052800	50	20–23	Core #50 20–23	5/14/10	--	--	--	--	100.0	99.6
462501117052800	50	62–65	Core #50 62–65	5/14/10	--	--	--	--	100.0	99.7
462510117053900	52	0–14	Core #52 0–14	5/14/10	--	--	--	--	--	--
462510117053900	52	16–19	Core #52 16–19	5/14/10	--	--	--	--	--	--
462510117053900	52	54–57	Core #52 54–57	5/14/10	--	--	--	--	--	--
462510117053900	52	104–107	Core #52 104–107	5/14/10	--	--	--	--	--	--
462506117050400	53	0–2	Core #53 0–2	5/12/10	--	--	--	100.0	99.9	99.5
462506117050400	53	27–30	Core #53 27–30	5/12/10	--	--	--	--	100.0	99.7
462506117050400	53	63–66	Core #53 63–66	5/12/10	--	--	--	--	100.0	98.3
462509117050300	54	2–5	Core #54 2–5	5/15/10	--	--	--	100.0	99.7	94.7
462509117050300	54	73–75	Core #54 73–75	5/15/10	--	--	--	--	100.0	89.7
462509117050300	54	103–106	Core #54 103–106	5/15/10	--	--	--	100.0	99.6	94.7
462520117042900	56	0–5	Core #56 0–5	5/15/10	--	--	--	--	100.0	99.7
462523117042900	57	0–1	Core #57 0–1	5/15/10	--	--	--	--	100.0	99.7

Appendix 2. Grain-size data from bed-sediment core samples collected in Lower Granite Reservoir and the Clearwater and Snake Rivers just above their confluence, 2010.—Continued

[# , number; cm, centimeter; mm, millimeter; --, not analyzed]

Sample identifier	Date	Percent finer than 0.25 mm; medium/ fine sand	Percent finer than 0.125 mm; fine/very fine sand	Percent finer than 0.0625 mm; very fine sand/ coarse silt	Percent finer than 0.031 mm; coarse/ medium silt	Percent finer than 0.016 mm; medium/ fine silt	Percent finer than 0.008 mm; fine/very fine silt	Percent finer than 0.004 mm; very fine silt/clay	Percent finer than 0.002 mm; silt/clay for mineral analysis	Percent finer than 0.001 mm; finer than clay
Lower Granite Reservoir—Continued										
Core #41 6–8	5/12/10	51.8	2.4	0.7	--	--	--	--	--	--
Core #43 3–5	5/12/10	99.4	97.6	93.6	88.3	70.5	57.5	46.6	37.8	23.9
Core #43 15–18	5/12/10	82.6	4.7	1.0	--	--	--	--	--	--
Core #43 53–56	5/12/10	99.7	96.9	73.3	53.6	34.9	25.6	20.1	16.3	14.4
Core #43 120–123	5/12/10	93.9	60.1	46.4	39.8	32.2	25.5	20.5	16.8	14.9
Core #44 0–4	5/12/10	22.6	3.0	1.1	--	--	--	--	--	--
Core #46 50–53	5/13/10	97.2	16.6	6.0	--	--	--	--	--	--
Core #46 55–58	5/13/10	99.5	83.8	72.0	59.8	43.1	31.8	24.1	18.9	16.2
Core #46 80–83	5/13/10	98.4	46.8	32.2	28.6	23.0	18.6	14.4	11.5	8.2
Core #46 97–100	5/13/10	96.4	11.1	1.7	--	--	--	--	--	--
Core #47 5–8	5/13/10	88.9	12.2	3.6	--	--	--	--	--	--
Core #47 51–54	5/13/10	93.2	13.8	2.3	--	--	--	--	--	--
Core #47 109–112	5/13/10	81.4	9.2	1.7	--	--	--	--	--	--
Core #48 0–2	5/12/10	13.6	1.8	0.6	--	--	--	--	--	--
Core #49 2–5	5/14/10	98.2	7.1	0.8	--	--	--	--	--	--
Core #49 30–33	5/14/10	99.8	99.0	88.1	67.5	45.5	31.5	24.7	19.7	17.9
Core #49 86–89	5/14/10	98.7	80.0	22.4	14.2	10.3	8.0	5.9	4.8	3.4
Core #49 98–101	5/14/10	99.8	96.5	89.9	79.9	60.0	41.6	29.4	21.9	18.8
Core #49 128–131	5/14/10	99.2	60.1	12.6	--	--	--	--	--	--
Core #50 0–2	5/14/10	69.5	36.8	27.7	25.0	21.4	17.8	14.3	11.3	10.0
Core #50 20–23	5/14/10	46.1	1.4	0.4	--	--	--	--	--	--
Core #50 62–65	5/14/10	37.7	2.0	0.6	--	--	--	--	--	--
Core #52 0–14	5/14/10	--	--	96.5	81.8	55.9	39.2	28.6	21.1	15.8
Core #52 16–19	5/14/10	--	--	96.7	81.2	54.4	42.0	32.9	27.2	19.2
Core #52 54–57	5/14/10	--	--	96.5	78.2	55.7	40.9	32.0	26.8	16.8
Core #52 104–107	5/14/10	--	--	98.2	85.0	59.3	41.9	32.2	25.8	19.6
Core #53 0–2	5/12/10	84.8	52.4	39.1	33.6	26.2	20.4	15.9	12.2	7.0
Core #53 27–30	5/12/10	67.8	2.5	0.5	--	--	--	--	--	--
Core #53 63–66	5/12/10	49.0	5.7	2.8	--	--	--	--	--	--
Core #54 2–5	5/15/10	10.0	0.8	0.2	--	--	--	--	--	--
Core #54 73–75	5/15/10	29.5	23.3	16.3	14.4	12.0	9.4	7.5	6.1	3.8
Core #54 103–106	5/15/10	29.7	25.8	20.7	15.8	10.5	7.7	6.0	4.8	3.6
Core #56 0–5	5/15/10	78.7	42.4	34.0	32.7	26.5	20.7	15.9	12.1	7.1
Core #57 0–1	5/15/10	15.0	0.8	0.3	--	--	--	--	--	--

Appendix 2. Grain-size data from bed-sediment core samples collected in Lower Granite Reservoir and the Clearwater and Snake Rivers just above their confluence, 2010.—Continued

[# , number; cm, centimeter; mm, millimeter; --, not analyzed]

USGS station number	Core identifier	Core sample interval analyzed (cm)	Sample identifier	Date	Percent finer than 16 mm; coarse/medium pebbles	Percent finer than 8 mm; medium/fine pebbles	Percent finer than 4 mm; fine/very fine pebbles	Percent finer than 2 mm; very fine pebbles/very coarse sand	Percent finer than 1 mm; very coarse sand/coarse sand	Percent finer than 0.50 mm; coarse/medium sand
				Lower Granite Reservoir—Continued						
462540117033500	59	0–3	Core #59 0–3	5/15/10	--	--	--	--	100.0	99.7
462542117033601	60	0–2	Core #60 0–2	5/15/10	--	--	--	--	100.0	93.3
462542117033601	60	6–9	Core #60 6–9	5/15/10	--	--	--	100.0	99.9	99.1
462542117033601	60	50–53	Core #60 50–53	5/15/10	--	--	--	100.0	99.9	99.3
462541117030300	62	84–87	Core #62 84–87	5/12/10	--	--	--	100.0	99.9	99.6
462541117030300	62	94–97	Core #62 94–97	5/12/10	--	--	--	100.0	99.9	99.2
462546117030500	63	0–2	Core #63 0–2	5/20/10	--	--	--	100.0	98.3	92.3
462546117030500	63	10–13	Core #63 10–13	5/20/10	--	--	--	100.0	99.7	83.7
462536117023500	65	60–63	Core #65 60–63	5/11/10	--	--	--	--	100.0	99.2
462536117023500	65	65–68	Core #65 65–68	5/11/10	--	--	--	--	100.0	99.4
462536117023500	65	85–88	Core #65 85–88	5/11/10	--	--	--	--	100.0	98.3
462542117024801	66	0–1	Core #66 0–1	5/20/10	--	--	--	--	100.0	99.7
462542117024801	66	10–13	Core #66 10–13	5/20/10	--	--	--	100.0	99.9	97.7
				Confluence						
462535117020701	70	0–2	Core #70 0–2	5/14/10	--	--	--	--	100.0	99.4
462535117020701	70	4–7	Core #70 4–7	5/14/10	--	--	--	100.0	99.9	97.3
462535117020701	70	26–28	Core #70 26–28	5/14/10	--	--	--	--	100.0	98.7
462535117020701	70	35–36	Core #70 35–36	5/14/10	--	--	--	--	100.0	98.4
462535117020701	70	38–41	Core #70 38–41	5/14/10	--	--	--	100.0	99.8	98.9
462535117020701	70	50–52	Core #70 50–52	5/14/10	--	--	100.0	99.5	98.9	96.0
462537117020500	71	2–5	Core #71 2–5	5/14/10	--	--	--	100.0	99.9	99.3
462537117020500	71	43–46	Core #71 43–46	5/14/10	--	--	--	--	100.0	99.8
462537117020500	71	90–93	Core #71 90–93	5/14/10	--	--	--	--	--	--
462537117020500	71	135–137	Core #71 135–137	5/14/10	--	--	--	--	100.0	99.4
462537117020500	71	144–146	Core #71 144–146	5/14/10	--	--	100.0	99.3	99.1	98.7
				Snake River						
462522117021500	72	0–0.5	Core #72 0–0.5	5/19/10	--	--	--	100.0	99.7	97.6
462522117021501	73	0–2	Core #73 0–2	5/19/10	--	--	--	--	100.0	98.4
462440117021300	78	0–0.5	Core #78 0–0.5	5/19/10	--	--	--	--	100.0	99.7
462437117020601	80	0–1	Core #80 0–1	5/19/10	--	--	--	--	100.0	98.3
462426117021901	81	0–3	Core #81 0–3	5/19/10	--	--	--	100.0	99.2	96.3
462426117021600	82	0–3	Core #82 0–3	10/13/10	--	100.0	99.8	99.7	99.2	81.5
462413117022100	84	5–15	Core #84 5–15	10/13/10	--	--	--	100.0	99.9	90.6
462413117022100	84	25–35	Core #84 25–35	10/13/10	--	100.0	99.8	99.7	99.4	89.5

Appendix 2. Grain-size data from bed-sediment core samples collected in Lower Granite Reservoir and the Clearwater and Snake Rivers just above their confluence, 2010.—Continued

[# , number; cm, centimeter; mm, millimeter; --, not analyzed]

Sample identifier	Date	Percent finer than 0.25 mm; medium/ fine sand	Percent finer than 0.125 mm; fine/very fine sand	Percent finer than 0.0625 mm; very fine sand/ coarse silt	Percent finer than 0.031 mm; coarse/ medium silt	Percent finer than 0.016 mm; medium/ fine silt	Percent finer than 0.008 mm; fine/very fine silt	Percent finer than 0.004 mm; very fine silt/clay	Percent finer than 0.002 mm; silt/clay for mineral analysis	Percent finer than 0.001 mm; finer than clay
Lower Granite Reservoir—Continued										
Core #59 0–3	5/15/10	55.4	18.1	3.9	2.9	2.2	1.8	1.5	1.2	0.9
Core #60 0–2	5/15/10	80.4	67.0	36.7	33.0	27.1	22.2	18.4	15.5	10.9
Core #60 6–9	5/15/10	22.8	2.3	0.3	--	--	--	--	--	--
Core #60 50–53	5/15/10	23.2	1.5	0.4	--	--	--	--	--	--
Core #62 84–87	5/12/10	50.6	2.3	0.3	--	--	--	--	--	--
Core #62 94–97	5/12/10	74.0	3.5	1.0	--	--	--	--	--	--
Core #63 0–2	5/20/10	26.0	7.6	2.8	--	--	--	--	--	--
Core #63 10–13	5/20/10	5.9	0.7	0.1	--	--	--	--	--	--
Core #65 60–63	5/11/10	26.0	1.1	0.3	--	--	--	--	--	--
Core #65 65–68	5/11/10	43.6	1.6	0.3	--	--	--	--	--	--
Core #65 85–88	5/11/10	14.2	1.1	0.4	--	--	--	--	--	--
Core #66 0–1	5/20/10	96.7	90.8	71.7	58.4	44.6	34.8	28.0	24.2	21.7
Core #66 10–13	5/20/10	14.0	2.0	0.4	--	--	--	--	--	--
Confluence										
Core #70 0–2	5/14/10	84.5	66.7	58.1	52.0	41.5	33.4	27.4	23.2	21.4
Core #70 4–7	5/14/10	44.1	3.6	1.0	--	--	--	--	--	--
Core #70 26–28	5/14/10	59.6	3.4	0.9	--	--	--	--	--	--
Core #70 35–36	5/14/10	74.7	31.9	28.1	26.5	23.6	20.0	16.5	14.0	12.8
Core #70 38–41	5/14/10	77.2	6.6	2.2	--	--	--	--	--	--
Core #70 50–52	5/14/10	45.0	6.8	2.6	--	--	--	--	--	--
Core #71 2–5	5/14/10	69.9	3.8	1.2	--	--	--	--	--	--
Core #71 43–46	5/14/10	98.1	89.6	81.6	67.1	45.7	34.6	28.0	23.8	19.6
Core #71 90–93	5/14/10	--	--	95.1	76.0	49.1	36.9	29.9	25.2	20.5
Core #71 135–137	5/14/10	94.3	20.0	5.2	4.6	3.7	2.4	1.6	1.3	0.9
Core #71 144–146	5/14/10	97.9	93.5	71.1	52.9	36.2	27.9	21.8	17.4	14.2
Snake River										
Core #72 0–0.5	5/19/10	16.2	1.0	0.1	--	--	--	--	--	--
Core #73 0–2	5/19/10	26.8	3.6	0.3	--	--	--	--	--	--
Core #78 0–0.5	5/19/10	48.3	3.1	0.2	--	--	--	--	--	--
Core #80 0–1	5/19/10	41.9	6.3	0.8	--	--	--	--	--	--
Core #81 0–3	5/19/10	26.5	1.5	0.2	--	--	--	--	--	--
Core #82 0–3	10/13/10	8.6	0.8	0.3	--	--	--	--	--	--
Core #84 5–15	10/13/10	8.5	1.0	0.4	--	--	--	--	--	--
Core #84 25–35	10/13/10	7.9	0.6	0.3	--	--	--	--	--	--

Appendix 2. Grain-size data from bed-sediment core samples collected in Lower Granite Reservoir and the Clearwater and Snake Rivers just above their confluence, 2010.—Continued

[# , number; cm, centimeter; mm, millimeter; --, not analyzed]

USGS station number	Core identifier	Core sample interval analyzed (cm)	Sample identifier	Date	Percent finer than 16 mm; coarse/medium pebbles	Percent finer than 8 mm; medium/fine pebbles	Percent finer than 4 mm; fine/very fine pebbles	Percent finer than 2 mm; very fine pebbles/very coarse sand	Percent finer than 1 mm; very coarse sand/coarse sand	Percent finer than 0.50 mm; coarse/medium sand
Snake River—Continued										
462413117022100	84	45–55	Core #84 45–55	10/13/10	--	--	--	100.0	99.7	91.2
462413117022100	84	65–75	Core #84 65–75	10/13/10	--	--	100.0	99.6	96.8	70.0
462413117022100	84	85–95	Core #84 85–95	10/13/10	--	--	--	100.0	99.9	90.0
462413117021900	85	5–15	Core #85 5–15	10/13/10	--	--	--	100.0	99.6	82.6
462413117021900	85	25–35	Core #85 25–35	10/13/10	--	100.0	99.9	99.5	83.1	6.2
462413117021900	85	45–55	Core #85 45–55	10/13/10	--	--	--	100.0	98.3	67.2
462413117021900	85	55–65	Core #85 55–65	10/13/10	--	--	100.0	99.7	98.8	79.3
462348117022801	87	0–19	Core #87 0–19	5/19/10	--	--	--	100.0	97.9	75.1
462348117022801	87	16–20	Core #87 16–20	10/13/10	--	100.0	99.8	99.8	99.8	96.3
462348117022801	87	50–55	Core #87 50–55	10/13/10	--	--	--	100.0	99.6	94.0
462348117022801	87	68–72	Core #87 68–72	10/13/10	--	--	--	--	--	--
462348117022801	87	77–82	Core #87 77–82	10/13/10	--	--	--	--	100.0	99.5
462352117022101	88	0–3	Core #88 0–3	5/19/10	--	--	--	100.0	99.9	97.8
462348117021701	89	0–3	Core #89 0–3	5/19/10	--	--	--	100.0	99.9	99.0

Appendix 2. Grain-size data from bed-sediment core samples collected in Lower Granite Reservoir and the Clearwater and Snake Rivers just above their confluence, 2010.—Continued

[# , number; cm, centimeter; mm, millimeter; --, not analyzed]

Sample identifier	Date	Percent finer than 0.25 mm; medium/ fine sand	Percent finer than 0.125 mm; fine/very fine sand	Percent finer than 0.0625 mm; very fine sand/ coarse silt	Percent finer than 0.031 mm; coarse/ medium silt	Percent finer than 0.016 mm; medium/ fine silt	Percent finer than 0.008 mm; fine/very fine silt	Percent finer than 0.004 mm; very fine silt/clay	Percent finer than 0.002 mm; silt/clay for mineral analysis	Percent finer than 0.001 mm; finer than clay
				Snake River—Continued						
Core #84 45–55	10/13/10	6.8	0.7	0.3	--	--	--	--	--	--
Core #84 65–75	10/13/10	4.0	0.7	0.4	--	--	--	--	--	--
Core #84 85–95	10/13/10	5.9	0.7	0.3	--	--	--	--	--	--
Core #85 5–15	10/13/10	2.8	0.3	0.2	--	--	--	--	--	--
Core #85 25–35	10/13/10	0.7	0.2	0.2	--	--	--	--	--	--
Core #85 45–55	10/13/10	1.7	0.3	0.2	--	--	--	--	--	--
Core #85 55–65	10/13/10	6.2	0.8	0.2	--	--	--	--	--	--
Core #87 0–19	5/19/10	13.4	4.3	0.6	--	--	--	--	--	--
Core #87 16–20	10/13/10	17.3	0.8	0.2	--	--	--	--	--	--
Core #87 50–55	10/13/10	53.5	40.5	35.4	32.5	24.4	16.9	12.3	9.8	8.1
Core #87 68–72	10/13/10	--	100.0	94.0	85.0	62.2	43.5	32.3	25.5	17.7
Core #87 77–82	10/13/10	91.2	52.4	21.7	18.4	14.8	12.6	10.7	9.0	7.6
Core #88 0–3	5/19/10	73.7	7.9	0.5	--	--	--	--	--	--
Core #89 0–3	5/19/10	57.8	13.6	1.1	--	--	--	--	--	--

Appendix 3—Analytical Data for Major and Trace Elements in Bed-Sediment Core Samples

Appendix 3. Analytical data for major and trace elements in bed-sediment core samples collected in Lower Granite Reservoir and the Clearwater and Snake Rivers just above their confluence, 2010.

[Concentrations in micrograms per gram unless otherwise noted; #, number; <, less than lower reporting limit]

USGS station number	Sample identifier	Date	Set number	Calcium	Magnesium	Potassium	Sodium	Total carbon (percent)	Inorganic carbon (percent)	Phosphorus	Aluminum
					Clearwater River						
462532117011101	Core #9 18–21	5/13/2010	11150	21,800	10,600	13,300	16,100	1.92	0.02	950	80,400
462532117011101	Core #9 34–37	5/13/2010	11150	24,200	10,700	15,100	20,600	1.02	0.01	818	74,500
462532117011101	Core #9 50–53	5/13/2010	11150	20,200	9,920	13,400	15,600	2.84	0.01	956	80,100
					Lower Granite Reservoir						
463216117150001	Core #31 0–3	4/6/2010	11150	22,400	10,200	16,500	15,700	6.02	0.04	1,090	67,900
463216117150001	Core #31 14–17	4/6/2010	11150	22,600	10,700	19,700	18,900	3.76	0.03	1,020	73,900
463216117150001	Core #31 28–31	4/6/2010	11150	21,400	11,100	19,000	14,400	6.55	0.06	1,230	74,200
463216117150001	Core #31 42–45	4/6/2010	11150	22,900	11,300	16,300	13,700	7.62	0.05	1,320	68,300
463216117150001	Core #31 56–59	4/6/2010	11150	23,700	11,700	14,600	13,700	7.90	0.06	1,420	66,300
463216117150001	Core #31 70–73	4/6/2010	11150	22,800	11,900	18,900	16,000	5.07	0.05	1,060	69,300
463216117150001	Core #31 84–87	4/6/2010	11150	24,100	12,300	18,000	14,900	6.82	0.09	1,260	70,700
463216117150001	Core #31 98–101	4/6/2010	11150	25,700	12,000	17,900	18,200	4.44	0.04	1,060	72,300
463216117150001	Core #31 112–115	4/6/2010	11150	22,900	11,500	17,100	15,900	5.00	0.04	1,120	70,700
463216117150001	Core #31 126–129	4/6/2010	11150	25,300	12,600	16,900	16,300	4.88	0.05	1,180	72,500
463216117150001	Core #31 140–143	4/6/2010	11150	22,600	11,400	16,400	14,100	6.28	0.05	1,250	70,500
463216117150001	Core #31 154–157	4/6/2010	11150	25,400	11,400	16,500	17,100	4.15	0.03	1,090	72,400
463216117150001	Core #31 164–167	4/6/2010	11150	27,800	12,700	16,600	18,800	2.78	0.04	1,020	74,800
462520117122001	Core #38 7–10	5/12/2010	11150	26,200	10,700	18,500	20,100	2.04	0.01	864	70,400
462520117122001	Core #38 12–15	5/12/2010	11150	22,600	10,200	13,800	13,600	6.11	0.04	1,340	64,900
462520117122001	Core #38 60–63	5/12/2010	11150	21,900	10,600	20,100	23,500	0.22	0.01	611	74,300
462520117122001	Core #38 98–101	5/12/2010	11150	25,000	11,300	19,500	24,100	0.17	0.02	722	76,200
462520117122001	Core #38 105–108	5/12/2010	11150	30,500	12,300	12,800	17,100	3.29	0.07	1,070	72,900
462520117122001	Core #38 155–158	5/12/2010	11150	25,900	11,000	12,300	14,700	3.65	0.07	1,180	71,700
462515117065401	Core #47 5–8	5/13/2010	11150	18,900	8,340	22,500	22,600	4.43	0.02	561	72,100
462515117065401	Core #47 51–54	5/13/2010	11150	18,900	9,030	23,000	24,500	0.94	0.02	529	78,200
462515117065401	Core #47 109–112	5/13/2010	11150	22,600	9,880	19,900	24,800	0.16	0.01	602	74,600
462542117033601	Core #60 0–2	5/15/2010	11150	18,600	7,280	13,400	11,400	17.10	0.06	831	45,500
462542117033601	Core #60 6–9	5/15/2010	11150	18,600	6,120	23,300	22,900	0.12	<0.01	432	66,400
462542117033601	Core #60 50–53	5/15/2010	11150	26,300	9,640	18,900	21,900	0.12	0.01	521	65,600
462542117024801	Core #66 10–13	5/20/2010	11150	19,600	6,540	21,300	22,400	0.14	<0.01	413	64,900

Appendix 3. Analytical data for major and trace elements in bed-sediment core samples collected in Lower Granite Reservoir and the Clearwater and Snake Rivers just above their confluence, 2010.—Continued

[Concentrations in micrograms per gram unless otherwise noted; #, number; <, less than lower reporting limit]

USGS station number	Sample identifier	Date	Set number	Calcium	Magne-sium	Potas-sium	Sodium	Total carbon (percent)	Inorganic carbon (percent)	Phos-phorus	Alumi-num
Confluence											
462535117020701	Core #70 0–2	5/14/2010	11150	17,400	8,470	14,900	15,900	5.69	0.03	1,040	71,300
462535117020701	Core #70 4–7	5/14/2010	11150	18,900	6,810	20,400	23,700	0.21	<0.01	420	71,700
462535117020701	Core #70 26–28	5/14/2010	11150	21,400	8,260	19,300	23,400	0.18	<0.01	474	73,200
462535117020701	Core #70 35–36	5/14/2010	11150	17,300	8,270	13,700	14,900	5.64	0.04	1,080	68,600
462535117020701	Core #70 38–41	5/14/2010	11150	22,200	8,960	19,200	23,900	0.42	<0.01	544	76,900
462535117020701	Core #70 50–52	5/14/2010	11150	19,100	8,130	20,000	22,900	0.74	<0.01	514	75,600
Snake River											
462522117021501	Core #73 0–2	5/19/2010	11150	19,500	7,410	20,700	23,500	0.14	<0.01	440	69,000
462437117020601	Core #80 0–1	5/19/2010	11150	20,500	8,720	20,800	23,700	0.26	0.01	529	70,500
462426117021901	Core #81 0–3	5/19/2010	11150	17,500	6,840	23,200	23,000	0.13	<0.01	384	70,700
462413117022101	Core #84 5–15	10/13/2010	11637	20,200	7,600	19,300	21,000	0.11	<0.01	471	61,200
462413117022101	Core #84 25–35	10/13/2010	11637	18,700	7,140	18,600	20,100	0.11	<0.01	468	59,300
462413117022101	Core #84 45–55	10/13/2010	11637	19,400	7,060	21,000	22,100	0.10	<0.01	453	65,500
462413117022101	Core #84 65–75	10/13/2010	11637	15,000	6,690	21,900	19,500	0.12	0.01	400	60,300
462413117022101	Core #84 85–95	10/13/2010	11637	15,900	5,890	19,500	19,600	0.11	0.01	402	57,700
462412117021801	Core #85 5–15	10/13/2010	11637	17,500	6,120	19,900	20,000	0.17	0.01	397	58,200
462412117021801	Core #85 25–35	10/13/2010	11637	18,300	6,740	18,000	19,400	0.12	<0.01	438	56,400
462412117021801	Core #85 45–55	10/13/2010	11637	21,800	8,770	18,600	20,500	0.12	<0.01	506	61,300
462412117021801	Core #85 55–65	10/13/2010	11637	19,300	7,180	18,600	20,000	0.11	<0.01	477	58,800
462348117022801	Core #87 0–19	5/19/2010	11150	18,500	7,330	19,400	21,400	0.59	0.01	472	63,700
462352117022101	Core #88 0–3	5/19/2010	11150	19,400	7,770	23,500	24,600	0.16	0.01	520	75,200
462348117021701	Core #89 0–3	5/19/2010	11150	19,200	7,640	23,900	24,000	0.17	0.01	499	72,800

Appendix 3. Analytical data for major and trace elements in bed-sediment core samples collected in Lower Granite Reservoir and the Clearwater and Snake Rivers just above their confluence, 2010.—Continued

[Concentrations in micrograms per gram unless otherwise noted; #, number; <, less than lower reporting limit]

Sample identifier	Date	Barium	Beryllium	Bismuth	Cadmium	Cerium	Cesium	Chromium	Cobalt	Copper	Gallium	Iron
						Clearwater River						
Core #9 18–21	5/13/2010	684	1.7	5.48	0.18	64.4	2.7	46.7	25.2	33.5	20.0	54,000
Core #9 34–37	5/13/2010	735	1.2	4.78	0.12	48.0	1.8	35.4	17.4	740	17.3	40,600
Core #9 50–53	5/13/2010	676	1.5	5.63	0.21	67.3	3.1	44.8	23.3	38.2	19.9	52,800
						Lower Granite Reservoir						
Core #31 0–3	4/6/2010	673	1.8	6.70	0.34	60.9	4.2	42.1	18.1	33.1	19.4	40,900
Core #31 14–17	4/6/2010	765	2.0	6.80	0.29	68.2	4.1	48.7	17.3	30.2	20.1	38,400
Core #31 28–31	4/6/2010	689	2.6	9.61	0.41	91.1	6.8	46.4	23.7	46.9	22.5	43,500
Core #31 42–45	4/6/2010	664	2.1	8.50	0.46	75.4	5.2	49.1	22.2	43.4	21.0	44,500
Core #31 56–59	4/6/2010	644	2.1	7.70	0.42	71.1	4.6	44.9	23.2	46.1	19.9	47,100
Core #31 70–73	4/6/2010	775	2.1	14.3	0.37	76.8	5.3	52.9	18.9	38.6	20.6	40,800
Core #31 84–87	4/6/2010	684	2.2	9.01	0.45	83.3	5.6	53.6	21.4	44.5	21.2	44,900
Core #31 98–101	4/6/2010	714	1.7	6.49	0.32	65.5	4.3	52.9	21.2	36.7	19.8	42,000
Core #31 112–115	4/6/2010	667	1.8	7.08	0.41	69.9	4.7	51.8	19.6	39.9	20.1	42,300
Core #31 126–129	4/6/2010	688	1.9	7.38	0.37	65.7	4.6	54.1	22.8	44.8	20.8	45,600
Core #31 140–143	4/6/2010	655	2.2	8.81	0.42	74.3	5.4	51.0	22.8	44.6	20.7	44,400
Core #31 154–157	4/6/2010	697	1.7	6.64	0.36	59.2	3.9	51.7	22.4	36.2	19.7	42,900
Core #31 164–167	4/6/2010	723	1.5	5.90	0.27	58.1	3.2	52.4	20.9	36.7	19.8	45,000
Core #38 7–10	5/12/2010	762	1.6	5.21	0.19	60.3	2.7	48.1	16.9	24.5	18.7	37,400
Core #38 12–15	5/12/2010	619	1.8	6.41	0.34	56.4	4.0	44.9	20.0	35.0	18.5	41,800
Core #38 60–63	5/12/2010	822	1.6	4.62	0.10	46.8	2.2	43.8	15.7	18.5	17.3	32,400
Core #38 98–101	5/12/2010	804	1.7	4.56	0.11	56.6	2.1	49.0	16.3	18.2	17.7	33,400
Core #38 105–108	5/12/2010	674	1.4	4.66	0.24	52.9	2.5	38.5	27.6	42.5	20.1	63,400
Core #38 155–158	5/12/2010	679	1.4	5.10	0.25	63.7	2.8	42.4	26.4	39.2	20.3	58,600
Core #47 5–8	5/13/2010	868	2.0	5.02	0.17	41.2	2.7	34.3	12.8	17.1	17.2	26,800
Core #47 51–54	5/13/2010	869	1.7	4.82	0.09	43.2	2.8	35.7	12.1	17.0	17.6	26,800
Core #47 109–112	5/13/2010	824	1.6	4.51	0.09	39.6	2.0	40.6	13.5	16.0	16.9	29,500
Core #60 0–2	5/15/2010	547	1.7	5.07	0.32	43.1	2.9	31.6	13.6	41.2	13.3	27,200
Core #60 6–9	5/15/2010	886	1.5	4.57	0.06	31.7	1.9	27.2	9.9	13.0	15.8	19,900
Core #60 50–53	5/15/2010	771	1.3	4.17	0.09	62.0	1.5	56.4	13.6	16.7	16.5	34,000
Core #66 10–13	5/20/2010	838	1.4	4.38	0.06	38.5	1.6	28.0	10.0	13.4	15.5	21,200

Appendix 3. Analytical data for major and trace elements in bed-sediment core samples collected in Lower Granite Reservoir and the Clearwater and Snake Rivers just above their confluence, 2010.—Continued

[Concentrations in micrograms per gram unless otherwise noted; #, number; <, less than lower reporting limit]

Sample identifier	Date	Barium	Beryl-lium	Bis-muth	Cad-mium	Cerium	Cesium	Chro-mium	Cobalt	Copper	Gallium	Iron
Confluence												
Core #70 0–2	5/14/2010	700	1.5	5.60	0.18	48.5	2.9	40.4	14.6	39.6	17.4	37,800
Core #70 4–7	5/14/2010	891	1.3	5.08	0.06	36.7	1.5	23.3	8.7	10.7	15.8	22,400
Core #70 26–28	5/14/2010	853	1.4	4.94	0.06	43.4	1.5	28.8	9.9	12.3	16.4	27,100
Core #70 35–36	5/14/2010	666	1.5	5.27	0.20	50.7	2.4	41.9	16.5	27.4	17.0	36,500
Core #70 38–41	5/14/2010	848	1.4	5.05	0.07	37.3	1.7	32.4	11.8	12.9	17.1	30,100
Core #70 50–52	5/14/2010	886	1.4	4.96	0.08	32.7	1.8	26.5	12.2	33.8	16.7	29,800
Snake River												
Core #73 0–2	5/19/2010	839	1.6	4.24	0.07	36.3	1.7	31.9	9.5	11.4	15.3	21,300
Core #80 0–1	5/19/2010	828	1.4	4.38	0.09	55.6	1.8	39.9	11.1	12.4	16.2	25,400
Core #81 0–3	5/19/2010	920	1.6	4.64	0.07	51.7	2.0	35.1	11.1	12.6	16.5	27,200
Core #84 5–15	10/13/2010	943	1.5	4.11	0.08	30.9	1.6	28.7	11.1	14.8	15.2	24,300
Core #84 25–35	10/13/2010	910	1.6	4.34	0.06	32.3	1.6	27.1	10.3	15.4	14.5	23,100
Core #84 45–55	10/13/2010	1,040	1.8	4.50	0.07	29.4	1.9	24.6	10.8	14.4	16.0	22,600
Core #84 65–75	10/13/2010	1,040	1.8	10.4	0.02	34.7	2.5	22.9	11.1	18.9	16.3	22,300
Core #84 85–95	10/13/2010	1,000	1.7	4.38	0.06	30.1	1.9	20.3	9.7	74.6	14.5	19,500
Core #85 5–15	10/13/2010	936	1.3	5.06	0.07	31.2	1.7	23.1	9.2	12.4	14.4	20,000
Core #85 25–35	10/13/2010	855	1.4	4.03	0.06	39.2	1.6	20.1	10.0	13.2	13.9	22,700
Core #85 45–55	10/13/2010	923	1.5	4.40	0.09	31.0	1.6	31.0	12.3	17.2	15.2	27,500
Core #85 55–65	10/13/2010	886	1.5	4.02	0.07	35.4	1.6	25.0	10.4	14.9	14.6	23,900
Core #87 0–19	5/19/2010	776	1.3	4.08	0.07	34.8	1.6	26.6	10.8	17.7	14.7	24,000
Core #88 0–3	5/19/2010	879	1.8	4.80	0.08	56.2	2.3	36.2	10.4	12.7	17.4	25,100
Core #89 0–3	5/19/2010	883	1.6	4.81	0.08	43.5	2.3	35.7	10.4	12.4	17.1	24,500

Appendix 3. Analytical data for major and trace elements in bed-sediment core samples collected in Lower Granite Reservoir and the Clearwater and Snake Rivers just above their confluence, 2010.—Continued

[Concentrations in micrograms per gram unless otherwise noted; #, number; <, less than lower reporting limit]

Sample identifier	Date	Lanthanum	Lead	Lithium	Manganese	Mercury	Molybdenum	Nickel	Niobium	Rubidium	Scandium
Clearwater River											
Core #9 18–21	5/13/2010	31.8	14.5	20.7	970	0.03	0.76	23.4	13	62.9	20.2
Core #9 34–37	5/13/2010	24.5	12.5	14.8	746	0.02	0.55	17.0	10	56.1	15.1
Core #9 50–53	5/13/2010	33.3	14.6	22.2	998	0.03	0.80	22.1	13	65.7	19.9
Lower Granite Reservoir											
Core #31 0–3	4/6/2010	32.8	17.5	26.8	817	0.08	1.2	20.2	14	80.0	15.3
Core #31 14–17	4/6/2010	36.2	17.4	25.4	735	0.08	1.1	20.9	15	90.4	14.1
Core #31 28–31	4/6/2010	49.4	24.3	33.2	1,090	0.14	1.6	22.0	18	101.0	15.2
Core #31 42–45	4/6/2010	38.9	21.7	32.5	1,160	0.28	1.8	24.0	16	83.9	16.1
Core #31 56–59	4/6/2010	38.2	19.9	27.2	1,110	0.14	1.5	23.8	14	74.5	17.6
Core #31 70–73	4/6/2010	40.6	38.7	27.4	852	0.20	2.1	27.4	17	92.7	14.7
Core #31 84–87	4/6/2010	43.6	23.7	29.2	1,100	0.24	1.9	28.2	18	90.6	16.0
Core #31 98–101	4/6/2010	34.4	16.9	24.2	853	0.08	1.2	25.4	17	85.4	15.4
Core #31 112–115	4/6/2010	36.4	18.4	26.6	787	0.09	1.9	25.9	16	86.2	15.7
Core #31 126–129	4/6/2010	34.9	19.4	26.8	964	0.15	2.8	27.5	16	81.7	16.9
Core #31 140–143	4/6/2010	39.7	22.6	28.7	984	0.14	3.4	25.5	16	84.5	16.2
Core #31 154–157	4/6/2010	31.6	17.5	24.5	783	0.09	2.1	24.0	14	75.6	16.2
Core #31 164–167	4/6/2010	30.0	15.5	20.7	790	0.09	0.86	26.2	14	70.8	17.5
Core #38 7–10	5/12/2010	31.9	13.9	19.1	694	0.05	0.69	19.9	13	75.1	14.6
Core #38 12–15	5/12/2010	30.5	16.8	23.6	930	0.08	1.0	22.5	12	67.5	16.2
Core #38 60–63	5/12/2010	24.7	12.4	17.5	532	0.02	1.3	18.1	12	76.1	12.1
Core #38 98–101	5/12/2010	31.0	12.0	15.9	571	0.02	0.58	17.3	13	71.1	13.5
Core #38 105–108	5/12/2010	25.8	12.3	17.8	1,230	0.04	1.0	21.8	12	57.4	23.5
Core #38 155–158	5/12/2010	31.3	13.6	20.6	1,220	0.04	0.96	22.4	13	61.0	22.9
Core #47 5–8	5/13/2010	22.9	13.5	20.0	482	0.03	0.88	15.1	12	88.6	9.1
Core #47 51–54	5/13/2010	22.9	12.9	21.0	437	0.02	0.47	14.9	13	93.7	9.3
Core #47 109–112	5/13/2010	20.6	12.1	14.9	509	0.04	0.51	16.8	11	72.4	11.6
Core #60 0–2	5/15/2010	24.5	13.5	18.2	798	0.07	1.3	17.2	10	64.0	8.3
Core #60 6–9	5/15/2010	17.0	12.4	13.2	349	0.01	0.42	11.8	9.2	84.7	7.6
Core #60 50–53	5/15/2010	33.4	11.1	11.7	753	0.26	0.64	17.6	16	65.8	13.7
Core #66 10–13	5/20/2010	20.1	11.7	12.1	394	0.02	0.54	12.8	8.8	76.0	8.4

Appendix 3. Analytical data for major and trace elements in bed-sediment core samples collected in Lower Granite Reservoir and the Clearwater and Snake Rivers just above their confluence, 2010.—Continued

[Concentrations in micrograms per gram unless otherwise noted; #, number; <, less than lower reporting limit]

Sample identifier	Date	Lanthanum	Lead	Lithium	Manganese	Mercury	Molybdenum	Nickel	Niobium	Rubidium	Scandium
					Confluence						
Core #70 0–2	5/14/2010	27.2	14.5	21.5	673	0.05	0.63	20.1	10	69.3	13.1
Core #70 4–7	5/14/2010	19.9	13.6	13.1	346	0.01	0.31	10.0	7.0	66.9	8.1
Core #70 26–28	5/14/2010	23.0	13.1	13.0	437	0.01	0.32	11.5	9.5	64.4	9.8
Core #70 35–36	5/14/2010	27.3	14.1	20.0	734	0.06	0.76	21.1	8.7	58.1	13.4
Core #70 38–41	5/14/2010	19.3	13.0	14.1	480	0.01	0.37	13.0	8.5	65.6	11.0
Core #70 50–52	5/14/2010	17.7	12.9	15.0	478	0.01	0.35	12.6	7.9	70.8	9.9
					Snake River						
Core #73 0–2	5/19/2010	18.4	11.7	13.3	411	0.01	0.46	12.7	8.2	72.4	8.8
Core #80 0–1	5/19/2010	30.6	11.7	14.0	553	0.02	0.56	15.2	11	75.7	10.6
Core #81 0–3	5/19/2010	28.6	12.2	15.0	574	2.32	0.50	12.9	15	85.3	8.5
Core #84 5–15	10/13/2010	15.9	11.3	13.7	491	0.01	0.44	12.4	9.7	71.7	9.7
Core #84 25–35	10/13/2010	16.6	11.8	13.4	418	0.01	0.43	11.7	8.5	69.9	8.9
Core #84 45–55	10/13/2010	15.6	12.3	15.6	394	0.03	0.44	11.7	8.8	80.2	8.7
Core #84 65–75	10/13/2010	18.8	28.6	20.8	389	0.02	0.47	12.7	12	92.3	7.6
Core #84 85–95	10/13/2010	15.8	11.8	14.4	346	0.01	0.40	10.0	8.7	79.5	7.2
Core #85 5–15	10/13/2010	16.7	13.7	11.8	368	0.01	0.42	10.6	8.7	76.2	7.5
Core #85 25–35	10/13/2010	21.4	11.1	11.4	410	0.01	0.44	10.0	7.8	68	8.7
Core #85 45–55	10/13/2010	15.8	12.0	12.5	535	0.15	0.50	13.1	8.2	69.1	11.4
Core #85 55–65	10/13/2010	19.0	11.0	12.4	439	0.01	0.53	11.2	8.3	70.3	9.3
Core #87 0–19	5/19/2010	18.7	10.9	12.6	470	0.01	0.49	12.5	8.2	71.3	9.5
Core #88 0–3	5/19/2010	30.4	13.0	17.1	562	0.02	0.45	13.8	12	90.4	9.0
Core #89 0–3	5/19/2010	24.8	12.9	15.7	500	0.02	0.44	14.4	13	90.3	8.9

Appendix 3. Analytical data for major and trace elements in bed-sediment core samples collected in Lower Granite Reservoir and the Clearwater and Snake Rivers just above their confluence, 2010.—Continued

[Concentrations in micrograms per gram unless otherwise noted; #, number; <, less than lower reporting limit]

Sample identifier	Date	Silver	Strontium	Thallium	Titanium	Vanadium	Yttrium	Zinc	Antimony	Arsenic	Organic carbon, percent	Thorium	Uranium
Clearwater River													
Core #9 18–21	5/13/2010	<0.01	281	0.38	7,760	201	27.6	98.2	0.39	3.2	1.90	7.95	2.29
Core #9 34–37	5/13/2010	<0.01	355	0.31	5,720	146	19.9	390	0.23	2.1	1.01	5.71	1.60
Core #9 50–53	5/13/2010	<0.01	265	0.40	7,280	191	28.7	99.3	0.45	3.8	2.83	8.45	2.46
Lower Granite Reservoir													
Core #31 0–3	4/6/2010	<0.01	295	0.45	4,990	130	27.8	107	1.0	9.7	5.98	8.71	5.57
Core #31 14–17	4/6/2010	<0.01	333	0.47	4,750	122	24.6	113	1.1	8.8	3.73	9.76	4.65
Core #31 28–31	4/6/2010	0.094	278	0.54	4,630	122	36.0	117	1.5	23.5	6.49	13.2	17.0
Core #31 42–45	4/6/2010	0.099	286	0.49	5,040	135	32.2	119	1.9	18.1	7.57	10.4	15.5
Core #31 56–59	4/6/2010	0.020	283	0.44	5,450	150	33.5	116	1.1	13.3	7.84	9.88	12.9
Core #31 70–73	4/6/2010	0.095	297	0.52	4,620	124	29.4	108	1.7	10.6	5.02	11.6	11.7
Core #31 84–87	4/6/2010	0.037	291	0.50	5,110	134	33.1	117	1.5	11.6	6.73	12.7	14.1
Core #31 98–101	4/6/2010	<0.01	328	0.47	5,210	131	26.9	103	0.81	7.5	4.40	10.7	4.93
Core #31 112–115	4/6/2010	<0.01	295	0.48	5,100	129	29.7	109	0.85	8.6	4.96	11.2	6.11
Core #31 126–129	4/6/2010	<0.01	310	0.46	5,480	147	29.2	111	1.8	11.1	4.83	9.82	11.1
Core #31 140–143	4/6/2010	<0.01	274	0.48	5,180	136	32.4	117	1.2	12.1	6.23	11.2	12.8
Core #31 154–157	4/6/2010	<0.01	318	0.42	5,470	141	26.1	107	0.80	8.7	4.12	8.58	6.04
Core #31 164–167	4/6/2010	<0.01	349	0.40	6,170	160	25.2	102	0.81	6.1	2.74	7.62	3.73
Core #38 7–10	5/12/2010	<0.01	365	0.40	5,150	134	21.7	85.2	0.59	4.2	2.03	8.57	3.22
Core #38 12–15	5/12/2010	0.033	272	0.40	4,980	136	29.3	108	0.77	7.4	6.07	7.83	5.86
Core #38 60–63	5/12/2010	<0.01	383	0.40	4,540	117	15.6	68.9	0.77	2.7	0.21	6.38	1.54
Core #38 98–101	5/12/2010	<0.01	390	0.38	5,000	130	17.5	69.5	0.70	2.6	0.15	7.07	1.56
Core #38 105–108	5/12/2010	<0.01	309	0.36	8,320	241	32.1	113	0.45	3.5	3.22	6.36	2.45
Core #38 155–158	5/12/2010	<0.01	277	0.38	8,030	225	32.6	115	0.46	3.9	3.58	6.96	2.81
Core #47 5–8	5/13/2010	<0.01	369	0.45	3,250	83.1	15.6	63.1	0.66	4.1	4.41	6.06	3.47
Core #47 51–54	5/13/2010	<0.01	381	0.46	3,290	81.8	13.6	61.9	0.46	3.0	0.92	6.42	2.37
Core #47 109–112	5/13/2010	<0.01	396	0.37	4,060	109	14.7	62.8	0.53	2.5	0.15	5.76	1.49
Core #60 0–2	5/15/2010	<0.01	239	0.35	2,560	80.8	20.3	79.5	1.1	9.0	17.04	5.34	8.17
Core #60 6–9	5/15/2010	<0.01	395	0.41	2,320	70.2	10.7	46.1	0.40	2.4	0.12	5.05	1.17
Core #60 50–53	5/15/2010	<0.01	394	0.33	5,720	141	19.2	61.4	0.47	2.7	0.11	7.41	1.59
Core #66 10–13	5/20/2010	<0.01	371	0.39	2,730	78.3	11.5	45.2	0.56	2.5	0.14	5.13	1.29

Appendix 3. Analytical data for major and trace elements in bed-sediment core samples collected in Lower Granite Reservoir and the Clearwater and Snake Rivers just above their confluence, 2010.—Continued

[Concentrations in micrograms per gram unless otherwise noted; #, number; <, less than lower reporting limit]

Sample identifier	Date	Silver	Strontium	Thallium	Titanium	Vanadium	Yttrium	Zinc	Antimony	Arsenic	Organic carbon, percent	Thorium	Uranium
						Confluence							
Core #70 0–2	5/14/2010	<0.01	302	0.39	4,500	112	22.2	92.5	0.38	4.1	5.66	5.72	3.28
Core #70 4–7	5/14/2010	<0.01	414	0.35	2,720	72.1	9.8	47.4	0.10	1.1	0.21	4.96	0.98
Core #70 26–28	5/14/2010	<0.01	423	0.32	3,910	89.7	13.6	54.6	0.20	1.0	0.18	5.34	1.20
Core #70 35–36	5/14/2010	<0.01	277	0.35	4,280	114	22.7	83.2	0.36	5.0	5.60	5.49	3.42
Core #70 38–41	5/14/2010	<0.01	420	0.33	3,910	101	13.0	64.6	0.10	1.5	0.42	4.63	1.41
Core #70 50–52	5/14/2010	<0.01	405	0.36	3,580	93.6	12.8	69.3	0.20	1.6	0.74	3.79	1.26
						Snake River							
Core #73 0–2	5/19/2010	<0.01	373	0.36	2,700	76.4	11.3	44.2	0.36	2.4	0.14	6.69	1.36
Core #80 0–1	5/19/2010	<0.01	370	0.38	3,420	92.6	14.7	50.8	0.42	2.2	0.25	7.57	1.36
Core #81 0–3	5/19/2010	<0.01	372	0.42	3,970	98.7	14.1	53.2	0.40	2.3	0.13	7.82	1.42
Core #84 5–15	10/13/2010	0.039	361	0.35	3,190	88.5	14.0	49.0	0.10	2.2	0.11	4.22	1.10
Core #84 25–35	10/13/2010	0.030	344	0.36	3,010	86.0	13.0	49.1	0.22	2.5	0.11	4.63	1.17
Core #84 45–55	10/13/2010	0.031	388	0.41	2,850	80.9	12.7	47.5	0.20	2.8	0.10	4.73	1.21
Core #84 65–75	10/13/2010	0.029	324	0.47	2,640	71.4	13.1	54.0	0.38	3.1	0.11	5.88	1.59
Core #84 85–95	10/13/2010	0.069	342	0.40	2,470	69.5	11.9	72.4	0.22	2.3	0.10	4.76	1.21
Core #85 5–15	10/13/2010	0.075	341	0.39	2,500	70.9	11.6	45.2	0.75	2.4	0.16	4.80	1.13
Core #85 25–35	10/13/2010	0.035	323	0.35	2,830	82.5	12.9	47.5	0.28	2.5	0.12	5.95	1.11
Core #85 45–55	10/13/2010	0.027	348	0.35	3,470	105	15.1	54.7	0.25	2.5	0.12	4.38	1.21
Core #85 55–65	10/13/2010	0.026	329	0.34	3,020	87.4	13.3	48.6	0.20	2.4	0.11	5.42	1.17
Core #87 0–19	5/19/2010	<0.01	327	0.37	3,030	88.1	12.5	51.2	0.66	2.7	0.58	5.17	1.26
Core #88 0–3	5/19/2010	<0.01	380	0.44	3,410	84.7	14.6	72.5	0.47	2.9	0.15	7.65	1.44
Core #89 0–3	5/19/2010	<0.01	379	0.45	3,370	81.8	13.1	53.4	0.44	2.2	0.16	6.42	1.43

Appendix 4—Quality-Assurance and Quality-Control Data for Major and Trace Elements in Bed-Sediment Core Samples

Appendix 4. Quality-assurance and quality-control data for major and trace elements in bed-sediment core samples collected in Lower Granite Reservoir and the Clearwater and Snake Rivers just above their confluence, 2010.

[Concentrations in micrograms per gram unless otherwise noted; #, number; <, less than lower reporting limit; %, percent; NIST, National Institute of Standards and Technology; --, not analyzed]

Type of quality-control sample	Sample identifier	Set number	Calcium	Magnesium	Potassium	Sodium	Phosphorus	Aluminum
Environmental	Core #31 164–167	11150	27,800	12,700	16,600	18,800	1,020	74,800
Laboratory replicate	Core #31 164–167 replicate	11150	27,400	12,600	16,200	18,600	1,010	75,000
Laboratory replicate	Core #31 164–167 replicate	11150	27,500	12,600	16,500	18,900	1,040	73,700
Blank	Blank	11150	<100	<6	<15	<25	<5	<50
Blank	Blank	11150	<100	<6	<15	44.2	<5	<50
Blank	Blank	11150	<100	<6	<15	<25	<5	<50
Blank	Blank	11150	<100	<6	<15	<25	<5	<50
Blank	Blank	11150	<100	<6	<15	<25	<5	<50
Blank	Blank	11150	<100	<6	<15	<25	<5	<50
Standard reference material	MAG-1 found	11150	10,600	17,900	30,900	28,100	693	84,200
Standard reference material	MAG-1 true (Potts and others, 1992)	11150	9,790	18,090	29,500	28,400	711	86,660
Standard reference material	Percent recovery	11150	108.3%	98.9%	104.7%	98.9%	97.5%	97.2%
Standard reference material	NIST 8704 found	11150	27,600	11,300	20,400	5,800	955	60,200
Standard reference material	NIST 8704 true (National Institute of Standards and Technology, 2008)	11150	26,410	12,000	20,010	5,530	--	61,000
Standard reference material	Percent recovery	11150	104.5%	94.2%	101.9%	104.9%	--	98.7%
Standard reference material	SCO-1 found	11150	19,800	15,500	23,100	6,800	869	71,800
Standard reference material	SCO-1 true (Potts and others, 1992)	11150	18,700	16,400	23,000	6,670	899	72,370
Standard reference material	Percent recovery	11150	105.9%	94.5%	100.4%	101.9%	96.7%	99.2%
Standard reference material	NIST 2709 found	11150	20,900	15,900	21,500	12,400	644	79,500
Standard reference material	NIST 2709 true (National Institute of Standards and Technology, 2003a)	11150	18,900	15,100	20,300	11,600	620	75,000
Standard reference material	Percent recovery	11150	110.6%	105.3%	105.9%	106.9%	103.9%	106.0%
Standard reference material	GSD-8 found	11150	2,290	2,040	36,300	4,590	180	61,900
Standard reference material	GSD-8 true (Potts and others, 1992)	11150	1,790	1,510	23,500	3,490	130	40,800
Standard reference material	Percent recovery	11150	127.9%	135.1%	154.5%	131.5%	138.5%	151.7%
Standard reference material	NIST-2711 found	11150	27,100	10,100	24,300	11,600	807	65,200
Standard reference material	NIST-2711 true (National Institute of Standards and Technology, 2003b)	11150	28,800	10,500	24,500	11,400	860	65,300
Standard reference material	Percent recovery	11150	94.1%	96.2%	99.2%	101.8%	93.8%	99.8%
Standard reference material	GSD-5 found	11150	39,500	5,510	18,200	2,580	596	81,900
Standard reference material	GSD-5 true (Potts and others, 1992)	11150	38,200	5,900	17,400	2,970	610	81,300
Standard reference material	Percent recovery	11150	103.4%	93.4%	104.6%	86.9%	97.7%	100.7%
Standard reference material	GSD-3 found	11150	1,550	3,950	20,900	2,130	602	66,600
Standard reference material	GSD-3 true (Potts and others, 1992)	11150	1,570	4,200	20,400	2,370	610	63,700
Standard reference material	Percent recovery	11150	98.7%	94.0%	102.5%	89.9%	98.7%	104.6%

Appendix 4. Quality-assurance and quality-control data for major and trace elements in bed-sediment core samples collected in Lower Granite Reservoir and the Clearwater and Snake Rivers just above their confluence, 2010.—Continued

[Concentrations in micrograms per gram unless otherwise noted; #, number; <, less than lower reporting limit; %, percent; NIST, National Institute of Standards and Technology; --, not analyzed]

Type of quality-control sample	Sample identifier	Set number	Calcium	Magnesium	Potassium	Sodium	Phosphorus	Aluminum
Standard reference material	MAG-1 found	11150	10,500	17,800	29,800	29,000	680	87,800
Standard reference material	MAG-1 true (Potts and others, 1992)	11150	9,790	18,090	29,500	28,400	711	86,660
Standard reference material	Percent recovery	11150	107.3%	98.4%	101.0%	102.1%	95.6%	101.3%
Standard reference material	NIST 8704 found	11150	26,400	11,600	19,500	5,910	917	62,000
Standard reference material	NIST 8704 true (National Institute of Standards and Technology, 2008)	11150	26,410	12,000	20,010	5,530	--	61,000
Standard reference material	Percent recovery	11150	100.0%	96.7%	97.5%	106.9%	--	101.6%
Environmental	Core #84 65–75	11637	15,000	6,690	21,900	19,500	400	60,300
Laboratory replicate	Core #84 65–75 replicate	11637	14,500	6,590	21,100	19,500	401	59,200
Blank	Blank	11637	<100	13.4	<15	<25	<5	<50
Blank	Blank	11637	<100	<6	<15	<25	7.6	<50
Blank	Blank	11637	<100	<6	<15	112	21	<50
Blank	Blank	11637	<100	<6	<15	<25	6	<50
Blank	Blank	11637	<100	<6	<15	<25	<5	<50
Standard reference material	MAG-1 found	11637	10,900	18,900	32,100	30,300	739	88,800
Standard reference material	MAG-1 true (Potts and others, 1992)	11637	9,790	18,090	29,500	28,400	711	86,660
Standard reference material	Percent recovery	11637	111.3%	104.5%	108.8%	106.7%	103.9%	102.5%
Standard reference material	NIST 8704 found	11637	29,400	12,900	21,900	6,340	1,040	66,100
Standard reference material	NIST 8704 true (National Institute of Standards and Technology, 2008)	11637	26,410	12,000	20,010	5,530	--	61,000
Standard reference material	Percent recovery	11637	111.3%	107.5%	109.4%	114.6%	--	108.4%
Standard reference material	SCO-1 found	11637	19,500	16,500	23,700	6,900	912	74,300
Standard reference material	SCO-1 true (Potts and others, 1992)	11637	18,700	16,400	23,000	6,670	899	72,370
Standard reference material	Percent recovery	11637	104.3%	100.6%	103.0%	103.4%	101.4%	102.7%
Standard reference material	NIST 2709 found	11637	21,200	16,100	21,900	12,400	670	80,700
Standard reference material	NIST 2709 true (National Institute of Standards and Technology, 2003a)	11637	18,900	15,100	20,300	11,600	620	75,000
Standard reference material	Percent recovery	11637	112.2%	106.6%	107.9%	106.9%	108.1%	107.6%
Standard reference material	GSD-8 found	11637	1,510	1,390	24,000	3,130	127	40,300
Standard reference material	GSD-8 true (Potts and others, 1992)	11637	1,790	1,510	23,500	3,490	130	40,800
Standard reference material	Percent recovery	11637	84.4%	92.1%	102.1%	89.7%	97.7%	98.8%
Standard reference material	NIST 2709 found	11637	19,000	14,500	19,700	11,300	595	71,500
Standard reference material	NIST 2709 true (National Institute of Standards and Technology, 2003a)	11637	18,900	15,100	20,300	11,600	620	75,000
Standard reference material	Percent recovery	11637	100.5%	96.0%	97.0%	97.4%	96.0%	95.3%

Appendix 4. Quality-assurance and quality-control data for major and trace elements in bed-sediment core samples collected in Lower Granite Reservoir and the Clearwater and Snake Rivers just above their confluence, 2010.—Continued

[Concentrations in micrograms per gram unless otherwise noted; #, number; <, less than lower reporting limit; %, percent; NIST, National Institute of Standards and Technology; --, not analyzed]

Type of quality-control sample	Sample identifier	Set number	Barium	Beryllium	Bismuth	Cadmium	Cerium	Cesium
Environmental	Core #31 164–167	11150	723	1.5	5.90	0.27	58.1	3.2
Laboratory replicate	Core #31 164–167 replicate	11150	712	1.6	6.42	0.28	58.9	3.3
Laboratory replicate	Core #31 164–167 replicate	11150	715	1.5	5.97	0.27	58.9	3.2
Blank	Blank	11150	<0.25	<0.03	<0.06	<0.007	<0.1	0.003
Blank	Blank	11150	<0.25	<0.03	<0.06	<0.007	<0.1	0.008
Blank	Blank	11150	0.73	<0.03	1.27	<0.007	0.26	0.007
Blank	Blank	11150	<0.25	<0.03	<0.06	<0.007	<0.1	0.005
Blank	Blank	11150	<0.25	<0.03	<0.06	<0.007	<0.1	<0.003
Blank	Blank	11150	<0.25	0.03	<0.06	<0.007	<0.1	<0.003
Standard reference material	MAG-1 found	11150	489	2.5	9.15	0.19	75.6	8.8
Standard reference material	MAG-1 true (Potts and others, 1992)	11150	479	3.2	0.34	0.202	88	8.6
Standard reference material	Percent recovery	11150	102.1%	78.1%	2,691.2%	94.1%	85.9%	102.3%
Standard reference material	NIST 8704 found	11150	415	1.5	55.2	3.1	55.9	5.9
Standard reference material	NIST 8704 true (National Institute of Standards and Technology, 2008)	11150	413	--	--	2.94	66.5	5.83
Standard reference material	Percent recovery	11150	100.5%	--	--	105.4%	84.1%	101.2%
Standard reference material	SCO-1 found	11150	577	1.4	11.7	0.14	54.5	8.1
Standard reference material	SCO-1 true (Potts and others, 1992)	11150	570	1.84	0.37	0.14	62	7.8
Standard reference material	Percent recovery	11150	101.2%	76.1%	3,162.2%	100.0%	87.9%	103.8%
Standard reference material	NIST 2709 found	11150	985	3.1	7.18	0.4	46.4	6
Standard reference material	NIST 2709 true (National Institute of Standards and Technology, 2003a)	11150	968	--	--	0.38	42	5.3
Standard reference material	Percent recovery	11150	101.8%	--	--	105.3%	110.5%	113.2%
Standard reference material	GSD-8 found	11150	653	2.1	11.5	<0.007	77.5	5
Standard reference material	GSD-8 true (Potts and others, 1992)	11150	480	2	0.19	0.081	54	3.6
Standard reference material	Percent recovery	11150	136.0%	105.0%	6,052.6%	--	143.5%	138.9%
Standard reference material	NIST-2711 found	11150	726	1.9	415	40.5	73.2	7
Standard reference material	NIST-2711 true (National Institute of Standards and Technology, 2003b)	11150	726	--	--	41.7	69	6.1
Standard reference material	Percent recovery	11150	100.0%	--	--	97.1%	106.1%	114.8%
Standard reference material	GSD-5 found	11150	435	1.8	44	0.9	88.8	9.3
Standard reference material	GSD-5 true (Potts and others, 1992)	11150	440	2.3	2.4	0.82	89	9.4
Standard reference material	Percent recovery	11150	98.9%	78.3%	1,833.3%	109.8%	99.8%	98.9%
Standard reference material	GSD-3 found	11150	616	1.1	15.9	0.2	61.8	7.9
Standard reference material	GSD-3 true (Potts and others, 1992)	11150	615	1.5	0.79	0.1	64	7.8
Standard reference material	Percent recovery	11150	100.2%	73.3%	2,012.7%	200.0%	96.6%	101.3%

Appendix 4. Quality-assurance and quality-control data for major and trace elements in bed-sediment core samples collected in Lower Granite Reservoir and the Clearwater and Snake Rivers just above their confluence, 2010.—Continued

[Concentrations in micrograms per gram unless otherwise noted; #, number; <, less than lower reporting limit; %, percent; NIST, National Institute of Standards and Technology; --, not analyzed]

Type of quality-control sample	Sample identifier	Set number	Barium	Beryllium	Bismuth	Cadmium	Cerium	Cesium
Standard reference material	MAG-1 found	11150	489	2.7	9.53	0.19	74.9	9
Standard reference material	MAG-1 true (Potts and others, 1992)	11150	479	3.2	0.34	0.202	88	8.6
Standard reference material	Percent recovery	11150	102.1%	84.4%	2,802.9%	94.1%	85.1%	104.7%
Standard reference material	NIST 8704 found	11150	423	1.7	55.3	3	53.5	6.2
Standard reference material	NIST 8704 true (National Institute of Standards and Technology, 2008)	11150	413	--	--	2.94	66.5	5.83
Standard reference material	Percent recovery	11150	102.4%	--	--	102.0%	80.5%	106.3%
Environmental	Core #84 65–75	11637	1,040	1.8	10.4	0.02	34.7	2.5
Laboratory replicate	Core #84 65–75 replicate	11637	1,010	1.9	10.4	0.02	35.6	2.4
Blank	Blank	11637	<0.25	<0.03	<0.06	<0.007	<0.1	0.004
Blank	Blank	11637	<0.25	<0.03	<0.06	<0.007	<0.1	0.004
Blank	Blank	11637	0.27	<0.03	0.15	<0.007	<0.1	0.004
Blank	Blank	11637	<0.25	<0.03	<0.06	<0.007	<0.1	<0.003
Blank	Blank	11637	<0.25	<0.03	<0.06	<0.007	<0.1	<0.003
Standard reference material	MAG-1 found	11637	544	2.9	10.7	0.31	91.7	9.6
Standard reference material	MAG-1 true (Potts and others, 1992)	11637	479	3.20	0.34	0.20	88.0	8.60
Standard reference material	Percent recovery	11637	113.6%	90.6%	3,147.1%	153.5%	104.2%	111.6%
Standard reference material	NIST 8704 found	11637	481	1.8	60.6	3.4	65.1	6.8
Standard reference material	NIST 8704 true (National Institute of Standards and Technology, 2008)	11637	413	--	--	2.94	66.5	5.83
Standard reference material	Percent recovery	11637	116.5%	--	--	115.6%	97.9%	116.6%
Standard reference material	SCO-1 found	11637	628	1.6	12.4	0.15	60.1	8.7
Standard reference material	SCO-1 true (Potts and others, 1992)	11637	570	1.84	0.37	0.14	62.0	7.80
Standard reference material	Percent recovery	11637	110.2%	87.0%	3,351.4%	107.1%	96.9%	111.5%
Standard reference material	NIST 2709 found	11637	1,060	2.9	7.44	0.41	49.1	6.3
Standard reference material	NIST 2709 true (National Institute of Standards and Technology, 2003a)	11637	968	--	--	0.38	42.0	5.30
Standard reference material	Percent recovery	11637	109.5%	--	--	107.9%	116.9%	118.9%
Standard reference material	GSD-8 found	11637	484	1.6	8.15	0.03	55.2	3.6
Standard reference material	GSD-8 true (Potts and others, 1992)	11637	480	2.00	0.19	0.08	54.0	3.60
Standard reference material	Percent recovery	11637	100.8%	80.0%	4,289.5%	37.0%	102.2%	100.0%
Standard reference material	NIST 2709 found	11637	905	2.9	6.58	0.34	42	5.4
Standard reference material	NIST 2709 true (National Institute of Standards and Technology, 2003a)	11637	968	--	--	0.38	42.0	5.30
Standard reference material	Percent recovery	11637	93.5%	--	--	89.5%	100.0%	101.9%

Appendix 4. Quality-assurance and quality-control data for major and trace elements in bed-sediment core samples collected in Lower Granite Reservoir and the Clearwater and Snake Rivers just above their confluence, 2010.—Continued

[Concentrations in micrograms per gram unless otherwise noted; #, number; <, less than lower reporting limit; %, percent; NIST, National Institute of Standards and Technology; --, not analyzed]

Type of quality-control sample	Sample identifier	Set number	Chromium	Cobalt	Copper	Gallium	Iron	Lanthanum	Lead
Environmental	Core #31 164–167	11150	52.4	20.9	36.7	19.8	45,000	30.0	15.5
Laboratory replicate	Core #31 164–167 replicate	11150	52.4	20.8	39.3	19.6	44,800	30.4	16.8
Laboratory replicate	Core #31 164–167 replicate	11150	52.9	20.7	36.6	19.8	45,300	30.1	15.8
Blank	Blank	11150	<0.5	<0.03	<2	<0.015	<50	<0.05	<0.4
Blank	Blank	11150	<0.5	<0.03	<2	<0.015	<50	<0.05	<0.4
Blank	Blank	11150	<0.5	<0.03	<2	<0.015	<50	0.16	3.35
Blank	Blank	11150	<0.5	<0.03	<2	<0.015	<50	<0.05	<0.4
Blank	Blank	11150	<0.5	<0.03	<2	<0.015	<50	<0.05	<0.4
Blank	Blank	11150	<0.5	<0.03	<2	<0.015	<50	<0.05	<0.4
Standard reference material	MAG-1 found	11150	104	23.1	30.2	24.5	49,100	36.8	24.3
Standard reference material	MAG-1 true (Potts and others, 1992)	11150	97	20.4	30	20.4	47,600	43	24
Standard reference material	Percent recovery	11150	107.2%	113.2%	100.7%	120.1%	103.2%	85.6%	101.3%
Standard reference material	NIST 8704 found	11150	121	14	91.4	16.7	40,200	26.6	146
Standard reference material	NIST 8704 true (National Institute of Standards and Technology, 2008)	11150	121.9	13.6	--	--	39,700	--	150
Standard reference material	Percent recovery	11150	99.3%	102.9%	--	--	101.3%	--	97.3%
Standard reference material	SCO-1 found	11150	71.9	11.9	32.4	18.4	35,800	27.6	31.2
Standard reference material	SCO-1 true (Potts and others, 1992)	11150	68	10.5	28.7	15	35,900	29.5	31
Standard reference material	Percent recovery	11150	105.7%	113.3%	112.9%	122.7%	99.7%	93.6%	100.6%
Standard reference material	NIST 2709 found	11150	122	14.4	37.8	18	36,900	23.5	18.7
Standard reference material	NIST 2709 true (National Institute of Standards and Technology, 2003a)	11150	130	13.4	34.6	14	35,000	23	18.9
Standard reference material	Percent recovery	11150	93.8%	107.5%	109.2%	128.6%	105.4%	102.2%	98.9%
Standard reference material	GSD-8 found	11150	7.9	5	8.8	16.7	22,200	37.9	30.9
Standard reference material	GSD-8 true (Potts and others, 1992)	11150	7.6	3.6	4.1	10.8	15,380	30	21
Standard reference material	Percent recovery	11150	103.9%	138.9%	214.6%	154.6%	144.3%	126.3%	147.1%
Standard reference material	NIST-2711 found	11150	43.1	10.1	112	17.2	28,400	38.4	1100
Standard reference material	NIST-2711 true (National Institute of Standards and Technology, 2003b)	11150	47	10	114	15	28,900	40	1162
Standard reference material	Percent recovery	11150	91.7%	101.0%	98.2%	114.7%	98.3%	96.0%	94.7%
Standard reference material	GSD-5 found	11150	69.1	20.3	140	22.4	41,200	39.4	115
Standard reference material	GSD-5 true (Potts and others, 1992)	11150	70	18.9	137	20.3	41,000	46	112
Standard reference material	Percent recovery	11150	98.7%	107.4%	102.2%	110.3%	100.5%	85.7%	102.7%
Standard reference material	GSD-3 found	11150	80.2	11.6	183	16.7	45,900	32.7	42
Standard reference material	GSD-3 true (Potts and others, 1992)	11150	87	11.7	177	15.9	45,500	39	40
Standard reference material	Percent recovery	11150	92.2%	99.1%	103.4%	105.0%	100.9%	83.8%	105.0%

Appendix 4. Quality-assurance and quality-control data for major and trace elements in bed-sediment core samples collected in Lower Granite Reservoir and the Clearwater and Snake Rivers just above their confluence, 2010.—Continued

[Concentrations in micrograms per gram unless otherwise noted; #, number; <, less than lower reporting limit; %, percent; NIST, National Institute of Standards and Technology; --, not analyzed]

Type of quality-control sample	Sample identifier	Set number	Chro-mium	Cobalt	Copper	Gallium	Iron	Lantha-num	Lead
Standard reference material	MAG-1 found	11150	97.6	22	29.7	23.6	47,600	37.4	24.6
Standard reference material	MAG-1 true (Potts and others, 1992)	11150	97	20.4	30	20.4	47,600	43	24
Standard reference material	Percent recovery	11150	100.6%	107.8%	99.0%	115.7%	100.0%	87.0%	102.5%
Standard reference material	NIST 8704 found	11150	115	13.6	89.7	16.2	38,600	25.7	145
Standard reference material	NIST 8704 true (National Institute of Standards and Technology, 2008)	11150	121.9	13.6	--	--	39,700	--	150
Standard reference material	Percent recovery	11150	94.3%	100.0%	--	--	97.2%	--	96.7%
Environmental	Core #84 65–75	11637	22.9	11.1	18.9	16.3	22,300	18.8	28.6
Laboratory replicate	Core #84 65–75 replicate	11637	21.3	10.9	19.7	16.1	21,700	19.4	28.7
Blank	Blank	11637	<0.5	<0.03	<2	<0.015	<50	<0.05	<0.4
Blank	Blank	11637	<0.5	<0.03	<2	<0.015	<50	<0.05	<0.4
Blank	Blank	11637	<0.5	<0.03	<2	<0.015	<50	<0.05	0.41
Blank	Blank	11637	<0.5	<0.03	<2	<0.015	<50	<0.05	<0.4
Blank	Blank	11637	<0.5	<0.03	<2	0.02	<50	<0.05	<0.4
Standard reference material	MAG-1 found	11637	107	23.8	32	25.9	51,300	44	28.3
Standard reference material	MAG-1 true (Potts and others, 1992)	11637	97	20.4	30.0	20.4	47,600	43.0	24.0
Standard reference material	Percent recovery	11637	110.3%	116.7%	106.7%	127.0%	107.8%	102.3%	117.9%
Standard reference material	NIST 8704 found	11637	127	15	98.1	18.1	43,600	31.1	162
Standard reference material	NIST 8704 true (National Institute of Standards and Technology, 2008)	11637	122	13.6	--	--	39,700	--	150.0
Standard reference material	Percent recovery	11637	104.2%	110.3%	--	--	109.8%	--	108.0%
Standard reference material	SCO-1 found	11637	72.2	12.1	30.2	19	37,100	30.3	33.1
Standard reference material	SCO-1 true (Potts and others, 1992)	11637	68.0	10.5	28.7	15.0	35,900	29.5	31.0
Standard reference material	Percent recovery	11637	106.2%	115.2%	105.2%	126.7%	103.3%	102.7%	106.8%
Standard reference material	NIST 2709 found	11637	120	14.8	38.8	19.2	38,300	24.3	19.9
Standard reference material	NIST 2709 true (National Institute of Standards and Technology, 2003a)	11637	130	13.4	34.6	14.0	35,000	23.0	18.9
Standard reference material	Percent recovery	11637	92.3%	110.4%	112.1%	137.1%	109.4%	105.7%	105.3%
Standard reference material	GSD-8 found	11637	9.7	3.4	5	11.1	15,000	26.7	22
Standard reference material	GSD-8 true (Potts and others, 1992)	11637	7.60	3.6	4.1	10.8	15,380	30.0	21.0
Standard reference material	Percent recovery	11637	127.6%	94.4%	122.0%	102.8%	97.5%	89.0%	104.8%
Standard reference material	NIST 2709 found	11637	104	12.7	33.4	16.1	33,800	21	17.5
Standard reference material	NIST 2709 true (National Institute of Standards and Technology, 2003a)	11637	130	13.4	34.6	14.0	35,000	23.0	18.9
Standard reference material	Percent recovery	11637	80.0%	94.8%	96.5%	115.0%	96.6%	91.3%	92.6%

Appendix 4. Quality-assurance and quality-control data for major and trace elements in bed-sediment core samples collected in Lower Granite Reservoir and the Clearwater and Snake Rivers just above their confluence, 2010.—Continued

[Concentrations in micrograms per gram unless otherwise noted; #, number; <, less than lower reporting limit; %, percent; NIST, National Institute of Standards and Technology; --, not analyzed]

Type of quality-control sample	Sample identifier	Set number	Lithium	Manganese	Molybdenum	Nickel	Niobium	Rubidium
Environmental	Core #31 164–167	11150	20.7	790	0.86	26.2	14	70.8
Laboratory replicate	Core #31 164–167 replicate	11150	22.0	798	0.88	25.6	14	70.2
Laboratory replicate	Core #31 164–167 replicate	11150	21.3	806	0.91	25.9	14	70.4
Blank	Blank	11150	<0.3	<0.7	<0.05	<0.3	0.2	<0.014
Blank	Blank	11150	0.3	<0.7	<0.05	<0.3	0.7	<0.014
Blank	Blank	11150	<0.3	<0.7	<0.05	<0.3	0.48	<0.014
Blank	Blank	11150	<0.3	<0.7	<0.05	<0.3	0.34	<0.014
Blank	Blank	11150	<0.3	<0.7	<0.05	<0.3	0.1	<0.014
Blank	Blank	11150	<0.3	<0.7	<0.05	<0.3	<0.1	<0.014
Standard reference material	MAG-1 found	11150	74.3	780	1.1	51.9	14	158
Standard reference material	MAG-1 true (Potts and others, 1992)	11150	79	760	1.6	53	12	149
Standard reference material	Percent recovery	11150	94.1%	102.6%	68.8%	97.9%	116.7%	106.0%
Standard reference material	NIST 8704 found	11150	44.3	585	4.6	43.2	7.6	107
Standard reference material	NIST 8704 true (National Institute of Standards and Technology, 2008)	11150	--	544	--	42.9	--	--
Standard reference material	Percent recovery	11150	--	107.5%	--	100.7%	--	--
Standard reference material	SCO-1 found	11150	42	409	1.3	27.7	10	119
Standard reference material	SCO-1 true (Potts and others, 1992)	11150	45	410	1.37	27	11	112
Standard reference material	Percent recovery	11150	93.3%	99.8%	94.9%	102.6%	90.9%	106.3%
Standard reference material	NIST 2709 found	11150	55.5	594	2.2	88	11	103
Standard reference material	NIST 2709 true (National Institute of Standards and Technology, 2003a)	11150	--	538	2	88	--	96
Standard reference material	Percent recovery	11150	--	110.4%	110.0%	100.0%	--	107.3%
Standard reference material	GSD-8 found	11150	17.6	510	0.82	2.4	51	198
Standard reference material	GSD-8 true (Potts and others, 1992)	11150	13.2	310	0.54	2.7	35	132
Standard reference material	Percent recovery	11150	133.3%	164.5%	151.9%	88.9%	145.7%	150.0%
Standard reference material	NIST-2711 found	11150	26.5	655	1.7	20	16	120
Standard reference material	NIST-2711 true (National Institute of Standards and Technology, 2003b)	11150	--	638	1.6	20.6	--	110
Standard reference material	Percent recovery	11150	--	102.7%	106.3%	97.1%	--	109.1%
Standard reference material	GSD-5 found	11150	43.3	1,220	1.3	37.6	11	128
Standard reference material	GSD-5 true (Potts and others, 1992)	11150	45	1,160	1.2	34	19	118
Standard reference material	Percent recovery	11150	96.2%	105.2%	108.3%	110.6%	57.9%	108.5%
Standard reference material	GSD-3 found	11150	32.4	424	96.9	27.2	6.8	83.2
Standard reference material	GSD-3 true (Potts and others, 1992)	11150	33	390	92	25.6	16	79
Standard reference material	Percent recovery	11150	98.2%	108.7%	105.3%	106.3%	42.5%	105.3%

Appendix 4. Quality-assurance and quality-control data for major and trace elements in bed-sediment core samples collected in Lower Granite Reservoir and the Clearwater and Snake Rivers just above their confluence, 2010.—Continued

[Concentrations in micrograms per gram unless otherwise noted; #, number; <, less than lower reporting limit; %, percent; NIST, National Institute of Standards and Technology; --, not analyzed]

Type of quality-control sample	Sample identifier	Set number	Lithium	Manganese	Molybdenum	Nickel	Niobium	Rubidium
Standard reference material	MAG-1 found	11150	74.8	743	1.1	50.5	12	149
Standard reference material	MAG-1 true (Potts and others, 1992)	11150	79	760	1.6	53	12	149
Standard reference material	Percent recovery	11150	94.7%	97.8%	68.8%	95.3%	100.0%	100.0%
Standard reference material	NIST 8704 found	11150	44.3	559	4.5	42.6	7	102
Standard reference material	NIST 8704 true (National Institute of Standards and Technology, 2008)	11150	--	544	--	42.9	--	--
Standard reference material	Percent recovery	11150	--	102.8%	--	99.3%	--	--
Environmental	Core #84 65–75	11637	0.02	389	0.47	12.7	12	92.3
Laboratory replicate	Core #84 65–75 replicate	11637	--	375	0.47	12	12	91.7
Blank	Blank	11637	<0.3	2.3	<0.05	<0.3	<0.1	<0.014
Blank	Blank	11637	<0.3	<0.7	<0.05	<0.3	2	<0.014
Blank	Blank	11637	<0.3	<0.7	<0.05	<0.3	0.58	<0.014
Blank	Blank	11637	<0.3	<0.7	<0.05	<0.3	0.31	<0.014
Blank	Blank	11637	0.8	<0.7	<0.05	<0.3	0.2	<0.014
Standard reference material	MAG-1 found	11637	79.2	809	1.2	54.5	15	161
Standard reference material	MAG-1 true (Potts and others, 1992)	11637	79.0	760	1.60	53.0	12.0	149
Standard reference material	Percent recovery	11637	100.3%	106.4%	75.0%	102.8%	125.0%	108.1%
Standard reference material	NIST 8704 found	11637	48	625	4.1	47.8	9.7	114
Standard reference material	NIST 8704 true (National Institute of Standards and Technology, 2008)	11637	--	544	--	42.9	--	--
Standard reference material	Percent recovery	11637	--	114.9%	--	111.4%	--	--
Standard reference material	SCO-1 found	11637	44.9	413	1.2	27.9	10	120
Standard reference material	SCO-1 true (Potts and others, 1992)	11637	45.0	410	1.37	27.0	11.0	112
Standard reference material	Percent recovery	11637	99.8%	100.7%	87.6%	103.3%	90.9%	107.1%
Standard reference material	NIST 2709 found	11637	56.3	610	2.2	90	9.4	105
Standard reference material	NIST 2709 true (National Institute of Standards and Technology, 2003a)	11637	--	538	2	88.0	--	96
Standard reference material	Percent recovery	11637	--	113.4%	110.0%	102.3%	--	109.4%
Standard reference material	GSD-8 found	11637	11.8	336	0.56	1.6	33	135
Standard reference material	GSD-8 true (Potts and others, 1992)	11637	13.2	310	0.54	2.7	35.0	132
Standard reference material	Percent recovery	11637	89.4%	108.4%	103.7%	59.3%	94.3%	102.3%
Standard reference material	NIST 2709 found	11637	52	540	1.9	77.8	8.9	90.7
Standard reference material	NIST 2709 true (National Institute of Standards and Technology, 2003a)	11637	--	538	2	88.0	--	96
Standard reference material	Percent recovery	11637	--	100.4%	95.0%	88.4%	--	94.5%

Appendix 4. Quality-assurance and quality-control data for major and trace elements in bed-sediment core samples collected in Lower Granite Reservoir and the Clearwater and Snake Rivers just above their confluence, 2010.—Continued

[Concentrations in micrograms per gram unless otherwise noted; #, number; <, less than lower reporting limit; %, percent; NIST, National Institute of Standards and Technology; --, not analyzed]

Type of quality-control sample	Sample identifier	Set number	Scandium	Silver	Strontium	Thallium	Titanium	Vanadium
Environmental	Core #31 164–167	11150	17.5	<0.01	349	0.40	6,170	160
Laboratory replicate	Core #31 164–167 replicate	11150	17.3	<0.01	343	0.40	6,090	158
Laboratory replicate	Core #31 164–167 replicate	11150	17.5	<0.01	347	0.41	6,180	161
Blank	Blank	11150	<0.04	12.3	<0.8	<0.08	<40	<0.15
Blank	Blank	11150	<0.04	<0.01	<0.8	<0.08	<40	<0.15
Blank	Blank	11150	<0.04	<0.01	<0.8	<0.08	<40	<0.15
Blank	Blank	11150	<0.04	<0.01	<0.8	<0.08	<40	<0.15
Blank	Blank	11150	<0.04	2.17	<0.8	<0.08	<40	<0.15
Blank	Blank	11150	<0.04	0.816	<0.8	<0.08	<40	<0.15
Standard reference material	MAG-1 found	11150	18	<0.01	148	0.71	3,400	153
Standard reference material	MAG-1 true (Potts and others, 1992)	11150	17.2	0.08	146	0.59	4,500	140
Standard reference material	Percent recovery	11150	104.7%	--	101.4%	120.3%	75.6%	109.3%
Standard reference material	NIST 8704 found	11150	11.4	<0.01	137	1.06	2,200	97.8
Standard reference material	NIST 8704 true (National Institute of Standards and Technology, 2008)	11150	11.26	--	--	--	4,570	94.6
Standard reference material	Percent recovery	11150	101.2%	--	--	--	48.1%	103.4%
Standard reference material	SCO-1 found	11150	11.9	<0.01	175	0.69	2,880	145
Standard reference material	SCO-1 true (Potts and others, 1992)	11150	10.8	0.134	174	0.72	3,760	131
Standard reference material	Percent recovery	11150	110.2%	--	100.6%	95.8%	76.6%	110.7%
Standard reference material	NIST 2709 found	11150	12.8	<0.01	248	0.68	3,250	127
Standard reference material	NIST 2709 true (National Institute of Standards and Technology, 2003a)	11150	12	--	231	0.74	3,420	112
Standard reference material	Percent recovery	11150	106.7%	--	107.4%	91.9%	95.0%	113.4%
Standard reference material	GSD-8 found	11150	7.5	<0.01	74.9	1.08	4,270	36
Standard reference material	GSD-8 true (Potts and others, 1992)	11150	5.7	0.062	52	0.78	3,660	26
Standard reference material	Percent recovery	11150	131.6%	--	144.0%	138.5%	116.7%	138.5%
Standard reference material	NIST-2711 found	11150	9.3	2.64	253	2.55	2,300	85.8
Standard reference material	NIST-2711 true (National Institute of Standards and Technology, 2003b)	11150	9	4.63	245.3	2.47	3,060	81.6
Standard reference material	Percent recovery	11150	103.3%	57.0%	103.1%	103.2%	75.2%	105.1%
Standard reference material	GSD-5 found	11150	13.9	<0.01	219	1.19	3,370	114
Standard reference material	GSD-5 true (Potts and others, 1992)	11150	14.5	0.36	204	1.16	5,400	109
Standard reference material	Percent recovery	11150	95.9%	--	107.4%	102.6%	62.4%	104.6%
Standard reference material	GSD-3 found	11150	12.9	<0.01	93.7	0.48	3,200	124
Standard reference material	GSD-3 true (Potts and others, 1992)	11150	14.3	0.59	90	0.58	6,360	120
Standard reference material	Percent recovery	11150	90.2%	--	104.1%	82.8%	50.3%	103.3%

Appendix 4. Quality-assurance and quality-control data for major and trace elements in bed-sediment core samples collected in Lower Granite Reservoir and the Clearwater and Snake Rivers just above their confluence, 2010.—Continued

[Concentrations in micrograms per gram unless otherwise noted; #, number; <, less than lower reporting limit; %, percent; NIST, National Institute of Standards and Technology; --, not analyzed]

Type of quality-control sample	Sample identifier	Set number	Scandium	Silver	Strontium	Thallium	Titanium	Vanadium
Standard reference material	MAG-1 found	11150	17.5	<0.01	141	0.73	3,150	145
Standard reference material	MAG-1 true (Potts and others, 1992)	11150	17.2	0.08	146	0.59	4,500	140
Standard reference material	Percent recovery	11150	101.7%	--	96.6%	123.7%	70.0%	103.6%
Standard reference material	NIST 8704 found	11150	11.6	<0.01	133	1.06	2,080	94.9
Standard reference material	NIST 8704 true (National Institute of Standards and Technology, 2008)	11150	11.26	--	--	--	4,570	94.6
Standard reference material	Percent recovery	11150	103.0%	--	--	--	45.5%	100.3%
Environmental	Core #84 65–75	11637	7.6	0.029	324	0.47	2,640	71.4
Laboratory replicate	Core #84 65–75 replicate	11637	7.4	0.039	323	0.47	2,580	69.9
Blank	Blank	11637	<0.04	0.029	<0.8	<0.08	<40	<0.15
Blank	Blank	11637	<0.04	<0.01	<0.8	<0.08	<40	<0.15
Blank	Blank	11637	<0.04	<0.01	<0.8	<0.08	<40	<0.15
Blank	Blank	11637	<0.04	<0.01	<0.8	<0.08	<40	<0.15
Blank	Blank	11637	<0.04	<0.01	<0.8	<0.08	<40	<0.15
Standard reference material	MAG-1 found	11637	18.6	0.065	155	0.75	3,640	155
Standard reference material	MAG-1 true (Potts and others, 1992)	11637	17.2	0.08	146	0.59	4,500	140
Standard reference material	Percent recovery	11637	108.1%	81.3%	106.2%	127.1%	80.9%	110.7%
Standard reference material	NIST 8704 found	11637	12.8	0.317	152	1.14	2,670	103
Standard reference material	NIST 8704 true (National Institute of Standards and Technology, 2008)	11637	11.3	--	--	--	4,570	94.6
Standard reference material	Percent recovery	11637	113.7%	--	--	--	58.4%	108.9%
Standard reference material	SCO-1 found	11637	12.5	0.103	181	0.72	2,850	143
Standard reference material	SCO-1 true (Potts and others, 1992)	11637	10.8	0.134	174	0.72	3,760	131
Standard reference material	Percent recovery	11637	115.7%	76.9%	104.0%	100.0%	75.8%	109.2%
Standard reference material	NIST 2709 found	11637	13.3	0.339	255	0.66	3,190	126
Standard reference material	NIST 2709 true (National Institute of Standards and Technology, 2003a)	11637	12.0	--	231	0.74	3,420	112.0
Standard reference material	Percent recovery	11637	110.8%	--	110.4%	89.2%	93.3%	112.5%
Standard reference material	GSD-8 found	11637	5	<0.01	51.4	0.72	2,750	24.6
Standard reference material	GSD-8 true (Potts and others, 1992)	11637	5.7	0.062	52.0	0.78	3,660	26
Standard reference material	Percent recovery	11637	87.7%	--	98.8%	92.3%	75.1%	94.6%
Standard reference material	NIST 2709 found	11637	11.3	0.306	218	0.65	2,840	109
Standard reference material	NIST 2709 true (National Institute of Standards and Technology, 2003a)	11637	12.0	--	231	0.74	3,420	112.0
Standard reference material	Percent recovery	11637	94.2%	--	94.4%	87.8%	83.0%	97.3%

Appendix 4. Quality-assurance and quality-control data for major and trace elements in bed-sediment core samples collected in Lower Granite Reservoir and the Clearwater and Snake Rivers just above their confluence, 2010.—Continued

[Concentrations in micrograms per gram unless otherwise noted; #, number; <, less than lower reporting limit; %, percent; NIST, National Institute of Standards and Technology; --, not analyzed]

Type of quality-control sample	Sample identifier	Set number	Yttrium	Zinc	Antimony	Arsenic	Thorium	Uranium
Environmental	Core #31 164–167	11150	25.2	102	0.81	6.1	7.62	3.73
Laboratory replicate	Core #31 164–167 replicate	11150	24.7	102	2.0	6.2	8.36	3.81
Laboratory replicate	Core #31 164–167 replicate	11150	25.0	103	0.77	6.0	7.82	3.85
Blank	Blank	11150	<0.05	<3	0.32	<1	<0.1	<0.02
Blank	Blank	11150	<0.05	<3	<0.04	<1	<0.1	<0.02
Blank	Blank	11150	<0.05	<3	<0.04	<1	<0.1	<0.02
Blank	Blank	11150	<0.05	<3	<0.04	<1	<0.1	<0.02
Blank	Blank	11150	<0.05	<3	0.23	<1	<0.1	<0.02
Blank	Blank	11150	<0.05	<3	0.22	<1	<0.1	<0.02
Standard reference material	MAG-1 found	11150	19.8	136	1	9.8	11	2.47
Standard reference material	MAG-1 true (Potts and others, 1992)	11150	28	130	0.96	9.2	11.9	2.7
Standard reference material	Percent recovery	11150	70.7%	104.6%	104.2%	106.5%	92.4%	91.5%
Standard reference material	NIST 8704 found	11150	20	393	2.9	17	8.44	2.72
Standard reference material	NIST 8704 true (National Institute of Standards and Technology, 2008)	11150	--	408	3.07	--	9.07	3.09
Standard reference material	Percent recovery	11150	--	96.3%	94.5%	--	93.1%	88.0%
Standard reference material	SCO-1 found	11150	17.8	107	2.6	12.7	8.92	2.7
Standard reference material	SCO-1 true (Potts and others, 1992)	11150	26	103	2.5	12.4	9.7	3
Standard reference material	Percent recovery	11150	68.5%	103.9%	104.0%	102.4%	92.0%	90.0%
Standard reference material	NIST 2709 found	11150	16.2	111	7.4	19.2	11.1	3.06
Standard reference material	NIST 2709 true (National Institute of Standards and Technology, 2003a)	11150	18	106	7.9	17.7	11	3
Standard reference material	Percent recovery	11150	90.0%	104.7%	93.7%	108.5%	100.9%	102.0%
Standard reference material	GSD-8 found	11150	19.2	65.9	0.39	4	19.5	4.37
Standard reference material	GSD-8 true (Potts and others, 1992)	11150	18	43	0.24	2.4	13.4	3
Standard reference material	Percent recovery	11150	106.7%	153.3%	162.5%	166.7%	145.5%	145.7%
Standard reference material	NIST-2711 found	11150	24.7	340	19.6	103	13.5	2.49
Standard reference material	NIST-2711 true (National Institute of Standards and Technology, 2003b)	11150	25	350.4	19.4	105	14	2.6
Standard reference material	Percent recovery	11150	98.8%	97.0%	101.0%	98.1%	96.4%	95.8%
Standard reference material	GSD-5 found	11150	16.9	257	4.2	78.1	14.7	2.37
Standard reference material	GSD-5 true (Potts and others, 1992)	11150	26	243	3.9	75	15.2	2.6
Standard reference material	Percent recovery	11150	65.0%	105.8%	107.7%	104.1%	96.7%	91.2%
Standard reference material	GSD-3 found	11150	12	52.6	6.5	18.6	8.54	1.43
Standard reference material	GSD-3 true (Potts and others, 1992)	11150	22	52	5.4	17.6	9.2	1.86
Standard reference material	Percent recovery	11150	54.5%	101.2%	120.4%	105.7%	92.8%	76.9%

Appendix 4. Quality-assurance and quality-control data for major and trace elements in bed-sediment core samples collected in Lower Granite Reservoir and the Clearwater and Snake Rivers just above their confluence, 2010.—Continued

[Concentrations in micrograms per gram unless otherwise noted; #, number; <, less than lower reporting limit; %, percent; NIST, National Institute of Standards and Technology; --, not analyzed]

Type of quality-control sample	Sample identifier	Set number	Yttrium	Zinc	Antimony	Arsenic	Thorium	Uranium
Standard reference material	MAG-1 found	11150	19.2	132	1	9.2	11.5	2.63
Standard reference material	MAG-1 true (Potts and others, 1992)	11150	28	130	0.96	9.2	11.9	2.7
Standard reference material	Percent recovery	11150	68.6%	101.5%	104.2%	100.0%	96.6%	97.4%
Standard reference material	NIST 8704 found	11150	19.6	385	2.9	16.5	8.3	2.81
Standard reference material	NIST 8704 true (National Institute of Standards and Technology, 2008)	11150	--	408	3.07	--	9.07	3.09
Standard reference material	Percent recovery	11150	--	94.4%	94.5%	--	91.5%	90.9%
Environmental	Core #84 65–75	11637	13.1	54.0	0.38	3.1	5.88	1.59
Laboratory replicate	Core #84 65–75 replicate	11637	12.2	53.4	0.27	3.0	5.93	1.44
Blank	Blank	11637	<0.05	<3	0.2	<1	<0.1	<0.02
Blank	Blank	11637	<0.05	<3	0.05	<1	<0.1	<0.02
Blank	Blank	11637	<0.05	<3	<0.04	<1	<0.1	<0.02
Blank	Blank	11637	<0.05	<3	<0.04	<1	<0.1	<0.02
Blank	Blank	11637	<0.05	<3	0.34	<1	<0.1	<0.02
Standard reference material	MAG-1 found	11637	22.2	142	0.91	9.9	12.9	2.92
Standard reference material	MAG-1 true (Potts and others, 1992)	11637	28.0	130	0.96	9.2	11.9	2.70
Standard reference material	Percent recovery	11637	79.3%	109.2%	94.8%	107.6%	108.4%	108.1%
Standard reference material	NIST 8704 found	11637	22.8	431	3.4	18.2	9.57	3.14
Standard reference material	NIST 8704 true (National Institute of Standards and Technology, 2008)	11637	--	408	3.07	--	9.1	3.09
Standard reference material	Percent recovery	11637	--	105.6%	110.7%	--	105.5%	101.6%
Standard reference material	SCO-1 found	11637	18.7	108	2.6	12.8	10.1	3.02
Standard reference material	SCO-1 true (Potts and others, 1992)	11637	26.0	103	2.50	12.4	9.7	3.00
Standard reference material	Percent recovery	11637	71.9%	104.9%	104.0%	103.2%	104.1%	100.7%
Standard reference material	NIST 2709 found	11637	16.6	114	7.1	19.4	12.1	3.12
Standard reference material	NIST 2709 true (National Institute of Standards and Technology, 2003a)	11637	18.0	106	7.90	17.7	11.0	3.00
Standard reference material	Percent recovery	11637	92.2%	107.5%	89.9%	109.6%	110.0%	104.0%
Standard reference material	GSD-8 found	11637	13.3	47	0.05	2.7	13.5	3.05
Standard reference material	GSD-8 true (Potts and others, 1992)	11637	18.0	43.0	0.24	2.4	13.4	3.00
Standard reference material	Percent recovery	11637	73.9%	109.3%	20.8%	112.5%	100.7%	101.7%
Standard reference material	NIST 2709 found	11637	14.3	99.3	6.7	16.8	10.4	2.78
Standard reference material	NIST 2709 true (National Institute of Standards and Technology, 2003a)	11637	18.0	106	7.90	17.7	11.0	3.00
Standard reference material	Percent recovery	11637	79.4%	93.7%	84.8%	94.9%	94.5%	92.7%

Publishing support provided by
Lafayette Publishing Service Center

Information regarding water resources in Texas is available at
http://tx.usgs.gov/

Braun and others—**Grain-Size Distribution and Selected Major and Trace Element Concentrations in Bed-Sediment Cores**—SIR 2012–5219

ISBN 978-1-4113-3512-7

Printed on recycled paper

Lower Snake River Programmatic Sediment Management Plan Environmental Impact Statement

Appendix M

Sediment Transport in the Lower Snake and Clearwater River Basins, Idaho and Washington

Section 2. Bathymetric and Underwater Video Survey of Lower Granite Reservoir and Vicinity, Washington and Idaho, 2009-10

U.S. Geological Survey

Prepared in Cooperation with the U.S. Army Corps of Engineers

USGS
science for a changing world

Prepared in cooperation with the U.S. Army Corps of Engineers

Bathymetric and Underwater Video Survey of Lower Granite Reservoir and Vicinity, Washington and Idaho, 2009–10

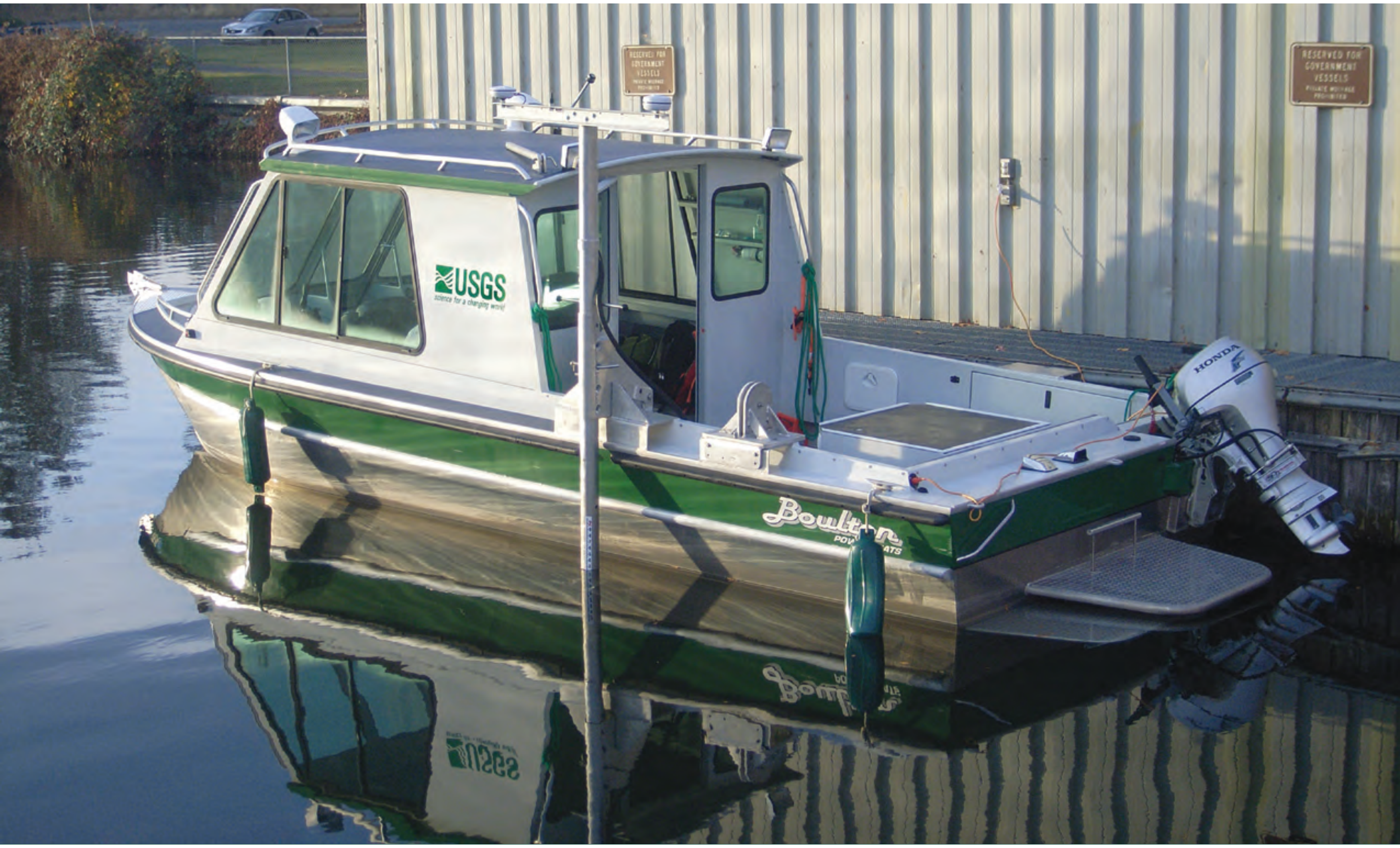

Scientific Investigations Report 2012–5089

U.S. Department of the Interior
U.S. Geological Survey

August 2014

Cover: U.S. Geological Survey hydrographic survey boat (25-foot jet) moored at the U.S. Army Corps of Engineers, Clarkston boat house in preparation for conducting surveys in the Lower Granite Reservoir, Washington.
Photograph taken by Ryan Fosness, U.S. Geological Survey, August 2009.

Bathymetric and Underwater Video Survey of Lower Granite Reservoir and Vicinity, Washington and Idaho, 2009–10

By Marshall L. Williams, Ryan L. Fosness, and Rhonda J. Weakland

Prepared in cooperation with the U.S. Army Corps of Engineers

Scientific Investigations Report 2012–5089

U.S. Department of the Interior
U.S. Geological Survey

U.S. Department of the Interior
KEN SALAZAR, Secretary

U.S. Geological Survey
Marcia K. McNutt, Director

U.S. Geological Survey, Reston, Virginia: 2012

For more information on the USGS—the Federal source for science about the Earth, its natural and living resources, natural hazards, and the environment, visit http://www.usgs.gov or call 1–888–ASK–USGS.

For an overview of USGS information products, including maps, imagery, and publications, visit http://www.usgs.gov/pubprod

To order this and other USGS information products, visit http://store.usgs.gov

Suggested citation:
Williams, M.L., Fosness, R.L., and Weakland, R.J., 2012, Bathymetric and underwater video survey of Lower Granite Reservoir and vicinity, Washington and Idaho, 2009–10: U.S. Geological Survey Scientific Investigations Report 2012–5089, 22 p.

Contents

Figures

Conversion Factors, Datums, and Abbreviations and Acronyms

Conversion Factors

Multiply	By	To obtain
	Length	
inch (in.)	2.54	centimeter (cm)
foot (ft)	0.3048	meter (m)
mile (mi)	1.609	kilometer (km)
	Flow	
million cubic yards per year (Myd^3/yr)	0.7646	million cubic meters per year (Mm^3/yr)

Datums

Vertical coordinate information is referenced to the Washington State Plane South, North American Datum 1983 (NAD 83).

Horizontal coordinate information is referenced to the North American Datum of 1983 (NAD 83).

Elevation, as used in this report, refers to distance above the vertical datum.

Abbreviations and Acronyms

ASCII	American Standard Code for Information Interchange
EM	engineering manual
GIS	Geospatial Information Systems
MBES	multibeam echosounder
QA	quality assurance
QC	quality control
RM	river mile
RTK-GPS	real-time kinematic-global positioning system
USACE	U.S. Army Corps of Engineers
USGS	U.S. Geological Survey
UVM	underwater video mapping

Bathymetric and Underwater Video Survey of Lower Granite Reservoir and Vicinity, Washington and Idaho, 2009–10

By, Marshall L. Williams, Ryan L. Fosness, and Rhonda J. Weakland

Abstract

The U.S. Geological Survey conducted a bathymetric survey of the Lower Granite Reservoir, Washington, using a multibeam echosounder, and an underwater video mapping survey during autumn 2009 and winter 2010. The surveys were conducted as part of the U.S. Army Corps of Engineer's study on sediment deposition and control in the reservoir. The multibeam echosounder survey was performed in 1-mile increments between river mile (RM) 130 and 142 on the Snake River, and between RM 0 and 2 on the Clearwater River. The result of the survey is a digital elevation dataset in ASCII coordinate positioning data (easting, northing, and elevation) useful in rendering a 3×3-foot point grid showing bed elevation and reservoir geomorphology. The underwater video mapping survey was conducted from RM 107.73 to 141.78 on the Snake River and RM 0 to 1.66 on the Clearwater River, along 61 U.S. Army Corps of Engineers established cross sections, and dredge material deposit transects. More than 900 videos and 90 bank photographs were used to characterize the sediment facies and ground-truth the multibeam echosounder data. Combined, the surveys were used to create a surficial sediment facies map that displays type of substrate, level of embeddedness, and presence of silt.

Introduction

As the farthest upstream of four impoundments on the lower Snake River, Lower Granite Reservoir (fig. 1) entraps the greatest volume of sediment flowing out of the upstream drainages—namely the Salmon, Grande Ronde, Imnaha, Clearwater, and the Snake Rivers. According to U.S. Army Corps of Engineers (USACE) (2003) calculations, the yearly sediment deposition into Lower Granite Reservoir has been 2.6 Myd^3/yr since completion of the impoundment in 1975. The USACE goes on to state that sedimentation is affecting the safety of commercial navigation in the Ports of Clarkston and Lewiston and reducing the storage capacity of the reservoir. Any increase in reservoir stage to overcome the effects of sedimentation will reduce the effectiveness of the levees necessary to prevent flooding. Historically, the USACE has dredged the sediment to keep navigation channels clear and to maintain adequate storage capacity. However, in recent years, other Federal agencies, affected Tribes, and special interest groups have questioned whether dredging negatively affects threatened or endangered species. To address these concerns, the USACE initiated a multi-year project to assess the status of sediment deposition in the reservoir, and to explore alternative sediment control measures. The bathymetric and underwater video surveys are a part of that effort.

During autumn 2009 and winter 2010, the U.S. Geological Survey (USGS), in cooperation with the USACE, conducted a hydrographic survey using a multibeam echosounder system (MBES) to develop a digital elevation dataset on 12 river miles of the Snake River, and 2 river miles of the Clearwater River upstream of the confluence with the Snake River (fig. 2). The confluence of the Snake and Clearwater Rivers is a transitional area where the rivers change from a free-flowing environment to one characterized by increased backwater effects created by the Lower Granite Dam. Data from the survey will be used by the USACE to develop a model that can help better understand and estimate sediment transport and deposition in the reservoir as part of its Programmatic Sediment Management Plan (U.S. Army Corps of Engineers, 2003). The digital elevation dataset also can be used to display riverbed elevation, geomorphology (scour holes, rock outcroppings), and bedforms (ripples and dunes) when viewed using a geographic data software. The survey acts as a snapshot of benthic geomorphology that can rapidly change due to reservoir stage, river discharge, and boat traffic.

At the same time that the hydrographic survey was being conducted, the USGS conducted an underwater video mapping (UVM) survey at discrete intervals along historical USACE survey lines and previous dredge-material deposit sites (fig. 3). The UVM survey provided geo-referenced videography that illustrated the type and size of sediment on the surface of the riverbed. The videography also was used to enhance the bathymetric data to create a surficial sediment facies map that the USACE will use to evaluate benthic habitat conditions. This report discusses the methods, equipment, quality assurance, and control information used to conduct the bathymetric and UVM surveys, and presents the results.

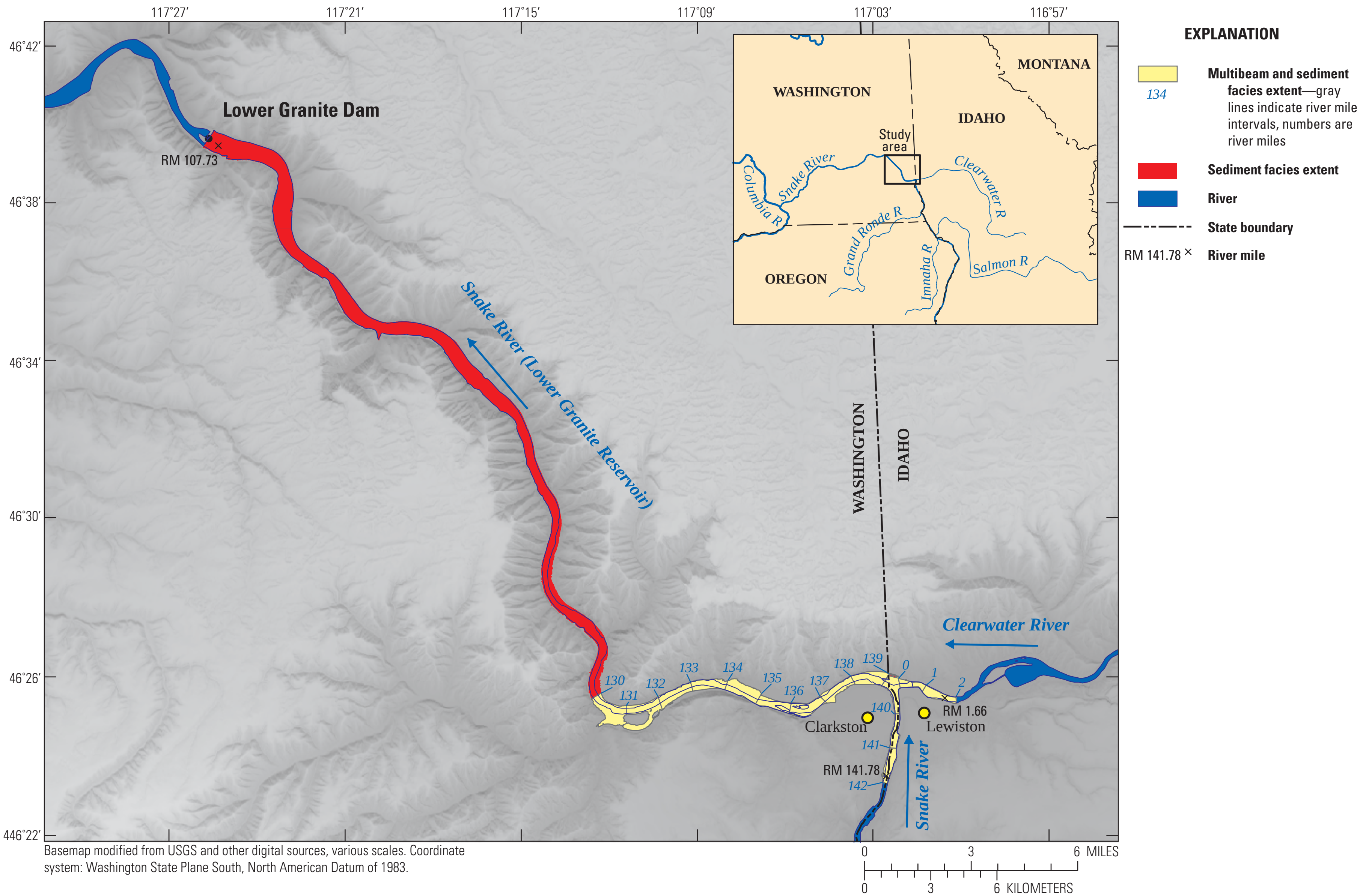

Figure 1. Location of Lower Granite Reservoir study area, Washington and Idaho.

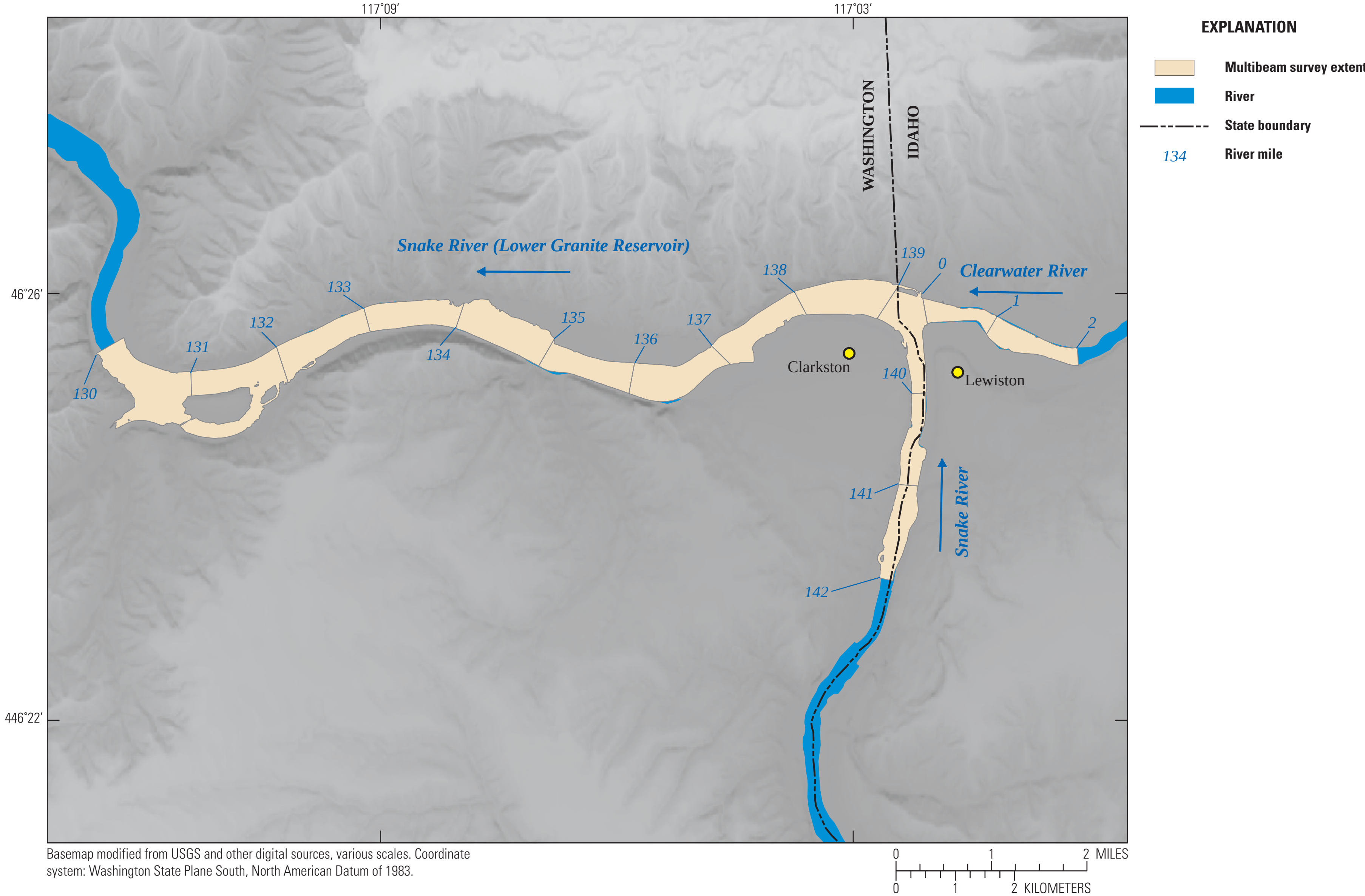

Basemap modified from USGS and other digital sources, various scales. Coordinate system: Washington State Plane South, North American Datum of 1983.

Figure 2. Bathymetric survey extents on the Snake and Clearwater River areas of Lower Granite Reservoir, Washington and Idaho.

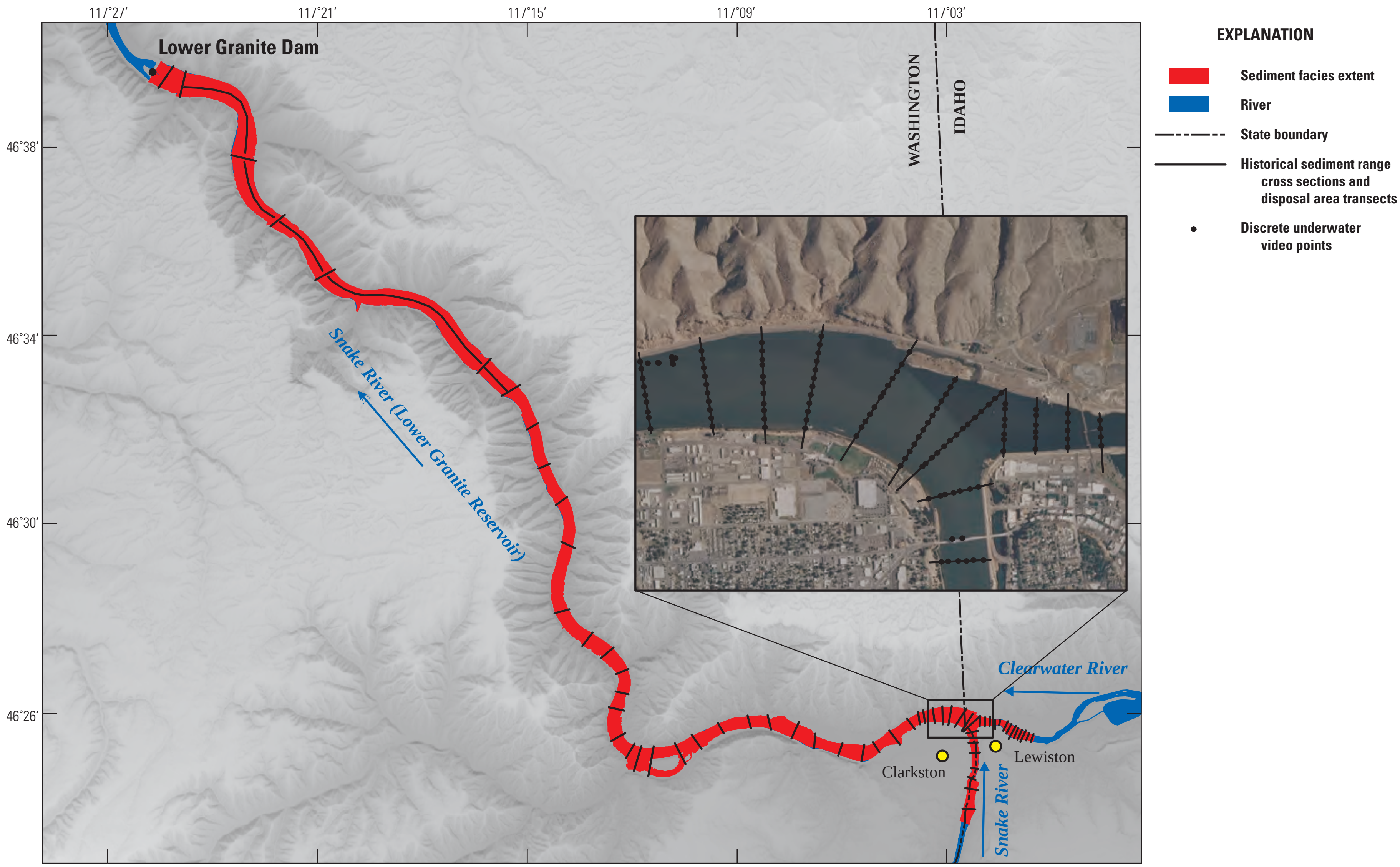

Basemap modified from USGS and other digital sources, various scales. Coordinate system: Washington State Plane South, North American Datum of 1983.

Figure 3. Map and aerial photograph showing underwater video mapping survey extents on the Snake and Clearwater River areas of Lower Granite Reservoir, Washington and Idaho. Historical cross sections are from U.S. Army Corps of Engineers surveys. Discrete underwater videos points are from U.S. Geological Survey mapping.

Multibeam Echosounder Hydrographic Survey

Methods

The hydrographic survey was from river mile (RM) 130 to 142 on the Snake River, and from RM 0 to 2 on the Clearwater River areas of Lower Granite Reservoir (fig. 2). The survey mapped the part of the river that was accessible to the boat and the echosounder equipment, but very shallow areas along the banks that were inaccessible or too shallow to be measured with echosounder equipment were not mapped. The survey was conducted in 1-mile segments, and the data were combined to provide a continuous digital elevation dataset of the reservoir within the limitations of the project (appendix A). The elevation points in the dataset were referenced to the USACE established benchmarks (table A1) using the real-time kinematic–global positioning system (RTK-GPS); therefore, point elevations were unaffected by reservoir stage changes.

Equipment

The bathymetric survey was conducted using state of the art equipment mounted to a 25-ft jet boat designed for hydrographic surveys of rivers and lakes. The hydrographic survey equipment used included an Odom Hydrographic Systems® ES-3 multibeam echosounder transducer capable of producing 480 beams; an International Industries® DSM-10 TSS dynamic motion sensor used to measure vertical displacement and attitude; and an Odom DIGIBAR-Pro profiling sound velocimeter to provide continuous near-surface velocity data. A Hemisphere® VS110 heading and position receiver using two GPS antennas mounted above the echosounder transducer provided precise heading data. RTK-GPS positioning was accomplished using a Trimble® R8/5800 GPS receiver mounted above the echosounder transducer and radio linked to a 35-watt Trimble® HPB450 transmitter to a Trimble® 5700 receiver using a Zephyr Geodedic GPS antenna over various USACE established survey benchmarks in the study area. Benchmarks used during this survey are listed in table A1. The echosounder data were collected using HYPACK® hydrographic survey software. All the raw data were processed through HYSWEEP® collection and editing software to eliminate backscatter distortion and false sounding data.

Quality Control and Quality Assurance

The USACE engineering manual (U.S. Army Corps of Engineers, 2004) provided guidance for quality assurance (QA) and quality control (QC) for this hydrographic survey. The survey team complied with the calibration and control criteria recommended by the manual for general surveys and studies. The sound velocity probes were factory calibrated just prior to the survey. A distilled water calibration assessment of the sound velocity probes also was done monthly, where the performance of the unit at a specific temperature was evaluated against the manufacturer calibration certificate. Sound velocity checks in the water column were conducted twice daily in the survey locations. Bar checks, where a metal plate is suspended by cable to a measured distance below the center or nadir beam of the transducer, were done at the beginning of every survey day to confirm that the system maintained the level of accuracy required by USACE performance standards. Horizontal and vertical accuracy quality assurance checks were done at the beginning and end of each survey day by placing the Trimble® R8/5800 GPS receiver on a 2-meter survey rod at a published benchmark and comparing the measured elevation and horizontal coordinates against published values. Additionally, the RTK-GPS base station antenna was measured at the end of each day and was compared to initial setup values to ensure that the equipment had remained stable throughout the day. The MBES quality assurance performance test was applied during the project to ensure that system performance was within USACE elevation/depth accuracy recommendations. Survey speeds typically were 6–7 knots or less to minimize latency error (the time delay between the measurement and the time when the processed data become available). A detailed description of positional accuracy and the results of the MBES quality assurance performance test are available in the metadata for the hydrographic survey in appendix A.

Results of the Hydrographic Survey

The digital elevation data in appendix A are presented as ASCII coordinate positioning data (easting, northing, and elevation), often referred to as xyz positional data. The survey was conducted using the Washington State Plane South, North American Datum of 1983 (NAD83) horizontal coordinate system in units of U.S. survey feet, and the vertical coordinate system of the North American Vertical Datum of 1988 (NAVD88) in units of U.S. survey feet. The digital elevation dataset consists of more than 1 million points in a 3×3-ft point grid. The primary purpose of these data is to support the USACE's sediment transport modeling effort. However, these data also can provide a visual representation of bed geomorphology useful for other purposes, such as habitat assessment. Figure 4 shows a two-dimensional overhead view of part of the surveyed area and includes areas of dune formation, scour holes, basalt rock formation, and areas where bed material was removed for levee source material.

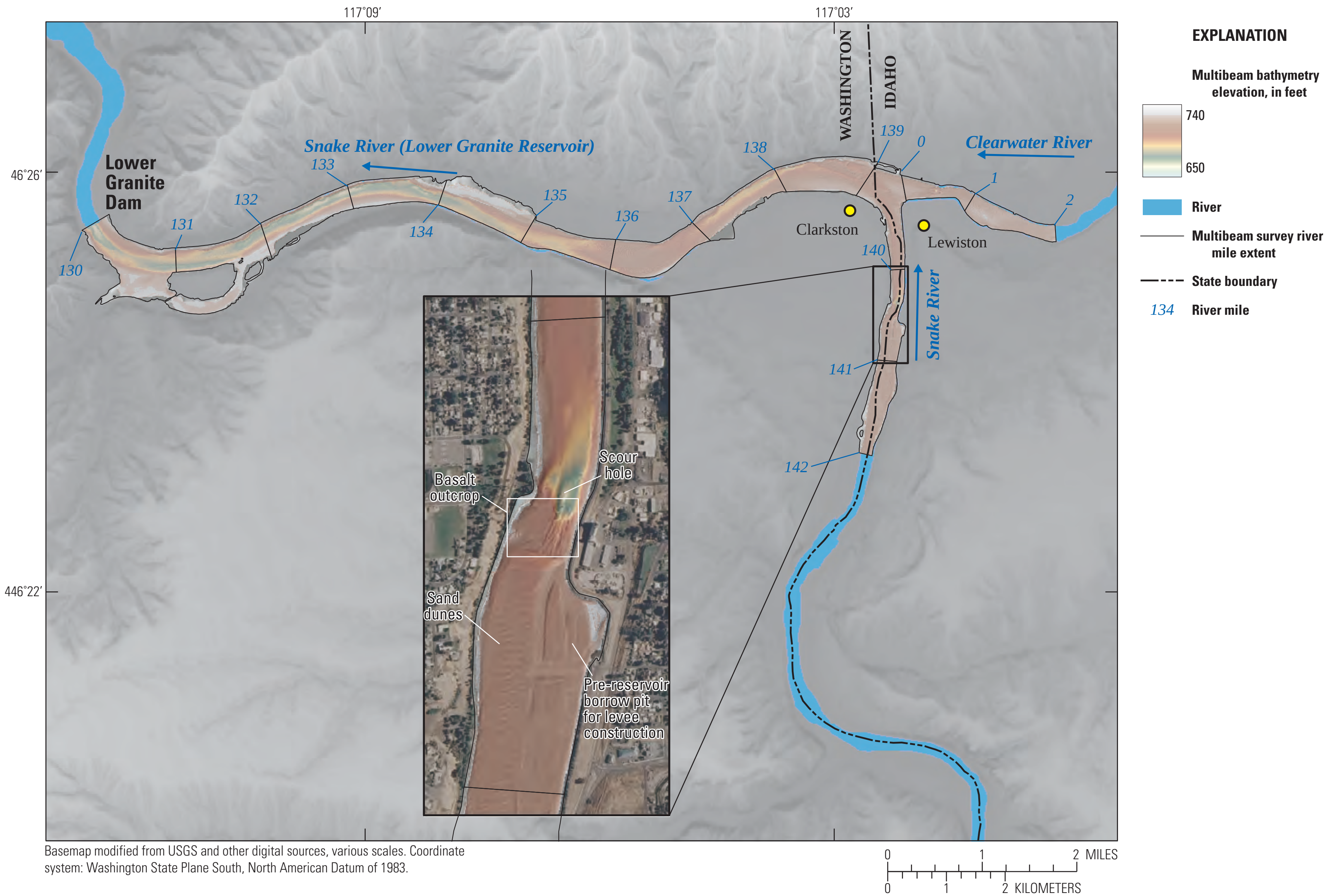

Figure 4. Example of a bathymetric map and bed morphology from the digital dataset, Snake and Clearwater Rivers, Washington and Idaho. Inset is an overhead image of the Snake River near RM 140.

Underwater Video Map Survey

A surficial sediment facies map should be the first step in any geologic study that simulates sediment processes and defines benthic habitats. Traditional facies maps are created by collecting sediment samples from the bed of the water body and analyzing the samples for grain and rock size and sediment type. The level of effort and cost for such an endeavor limits the number of samples available to create the facies map, and much of traditional map detail is through interpolation. Current underwater video technology, coupled with the high-resolution MBES data, allow for much finer detail in creating sediment facies maps. The video record captures the primary attributes of the substrate such as bottom type, texture, small bedforms, indications of disturbance, unusual features, and embeddedness. The video record also provides ground-truthing of the sediment type that may be interpreted from the MBES data. For bedforms that are greater than the field of view of the camera, especially in limited light conditions, the MBES bed elevation data provide the fidelity to define larger geomorphological features. Coupled, the modern technology provides a great deal of data that are useful in creating sediment facies maps.

Methods and Equipment

The underwater digital point video of sediment facies was recorded from RM 107.73 to 141.78 on the Snake River, and between RM 0 and 1.66 on the Clearwater River (fig. 3). Videos of less than 1 minute were recorded at locations spaced approximately every 165 ft along transects previously established by the USACE (fig. 3). These transects included 61 cross sections that had been used previously to measure sediment accumulation for the evaluation of reservoir capacity, and to ensure depths were adequate for river navigation. Five longitudinal dredge material deposit areas also were surveyed. The geographic coordinates for the center point of the transects and disposal lines are defined in appendix B, table B1 for the Clearwater River, and table B2 for the Snake River.

The videos were collected using a tether-suspended, high-resolution color video camera with a 79-degree field of view and 16 white LED variable-intensity lights. Underwater, high-power laser pointers mounted in parallel on the camera housing emitted two laser points with a 4-in. separation on the substrate surface. The laser points provide a reference distance in order to estimate the size of the substrate on the riverbed. The camera was lowered through the water column until it was near the riverbed and recorded video for as much time as was required to characterize the substrate. For quality control, the lasers were adjusted prior to camera deployment by measuring the distance between the laser points, first with the camera positioned at 4 in., and then at 6 ft from a reflective surface to ensure that they were mounted parallel to each other. In areas that were too shallow for the boat to operate safely, geo-tagged bank photographs were taken to show the type of sediment at the edge of water. This information was incorporated into the geospatial information system (GIS) facies map product.

The geographic position of the camera, time of recording, and depth of the water below the boat transom were continuously superimposed on the video recording. Geographic positioning and time of recording was obtained from a Trimble® mapping grade GPS receiver. The depth displayed on the video recording is provided by an echosounder fixed-mounted on the boat hull to provide the approximate depth below the transom in meters.

Data Processing and Analysis

More than 900 video recordings (appendixes C and D) were analyzed to determine the sediment type and level of embeddedness (which indicates whether sand or silt has filled the interstices of coarse material) for each location. Analysis of the recording was used in combination with bathymetry to create a surficial sediment facies map through ESRI ArcGIS® software. Small bedforms (for example, plane bedform or ripples) are listed as a video point attribute in the GIS tables, but are not visually rendered on the map. Larger bedforms, such as dunes, typically are larger than the camera's field of view and are best observed from the bathymetric dataset, or as a layer in the GIS facies map product.

The surficial sediment facies map uses the following rock diameters and sediment classifications to define facies map areas: bedrock, boulder (>10.1 in.), cobble (>2.5–10.1 in.), gravel (>0.08–2.5 in.), sand (0.002–<0.08 in.), silt (<0.002 in.), and riprap material (Wentworth, 1922). For the purposes of this study, the presentation of coarse substrates on the facies map (for example, boulder, cobble, and gravel) were combined into one category because they can change quickly over a small area. The facies map uses different patterns to distinguish between categories and hatching to indicate the presence of fines. An average percent of embeddedness (the percent to which coarse substrate is surrounded or covered by sand or silt) is depicted by a color ramp on the facies map. For example, one color will be used for a 0–20 percent embeddedness range, where little to no observable silt or sand is filling the interstitial spaces or covering the rocks; a different color will depict the range of 81 to 100 percent where the rocks would be nearly or completely covered by fine sediment. The range for each color is provided in the GIS product.

Underwater Video Mapping Survey Results

The UVM survey analysis was used with the bathymetric survey results to create a surficial sediment facies map as a GIS product (example shown in figure 5). The surface substrate type and embeddedness are variable in the upper reach of the study area, although areas downstream of the confluence affected by backwater from the dam may have only fine grain sediments. Use of the bathymetry in creating the GIS facies map allowed for inclusion of bedform features in what otherwise might be considered a featureless bottom, if determined from analysis of the videos alone. When paired, the UVM and MBES surveys provide information on the benthic geomorphology and habitat conditions of the Lower Granite Reservoir at a level that had not been previously attained.

Future Application and Enhancements

The data provided in this report can be useful in numerous ways. Comparative analysis of ASCII elevation dataset with historical surveys can illustrate areas of sediment deposition, changes in channel morphology, assessment of reservoir capacity, and evaluation of levee effectiveness in the area surveyed. Augmentation of these data with hydrologic streamflow data focused in areas of coarse-grained sediment transition to areas of greater embeddedness of fine grain sediments, and then broadly across the study area using acoustic Doppler current profiler technology can help refine sediment transport modeling efforts for a more accurate model.

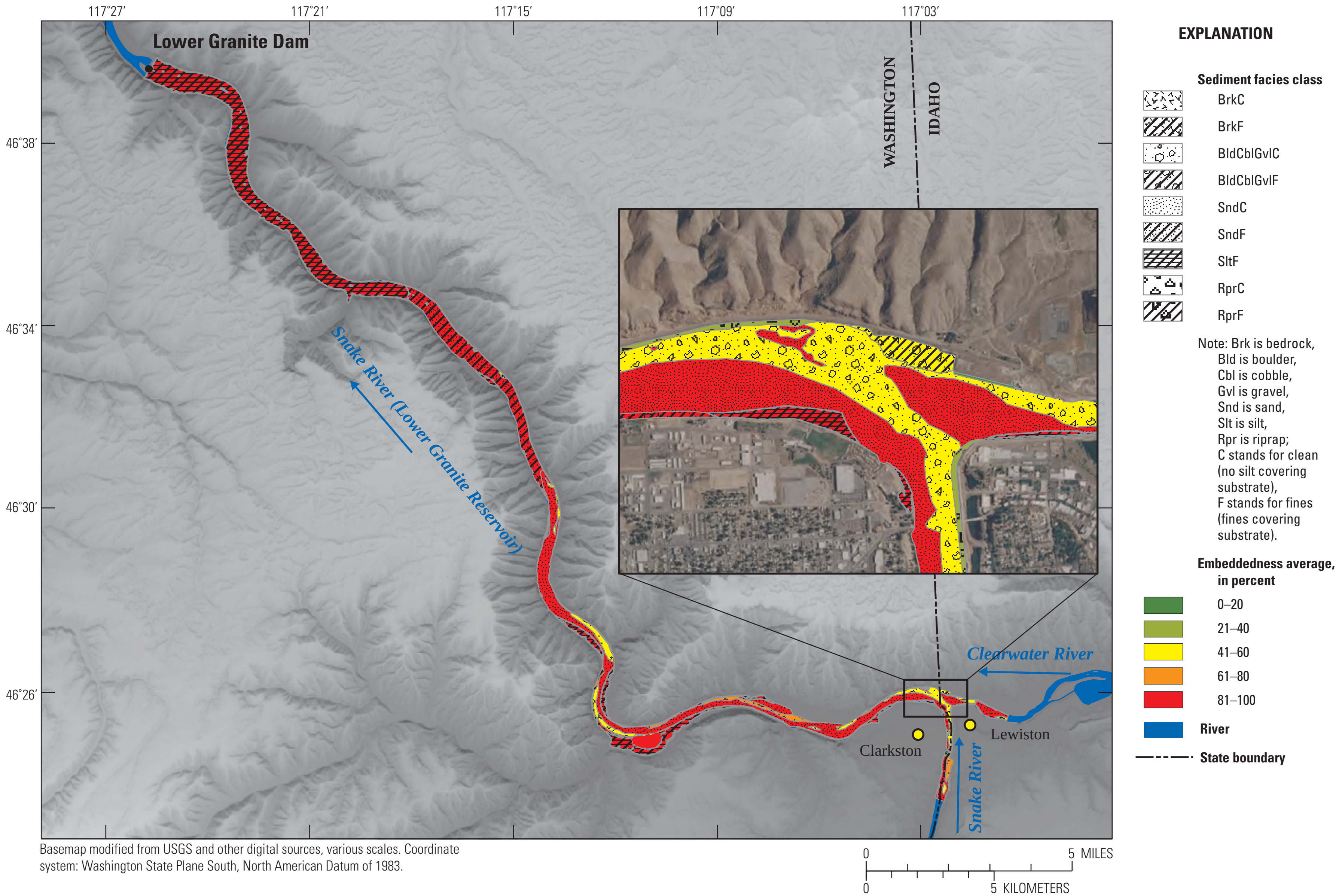

Basemap modified from USGS and other digital sources, various scales. Coordinate system: Washington State Plane South, North American Datum of 1983.

Figure 5. Sample of surficial sediment facies map of the Snake and Clearwater Rivers, Washington and Idaho.

Summary

The U.S. Geological Survey, in cooperation with the U.S. Army Corps of Engineers, conducted a bathymetric survey of the Lower Granite Reservoir, Washington, using a multibeam echosounder, and an underwater video mapping survey during autumn 2009 and winter 2010. The surveys were conducted as part of the U.S. Army Corps of Engineer's study on sediment deposition and control in the reservoir. The multibeam echosounder survey was performed in 1-mile increments between river mile (RM) 130 and 142 on the Snake River, and between RM 0 and 2 on the Clearwater River. The result of the survey is a digital elevation dataset in ASCII coordinate positioning data (easting, northing, and elevation) useful in rendering a 3×3-foot point grid showing bed elevation and reservoir geomorphology. The underwater video mapping survey was conducted from RM 107.73 to 141.78 on the Snake River and RM 0 to 1.66 on the Clearwater River, along 61 U.S. Army Corps of Engineers established cross sections, and dredge material deposit transects. More than 900 videos and 90 bank photographs were used to characterize the sediment facies and ground-truth the multibeam echosounder data. Combined, the surveys were used to create a surficial sediment facies map that displays type of substrate type, level of embeddedness, and presence of silt.

Acknowledgments

The authors and field personnel offer a special thanks to the USACE Clarkston Natural Resources Office staff for their gracious support in providing boat mooring, equipment storage, and the use of their facilities for the duration of this study.

References Cited

U.S. Army Corps of Engineers, 2003, Supplemental environmental analysis for the purposes of 2003–2004 dredging (Lower Snake and Clearwater Rivers, Washington and Idaho): U.S. Army Corps of Engineers, Walla Walla District, 100 p.

U.S. Army Corps of Engineers, 2004, Engineering and design—Hydrographic surveying: Washington, D.C., U.S. Army Corps of Engineers, EM 1110-2-1003, Change 1.

Wentworth, C.K., 1922, A scale of grade and class terms for clastic sediments: The Journal of Geology, v. 30, p. 377–392.

Appendix A. Multibeam Echosounder Data and Sediment Facies Map

Snake and Clearwater River Multibeam Echosounder Data

ASCII XYZ position and elevation data Metadata

Snake and Clearwater River Sediment Facies Map

GIS files for map

Table A1. Survey benchmarks.

Point listing name	Northing	Easting	Elevation (feet)
R21-RA	410565.402	2513935.089	747.97
R24-LA	416395.56	2513025.92	743.82
R27A-RA	415223.29	2501208.87	745.85
R28A-RA	415109.67	2497368.67	746.65
R29D-RA	417580.451	2481859.809	748.38
R31-LA	413164.38	2473552.19	764.35

This page left intentionally blank

Appendix B. Underwater Video Mapping Survey Transect Tables

Table B1. Underwater video mapping, Clearwater River, Idaho.

River mile	Type	Length (feet)	Easting (feet, Washington State Plane South)	Northing (feet, Washington State Plane South)
0.28	Cross section	1,310	2514558.108	417877.3041
0.41	Cross section	1,089	2515168.939	417818.9142
0.53	Cross section	1,130	2515783.093	417869.1791
0.67	Cross section	1,141	2516432.022	417492.1168
0.78	Cross section	748.9	2517019.141	417722.1255
0.92	Cross section	1,312	2517759.454	417280.8562
1.06	Cross section	1,367	2518167.193	416938.5179
1.16	Cross section	1,890	2518578.477	416488.9467
1.26	Cross section	1,427	2519071.113	416397.1885
1.36	Cross section	1,376	2519526.546	416213.3064
1.47	Cross section	1,610	2519954.69	416008.4692
1.56	Cross section	1,013	2520523.993	415947.9729
1.66	Cross section	1,094	2521074.225	415765.7706

Table B2. Underwater video mapping, Snake River, Washington.

River mile	Type	Length (feet)	Easting (feet, Washington State Plane South)	Northing (feet, Washington State Plane South)
107.73	Cross section	3,336	2412915.649	498263.0819
108.31	Cross section	3,280	2415041.396	497375.0198
110.00	Disposal line	14,050	2421886.205	495449.1141
111.24	Cross section	3,180	2422610.341	488148.1157
112.00	Disposal line	8,223	2423706.247	483667.758
113.12	Cross section	2,305	2426871.145	480340.8725
114.00	Disposal line	8,222	2430353.614	477579.0884
114.92	Cross section	2,801	2432785.091	473595.1037
117.00	Disposal line	23,210	2443999.23	470331.3617
119.56	Cross section	2,484	2452639.727	462208.8201
120.00	Disposal line	4,181	2454107.987	460527.9898
120.46	Cross section	2,731	2455978.219	459152.517
121.42	Cross section	1,665	2458714.545	454689.9359
122.69	Cross section	1,565	2460142.018	449702.9212
123.30	Cross section	1,756	2462311.381	445358.4231
124.94	Cross section	1,861	2463125.525	439871.907
126.07	Cross section	1,933	2462355.905	431585.1297
127.03	Cross section	2,126	2465565.422	428106.331
127.63	Cross section	2,117	2468000.434	426400.7354
128.27	Cross section	1,707	2469877.035	424065.6926
128.87	Cross section	1,629	2469865.525	421412.4978
129.27	Cross section	1,964	2469168.541	419409.8057
130.00	Cross section	2,066	2469368.937	415882.2926
130.44	Cross section	2,122	2470885.387	414174.117
130.66	Cross section	3,262	2471823.859	413224.3367
130.93	Cross section	3,807	2473487.722	412867.8886
131.62	Cross section	2,910	2477144.328	413829.3271

Table B2. Underwater video mapping, Snake River, Washington.—Continued

River mile	Type	Length (feet)	Easting (feet, Washington State Plane South)	Northing (feet, Washington State Plane South)
132.05	Cross section	2,148	2479188.89	415323.0343
132.71	Cross section	1,508	2482183.778	417030.3178
133.41	Cross section	1,676	2485753.914	417787.6633
133.98	Cross section	1,881	2488262.078	417740.6446
134.58	Cross section	2,221	2491484.273	416732.1745
135.15	Cross section	1,860	2493916.474	415403.1546
135.76	Cross section	1,655	2497120.087	414373.0329
136.29	Cross section	2,153	2499947.688	413917.833
136.69	Cross section	1,519	2501598.19	414622.2821
137.17	Cross section	2,211	2503894.728	415850.9087
137.69	Cross section	1,604	2505944.024	417545.031
137.94	Cross section	1,584	2506938.931	418253.5856
138.07	Cross section	1,575	2507593.291	418451.1655
138.34	Cross section	1,895	2508786.328	418586.1987
138.52	Cross section	2,251	2509885.094	418603.3159
138.71	Cross section	2,420	2510836.798	418576.519
138.94	Cross section	2,737	2512123.787	418309.8488
139.22	Cross section	2,483	2512976.353	417722.8096
139.29	Cross section	2,866	2513520.537	417544.379
139.43	Cross section	1,488	2513607.366	416528.4698
139.64	Cross section	1,178	2513698.334	415196.6179
139.91	Cross section	1,260	2513933.03	413932.7433
140.22	Cross section	916.6	2513876.90	411988.059
140.51	Cross section	1,022	2513556.897	410720.6452
140.75	Cross section	1,588	2513500.822	409394.7468
141.21	Cross section	1,619	2513167.011	406918.5852

Appendix C. Underwater Video Mapping Survey Videos

Table C1. Underwater videos, Clearwater River, Idaho, October 20, 2009.

[Maps and associated videos can be viewed in figures C1–C26, available at http://pubs.usgs.gov/sir/2012/5089]

10202009-2.mp4	10202009-23.mp4	10202009-44.mp4	10202009-65.mp4
10202009-3.mp4	10202009-24.mp4	10202009-45.mp4	10202009-66.mp4
10202009-4.mp4	10202009-25.mp4	10202009-46.mp4	10202009-67.mp4
10202009-5.mp4	10202009-26.mp4	10202009-47.mp4	10202009-68.mp4
10202009-6.mp4	10202009-27.mp4	10202009-48.mp4	10202009-69.mp4
10202009-7.mp4	10202009-28.mp4	10202009-49.mp4	10202009-70.mp4
10202009-8.mp4	10202009-29.mp4	10202009-50.mp4	10202009-71.mp4
10202009-9.mp4	10202009-30.mp4	10202009-51.mp4	10202009-72.mp4
10202009-10.mp4	10202009-31.mp4	10202009-52.mp4	10202009-73.mp4
10202009-11.mp4	10202009-32.mp4	10202009-53.mp4	10202009-74.mp4
10202009-12.mp4	10202009-33.mp4	10202009-54.mp4	10202009-75.mp4
10202009-13.mp4	10202009-34.mp4	10202009-55.mp4	10202009-76.mp4
10202009-14.mp4	10202009-35.mp4	10202009-56.mp4	10202009-77.mp4
10202009-15.mp4	10202009-36.mp4	10202009-57.mp4	10202009-78.mp4
10202009-16.mp4	10202009-37.mp4	10202009-58.mp4	10202009-79.mp4
10202009-17.mp4	10202009-38.mp4	10202009-59.mp4	10202009-80.mp4
10202009-18.mp4	10202009-39.mp4	10202009-60.mp4	10202009-81.mp4
10202009-19.mp4	10202009-40.mp4	10202009-61.mp4	10202009-82.mp4
10202009-20.mp4	10202009-41.mp4	10202009-62.mp4	
10202009-21.mp4	10202009-42.mp4	10202009-63.mp4	
10202009-22.mp4	10202009-43.mp4	10202009-64.mp4	

Table C2. Underwater videos, Snake River, Washington, October 21, 2009.

[Maps and associated videos can be viewed in figures C1–C26, available at http://pubs.usgs.gov/sir/2012/5089]

10212009-2.mp4	10212009-44.mp4	10212009-87.mp4	10212009-130.mp4
10212009-3.mp4	10212009-45.mp4	10212009-88.mp4	10212009-130.mp4
10212009-4.mp4	10212009-46.mp4	10212009-89.mp4	10212009-131.mp4
10212009-5.mp4	10212009-47.mp4	10212009-90.mp4	10212009-132.mp4
10212009-6.mp4	10212009-48.mp4	10212009-91.mp4	10212009-133.mp4
10212009-7.mp4	10212009-49.mp4	10212009-92.mp4	10212009-134.mp4
10212009-8.mp4	10212009-50.mp4	10212009-93.mp4	10212009-135.mp4
10212009-9.mp4	10212009-51.mp4	10212009-94.mp4	10212009-136.mp4
10212009-10.mp4	10212009-52.mp4	10212009-95.mp4	10212009-137.mp4
10212009-11.mp4	10212009-53.mp4	10212009-96.mp4	10212009-138.mp4
10212009-12.mp4	10212009-54.mp4	10212009-97.mp4	10212009-139.mp4
10212009-13.mp4	10212009-55.mp4	10212009-98.mp4	10212009-140.mp4
10212009-14.mp4	10212009-56.mp4	10212009-99.mp4	10212009-141.mp4
10212009-15.mp4	10212009-57.mp4	10212009-100.mp4	10212009-142.mp4
10212009-16.mp4	10212009-58.mp4	10212009-101.mp4	10212009-143.mp4
10212009-17.mp4	10212009-59.mp4	10212009-102.mp4	10212009-144.mp4
10212009-18.mp4	10212009-60.mp4	10212009-103.mp4	10212009-145.mp4
10212009-19.mp4	10212009-61.mp4	10212009-104.mp4	10212009-146.mp4
10212009-20.mp4	10212009-62.mp4	10212009-105.mp4	10212009-147.mp4
10212009-21.mp4	10212009-63.mp4	10212009-106.mp4	10212009-148.mp4
10212009-22.mp4	10212009-64.mp4	10212009-107.mp4	10212009-149.mp4
10212009-23.mp4	10212009-65.mp4	10212009-108.mp4	10212009-150.mp4
10212009-24.mp4	10212009-66.mp4	10212009-109.mp4	10212009-151.mp4
10212009-25.mp4	10212009-68.mp4	10212009-110.mp4	10212009-152.mp4
10212009-26.mp4	10212009-69.mp4	10212009-111.mp4	10212009-153.mp4
10212009-27.mp4	10212009-70.mp4	10212009-112.mp4	10212009-154.mp4
10212009-28.mp4	10212009-71.mp4	10212009-113.mp4	10212009-155.mp4
10212009-29.mp4	10212009-72.mp4	10212009-114.mp4	10212009-156.mp4
10212009-30.mp4	10212009-73.mp4	10212009-115.mp4	10212009-157.mp4
10212009-31.mp4	10212009-74.mp4	10212009-116.mp4	10212009-158.mp4
10212009-32.mp4	10212009-75.mp4	10212009-117.mp4	10212009-159.mp4
10212009-33.mp4	10212009-76.mp4	10212009-118.mp4	10212009-160.mp4
10212009-34.mp4	10212009-77.mp4	10212009-119.mp4	10212009-161.mp4
10212009-35.mp4	10212009-78.mp4	10212009-120.mp4	10212009-162.mp4
10212009-36.mp4	10212009-79.mp4	10212009-121.mp4	10212009-163.mp4
10212009-37.mp4	10212009-80.mp4	10212009-122.mp4	10212009-164.mp4
10212009-38.mp4	10212009-81.mp4	10212009-123.mp4	10212009-165.mp4
10212009-39.mp4	10212009-82.mp4	10212009-124.mp4	10212009-166.mp4
10212009-40.mp4	10212009-83.mp4	10212009-125.mp4	10212009-167.mp4
10212009-41.mp4	10212009-84.mp4	10212009-126.mp4	10212009-168.mp4
10212009-42.mp4	10212009-85.mp4	10212009-127.mp4	10212009-169.mp4
10212009-43.mp4	10212009-86.mp4	10212009-128.mp4	10212009-170.mp4
		10212009-129.mp4	

Table C3. Underwater videos, Snake River, Washington, October 22, 2009.

[Maps and associated videos can be viewed in figures C1–C26, available at http://pubs.usgs.gov/sir/2012/5089]

10222009-2.mp4	10222009-53.mp4	10222009-105.mp4	10222009-157.mp4
10222009-3.mp4	10222009-54.mp4	10222009-106.mp4	10222009-158.mp4
10222009-4.mp4	10222009-55.mp4	10222009-107.mp4	10222009-159.mp4
10222009-5.mp4	10222009-56.mp4	10222009-108.mp4	10222009-160.mp4
10222009-6.mp4	10222009-57.mp4	10222009-109.mp4	10222009-161.mp4
10222009-7.mp4	10222009-58.mp4	10222009-110.mp4	10222009-162.mp4
10222009-8.mp4	10222009-59.mp4	10222009-111.mp4	10222009-163.mp4
10222009-9.mp4	10222009-60.mp4	10222009-112.mp4	10222009-164.mp4
10222009-10.mp4	10222009-61.mp4	10222009-113.mp4	10222009-165.mp4
10222009-11.mp4	10222009-62.mp4	10222009-114.mp4	10222009-166.mp4
10222009-12.mp4	10222009-63.mp4	10222009-115.mp4	10222009-167.mp4
10222009-13.mp4	10222009-64.mp4	10222009-116.mp4	10222009-168.mp4
10222009-14.mp4	10222009-65.mp4	10222009-117.mp4	10222009-169.mp4
10222009-15.mp4	10222009-66.mp4	10222009-118.mp4	10222009-170.mp4
10222009-16.mp4	10222009-67.mp4	10222009-119.mp4	10222009-171.mp4
10222009-17.mp4	10222009-68.mp4	10222009-120.mp4	10222009-172.mp4
10222009-18.mp4	10222009-69.mp4	10222009-121.mp4	10222009-173.mp4
10222009-19.mp4	10222009-70.mp4	10222009-122.mp4	10222009-174.mp4
10222009-20.mp4	10222009-71.mp4	10222009-123.mp4	10222009-175.mp4
10222009-21.mp4	10222009-72.mp4	10222009-124.mp4	10222009-176.mp4
10222009-22.mp4	10222009-73.mp4	10222009-125.mp4	10222009-177.mp4
10222009-23.mp4	10222009-74.mp4	10222009-126.mp4	10222009-178.mp4
10222009-24.mp4	10222009-75.mp4	10222009-127.mp4	10222009-179.mp4
10222009-25.mp4	10222009-76.mp4	10222009-128.mp4	10222009-180.mp4
10222009-26.mp4	10222009-77.mp4	10222009-129.mp4	10222009-181.mp4
10222009-27.mp4	10222009-78.mp4	10222009-130.mp4	10222009-182.mp4
10222009-28.mp4	10222009-79.mp4	10222009-131.mp4	10222009-183.mp4
10222009-29.mp4	10222009-80.mp4	10222009-132.mp4	10222009-184.mp4
10222009-30.mp4	10222009-81.mp4	10222009-133.mp4	10222009-185.mp4
10222009-31.mp4	10222009-82.mp4	10222009-134.mp4	10222009-186.mp4
10222009-32.mp4	10222009-83.mp4	10222009-135.mp4	10222009-187.mp4
10222009-33.mp4	10222009-84.mp4	10222009-136.mp4	10222009-188.mp4
10222009-34.mp4	10222009-85.mp4	10222009-137.mp4	10222009-189.mp4
10222009-35.mp4	10222009-86.mp4	10222009-138.mp4	10222009-190.mp4
10222009-36.mp4	10222009-87.mp4	10222009-139.mp4	10222009-191.mp4
10222009-37.mp4	10222009-88.mp4	10222009-140.mp4	10222009-192.mp4
10222009-38.mp4	10222009-89.mp4	10222009-141.mp4	10222009-193.mp4
10222009-39.mp4	10222009-90.mp4	10222009-142.mp4	10222009-194.mp4
10222009-40.mp4	10222009-91.mp4	10222009-143.mp4	10222009-195.mp4
10222009-41.mp4	10222009-92.mp4	10222009-144.mp4	10222009-196.mp4
10222009-42.mp4	10222009-93.mp4	10222009-145.mp4	10222009-197.mp4
10222009-43.mp4	10222009-94.mp4	10222009-146.mp4	10222009-198.mp4
10222009-44.mp4	10222009-95.mp4	10222009-147.mp4	10222009-199.mp4
10222009-45.mp4	10222009-96.mp4	10222009-148.mp4	10222009-200.mp4
10222009-46.mp4	10222009-97.mp4	10222009-149.mp4	10222009-201.mp4
10222009-47.mp4	10222009-98.mp4	10222009-150.mp4	10222009-202.mp4
10222009-48.mp4	10222009-99.mp4	10222009-151.mp4	10222009-203.mp4
10222009-49.mp4	10222009-100.mp4	10222009-152.mp4	10222009-204.mp4
10222009-50.mp4	10222009-101.mp4	10222009-153.mp4	10222009-205.mp4
10222009-51.mp4	10222009-102.mp4	10222009-154.mp4	10222009-206.mp4
10222009-52.mp4	10222009-103.mp4	10222009-155.mp4	10222009-207.mp4
	10222009-104.mp4	10222009-156.mp4	

Table C4. Underwater videos, Snake River, Washington, February 1, 2010.

[Maps and associated videos can be viewed in figures C1–C26, available at http://pubs.usgs.gov/sir/2012/5089]

02012010-2.mp4	02012010-36.mp4	02012010-71.mp4	02012010-106.mp4
02012010-3.mp4	02012010-37.mp4	02012010-72.mp4	02012010-107.mp4
02012010-4.mp4	02012010-38.mp4	02012010-73.mp4	02012010-108.mp4
02012010-5.mp4	02012010-39.mp4	02012010-74.mp4	02012010-109.mp4
02012010-6.mp4	02012010-40.mp4	02012010-75.mp4	02012010-110.mp4
02012010-7.mp4	02012010-41.mp4	02012010-76.mp4	02012010-111.mp4
02012010-9.mp4	02012010-42.mp4	02012010-77.mp4	02012010-112.mp4
02012010-10.mp4	02012010-43.mp4	02012010-78.mp4	02012010-113.mp4
02012010-11.mp4	02012010-44.mp4	02012010-79.mp4	02012010-114.mp4
02012010-12.mp4	02012010-45.mp4	02012010-80.mp4	02012010-115.mp4
02012010-13.mp4	02012010-46.mp4	02012010-81.mp4	02012010-116.mp4
02012010-14.mp4	02012010-47.mp4	02012010-82.mp4	02012010-117.mp4
02012010-15.mp4	02012010-48.mp4	02012010-83.mp4	02012010-118.mp4
02012010-16.mp4	02012010-49.mp4	02012010-84.mp4	02012010-119.mp4
02012010-17.mp4	02012010-50.mp4	02012010-85.mp4	02012010-120.mp4
02012010-18.mp4	02012010-51.mp4	02012010-86.mp4	02012010-121.mp4
02012010-19.mp4	02012010-52.mp4	02012010-87.mp4	02012010-122.mp4
02012010-20.mp4	02012010-53.mp4	02012010-88.mp4	02012010-123.mp4
02012010-21.mp4	02012010-54.mp4	02012010-89.mp4	02012010-124.mp4
02012010-22.mp4	02012010-55.mp4	02012010-90.mp4	02012010-125.mp4
02012010-23.mp4	02012010-56.mp4	02012010-91.mp4	02012010-126.mp4
02012010-24.mp4	02012010-57.mp4	02012010-92.mp4	02012010-127.mp4
02012010-25.mp4	02012010-58.mp4	02012010-93.mp4	02012010-128.mp4
02012010-26.mp4	02012010-59.mp4	02012010-94.mp4	02012010-129.mp4
02012010-27.mp4	02012010-60.mp4	02012010-95.mp4	02012010-130.mp4
02012010-28.mp4	02012010-61.mp4	02012010-96.mp4	02012010-131.mp4
02012010-29.mp4	02012010-62.mp4	02012010-97.mp4	02012010-132.mp4
02012010-30.mp4	02012010-63.mp4	02012010-98.mp4	02012010-133.mp4
02012010-31.mp4	02012010-64.mp4	02012010-99.mp4	02012010-134.mp4
02012010-32.mp4	02012010-65.mp4	02012010-100.mp4	02012010-135.mp4
02012010-33.mp4	02012010-66.mp4	02012010-101.mp4	02012010-137.mp4
02012010-34.mp4	02012010-67.mp4	02012010-102.mp4	02012010-138.mp4
02012010-35.mp4	02012010-68.mp4	02012010-103.mp4	02012010-139.mp4
	02012010-70.mp4	02012010-104.mp4	
		02012010-105.mp4	

Table C5. Underwater videos, Snake River, Washington, February 2, 2010.

[Maps and associated videos can be viewed in figures C1–C26, available at http://pubs.usgs.gov/sir/2012/5089]

02022010-2.mp4	02022010-45.mp4	02022010-89.mp4	02022010-133.mp4
02022010-3.mp4	02022010-46.mp4	02022010-90.mp4	02022010-134.mp4
02022010-4.mp4	02022010-47.mp4	02022010-91.mp4	02022010-135.mp4
02022010-5.mp4	02022010-48.mp4	02022010-92.mp4	02022010-136.mp4
02022010-6.mp4	02022010-49.mp4	02022010-93.mp4	02022010-137.mp4
02022010-7.mp4	02022010-50.mp4	02022010-94.mp4	02022010-138.mp4
02022010-8.mp4	02022010-51.mp4	02022010-95.mp4	02022010-139.mp4
02022010-9.mp4	02022010-52.mp4	02022010-96.mp4	02022010-140.mp4
02022010-10.mp4	02022010-53.mp4	02022010-97.mp4	02022010-141.mp4
02022010-11.mp4	02022010-54.mp4	02022010-98.mp4	02022010-142.mp4
02022010-12.mp4	02022010-55.mp4	02022010-99.mp4	02022010-143.mp4
02022010-13.mp4	02022010-56.mp4	02022010-100.mp4	02022010-144.mp4
02022010-14.mp4	02022010-57.mp4	02022010-101.mp4	02022010-145.mp4
02022010-15.mp4	02022010-58.mp4	02022010-102.mp4	02022010-146.mp4
02022010-16.mp4	02022010-59.mp4	02022010-103.mp4	02022010-147.mp4
02022010-17.mp4	02022010-60.mp4	02022010-104.mp4	02022010-148.mp4
02022010-18.mp4	02022010-61.mp4	02022010-105.mp4	02022010-149.mp4
02022010-19.mp4	02022010-62.mp4	02022010-106.mp4	02022010-150.mp4
02022010-20.mp4	02022010-63.mp4	02022010-107.mp4	02022010-151.mp4
02022010-21.mp4	02022010-64.mp4	02022010-108.mp4	02022010-152.mp4
02022010-22.mp4	02022010-65.mp4	02022010-109.mp4	02022010-153.mp4
02022010-23.mp4	02022010-66.mp4	02022010-110.mp4	02022010-154.mp4
02022010-24.mp4	02022010-67.mp4	02022010-111.mp4	02022010-155.mp4
02022010-25.mp4	02022010-68.mp4	02022010-112.mp4	02022010-156.mp4
02022010-26.mp4	02022010-69.mp4	02022010-113.mp4	02022010-157.mp4
02022010-27.mp4	02022010-70.mp4	02022010-114.mp4	02022010-158.mp4
02022010-28.mp4	02022010-71.mp4	02022010-115.mp4	02022010-159.mp4
02022010-29.mp4	02022010-72.mp4	02022010-116.mp4	02022010-160.mp4
02022010-30.mp4	02022010-73.mp4	02022010-117.mp4	02022010-161.mp4
02022010-31.mp4	02022010-74.mp4	02022010-118.mp4	02022010-162.mp4
02022010-32.mp4	02022010-75.mp4	02022010-119.mp4	02022010-163.mp4
02022010-33.mp4	02022010-76.mp4	02022010-120.mp4	02022010-164.mp4
02022010-34.mp4	02022010-77.mp4	02022010-121.mp4	02022010-165.mp4
02022010-35.mp4	02022010-78.mp4	02022010-122.mp4	02022010-166.mp4
02022010-36.mp4	02022010-79.mp4	02022010-123.mp4	02022010-167.mp4
02022010-37.mp4	02022010-80.mp4	02022010-124.mp4	02022010-168.mp4
02022010-38.mp4	02022010-81.mp4	02022010-125.mp4	02022010-169.mp4
02022010-39.mp4	02022010-82.mp4	02022010-126.mp4	02022010-170.mp4
02022010-40.mp4	02022010-83.mp4	02022010-127.mp4	02022010-171.mp4
02022010-41.mp4	02022010-84.mp4	02022010-128.mp4	02022010-172.mp4
02022010-42.mp4	02022010-85.mp4	02022010-129.mp4	02022010-173.mp4
02022010-43.mp4	02022010-86.mp4	02022010-130.mp4	02022010-174.mp4
02022010-44.mp4	02022010-87.mp4	02022010-131.mp4	02022010-175.mp4
	02022010-88.mp4	02022010-132.mp4	

Table C6. Underwater videos, Snake River, Washington, February 3, 2010.

[Maps and associated videos can be viewed in figures C1–C26, available at http://pubs.usgs.gov/sir/2012/5089]

02032010-3.mp4	02032010-42.mp4	02032010-83.mp4	02032010-125.mp4
02032010-4.mp4	02032010-43.mp4	02032010-84.mp4	02032010-126.mp4
02032010-5.mp4	02032010-45.mp4	02032010-85.mp4	02032010-127.mp4
02032010-6.mp4	02032010-46.mp4	02032010-86.mp4	02032010-128.mp4
02032010-7.mp4	02032010-47.mp4	02032010-87.mp4	02032010-129.mp4
02032010-8.mp4	02032010-48.mp4	02032010-88.mp4	02032010-130.mp4
02032010-9.mp4	02032010-49.mp4	02032010-89.mp4	02032010-131.mp4
02032010-10.mp4	02032010-50.mp4	02032010-90.mp4	02032010-132.mp4
02032010-11.mp4	02032010-51.mp4	02032010-91.mp4	02032010-133.mp4
02032010-12.mp4	02032010-52.mp4	02032010-92.mp4	02032010-134.mp4
02032010-13.mp4	02032010-53.mp4	02032010-93.mp4	02032010-135.mp4
02032010-14.mp4	02032010-54.mp4	02032010-94.mp4	02032010-136.mp4
02032010-15.mp4	02032010-55.mp4	02032010-95.mp4	02032010-137.mp4
02032010-16.mp4	02032010-56.mp4	02032010-96.mp4	02032010-138.mp4
02032010-17.mp4	02032010-57.mp4	02032010-97.mp4	02032010-139.mp4
02032010-18.mp4	02032010-58.mp4	02032010-98.mp4	02032010-140.mp4
02032010-19.mp4	02032010-59.mp4	02032010-99.mp4	02032010-141.mp4
02032010-20.mp4	02032010-60.mp4	02032010-100.mp4	02032010-142.mp4
02032010-21.mp4	02032010-61.mp4	02032010-101.mp4	02032010-143.mp4
02032010-22.mp4	02032010-62.mp4	02032010-102.mp4	02032010-144.mp4
02032010-23.mp4	02032010-63.mp4	02032010-103.mp4	02032010-145.mp4
02032010-24.mp4	02032010-64.mp4	02032010-104.mp4	02032010-146.mp4
02032010-25.mp4	02032010-65.mp4	02032010-105.mp4	02032010-147.mp4
02032010-26.mp4	02032010-66.mp4	02032010-106.mp4	02032010-148.mp4
02032010-27.mp4	02032010-67.mp4	02032010-107.mp4	02032010-149.mp4
02032010-28.mp4	02032010-68.mp4	02032010-108.mp4	02032010-150.mp4
02032010-29.mp4	02032010-69.mp4	02032010-109.mp4	02032010-151.mp4
02032010-30.mp4	02032010-70.mp4	02032010-110.mp4	02032010-152.mp4
02032010-31.mp4	02032010-71.mp4	02032010-111.mp4	02032010-153.mp4
02032010-32.mp4	02032010-72.mp4	02032010-112.mp4	02032010-154.mp4
02032010-33.mp4	02032010-73.mp4	02032010-113.mp4	02032010-155.mp4
02032010-34.mp4	02032010-74.mp4	02032010-114.mp4	02032010-156.mp4
02032010-35.mp4	02032010-75.mp4	02032010-115.mp4	02032010-157.mp4
02032010-36.mp4	02032010-76.mp4	02032010-116.mp4	02032010-158.mp4
02032010-37.mp4	02032010-77.mp4	02032010-117.mp4	02032010-159.mp4
02032010-38.mp4	02032010-78.mp4	02032010-118.mp4	02032010-160.mp4
02032010-39.mp4	02032010-79.mp4	02032010-119.mp4	02032010-161.mp4
02032010-40.mp4	02032010-80.mp4	02032010-120.mp4	
02032010-41.mp4	02032010-81.mp4	02032010-121.mp4	
	02032010-82.mp4	02032010-122.mp4	
		02032010-123.mp4	

Table C7. Underwater videos, Snake River, Washington, February 4, 2010.

[Maps and associated videos can be viewed in figures C1–C26, available at http://pubs.usgs.gov/sir/2012/5089]

02042010-2.mp4	02042010-10.mp4	02042010-23.mp4	02042010-34.mp4
02042010-3.mp4	02042010-11.mp4	02042010-29.mp4	02042010-35.mp4
02042010-4.mp4	02042010-12.mp4	02042010-30.mp4	02042010-39.mp4
02042010-5.mp4	02042010-13.mp4	02042010-31.mp4	02042010-40.mp4
02042010-6.mp4	02042010-14.mp4	02042010-32.mp4	02042010-41.mp4
02042010-8.mp4	02042010-15.mp4	02042010-33.mp4	02042010-42.mp4

Appendix D. Bank Photographs

Table D1. Geo-tagged bank photographs, Clearwater and Snake Rivers, October 21–22, 2010.

Click on a file name to view the photograph.

102109_074718_tag.jpg	102109_134448_tag.jpg	102209_083243_tag.jpg	102209_132242_tag.jpg
102109_081505_tag.jpg	102109_135039_tag.jpg	102209_083629_tag.jpg	102209_132521_tag.jpg
102109_082226_tag.jpg	102109_140644_tag.jpg	102209_012235_tag.jpg	102209_133505_tag.jpg
102109_083838_tag.jpg	102109_141019_tag.jpg	102209_090734_tag.jpg	102209_134028_tag.jpg
102109_084317_tag.jpg	102109_142431_tag.jpg	102209_091100_tag.jpg	102209_134433_tag.jpg
102109_085349_tag.jpg	102109_142747_tag.jpg	102209_092450_tag.jpg	102209_135750_tag.jpg
102109_090108_tag.jpg	102109_144017_tag.jpg	102209_092907_tag.jpg	102209_140049_tag.jpg
102109_090913_tag.jpg	102109_144425_tag.jpg	102209_020951_tag.jpg	102209_141820_tag.jpg
102109_091627_tag.jpg	102109_150216_tag.jpg	102209_021642_tag.jpg	102209_143401_tag.jpg
102109_092605_tag.jpg	102109_151053_tag.jpg	102209_100048_tag.jpg	102209_145226_tag.jpg
102109_093115_tag.jpg	102109_152803_tag.jpg	102209_100150_tag.jpg	102209_145844_tag.jpg
102109_093947_tag.jpg	102109_153406_tag.jpg	102209_100639_tag.jpg	102209_151753_tag.jpg
102109_094639_tag.jpg	102109_154535_tag.jpg	102209_103840_tag.jpg	102209_152251_tag.jpg
102109_100042_tag.jpg	102109_155108_tag.jpg	102209_104517_tag.jpg	102209_153657_tag.jpg
102109_103514_tag.jpg	102109_160534_tag.jpg	102209_104531_tag.jpg	102209_154331_tag.jpg
102109_110124_tag.jpg	102209_073220_tag.jpg	102209_033617_tag.jpg	102209_160204_tag.jpg
102109_110438_tag.jpg	102209_074629_tag.jpg	102209_033923_tag.jpg	102209_160439_tag.jpg
102109_113235_tag.jpg	102209_075258_tag.jpg	102209_115010_tag.jpg	102209_162218_tag.jpg
102109_113813_tag.jpg	102209_080633_tag.jpg	102209_123723_tag.jpg	
102109_120724_tag.jpg	102209_080645_tag.jpg	102209_125121_tag.jpg	
102109_130517_tag.jpg	102209_081343_tag.jpg	102209_125416_tag.jpg	
102109_132302_tag.jpg	102209_082747_tag.jpg	102209_130852_tag.jpg	
102109_132302-1_tag.jpg	102209_082747-1_tag.jpg	102209_131219_tag.jpg	
102109_132630_tag.jpg	102209_082845_tag.jpg	102209_131236_tag.jpg	

This page left intentionally blank

Publishing support provided by the U.S. Geological Survey
Publishing Network, Tacoma Publishing Service Center

For more information concerning the research in this report, contact the
Director, Idaho Water Science Center
U.S. Geological Survey
230 Collins Road
Boise, Idaho 83702
http://id.water.usgs.gov

USGS

Williams and others—**Bathymetric and Underwater Video Survey of Lower Granite Reservoir and Vicinity, Washington and Idaho, 2009–10**—Scientific Investigations Report 2012–5089

Lower Snake River Programmatic Sediment Management Plan Environmental Impact Statement

Appendix M

Sediment Transport in the Lower Snake and Clearwater River Basins, Idaho and Washington

Section 3. Use of Surrogate Technologies to Estimate Suspended Sediment in the Clearwater River, Idaho, and Snake River, Washington, 2008-10

U.S. Geological Survey

Prepared in Cooperation with the U.S. Army Corps of Engineers

Appendix M – Sediment Transport in the Lower Snake and Clearwater River Basins, Idaho and Washington
Lower Snake River Programmatic Sediment Management Plan – Final EIS

Prepared in cooperation with the U.S. Army Corps of Engineers

Use of Surrogate Technologies to Estimate Suspended Sediment in the Clearwater River, Idaho, and Snake River, Washington, 2008–10

Scientific Investigations Report 2013-5052

U.S. Department of the Interior
U.S. Geological Survey

August 2014

Cover:
Background: Confluence of the Snake and Clearwater Rivers at Lewiston, Idaho, May 14, 2012.
From left to right

Inset 1: Laser In Situ Scattering and Transmissometry (LISST)-Streamside laser diffraction instrument—Clearwater River at Spalding, Idaho, March 19, 2009.
Inset 2: Acoustic Doppler velocity meters (ADVMs)—Snake River near Anatone, Washington, March 20, 2009.
Inset 3: Nephelometric turbidity probe—Clearwater River at Spalding, Idaho, May 7, 2008.

All photographs were taken by Molly Wood, U.S. Geological Survey.

Use of Surrogate Technologies to Estimate Suspended Sediment in the Clearwater River, Idaho, and Snake River, Washington, 2008–10

By Molly S. Wood, U.S. Geological Survey, and Gregg N. Teasdale, U.S. Army Corps of Engineers

Prepared in cooperation with the U.S. Army Corps of Engineers

Scientific Investigations Report 2013–5052

U.S. Department of the Interior
U.S. Geological Survey

U.S. Department of the Interior
KEN SALAZAR, Secretary

U.S. Geological Survey
Suzette M. Kimball, Acting Director

U.S. Geological Survey, Reston, Virginia: 2013

For more information on the USGS—the Federal source for science about the Earth, its natural and living resources, natural hazards, and the environment, visit http://www.usgs.gov or call 1–888–ASK–USGS.

For an overview of USGS information products, including maps, imagery, and publications, visit http://www.usgs.gov/pubprod

To order this and other USGS information products, visit http://store.usgs.gov

Suggested citation:
Wood, M.S., and Teasdale, G.N., 2013, Use of surrogate technologies to estimate suspended sediment in the Clearwater River, Idaho, and Snake River, Washington, 2008–10: U.S. Geological Survey Scientific Investigations Report 2013-5052, 30 p.

Contents

Figures

Figures—Continued

Tables

Conversion Factors and Datums

Conversion Factors

Inch/Pound to SI

Multiply	By	To obtain
	Length	
foot (ft)	0.3048	meter (m)
mile (mi)	1.609	kilometer (km)
	Area	
square mile (mi^2)	259.0	hectare (ha)
square mile (mi^2)	2.590	square kilometer (km^2)
	Flow rate	
foot per second (ft/s)	0.3048	meter per second (m/s)
cubic foot per second (ft^3/s)	0.02832	cubic meter per second (m^3/s)
	Mass	
ton, short (2,000 lb)	0.9072	megagram (Mg)
ton per day (ton/d)	0.9072	metric ton per day
ton per day (ton/d)	0.9072	megagram per day (Mg/d)
ton per year (ton/yr)	0.9072	megagram per year (Mg/yr)
ton per year (ton/yr)	0.9072	metric ton per year
	Pressure	
atmosphere, standard (atm)	101.3	kilopascal (kPa)
pound-force per square inch (lbf/in^2)	6.895	kilopascal (kPa)
pound per square foot (lb/ft^2)	0.04788	kilopascal (kPa)
pound per square inch (lb/in^2)	6.895	kilopascal (kPa)

Conversion Factors and Datums—Continued

Conversion Factors—Continued

SI to Inch/Pound

Multiply	By	To obtain
	Length	
centimeter (cm)	0.3937	inch (in.)
meter (m)	3.281	foot (ft)
	Volume	
liter (L)	33.82	ounce, fluid (fl. oz)
liter (L)	2.113	pint (pt)
liter (L)	1.057	quart (qt)
liter (L)	0.2642	gallon (gal)
liter (L)	61.02	cubic inch (in^3)
	Flow rate	
centimeter per second (cm/s)	0.03281	foot per second (ft/s)
centimeter per second (cm/s)	0.03281	foot per second (ft/s)
	Mass	
gram (g)	0.03527	ounce, avoirdupois (oz)
kilogram (kg)	2.205	pound avoirdupois (lb)
	Density	
kilogram per cubic meter (kg/m^3)	0.06242	pound per cubic foot (lb/ft^3)
gram per cubic centimeter (g/cm^3)	62.4220	pound per cubic foot (lb/ft^3)

Temperature in degrees Celsius (°C) may be converted to degrees Fahrenheit (°F) as follows:

$$°F=(1.8×°C)+32.$$

Temperature in degrees Fahrenheit (°F) may be converted to degrees Celsius (°C) as follows:

$$°C=(°F-32)/1.8.$$

Datums

Vertical coordinate information is referenced to the North American Vertical Datum of 1988 (NAVD 88).

Horizontal coordinate information is referenced to the North American Datum of 1983 (NAD 83).

Altitude, as used in this report, refers to distance above the vertical datum.

Use of Surrogate Technologies to Estimate Suspended Sediment in the Clearwater River, Idaho, and Snake River, Washington, 2008–10

By Molly S. Wood, U.S. Geological Survey, and Gregg N. Teasdale, U.S. Army Corps of Engineers

Abstract

Elevated levels of fluvial sediment can reduce the biological productivity of aquatic systems, impair freshwater quality, decrease reservoir storage capacity, and decrease the capacity of hydraulic structures. The need to measure fluvial sediment has led to the development of sediment surrogate technologies, particularly in locations where streamflow alone is not a good estimator of sediment load because of regulated flow, load hysteresis, episodic sediment sources, and non-equilibrium sediment transport. An effective surrogate technology is low maintenance and sturdy over a range of hydrologic conditions, and measured variables can be modeled to estimate suspended-sediment concentration (SSC), load, and duration of elevated levels on a real-time basis. Among the most promising techniques is the measurement of acoustic backscatter strength using acoustic Doppler velocity meters (ADVMs) deployed in rivers. The U.S. Geological Survey, in cooperation with the U.S. Army Corps of Engineers, Walla Walla District, evaluated the use of acoustic backscatter, turbidity, laser diffraction, and streamflow as surrogates for estimating real-time SSC and loads in the Clearwater and Snake Rivers, which adjoin in Lewiston, Idaho, and flow into Lower Granite Reservoir. The study was conducted from May 2008 to September 2010 and is part of the U.S. Army Corps of Engineers Lower Snake River Programmatic Sediment Management Plan to identify and manage sediment sources in basins draining into lower Snake River reservoirs.

Commercially available acoustic instruments have shown great promise in sediment surrogate studies because they require little maintenance and measure profiles of the surrogate parameter across a sampling volume rather than at a single point. The strength of acoustic backscatter theoretically increases as more particles are suspended in the water to reflect the acoustic pulse emitted by the ADVM. ADVMs of different frequencies (0.5, 1.5, and 3 Megahertz) were tested to target various sediment grain sizes. Laser diffraction and turbidity also were tested as surrogate technologies. Models between SSC and surrogate variables were developed using ordinary least-squares regression. Acoustic backscatter using the high frequency ADVM at each site was the best predictor of sediment, explaining 93 and 92 percent of the variability in SSC and matching sediment sample data within +8.6 and +10 percent, on average, at the Clearwater River and Snake River study sites, respectively. Additional surrogate models were developed to estimate sand and fines fractions of suspended sediment based on acoustic backscatter. Acoustic backscatter generally appears to be a better estimator of suspended sediment concentration and load over short (storm event and monthly) and long (annual) time scales than transport curves derived solely from the regression of conventional sediment measurements and streamflow. Changing grain sizes, the presence of organic matter, and aggregation of sediments in the river likely introduce some variability in the model between acoustic backscatter and SSC.

Introduction

The U.S. Geological Survey (USGS) Idaho Water Science Center, in cooperation with the U.S. Army Corps of Engineers (USACE), Walla Walla District, is evaluating surrogate technologies to estimate suspended-sediment concentrations (SSC) in the Clearwater River at Spalding, Idaho, and the Snake River near Anatone, Washington (fig. 1) to help quantify sediment transport to Lower Granite Reservoir in northern Idaho and eastern Washington. USACE is developing strategies for managing fluvial sediment transport and deposition in lower Snake River reservoirs, which has negatively affected navigation and flow conveyance. Historically, sediment deposition has been managed through periodic dredging of the federal navigation channel; however, USACE plans to identify more opportunities for controlling sediment by quantifying sediment sources and transport in contributing drainage basins, particularly the Clearwater, Snake, and Salmon River basins. Streamflow in the two river systems is partially regulated, meaning that some but not all of the flow is controlled by dam releases. Some flow passing each study site is contributed by unregulated (free-flowing) tributaries.

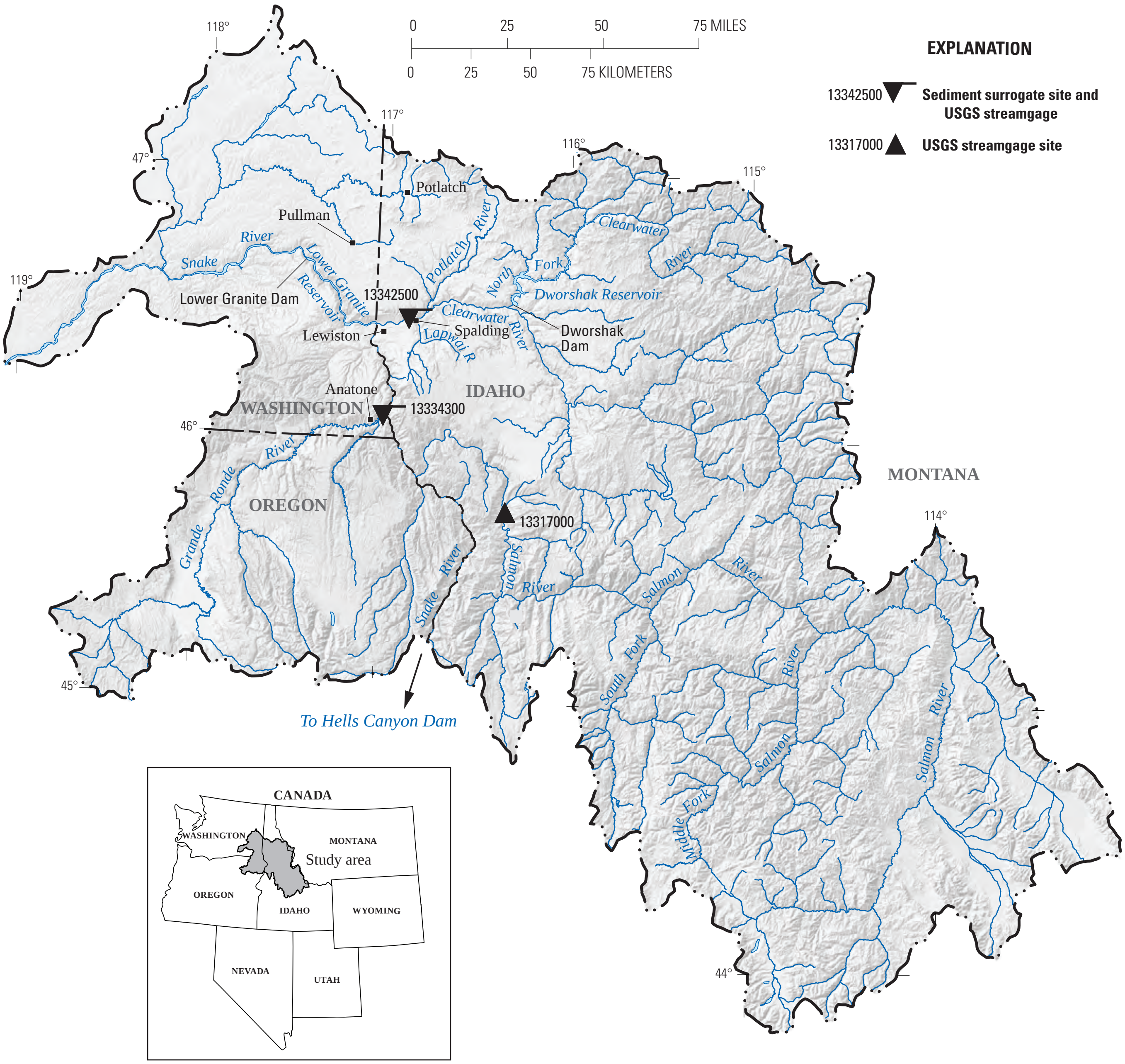

Figure 1. Study area and locations of sediment surrogate and U.S. Geological Survey (USGS) streamgage sites in the Clearwater River, Idaho, and Snake River, Washington, May 2008–September 2010.

The Lower Granite Lock and Dam forms the farthest upstream reservoir on the lower Snake River and captures sediment from about 27,000 mi^2 of forested and agricultural land in the Clearwater, Salmon, and Grande Ronde River basins (Teasdale, 2010). Levees were constructed along the Snake and Clearwater Rivers in Lewiston, Idaho, to contain the backwater of Lower Granite Dam and provide flood damage reduction up to the level of the Standard Project Flood, which is the streamflow expected to result from the most severe hydrologic and meteorological conditions that is characteristic of the drainage basins (U.S. Army Corps of Engineers, 2002). Sediment deposition has reduced the hydraulic capacity of the levees since completion of the dam in 1974. Periodic dredging has been performed by the USACE to maintain the navigation channel and recover hydraulic capacity of the levee system. An Environmental Impact Statement (EIS) for proposed dredging action prepared by the USACE in 2002 was suspended in litigation and the USACE is now revising the EIS as part of the development of a comprehensive Programmatic Sediment Management Plan (PSMP). The PSMP-EIS is evaluating alternatives to dredging, including drainage basin measures that may reduce sediment loads and the construction of structures within the reservoir to promote movement of sediment through the confluence. Accurate measurements of sediment concentration and load are necessary to plan and evaluate potential sediment management actions and to calibrate sediment yield and transport models.

The USGS conducted a sediment sampling program in the Clearwater and Snake Rivers from 1972 to 1979 and developed sediment-transport curves that related streamflow to suspended and bedload sediment samples to calculate continuous records of sediment concentration and load. The results of the 1970s study are presented in Jones and Seitz (1980). One of the goals of the 2008–10 sediment sampling program was to determine whether the 1970s sediment-transport curves are representative of current sediment-transport conditions. A detailed discussion of comparisons between results of the 1970s and 2008–10 sampling programs is provided in Clark and others (in press).

This report documents the ability and limitations of using sediment-surrogate technologies (surrogate technologies), such as acoustic backscatter, laser diffraction, and turbidity, to estimate SSC and load on continuous, 15-min intervals in the Snake and Clearwater Rivers draining to Lower Granite Reservoir. Surrogate technologies are evaluated to determine whether they provide improved estimates of SSC and load in comparison with sediment-transport curves generated using streamflow and sediment data collected during the 1970s and 2008–10 studies. Transport curves relying on streamflow as the explanatory variable may be poor estimators of SSC in these river systems, particularly during rain events, owing to "hysteresis" and varying sources of sediment (mostly from unregulated tributary inflows) that may not contribute a large percentage of the total flow but contribute a large amount of sediment. Sediment "hysteresis" means that sediment concentrations have different values at identical streamflow on the ascending and descending limbs of a hydrograph. A plot of streamflow and SSC during a storm event often appears to have a looped relation owing to hysteresis.

Additional sediment samples and surrogate data were collected in water year 2011 to validate the acoustic backscatter surrogate models described in this report; validation results are presented in Clark and others (in press). Clark and others (in press) also presents a comparison of suspended sediment-load estimates generated using the acoustic backscatter surrogate models described in this report and using a LOADEST (LOAD ESTimation) model, which is a FORTRAN (FORmula TRANslation) program for estimating constituent loads in streams and rivers based on streamflow and time variables (Runkel and others, 2004).

Background

The USGS has traditionally used streamflow as a surrogate to estimate instantaneous SSC and sediment loads based on guidelines in Porterfield (1972), Glysson (1987), and Nolan and others (2005). A relation is developed between streamflow and SSC or sediment load using log transformations on both variables or plotting on logarithmic scales. The relation, which may be linear or non-linear, is called a sediment-transport curve.

Uncertainties in sediment-transport curves have led to the development and evaluation of more direct, in-situ surrogate techniques. Acoustic instruments have shown great promise as sediment- surrogate technologies. They are tolerant of biological fouling and measure profiles across a sampling volume rather than at a single point in the stream (Gartner and Gray, 2005).

Acoustic backscatter has been used with success as a surrogate technology for SSC or suspended solids concentration in the San Francisco Bay (Gartner, 2004), Florida estuaries (Patino and Byrne, 2004), Colorado River (Topping and others, 2004, 2006), Hudson River (Wall and others, 2006), the Aegean Region in Turkey (Elci and others, 2009), and subtropical estuaries in Australia (Chanson and others, 2008). Although the primary purpose of these types of acoustic instruments is to measure water velocity, additional measures are useful to monitor suspended-sediment transport. As the instrument emits an acoustic pulse into the water and measures the Doppler-shifted frequency of the pulse as it bounces off acoustic reflectors (typically assumed to be primarily sediment particles), the strength of the returned pulse (backscatter) also is measured as it returns to the instrument along the beam path (SonTek/Yellow Springs Instruments, 2007). Backscatter should increase when more particles are present in the water. As a result, the backscatter measurement may be related to SSC.

Additional surrogate technologies have been used to monitor suspended-sediment transport. Turbidity has been successfully used as a surrogate for SSC in Kansas (Rasmussen and others, 2005), Oregon (Uhrich and Bragg, 2003), and Florida (Lietz and Debiak, 2005), among other locations. Turbidity probes typically used in these studies emit a near-infrared light at 780–900 nm and measure the amount of light scattered at an angle of 90 degrees (Yellow Springs Instruments, 2011). The greater the amount of light scattered, the higher the turbidity reading. In theory, this should equate to a larger amount of suspended material in the measurement volume.

The concept of laser diffraction is documented in Agrawal and others (2008) and has been used with success as a sediment surrogate in the Colorado River (Topping and others, 2004) and in laboratory experiments (Meral, 2008). Essentially, a laser is passed through a water sample and a receiving lens in the instrument focuses the light that is scattered by particles in the water onto a series of ring detectors. The detectors calculate a volumetric concentration of sediment in 32 size classes. Data can be converted to a mass concentration by multiplying the volumetric concentration by a known sediment density, or the volumetric concentrations can be used alone in a calibration with measured SSC.

Site Descriptions and Surrogate Instrument Configurations

Study sites were co-located with existing USGS streamgages to take advantage of existing infrastructure for mounting equipment and transmitting data and to facilitate computations of sediment loads. Acoustic frequencies were selected for this study to maximize sensitivity of backscatter to dominant sediment particle size (grain size) with low acoustic frequency for the sand-sized fraction (grain size between 0.63 and 2 mm) and high acoustic frequency for the fines fraction (grain size less than 0.63 mm) to minimize errors because of changing grain-size distribution, as recommended in Gartner (2004) and Topping and others (2004). The following sections describe characteristics of the two study sites and configuration of surrogate instruments.

Clearwater River Study Site

The Clearwater River study site is co-located with USGS streamgage No. 13342500 on the left streambank at Spalding, Idaho. Part of the streamflow passing the study site is regulated by Dworshak Dam located upstream of the site on the North Fork Clearwater River (fig. 1). The main stem Clearwater River is unregulated except for a few upstream irrigation diversions, which affect about 18 percent of the drainage area (U.S. Geological Survey, 2012). The site is equipped with a 0.5-MHz SonTek™/YSI Argonaut-SL acoustic Doppler velocity meter (ADVM), a 3-MHz SonTek™/YSI Argonaut-SL ADVM, a Yellow Springs Instruments (YSI™) 6600EDS water-quality sonde with a model 6136 nephelometric turbidity probe, and a Sequoia Scientific Laser In Situ Scattering and Transmissometry (LISST)-StreamSide laser diffraction instrument (fig. 2). The YSI™ 6136 nephelometric turbidity probe used in this study emits a near-infrared light at 780–900 nm and measures the amount of light scattered at an angle of 90 degrees (Yellow Springs Instruments, 2011). The site also is equipped with a datalogger and satellite telemetry for collecting and transmitting real-time data. The ADVMs, turbidity probe, and telemetry were installed in May 2008; the LISST-StreamSide was installed in July 2008. The LISST-StreamSide is deployed inside a gage house, and a pump draws water from the river into the LISST-StreamSide optical analyzer box. The intended advantage of the LISST-StreamSide over other commercially available, in-situ laser diffraction instruments as described in Gray and Gartner (2010) is improved data quality through reduced stream contact and resulting biological fouling. Unforeseen configuration problems in the LISST-StreamSide, which resulted in poor pump operation, the formation of bubbles in the line, and possible condensation on internal lenses, prevented reliable measurements for most of the study period. The manufacturer of the LISST-StreamSide, Sequoia Scientific, is working closely with the USGS to resolve the problems. Further testing is needed to determine whether the instrument will perform as intended, once these issues are resolved.

The ADVMs, turbidity probe, and LISST-StreamSide pump intake are mounted on a 44-ft aluminum slide-track mount that can be raised and lowered as needed to service equipment. The 0.5- and 3-MHz ADVMs measure backscatter in five discrete, equally sized cells in a horizontal sampling volume, at distances of 5.0–100 ft and 3.3–12 ft from the instrument, respectively. The sampling volume for each ADVM was selected based on acoustic frequency, abundance of acoustic reflectors along the beam path, and any obstructions in the beam path. The ADVMs were originally configured to measure backscatter in 10 cells, within a sampling volume twice as large as the current configuration. However, the sampling volume represented by the first five cells was determined to be optimum for developing the model between SSC and acoustic backscatter. In addition, data transfer limitations using Serial Data Interface-1200 baud rate (SDI-12) protocol, the communication protocol used to transfer data from the ADVMs to the dataloggers at both sites, prevents real-time display of data from more than five cells. As a result, only the first five cells could be practically used to compute real-time estimates of SSC and sediment load using developed surrogate models.

Figure 2. Sediment surrogate instruments deployed at the Clearwater River near Spalding, Idaho. Instruments are shown pulled up the slide track mount for servicing. Not shown: the pump and intake for the LISST-StreamSide was later installed on the back side of the aluminum plate attached to the acoustic Doppler velocity meters. Photograph taken by Molly Wood, U.S. Geological Survey, May 8, 2009.

The ADVMs average measurements collected over 2 min out of every 15 min. The water-quality sonde measures turbidity adjacent to the instrument every 15 min and is equipped with an automated wiper mechanism to reduce biological fouling on the face of the probe. The LISST-StreamSide measures volumetric SSC and grain-size distribution every 30 min. The sampling line for the LISST-StreamSide is flushed for 2–5 min prior to each measurement (duration changed during study period), and measurements are then averaged over 30 sec.

Snake River Study Site

The Snake River study site is co-located with USGS streamgage No. 13334300 on the left streambank near Anatone, Washington (fig. 1). Part of the streamflow passing the study site is regulated by numerous dams along the Snake River, including Hells Canyon Dam located 31 mi upstream. The Salmon and Grande Ronde Rivers join the Snake River upstream of the study site and contribute most of the sediment passing the site (Gregory Clark, U.S. Geological Survey, oral commun., 2011). The site is equipped with a 0.5-MHz SonTek™/YSI Argonaut-SL ADVM, a 1.5-MHz SonTek™/YSI Argonaut-SL ADVM, and a YSI™ 6600EDS water-quality sonde with a model 6136 turbidity probe (fig. 3).

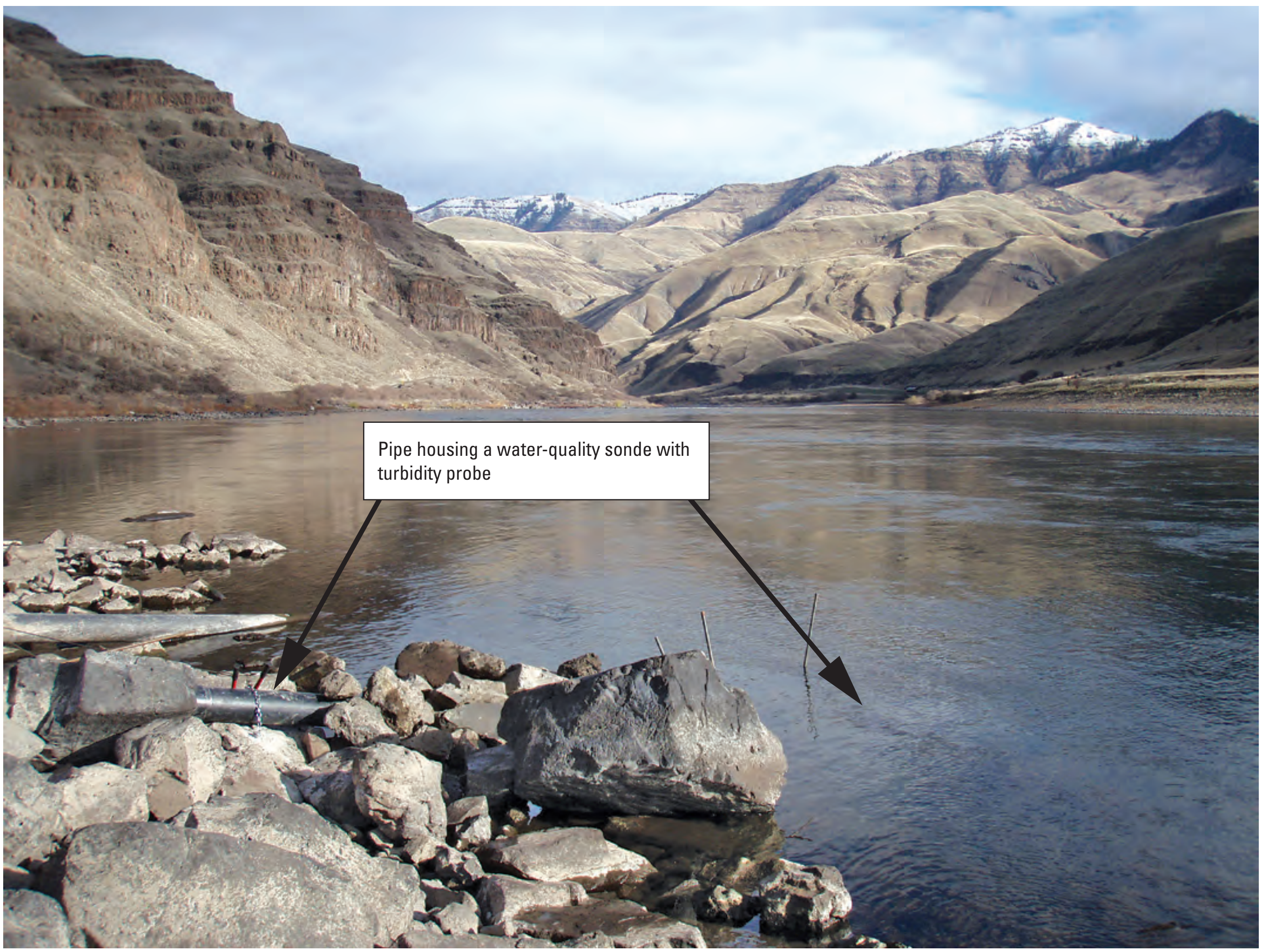

A. The pipe housing a Yellow Springs Instruments (YSI™) water-quality sonde with turbidity probe.

Figure 3. Sediment surrogate instruments deployed at the Snake River near Anatone, Washington. (Photographs *A* and *B* taken December 15, 2008 and March 30, 2009, respectively, by Molly Wood, U.S. Geological Survey.

B. The 1.5-MHz and 0.5-MHz SonTek™/YSI acoustic Doppler velocity meters (ADVMs) attached to an aluminum slide track mount about 1,000 ft upstream of the water-quality sonde.

Figure 3.—Continued

Like the Clearwater River study site, the Snake River site is equipped with a datalogger and satellite telemetry. The water-quality sonde and telemetry were installed in May 2008; the ADVMs were installed in April 2009. The water-quality sonde is mounted in a plastic pipe, drilled with holes to maintain hydraulic communication between the inside of the pipe and surrounding water, which extends into the river from the left bank near the gage house. The ADVMs could not be co-located with the streamgage and water-quality sonde because streambed features limited profiling across the channel. The ADVMs were installed in a more suitable measurement location about 1,000 ft upstream of the streamgage, on a 32-ft aluminum slide track mount that can be raised and lowered as needed to service the equipment.

The 0.5- and 1.5-MHz ADVMs are configured to measure backscatter in five discrete, equally sized cells in a horizontal sampling volume, 6.6–203 ft and 6.6–59 ft from the instrument, respectively. The ADVMs average measurements collected over 2 min out of every 15 min. The water-quality sonde measures turbidity adjacent to the instrument every 15 min and is equipped with an automated wiper mechanism.

Unlike the Clearwater River site, the ADVMs at the Snake River site are direct current-powered through a solar panel and battery. To avoid fluctuations in input voltage, which is common at sites powered by a solar panel and battery, that could lead to fluctuations in power during transmission of the acoustic pulse (Craig Huhta, SonTek/Yellow Springs Instruments, oral commun., 2012), both ADVMs are connected to a direct current voltage converter to maintain a constant voltage input to the instruments during measurements. The voltage converter changes direct current voltage from a solar panel and battery to a constant output of 13 volts to the ADVMs, to remove the potential uncertainty in backscatter measurements because of fluctuations in input voltage. This setup was deemed necessary because Wall and others (2006) noted that differing power-supply voltages supplied to acoustic Doppler current profilers used to estimate sediment in the Hudson River resulted in changes in transmit power of the acoustic pulse, which required corrections to the data. This phenomenon could cause fluctuations in backscatter measurements which are not a result of changes in SSC in the river.

Methods

The following sections describe the methods used to collect suspended-sediment samples, process and apply corrections to surrogate data, and develop surrogate models for the computation of continuous records of SSC and load.

Sediment Sample Collection

Suspended-sediment samples were collected using the equal-width-increment (EWI) sampling method (U.S. Geological Survey, 2006) with a cable-suspended, US D-96 depth-integrating, isokinetic water sampler and were analyzed at the USGS Cascades Volcano Observatory Sediment Laboratory in Vancouver, Washington. Sampling was targeted towards the ascending limb, the peak, and the descending limb of the snowmelt runoff hydrograph for each river. Thirty-three EWI suspended- sediment samples were collected at each site during May 2008–September 2010 (table 1) and were analyzed for concentration, percent fines smaller than 0.063 mm, and organic content through a loss-on-ignition test. A full grain-size analysis on the sand fraction was performed for some samples. Samples submitted for analysis were a composite representative of the entire cross section.

To quantify cross-sectional variability, 10 discrete depth-integrated samples, each from a separate vertical section, were collected and analyzed during 4 sampling events at the Clearwater River site and 5 sampling events at the Snake River site. EWI samples should have been collected with each of the discrete sample subsets because the average concentration from the discrete sample subsets may not necessarily equal the EWI sample concentration. However, EWI samples were collected concurrently for only two of the discrete sample subsets at the Snake River site. When discrete bottles were collected without a corresponding EWI sample, the results from the discrete samples were averaged for use in the analysis. Discrete and corresponding EWI samples were collected at flows of 48,000 and 105,000 ft^3/s at the Snake River site. Ratios were calculated between the EWI sample concentration and average concentration from discrete samples for these two sampling events. The ratios were 0.79 and 0.96 for the higher and lower flow sampling events, respectively, meaning that in both cases the EWI sample concentration was less than the average concentration from discrete samples. Sample results from the remaining three sampling events in the Snake River, when a corresponding EWI sample was not collected, were adjusted based on these ratios. Samples collected at 24,600 and 55,000 ft^3/s were adjusted using the 0.96 (lower flow) ratio and a sample collected at 103,000 ft^3/s was adjusted using the 0.79 (higher flow) ratio. For example, the average concentration for discrete samples collected on May 20, 2009, at a flow of 103,000 ft^3/s was 301 mg/L. The concentration was adjusted to 301 mg/L × 0.79 = 237 mg/L to estimate what the EWI sample concentration might have been for that sampling event. None of the samples on the Clearwater River site were adjusted in this way because no corresponding EWI samples were collected concurrently with the four discrete sample subsets.

Table 1. Suspended-sediment and streamflow data collected in the Clearwater River, Idaho, and Snake River, Washington, May 2008–September 2010.

[**Abbreviations:** USGS, U.S. Geological Survey; mg/L, milligrams per liter; ft^3/s, cubic feet per second; na, not applicable]

Characteristic	USGS streamgage		Units
	Clearwater River (13342500)	Snake River (13334300)	
Number of sediment samples collected during study period	33	33	na
Mean annual streamflow, period of record[1]	14,710	34,450	ft^3/s
Annual mean streamflow			
2008	16,220	31,310	ft^3/s
2009	16,040	33,080	ft^3/s
2010	10,830	29,130	ft^3/s
Total suspended-sediment concentration			
Mean	26	70	mg/L
Median	13	40	mg/L
Ranges			
Total suspended-sediment concentration	3–210	6–414	mg/L
Sand concentration	0.3–122	0.5–232	mg/L
Fines concentration	2–88	5–206	mg/L
Flows during sample collection	4,760–78,900	14,900–155,000	ft^3/s
Flows during study period (May 2008–September 2010)	2,190–79,700	10,900–173,000	ft^3/s

[1] Based on published period of record for streamgage, water years 1972–2010 for Clearwater River, 1958–2010 for Snake River.

Surrogate Instrument Data Corrections

The surrogate technologies required varying levels of correction to be used in SSC estimates from the raw measured values. Turbidity data were corrected for calibration drift and fouling errors as described in Wagner and others (2006). Laser diffraction data were recorded by the instrument in volumetric concentration in microliters per liter (μL/L), which can be multiplied by a known or assumed particle density to obtain mass concentration in milligrams per liter (mg/L). In this investigation, it was not practical to continuously measure particle density, so a regression model was developed between LISST volumetric concentration and the mass concentration of the physical samples. No corrections were applied to the LISST volumetric concentration data.

To correct acoustic backscatter data into a more meaningful estimator of SSC, multiple steps are required. Acoustic backscatter data were corrected for (1) beam spreading, (2) transmission losses owing to absorption by water, and (3) absorption or attenuation by sediment. Methods for correcting acoustic backscatter data are documented in Flammer (1962), Urick (1975), Thevenot and Kraus (1993), and Gartner (2004). Methods for correcting acoustic backscatter data differ and can significantly change estimates of sediment concentration. Selection of an appropriate method is an important decision in the analysis of acoustic backscatter data. Candidate methods were reviewed and those selected for this study are described in the following sections.

Acoustic Data Corrections

Mass concentration of suspended sediment can be related to acoustic backscatter using equation (1) in exponential form:

$$SSC = 10^{(\beta_0 + (\beta_1 \text{ABScorr}) + (\beta_2 EVi) + \ldots + (\beta_n EVn))} \quad (1)$$

where
- SSC is suspended-sediment concentration (mg/L)
- β_0 is the equation intercept,
- β_1 is the regression coefficient corresponding to ABS_{corr}, and
- ABS_{corr} is the range-normalized acoustic backscatter (ABS) corrected for two-way transmission losses (Thevenot and Kraus, 1993) in decibels (dB).

EVi through *EVn* are other explanatory variables used in the regression, and β_2 through β_n are the corresponding regression coefficients. The regression coefficients are determined by regressing mass concentration measurements of suspended sediment with measurements of ABS_{corr} and other explanatory variables during sample collection.

Backscatter data must be range-normalized or corrected for transmission losses through a multi-step process (fig. 4).

Corrected acoustic backscatter, $ABS_{corr,}$ is calculated using a form of the sonar equation from Urick (1975):

$$ABS_{corr} = K(E - E_r) + 20\log_{10}(R) + 2\alpha_w R + 2\alpha_s R \quad (2)$$

where
- ABS_{corr} is the range-normalized acoustic backscatter corrected for two-way transmission losses in dB,
- K is a scale factor used to convert uncorrected ABS in counts to dB,
- E is the raw amplitude of the uncorrected ABS as reported by the acoustic device (counts),
- E_r is the received signal strength indicator reference level or instrument noise floor (counts),
- R is the slant distance along the acoustic beam to the measurement location incorporating beam angle (25 degrees for SonTek™/YSI ADVMs) (m),
- α_w is the water absorption coefficient (dB/m), and
- α_s is the sediment attenuation coefficient (dB/m).

The scale factor used to convert uncorrected ABS in counts to dB typically ranges from 0.35 to 0.55 according to Deines (1999). For SonTek™/YSI ADVMs, the appropriate value for *K* when converting ABS from counts to dB is 0.43 (SonTek/Yellow Springs Instruments, 2007). The term E_r, or instrument noise floor, is specific to the ADVM and deployment location, and is the baseline echo measured by the instrument when no signal is transmitted. Local electronic interferences can affect E_r. E_r is measured automatically by the ADVMs used in this study immediately after a backscatter measurement is made. The term $K(E - E_r)$ is output from the SonTek™/YSI ADVMs directly as Signal to Noise Ratio (SNR) in each cell, so this term was used in all calculations because it incorporated actual measurements of the instrument noise floor (fig. 4, step 1).

Acoustic Beam Spreading

Losses owing to beam spreading, represented by the term $20\log_{10}(R)$ in equation (2), are different for acoustic backscatter data collected near the transducer, or within a zone called the near-field distance. The near-field distance is defined by $Rcritical = \pi r_t^2/\lambda$, where r_t is the transducer radius (cm) and λ is the acoustic wavelength, or the speed of sound in water (cm/s) divided by the acoustic frequency (Hz). At distances less than *Rcritical*, the near-field correction for spreading loss is defined by Downing and others (1995) as:

$$\Psi = \left[1 + 1.35Z + (2.5Z)^{3.2}\right] / \left[1.35Z + (2.5Z)^{3.2}\right] \quad (3)$$

where
- $Z = R/Rcritical$ and R is the slant range distance along the beam to the sampling volume of interest.

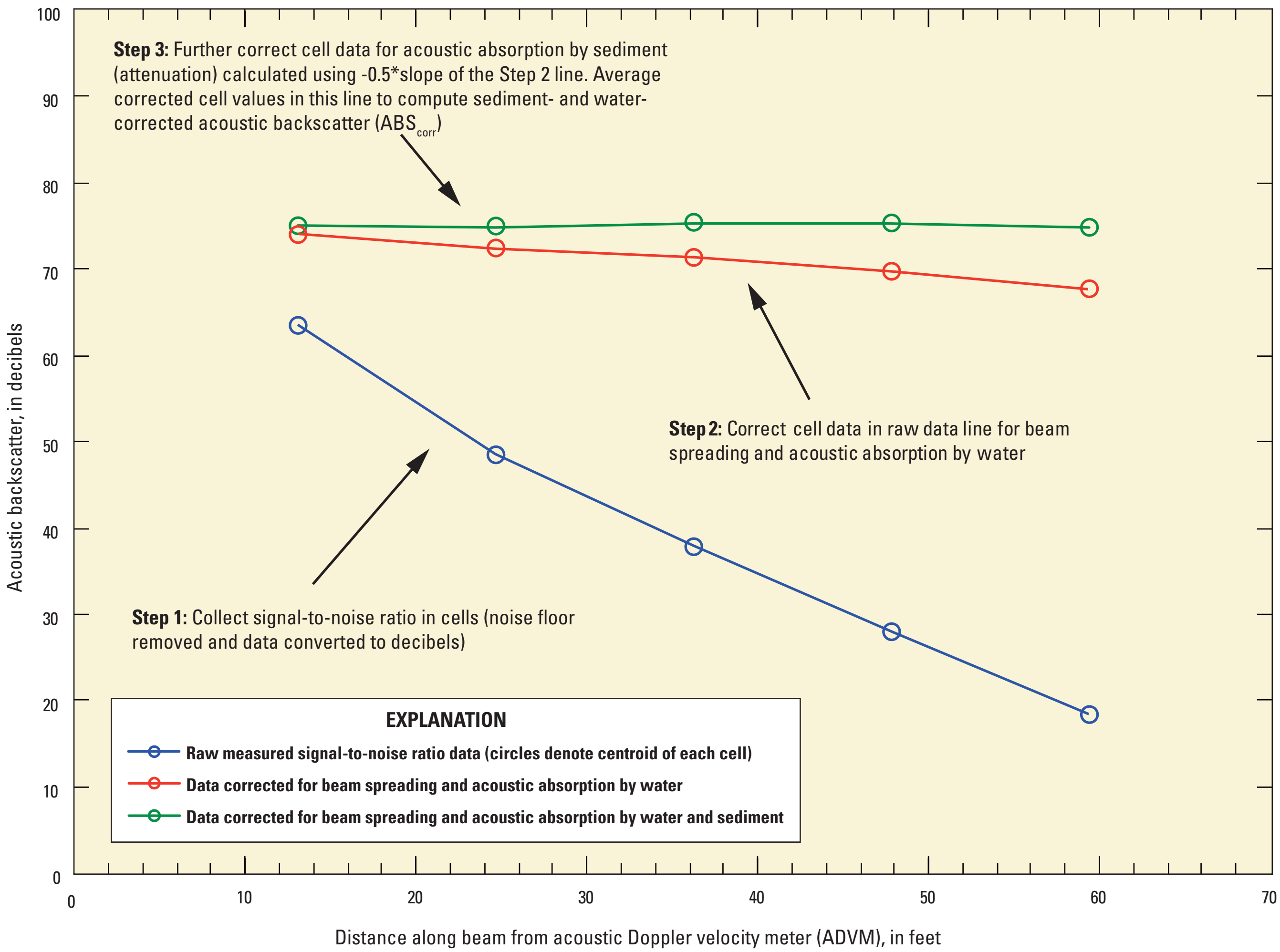

Figure 4. Process for calculation of range-normalized acoustic backscatter corrected for two-way transmission losses in the Clearwater River, Idaho, and Snake River, Washington.

At points within the near field, the term $20\log_{10}(R)$ in equation (2) becomes $20\log_{10}(R\psi)$. Cell 1 centroids for the ADVMs in the Clearwater and Snake Rivers were greater than *Rcritical* and so were not corrected for near-field spreading losses. Losses owing to beam spreading were calculated simply using the term $20\log_{10}(R)$.

Acoustic Absorption by Water

The water absorption coefficient, α_w, in equation (2) is a function of acoustic frequency, pressure, salinity, and temperature; and is calculated according to Schulkin and Marsh (1962):

$$\alpha_w = [SAf_t f^2/(f_t^2 + f^2) + Bf^2/f_t][1-(6.54\times10^{-4})(P)]\times 8.686 \qquad (4)$$

where

α_w is the water absorption coefficient (dB/m),
S is salinity (practical salinity units),
A is a constant for ionic relaxation process in sea water equal to 2.34×10^{-6},
f_t is the temperature-dependent relaxation frequency (kilohertz or kHz) defined as $21.9\times10^{[6-1520/(T+273)]}$,
T is temperature (°C),
f is the ADVM acoustic frequency (kHz),
B is a constant for viscosity mechanism in pure water, defined as 3.38×10^{-6} and
P is pressure (atmospheres or kg/cm^3).

In this analysis, the first term of the equation, $SAf_t f^2/(f_t^2+f^2)$, is assumed to be zero because salinity is negligible. Pressure, P, is considered 1 atmosphere because the difference in pressure between the elevations of the water surface at the sites (about 800 ft above sea level) and the depth of the deployed ADVMs is negligible.

The terms $20\log_{10}(R)$ and $2\alpha_w R$ in equation (2) represent the two-way transmission loss, or acoustic signal loss owing to beam spreading and acoustic absorption by water. Data corrected for these losses are represented by step 2 in figure 4.

Acoustic Absorption by Sediment

The last term in equation (2), $2\alpha_s R$, represents the two-way transmission loss owing to absorption or attenuation by sediment, and ideally should be calculated based on knowledge of source level, target strength, ensonified volume, and mass of suspended material in various size classes. Attenuation of an acoustic signal by suspended particles consists of viscous, scattering, and diffraction energy loss components (Flammer, 1962). Diffraction losses are described in more detail in Reichel and Nachtnebel (1994) and are not a concern at the study site, given the frequency of the selected ADVMs and measured sediment concentrations and particle sizes. A theoretical calculation of viscous and scattering losses can be made based on the following equation from Urick (1975):

$$2\alpha_s = \underbrace{(K(\gamma-1)^2\{S/[S^2+(\gamma+\tau)^2]\}}_{\textit{Viscous losses}} + \underbrace{(K^4 a_p^3)/6)(8.686)(SSC)}_{\textit{Scattered losses}} \quad (5)$$

where

SSC is the suspended-sediment concentration (mg/L)

$2\alpha_s$ is the two-way transmission loss owing to attenuation from suspended particles (dB/m),

K is $2\pi/\lambda$,

λ is acoustic wavelength or the speed of sound in water (cm/s) divided by acoustic frequency (Hz),

S is $[9/(4\beta a_p)][1+1/(\beta a_p)]$, β is $[\omega/2v]^{0.5}$, ω is $2\pi f$,

f is acoustic frequency (Hz),

v is the kinematic viscosity of water (Stokes),

a_p is particle radius (cm),

γ is the particle wet density divided by fluid density, and

τ is $0.5+9/(4\beta a_p)$.

It was not always practical to measure true values for some of the parameters in equation (5) given the expected non-uniformity in particle shape, size, and density. Topping and others (2004, 2006) proposed that the acoustic absorption by sediment (attenuation) can be calculated based on profiles of acoustic backscatter corrected for spherical beam spreading and absorption by water. In Topping and others (2004, 2006) and the study reported here, $2\alpha_s R$ in equation (2) was calculated for each cell by determining -0.5 times the slope of the line of $K(E-E_r)+20\log_{10}(R)+2\alpha_w R$ (represented by the line in fig. 4, step 2). This value, called sediment attenuation, or α_s, is then multiplied by $2\times R$ (the slant range distance along the beam to the sampling volume of interest). ABS_{corr} was then calculated for each cell according to equation (2) (fig. 4, step 3), and the average of ABS_{corr} from all cells was used to relate surrogate data to sediment sample data.

During some brief periods of low backscatter and low SSC, the line representing data corrected for beam spreading and acoustic absorption by water (fig. 4, step 2) curved upward in cells 4 or 5. This is not physically possible, and use of this data in the calculations would have resulted in erroneous estimates of the slope of the line, or sediment attenuation. During these periods, acoustic backscatter in the outer cell(s) may have been erroneous because it could not be distinguished from the instrument noise floor. When this occurred, these cells were discarded from the calculation of sediment attenuation. Only cells along the decreasing trend of the line representing data corrected for beam spreading and acoustic absorption by water were used to calculate sediment attenuation for further correction of the data in step 3 of figure 4.

Surrogate Model Development

Samples collected in 2008–10 were used to develop sediment-surrogate models at each site. Surrogate measurements (acoustic backscatter, turbidity, streamflow, and laser diffraction (laser diffraction was measured at the Clearwater River site but not the Snake River site) data) were averaged over a 1-hour period bracketing each sediment sample to obtain concurrent measurements for surrogate-model calibrations. Some samples were not included in the surrogate models because of intermittent equipment malfunctions, varying installation dates for surrogate instruments, and surrogate instruments being out of water for short periods of time during low-flow conditions.

Models between SSC and surrogate variables were developed using stepwise ordinary least-squares regression techniques in TIBCO Spotfire S+® statistical software (TIBCO Software Inc., 2008). Log transformations were performed on SSC, streamflow, LISST concentration, and at the Clearwater River site, turbidity, to improve distribution and fit prior to the evaluation in the regression model. Various transformations were evaluated on variables prior to use in the regressions, including the square root, cube root, reciprocal root, and reciprocal, as described in Helsel and Hirsch (2002). Use of the log transformation produced the best fit and most linear relations of other evaluated transformations. Acoustic backscatter data are already reported in a log-based scale and do not require a transformation. Regression models were selected based on statistical significance (p-values) of explanatory variables and various regression statistics, such as high coefficient of determination (R^2), low standard error, constant variance and random patterns in residuals plots, and low relative percent difference (RPD) between measured and estimated SSC, as defined in equation (6):

$$RPD = [(\text{Estimated SSC} - \text{Measured SSC})/\text{Measured SSC}]\times 100 \quad (6)$$

Additional forms of the regression models developed for the acoustic backscatter surrogates were evaluated in an attempt to improve fit at high SSC. One of the forms evaluated was a compound regression model composed of two linear segments with different slopes. A breakpoint in acoustic backscatter between the two linear segments was selected based on backscatter measured during times when upstream tributaries contributed high SSC. For example, in the Clearwater River, the evaluated breakpoint was 72 dB. Above this breakpoint, most of the samples in the Clearwater River were collected during times when high SSC was measured in the Potlatch River (fig. 1), an upstream tributary to the Clearwater River. Polynomial forms of the acoustic backscatter models also were evaluated, which included terms of backscatter and backscatter squared. None of the evaluated forms substantially improved the overall fit of the regression model to the measured data nor the variance in residuals plots, in comparison with the simple linear relations between corrected acoustic backscatter and log-transformed SSC.

A nonparametric bias correction factor described in Duan (1983) was applied to each regression model to correct for bias induced by log transformation and subsequent retransformation of the dependent variable. Duan's bias correction factor is calculated by averaging the values of 10 to the power of each residual of the dependent variable in the dataset used to develop the regression model. The factor was used to correct each value of SSC as well as upper and lower 95-percent confidence intervals estimated by a regression model. Sediment loads were calculated by multiplying estimates of SSC by rated streamflow at each study site.

Sediment-transport curves developed during the 1970s study and presented in Jones and Seitz (1980) were applied to streamflow data in the 2008–10 study to determine whether the relation between suspended sediment and streamflow changed between the two studies. Jones and Seitz (1980) did not use a bias correction factor in their equations. The original sediment-transport curves were not altered for the comparison with the 2008–10 study.

Use of Surrogate Models To Estimate Suspended Sediment

Stream conditions varied at each sediment-surrogate monitoring site. Measured SSC in the Clearwater River ranged from 3 to 210 mg/L, with a median of 13 mg/L, during the period of sample collection used for development of the surrogate models (May 2008–September 2010) (table 1). Fines content (<63 µm) ranged from 30 to 96 percent. In the Snake River, measured SSC ranged from 6 to 414 mg/L, with a median SSC of 40 mg/L. Fines content ranged from 32 to 94 percent. Fines content at both sites typically decreased with increasing concentration. Samples were collected over nearly the full range in streamflow at both sites; 96 and 86 percent of the range in flow was represented by samples at the Clearwater River and Snake River sites, respectively (table 1).

The acoustic surrogate models demonstrate the robust nature of acoustic technologies for use as sediment surrogates at the study sites. The higher frequency acoustic surrogate models were the best estimator of SSC of all of the evaluated surrogate technologies, based on regression statistics (tables 2 and 3). The ADVMs also required the least maintenance of the instruments evaluated; however, post-processing of the data was more difficult than for other surrogates. Substantial variability was observed in the turbidity and laser diffraction models, which may be due in part to cross-sectional variability in sediment concentration, which was verified through the collection of the discrete samples across each cross section as well as visual observations of sediment stratification during some site visits, typically after a runoff event. At each study site, tributary inflows enter the main channel on the left bank less than 2 mi upstream of the measurement site. During some storm runoff and snowmelt events, the tributaries discharge sediment-laden water that adjoins the left bank and persists downstream past the location of the surrogate equipment. However, turbulence induced by channel and bank features varied with streamflow and seemed to cause slight spatial variability in this zone, relative to the location of the surrogate instruments. This small-scale spatial variability likely resulted in the high variability in the calibrations of the laser diffraction and turbidity instruments. The ADVMs were less affected by this streamflow condition because they sample a larger part of the channel volume and capture more of the cross-sectional variability. The method for correcting acoustic backscatter for losses assumes that the suspended sediment within the sampling volume is relatively uniform in concentration and particle-size distribution, but the acoustic surrogates seem to be more tolerant of small amounts of spatial variability than the point measurements of the laser diffraction and turbidity instruments.

Clearwater River Study Site

Backscatter from the 3-MHz ADVM was the best estimator of SSC in the Clearwater River, likely because sediment is dominated by fine sands and silt which seems to be well-targeted by the high frequency ADVM (table 2). Surrogate models also were developed to estimate sand and fines concentrations separately based on 3-MHz acoustic backscatter. RPD was calculated between each pair of measured and estimated SSC values according to equation (6).

Table 2. Surrogate model results and regression statistics for the Clearwater River at Spalding, Idaho, May 2008–September 2010.

[**Sediment surrogate:** ADVM, acoustic Doppler velocity meter; MHz, megahertz. **Model:** SSC, suspended-sediment concentration in milligrams per liter (mg/L); ABS_{corr}, acoustic backscatter corrected for beam spreading and attenuation by water and sediment in decibels (dB); Turb, turbidity in Formazin Nephelometric Units (FNU); *Q*, streamflow in cubic feet per second (ft^3/s); LISST, suspended-sediment concentration estimated by the LISST StreamSide in microliter per liter (µL/L). R^2: Coefficient of determination. **Average RPD**: Relative percent difference. **BCF:** Duan's bias correction factor. **Abbreviation:** na, not applicable]

Sediment surrogate	Number of samples used for regression	Model	R^2	Average RPD (percent)	Standard error (mg/L)	BCF
3-MHz ADVM backscatter	30	$SSC = 10^{\left[(0.0557\times 3\text{-MHz\_ABScorr})-2.431\right]} \times 1.040$	0.93	+8.6	1.34	1.040
		$\text{Sand concentration} = 10^{\left[(0.0743\times 3\text{-MHz\_ABScorr})-4.147\right]} \times 1.146$	0.87	+34	1.71	1.146
		$\text{Fines concentration} = 10^{\left[(0.0461\times 3\text{-MHz\_ABScorr})-2.030\right]} \times 1.097$	0.78	+19	1.58	1.097
Turbidity	30	$SSC = 10^{\left[(0.872\times\log(\text{Turb}))+0.454\right]} \times 1.202$	0.64	+48	1.92	1.202
2008–10 sediment transport curve	33	$SSC = 10^{\left[(1.142\times\log Q)-3.840\right]} \times 1.284$	0.54	+64	2.10	1.284
1970s sediment transport curve[1]	135	$SSC = 0.000349 \times Q^{1.074}$	0.52	+54	2.69	na[2]
0.5-MHz ADVM backscatter	30	$SSC = 10^{\left[(0.0064\times 0.5\text{-MHz\_ABScorr})-0.676\right]} \times 1.916$	0.007	+204	2.97	1.916
Laser diffraction	15	$SSC = 10^{\left[(0.0459\times\log(\text{LISST}))+1.011\right]} \times 1.560$	0.003	+119	2.73	1.560

[1] As published in Jones and Seitz (1980).

[2] Bias correction factor was not used in the computation of concentrations and loads in Jones and Seitz (1980).

Table 3. Surrogate model results and regression statistics for the Snake River near Anatone, Washington, May 2008–September 2010.

[**Sediment surrogate:** ADVM, acoustic Doppler velocity meter; MHz, megahertz. **Model:** SSC, suspended-sediment concentration in milligrams per liter (mg/L); ABS_{corr}, acoustic backscatter corrected for beam spreading and attenuation by water and sediment in decibels (dB); Turb, turbidity in Formazin nephelometric units (FNU); Q, streamflow in cubic feet per second (ft^3/s); LISST, suspended-sediment concentration estimated by the LISST StreamSide in microliter per liter (µL/L). $\mathbf{R^2}$: Coefficient of determination. **Average RPD**: Relative percent difference. **BCF:** Duan's bias correction factor. **Abbreviation:** na, not applicable

Sediment surrogate	Number of samples used for regression	Model	R^2	Average RPD (percent)	Standard error (mg/L)	BCF
1.5-MHz ADVM backscatter	22	$SSC = 10^{\left[(0.0756 \times 1.5\text{-MHz\_ABScorr})-4.676\right]} \times 1.048$	0.92	+10	1.39	1.048
		$\text{Sand concentration} = 10^{\left[(0.105 \times 1.5\text{-MHz\_ABScorr})-7.636\right]} \times 1.129$	0.89	+24	1.73	1.129
		$\text{Fines concentration} = 10^{\left[(0.0615 \times 1.5\text{-MHz\_ABScorr})-3.730\right]} \times 1.084$	0.81	+19	1.54	1.084
2008–10 sediment transport curve	33	$SSC = 10^{\left[(1.761 \times \log(Q))-6.697\right]} \times 1.120$	0.83	+24	1.65	1.120
1970s sediment transport curve [1]	125	$SSC = 0.000003 \times Q^{1.460}$	0.61	-34	2.03	na [2]
Turbidity	29	$SSC = 10^{\left[(0.0181 \times \text{Turb})+1.249\right]} \times 1.209$	0.70	+48	1.93	1.209
0.5-MHz ADVM backscatter	22	$SSC = 10^{\left[(-0.0333 \times 0.5\text{-MHz\_ABScorr})+4.301\right]} \times 1.417$	0.33	+120	2.59	1.417

[1] As published in Jones and Seitz (1980).

[2] Bias correction factor was not used in the computation of concentrations and loads in Jones and Seitz (1980).

The model between 0.5 MHz acoustic backscatter and SSC was poor (R^2=0.007) because of a problem noted in the instrument noise level measurements. At high flows, the measured noise level increased substantially and was high relative to the raw backscatter measurement. The 0.5-MHz ADVM appears to be more sensitive to electrical and other noise that occurs in the water at high streamflows than the other evaluated frequencies (Craig Huhta, SonTek/Yellow Springs Instruments, oral commun., 2012). Because the instrument noise level is subtracted from the raw backscatter to compute SNR, in many cases this resulted in a low SNR when SSC was high. For comparison, a model was developed between the raw backscatter from the 0.5-MHz ADVM (without subtracting the noise level) and SSC, resulting in an improved R^2 of 0.89, but raw backscatter data collected during this period also could have been erroneous. Overall, the 3-MHz ADVM was still a better estimator of SSC than the other surrogates whether raw backscatter or SNR was used to develop the model.

Topping and others (2004) determined that in the Colorado River, the degree of sediment attenuation along the beam path is closely related to the fines fraction, and average backscatter is closely related to the sand fraction. However, backscatter alone was determined to be a good estimator of the fines and sand fractions, as well as overall SSC, in the Clearwater River. The model between 3-MHz acoustic backscatter and SSC (overall, sand, and fines) shows that a shift from a fines-dominated SSC to a sand-dominated SSC occurs around 60 mg/L or an ABS_{corr} for the 3-MHz ADVM of 75 dB (fig. 5). Non-zero attenuation at low SSC, likely because of the presence of organic matter, created significant variability in the relation between attenuation and the fines fraction, as well as overall SSC, at low concentrations. High variability in the individual sand and fines models is caused by many physical factors of sediment load and transport including the magnitude of the washload component, mobility of bed material and armor, non-equilibrium (supply limited) transport

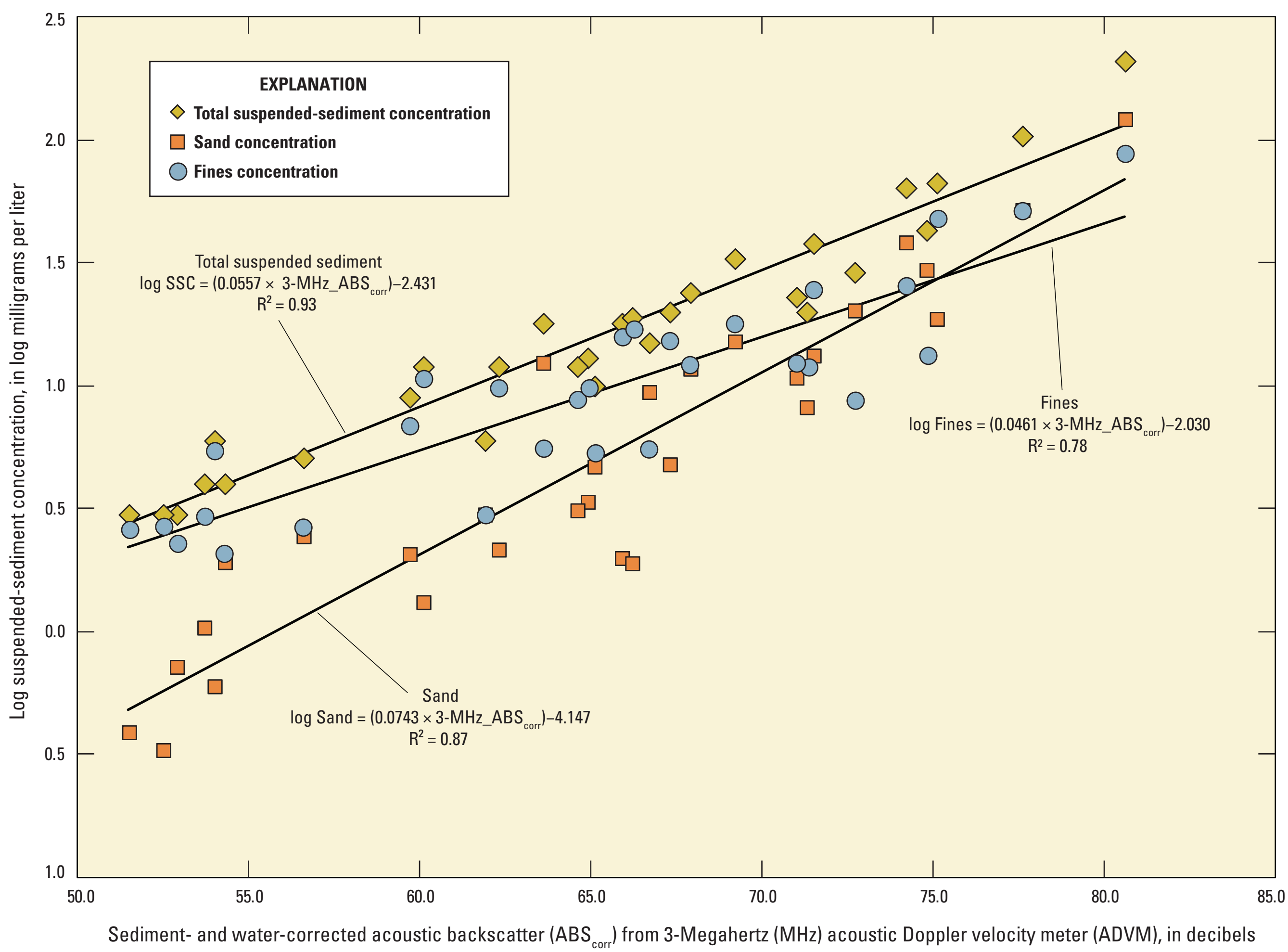

Figure 5. Surrogate regression models for total suspended sediment, sand, and fines concentrations based on acoustic backscatter for the Clearwater River near Spalding, Idaho.

of sediment, relative magnitudes of the tributary flows, timing of releases of stored water for water management, and proximity of episodic sediment sources. The uncertainty and stochasticity of the relations between these factors motivated the USACE's interest in the use of surrogate sediment measurement technology in this study.

The selected regression based on 3-MHz acoustic backscatter represented 93 percent of the variability in SSC and resulted in an average RPD between measured and estimated SSC of +8.6 percent. Standard error for the 3-MHz model was lower and variance in residuals was lower and more constant than for all other models indicating best fit. Best agreement (lowest RPD) was observed when fines were between about 70 and 85 percent of total SSC. Estimates of SSC when the sand fraction was high were not substantially improved by using the model with the 0.5-MHz ADVM, even when using a model that did not incorporate the continuously measured noise level. This is likely because most of the sand fraction is very fine and fine sand (<250 µm), which along with fines is well-represented by the 3-MHz ADVM.

Results of discrete samples collected to assess cross-sectional variability in SSC show that inflows from the upstream tributary Lapwai Creek are not well mixed with the Clearwater River at the study site under some conditions of flow. Segregation of Clearwater River and Lapwai Creek flows is supported by hydraulic analysis and observations made by aerial survey (Teasdale, 2005). Standard deviation among discrete samples ranged from 2 mg/L at low SSC to 24 mg/L at high SSC. Because water from Lapwai Creek adjoins the bank on the same side of the river as the surrogate instruments, they likely sample a zone of average to above-average SSC relative to the entire cross section. The biased sampling leads to an overestimate of sediment concentration when this phenomenon occurs. Even with this local effect, the ADVMs represent cross-sectional variability better than other surrogates. Alternative methods to correct bias imposed by non-uniform flow conditions are being evaluated.

Following a transformation back to original units, the selected regression model for estimating SSC at the Clearwater River site is:

$$SSC = 10^{[(0.0557 \times 3\text{-MHz\_ABScorr}) - 2.431]} \times 1.040 \qquad (7)$$

where

SSC is the suspended-sediment concentration (mg/L),

3-MHz_ABS_{corr} is the range-normalized acoustic backscatter from the 3-MHz ADVM corrected for two-way transmission losses (dB), and

1.040 is Duan's bias correction factor.

Measured and estimated SSC based on the selected model (eq. 7) compare well but deviate at higher SSC (>100 mg/L) (fig. 6). The upper and lower 95-percent confidence level for the sample with highest concentration, 210 mg/L, plotted well below the value estimated by the surrogate model. RPD for individual observations ranged from -43 to +80 percent, but most of the high RPDs occurred at low SSC, when small differences between estimated and measured values can result in high percent differences. At high SSC (>100 mg/L), mean RPD was -33 percent, meaning that in general, the regression model underestimated measured SSC when high. A possible reason for model underestimation at high SSC is that more sand is transported during these periods. Sand may travel lower in the water column than finer materials owing to higher mass and may not be captured within the sampling volume of the ADVMs, which are installed approximately mid-depth in the water column. An additional source of error may have been that 4 of the sample concentrations (5.1, 19, 38, and 104 mg/L) used to develop the surrogate model were averages of 10 concentrations of discrete samples collected across the cross section. However, none of these sample concentrations appear to be highly influential in the regression (fig. 5) so likely do not contribute to substantial model error. The USGS evaluated whether the inclusion of additional explanatory variables in the regression would improve estimates at high SSC. Some of the evaluated variables included the fraction

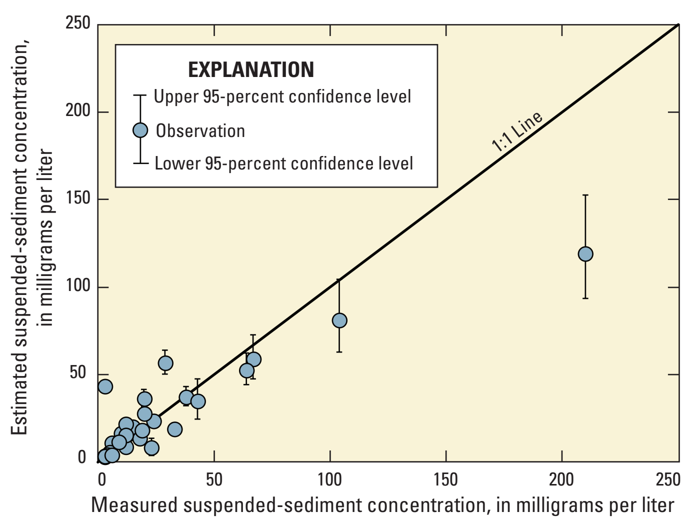

Figure 6. Measured and estimated total suspended sediment concentrations in the Clearwater River at Spalding, Idaho, based on a surrogate model with acoustic backscatter.

of unregulated flow passing the site, turbidity, the square of 3-MHz_ABS$_{corr}$, and ratios of attenuation and backscatter for the 3- and 0.5-MHz ADVMs. The fraction of unregulated flow term is discussed in more detail in Wood (2010). None of the variables substantially improved the regression statistics or SSC estimates in comparison with the base model using 3-MHz_ABS$_{corr}$ alone.

At low SSC (<100 mg/L), mean RPD was +16 percent; thus the regression model generally overestimated measured SSC when low. Average percent organic matter was 10 percent at high SSC and 23 percent at low SSC. High percent organic matter at low SSC is a possible cause of high positive RPD because the ADVMs likely detect the organic matter as sediment. Inaccuracy in the estimates of the low SSC range had a negligible effect on the estimation of the magnitude and timing of total suspended sediment load in this study, but may be of importance where chronic exposure to low levels of contaminated sediment is the concern.

Measured and estimated SSC for March–July 2010, based on the selected model with 3-MHz acoustic backscatter as well as with transport curves developed from 2008 to 2010 and 1970s samples, and streamflows, is presented in figure 7. Agreement between measured and estimated SSC is better for the 3-MHz ADVM than for the sediment-transport curves. At this site, sediment predictions based on streamflow are less accurate than those based on acoustic backscatter over a storm event. Sediment transport curves inadequately represent hysteresis of sediment concentration caused by the timing of inflows from sediment-laden tributaries and the other factors mentioned above.

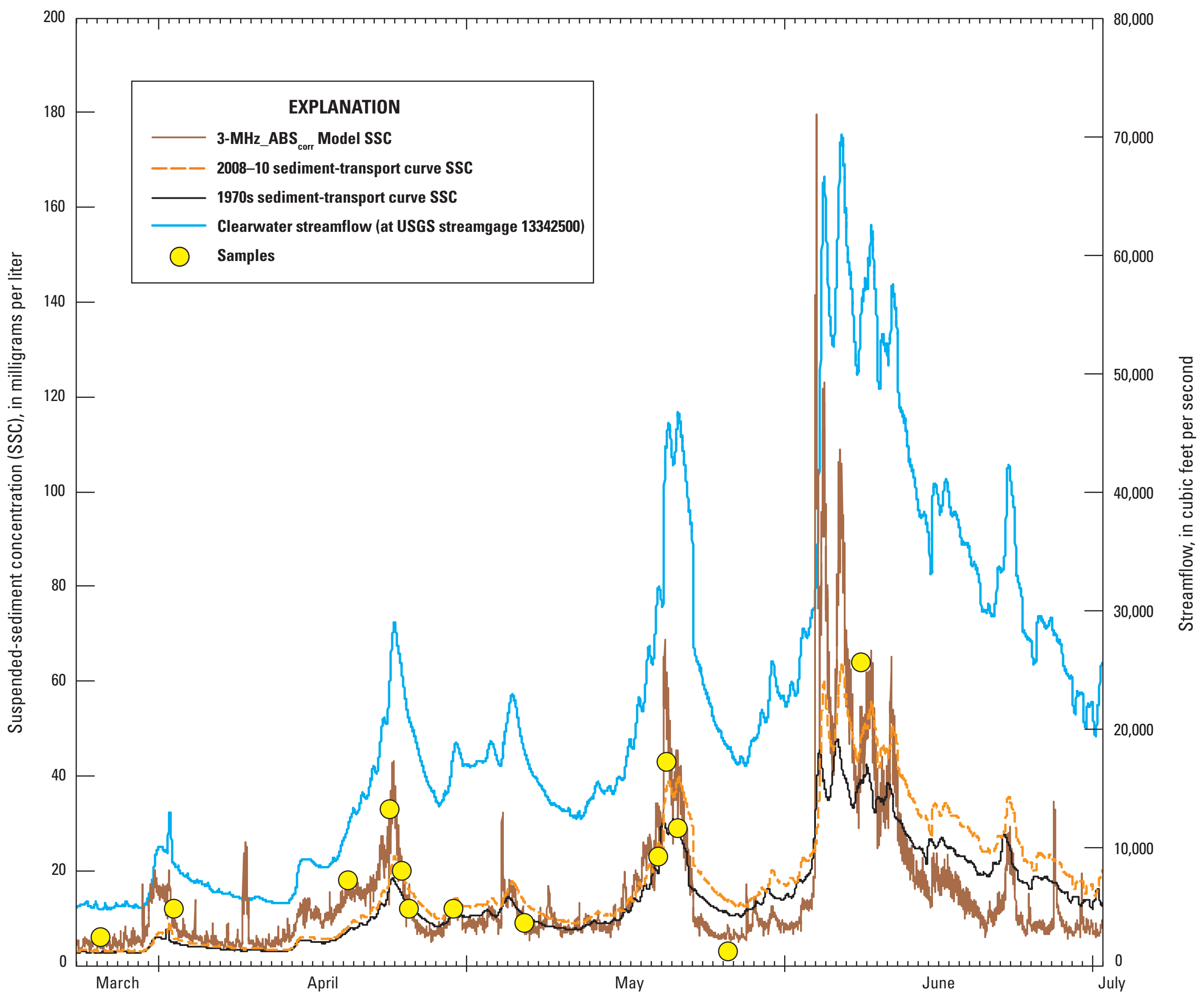

Figure 7. Estimated instantaneous values of total suspended-sediment concentration for March 23–July 1, 2010, in the Clearwater River near Spalding, Idaho, based on a surrogate model with acoustic backscatter and sediment-transport curves developed using data from the 2008–10 and 1970s studies.

Snake River Study Site

Acoustic backscatter was shown to be as good of an estimator for SSC in the Snake River as it was in the Clearwater River, despite the shorter period of record during which the ADVMs were installed and fewer samples available for the calibration (table 3). Similar to the Clearwater River, the model between 0.5-MHz ADVM backscatter and SSC was poor owing to high noise levels at high flows resulting in an inverse relation between SNR and SSC. A model developed between the raw backscatter from the 0.5-MHz ADVM (without subtracting the noise level) and SSC resulted in an improved R^2 of 0.67 but was still inferior to the model between the 1.5-MHz ADVM and SSC.

Discrete samples collected to assess cross-sectional variability in SSC show that inflows from the upstream tributary Grande Ronde River are not always well-mixed with the Snake River at the study site. Standard deviation among discrete samples was higher for the Snake River than for the Clearwater River, ranging from 15 mg/L at low SSC to 185 mg/L at high SSC. The surrogate instruments likely measure a zone of average to above-average SSC relative to the entire cross section because water from the Grande Ronde River adjoins the left bank and does not fully mix with the Snake River flow before the measurement site. As at the Clearwater River site, the ADVMs at the Snake River site are able to better represent cross-sectional variability than other surrogates.

Following a transformation back to original units, the selected regression model for estimating SSC at the Snake River site is:

$$SSC = 10^{[(0.0756 \times 1.5\text{-MHz\_ABScorr}) - 4.676]} \times 1.048 \quad (8)$$

where

SSC is the suspended-sediment concentration (mg/L),

$1.5\text{-MHz\_ABS}_{corr}$ is the range-normalized acoustic backscatter from the 1.5-MHz ADVM corrected for two-way transmission losses (dB), and

1.048 is Duan's bias correction factor.

Separate models were developed to estimate overall SSC as well as sand and fines fractions (fig. 8). The shift from a fines-dominated SSC to a sand-dominated SSC appears to occur at about 110 mg/L or an ABS_{corr} for the 1.5-MHz ADVM of 89 dB.

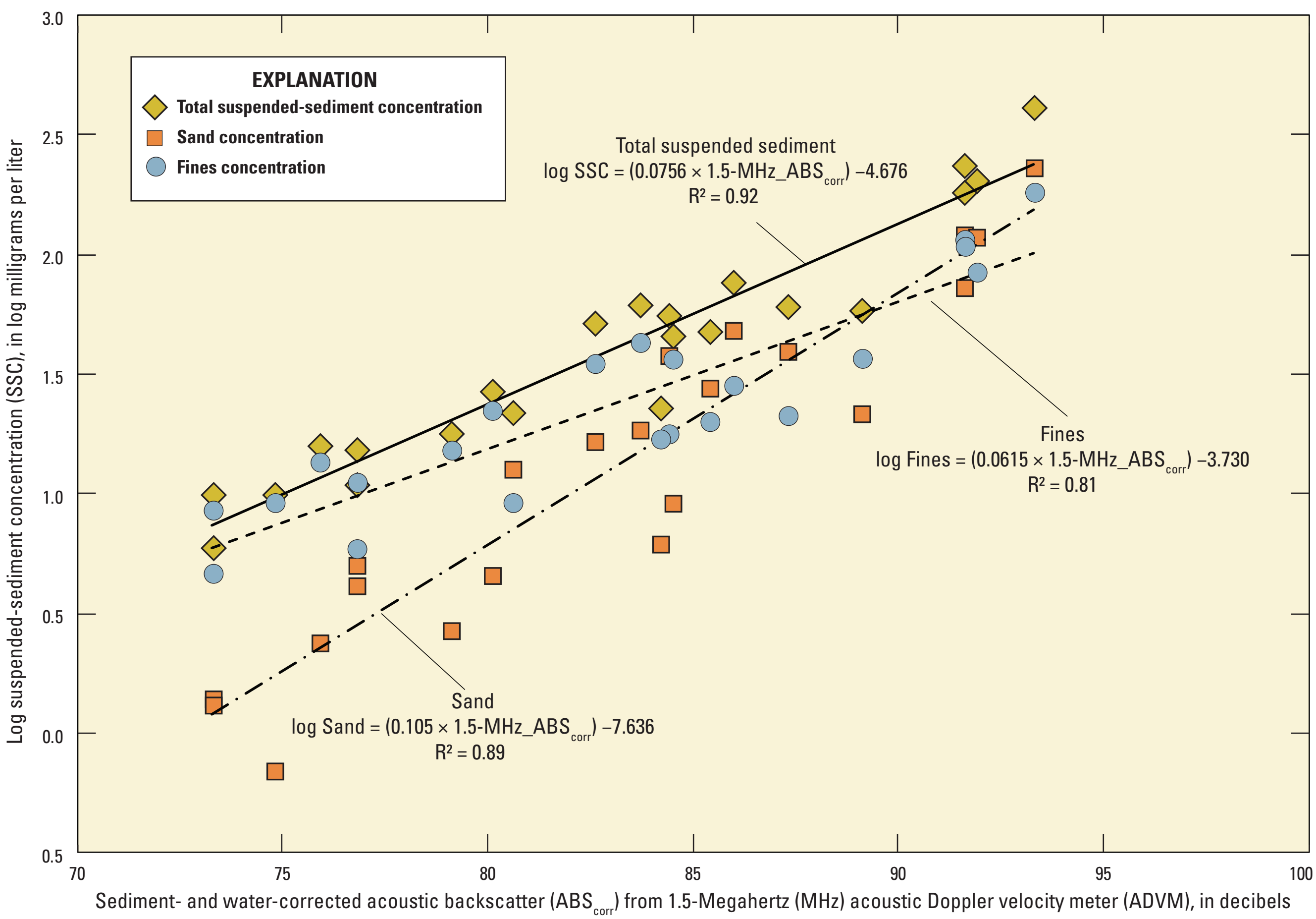

Figure 8. Surrogate regression models for total suspended sediment, sand, and fines concentrations based on acoustic backscatter for the Snake River near Anatone, Washington.

In general, agreement between measured and estimated SSC improved as the percentage of fines increased. Similar to the Clearwater River, estimates of SSC when the sand fraction was high were not significantly improved by using the model with the 0.5-MHz ADVM, even when using a model that did not incorporate the continuously measured noise level. Based on a grain-size analysis of the full sand fraction conducted for 12 of the samples, most of the sand fraction appears to be very fine and fine sand (<250 µm) with some medium sand (<500 µm), which along with fines appears to be fairly well-represented by the 1.5-MHz ADVM.

Measured and estimated SSC based on the selected model (eq. 8) shows good agreement but some deviation at high SSC (fig. 9). RPD for individual observations ranged from -40 to +123 percent, but many of the high RPDs were at low SSC, when small differences between the estimated and measured values can result in high percent differences. At high SSC (>100 mg/L), mean RPD was -16 percent, meaning that in general, the regression model underestimated true SSC when high. Similar to the Clearwater River, model underestimation at high SSC likely occurs because more sand is transported during these periods, which may travel lower in the water column than finer materials owing to higher mass and may not be captured within the sampling volume of the ADVMs. Estimates at high SSC may be improved by collecting samples to define the degree of vertical stratification of sediment and by installing another ADVM at a depth likely to capture the zone of sand transport. Similar to the Clearwater River analysis, the USGS evaluated whether the inclusion of additional explanatory variables in the regression would improve estimates at high SSC. Some of the evaluated variables included fraction of unregulated flow passing the site (discussed in Wood (2010) for a preliminary analysis of the Snake River data), turbidity, the square of 1.5-MHz_ABS_{corr}, and ratios of attenuation and backscatter for the 1.5- and 0.5-MHz ADVMs. In the final analysis, none of the variables substantially improved the regression statistics or SSC estimates in comparison with the base model using 1.5-MHz_ABS_{corr} alone.

At low SSC (<100 mg/L), mean RPD was +16 percent; thus, the regression model generally overestimated true SSC when low. Similar to the Clearwater River site, percent organic matter at low SSC was higher (16 percent) than at high SSC (5 percent) and is a possible cause of high positive RPD in those samples. Overall, however, measured and estimated SSC compared well, matching on average within 10 percent.

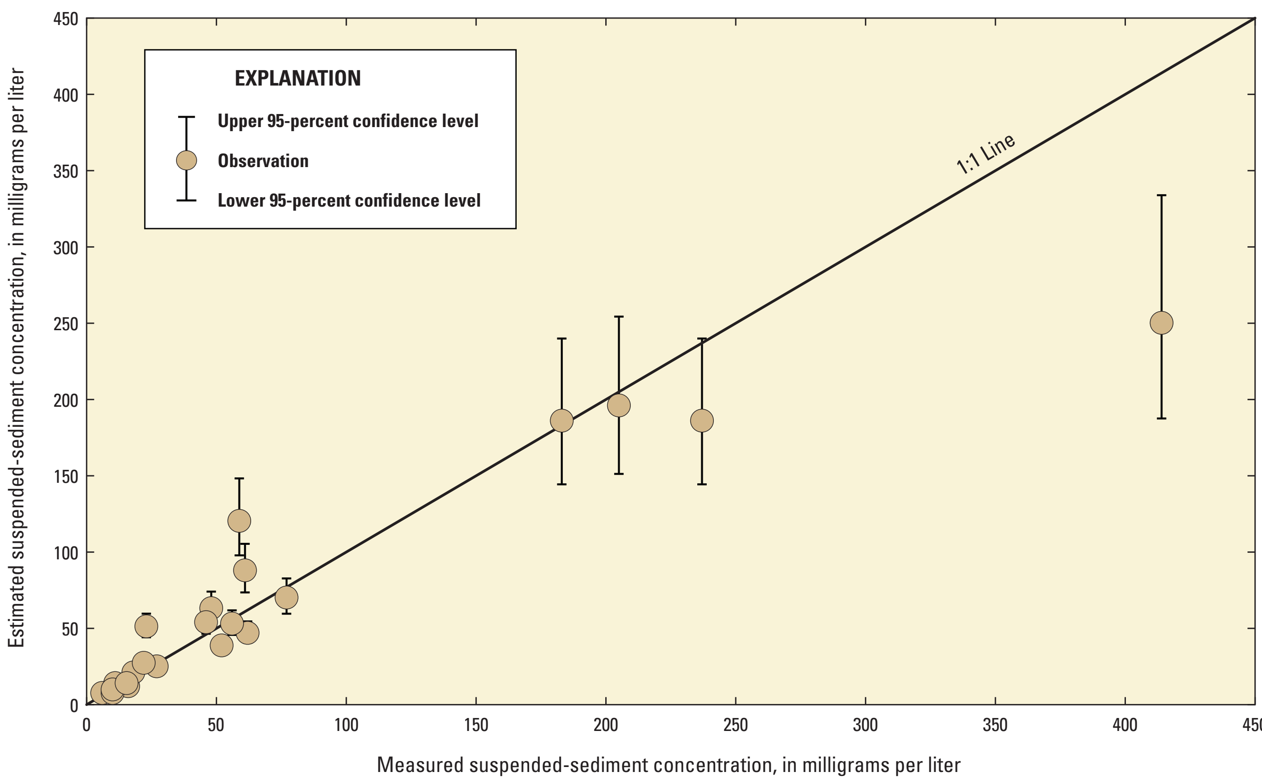

Figure 9. Measured and estimated total suspended-sediment concentrations in the Snake River near Anatone, Washington, based on a surrogate model with acoustic backscatter.

Measured and estimated SSC, based on the selected regression model as well as sediment- transport curves based on 2008–10 and 1970s samples and streamflows, are shown for a selected high flow event in June 2010 in figure 10. The highest SSC sample collected during the period of analysis (414 mg/L) was collected during this event but was not well-represented by any of the surrogate models. The peak in sediment concentration estimated by the acoustic backscatter model on June 3 on the ascending limb of the hydrograph was caused by an increase in sediment-laden inflows from the Salmon River. Because the increase in Salmon River flow was proportional to the increase in total flow at the study site, but sediment contributions were not, the increase in sediment concentrations estimated at the study site was not well-represented by the sediment-transport curves.

As a whole, the concentrations and loads calculated using the 1970s sediment-transport curve underestimate current sediment transport. If the estimates based on acoustic backscatter are assumed to be more accurate, then estimates using the 2008–10 sediment-transport curve underestimate sediment transport on the ascending limb and peak of the hydrograph and overestimate current sediment transport on the descending limb of the hydrograph. The differences between sediment loads estimated using sediment transport curves developed from 2008–10 and 1970s streamflows were much greater for the Snake River than the Clearwater River. Based on other sampling conducted by the USGS in the Snake River basin, the Salmon River transported more sediment (particularly sand) in the 2008–10 study than in the 1970s study (Clark and others, in press).

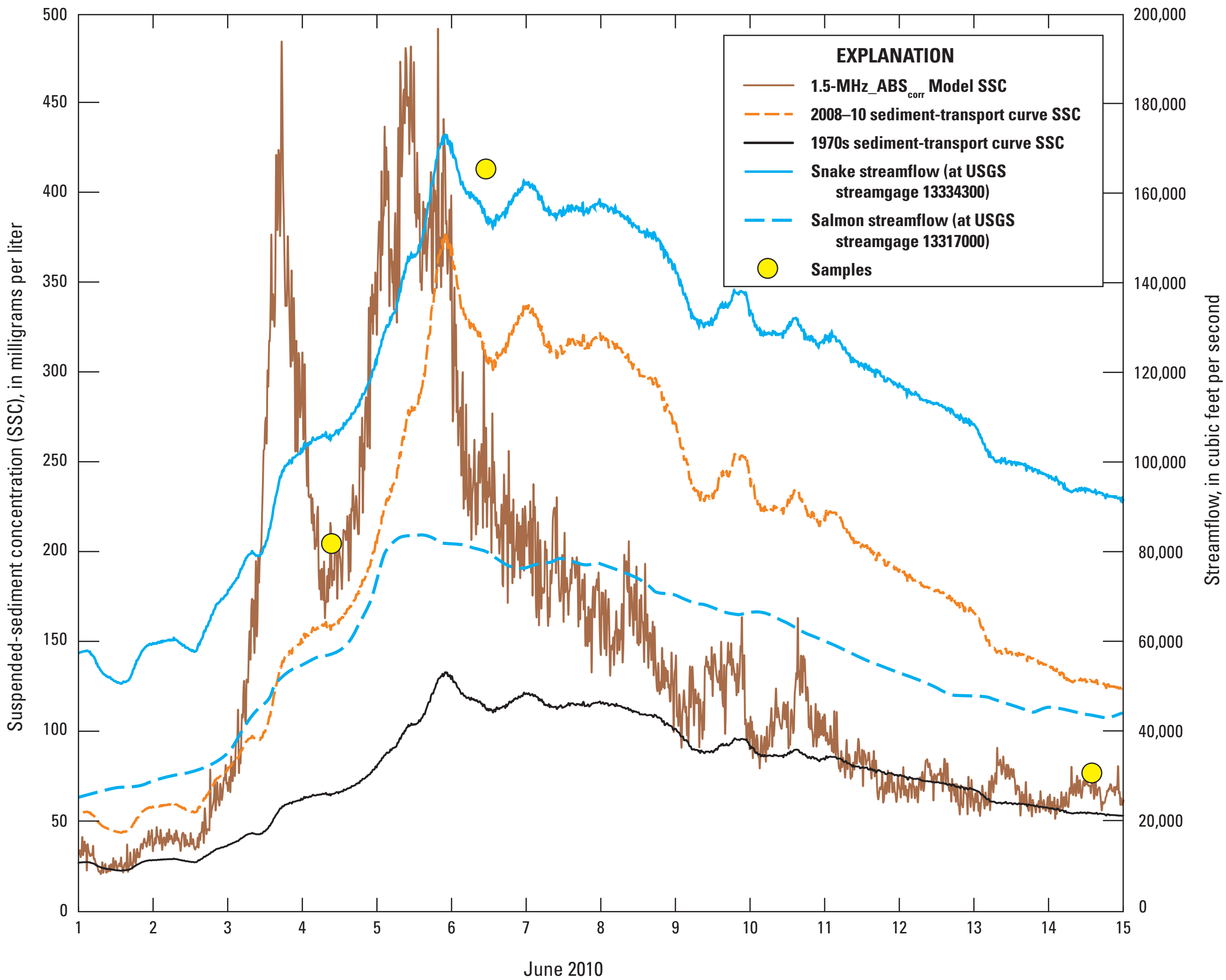

Figure 10. Estimated instantaneous values of suspended-sediment concentration during a storm event on June 1–15, 2010, in the Snake River near Anatone, Washington, based on a surrogate model with acoustic backscatter and sediment transport curves developed using data from the 2008–10 and 1970s studies.

Advantages of Acoustics over Sediment-Transport Curves in Sediment Monitoring

Use of regression models that relate measured SSC to streamflow is common practice in sedimentation engineering (Glysson, 1987; Gray and Simões, 2008) and is often necessary when sediment load must be predicted for forecast or hypothetical streamflows. In sediment load monitoring, SSC is often estimated on a continuous basis using a sediment-transport curve or linear regression, but such relations are often not accurate over short time scales because the regression prediction is for the mean SSC response. This is particularly true when estimating SSC for a particular storm event where sediment supply is the limiting factor of sediment transport and is not well represented by the mean response.

These inaccuracies arise in simple univariate regression because the same SSC is predicted at identical streamflows on the ascending and descending limbs of the hydrograph, although the actual sediment load may be strongly hysteretic. In addition, streamflows in rivers that are partially regulated may be comprised of relatively non-turbid water management releases, sediment-laden tributary inflows and overland runoff. Under these conditions, the dominant sediment sources may not contribute a large percentage of flow but contribute most of the sediment load. It follows that a large increase in flow owing to a regulated flow release may not equate to a corresponding increase in SSC. Furthermore, sudden increases in SSC because of increased sediment transport from unregulated tributaries will not be represented by a simple streamflow-sediment load regression derived for the main river unless such events were adequately represented in the regression dataset.

More complex approaches may be used to estimate composite load with separate regressions for each source, a multivariate relation (Helsel and Hirsch, 2002), or a model simulation. Load monitoring with ADVMs provides a more direct means to improve the accuracy of continuous sediment-load estimates.

The effect of tributary sediment inflow is seen in figure 7 which shows an increase in SSC estimated by acoustic backscatter in the Clearwater River on April 8, 2010, because of a storm event in the Lapwai River drainage that was not estimated by the 2008–10 or 1970s sediment-transport curves. In the Snake River in June 2010 (fig. 10), assuming that acoustic backscatter was the most accurate estimator of SSC, a small increase in flow on the ascending limb of the hydrograph owing to increases in flow from the Salmon River caused a large increase in estimated SSC that was not captured in 2008–10 and 1970s sediment-transport curve estimates.

The timing of sediment sample collection also has been traditionally targeted for capturing the peak of the hydrograph, which may or may not coincide with peak SSC. At the study sites, SSC estimated by the acoustic backscatter surrogate models typically peaks on the ascending limb of the hydrograph then decreases fairly rapidly after peak streamflow (figs. 7 and 10). It is rational that higher concentrations would be observed on the ascending limb owing to a “first flush” effect from overland runoff, tributary inflows, and resuspension of sediment from the stream channel. A surrogate model other than streamflow is needed to help guide sediment sampling efforts as well as to capture the variability in SSC during an event.

Comparison over Short Time Scales

To further quantify differences in suspended-sediment concentration and load estimates over short time scales, suspended-sediment loads were summed by month and for the duration of selected, well-defined hydrologic events. The range and distribution of SSC in the Clearwater River, analyzed by month during the period of analysis based on 3-MHz acoustic backscatter, shows several outliers with high SSC because the 3-MHz surrogate model tends to capture short-term increases in SSC (fig. 11*A*). Most storm and rain-on-snow events occur in April and May (including June 2010), and streamflow begins to decline in later June and July. Except for outliers, the estimated range and overall distribution in SSC is higher for the 2008–10 sediment-transport curves than for the acoustic backscatter models during the high flow months (April, May, June) and for months with declining flows (July, August) (fig. 11*B*). This pattern indicates that the 2008–10 sediment-transport curve does not represent conditions during individual storm events owing to hysteresis but, on a monthly basis, the transport curve overestimation of sediment on the descending limb of the hydrograph results in an overall net concentration that is higher than what is estimated using the acoustic backscatter model. Monthly SSC estimated by the 1970s sediment-transport curves were similar in pattern but slightly lower in magnitude compared with the 2008–10 sediment-transport curves. The 3-MHz surrogate model and 1970s and 2008–10 sediment-transport curves estimate similar concentrations during September through March when flows are fairly steady and storm events are infrequent. Monthly SSCs in the Snake River are similar in pattern but higher in magnitude compared to those in the Clearwater River.

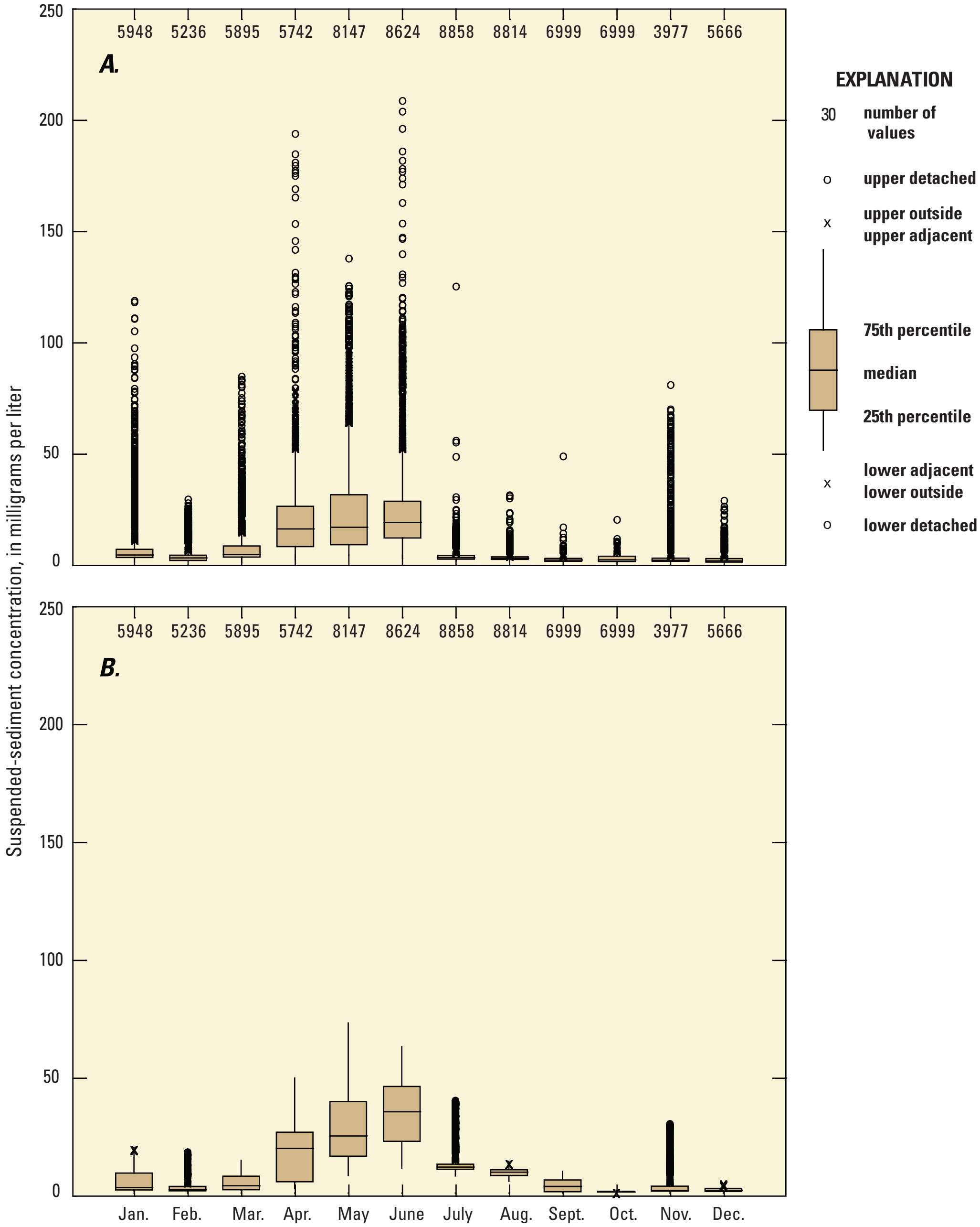

Figure 11. Distribution of total suspended-sediment concentration by month in the Clearwater River at Spalding, Idaho, based on (*A*) a surrogate model with 3MHz acoustic backscatter, (*B*) 2008–10 sediment transport curves, and (*C*) 1970s sediment transport curves, May 2008–September 2010.

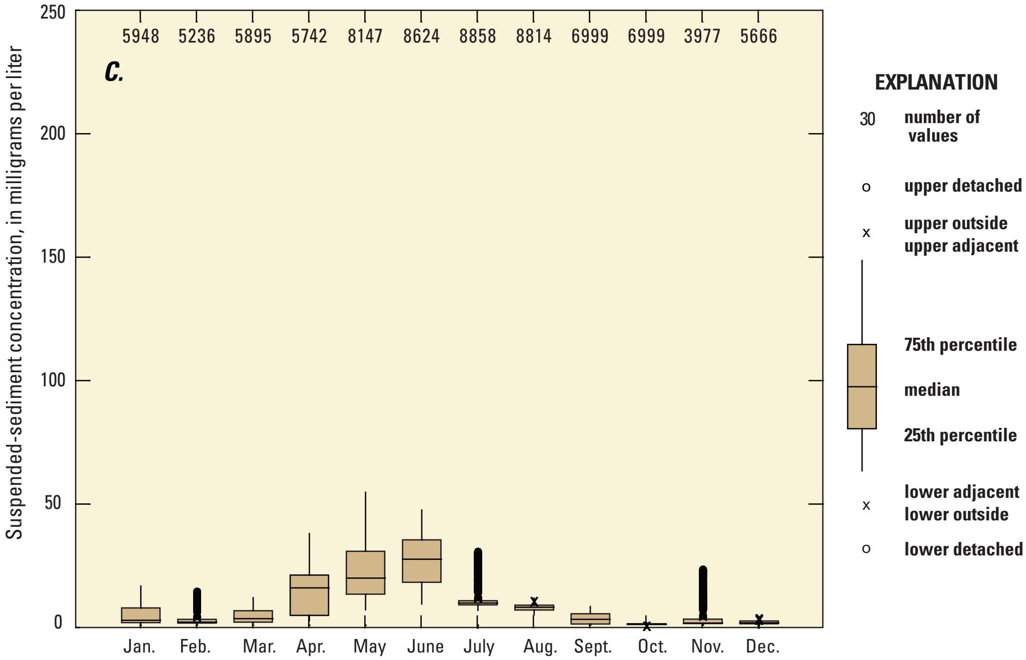

Figure 11.—Continued

Monthly patterns also are evident in figure 12, which presents total load by month for both study sites for the acoustic backscatter model and 1970s and 2008–10 sediment-transport curves. At the Clearwater River study site (fig. 12*A*), the 1970s sediment-transport curves estimate lower sediment loads during months when flow generally is increasing (April–May) and higher monthly sediment loads during months when flow is high or generally decreasing (June–August) relative to the acoustic backscatter model. At the Snake River study site, estimates generated from the 1970s sediment- transport curves are much lower than those generated from the acoustic backscatter model and 2008–10 sediment-transport curve during April–June and similar to those generated from the acoustic backscatter model during other months.

Differences in load estimates owing to hysteresis were further examined by summing estimated loads over the ascending and descending limbs of the hydrograph for several well-defined hydrologic events—seven in the Clearwater River and six in the Snake River (table 4). Load estimates based on acoustic backscatter were higher on the ascending limb (negative percent difference) and lower on the descending limb (positive percent difference) than estimates based on the 2008–10 sediment-transport curves in all cases except the descending limb for two events in the Clearwater River. Loads for these two events were low relative to other events. For all events combined, load estimates based on acoustic backscatter were 15 and 35 percent higher on the ascending limb and 30 and 49 percent lower on the descending limb than estimates based on 2008–10 sediment-transport curves for the Clearwater and Snake Rivers, respectively. Estimated SSC was usually higher on the ascending limb (especially for acoustic backscatter) but total loads were often higher on the descending limb because of a prolonged recession in flow. Loads estimated by the 1970s sediment-transport curves were not included in the storm event analysis because patterns are expected to be similar to the 2008–10 sediment-transport curves. In this study, acoustic backscatter appears to be a better estimator of sediment for load monitoring than streamflow alone over short time scales because it (1) is not affected by hysteresis, (2) provides a more direct, in-situ measurement of suspended sediment, and (3) better represents sediment sources from a combination of regulated and unregulated sources.

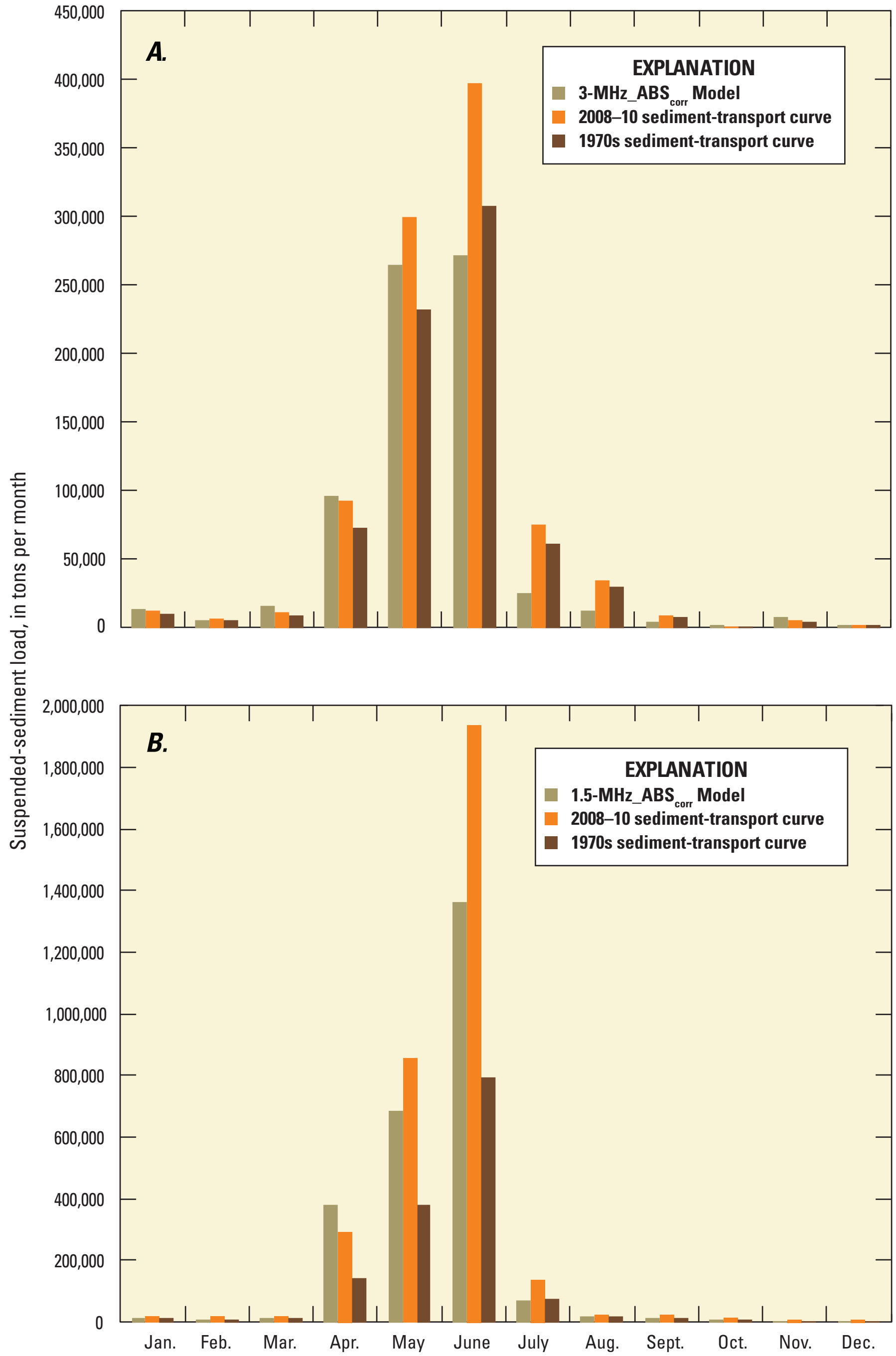

Figure 12. Total suspended-sediment load by month based on a surrogate model with acoustic backscatter and 2008–10 and 1970s sediment-transport curves for the (A) Clearwater River at Spalding, Idaho, May 2008–September 2010, and (B) Snake River near Anatone, Washington, April 2009–September 2010.

NOTE: Each month represents the total load that occurred during that month within the study period. For example, the total load for May in the Clearwater River is the sum of loads measured in May 2008, May 2009, and May 2010.

Table 4. Comparison of suspended sediment loads during selected storm events estimated using acoustic backscatter and sediment-transport curves based on 2008–10 streamflows in the Clearwater River at Spalding, Idaho, and Snake River near Anatone, Washington.

[**Abbreviations:** ABS_{corr}, acoustic backscatter corrected for beam spreading and attenuation by water and sediment in decibels (dB); na, not applicable]

Site	Event No.	Event dates	Sediment load for ascending limb of hydrograph (tons)			Sediment load for descending limb of hydrograph (tons)		
			3-MHz_ABS_{corr} or 1.5-MHz_ABS_{corr} model	2008–10 sediment transport curve	Percent difference	3-MHz_ABScorr or 1.5-MHz_ABS_{corr} model	2008–10 sediment transport curve	Percent difference
Clearwater River	na	na – All 7 events combined	172,000	148,000	-15	131,000	178,000	30
	1	May 13–24, 2008	59,400	56,700	-5	13,000	18,800	36
	2	November 12–30, 2008	2,070	1,120	-60	3,750	2,850	-27
	3	January 1–12, 2009	2,950	790	-116	3,540	2,700	-27
	4	April 21–May 1, 2009	13,000	12,900	-1	17,700	24,600	33
	5	May 18–June 12, 2009	9,130	8,170	-11	51,100	62,600	20
	6	May 14–26, 2010	14,700	11,200	-27	7,370	10,200	32
	7	June 2–July 5, 2010	70,600	57,200	-21	34,900	56,000	46
Snake River	na	na –All 6 events combined	585,000	409,000	-35	762,000	1,260,000	49
	1	April 18–May 3, 2009	122,000	68,500	-56	89,600	113,000	23
	2	May 5–11, 2009	48,600	39,400	-21	24,400	31,200	24
	3	May 18–24, 2009	98,400	84,100	-16	106,000	129,000	20
	4	April 20–27, 2010	15,700	11,300	-33	12,100	15,300	23
	5	May 16–30, 2010	33,000	26,600	-21	48,400	73,000	41
	6	June 2–19, 2010	267,000	180,000	-39	481,000	895,000	60

Comparison over Annual Time Scales

Total sediment loads were computed for the period of analysis using continuous estimates of SSC based on models with acoustic backscatter and sediment-transport curves based on 2008–10 and 1970s streamflows to determine how estimates compared over longer time scales (table 5). The period of analysis for each site was limited to the period when the ADVMs were deployed so that a direct comparison could be made between sediment-transport curves and acoustic surrogate models. On an annual basis, the 2008–10 sediment-transport curves produced load estimates that were +27 and +26 percent different for the Clearwater and Snake Rivers, respectively, from load estimates based on acoustic backscatter, meaning that the sediment-transport curves estimated more sediment than acoustic backscatter. Annual load estimates for the Clearwater River based on the 1970s transport curves were about 24 percent lower than estimates based on the 2008–10 sediment-transport curves; thus for a given flow, slightly more sediment was transported in the 2008–10 study than in the 1970s study. In the Snake River, load estimates based on the 1970s transport curves were 77 percent lower than estimates based on the 2008–10 transport curves and 54 percent lower than estimates based on acoustic backscatter. For a given streamflow, much more sediment was transported in the 2008–10 study than in the 1970s study in the Snake River. As stated previously, Clark and others (in press) noted that much more sand was transported in the Snake River during the 2008–10 study than in the 1970s study.

Overall, the acoustic backscatter model appears to be more accurate than sediment-transport curves over an annual time scale because of the patterns observed over shorter time scales (monthly and storm events). Based on the few samples collected on the receding limbs of storm hydrographs and during the long recession in flow from July to September, the sediment-transport curves overestimate sediment concentrations and loads during these flow conditions. As a result, computed annual suspended sediment is consistently higher for the sediment-transport curves than for the acoustic backscatter models.

Table 5. Comparison of total, daily, and annual suspended sediment loads estimated using acoustic backscatter and sediment-transport curves based on 2008–10 and 1970s streamflows in the Clearwater River at Spalding, Idaho, and Snake River near Anatone, Washington.

[**Sediment surrogate:** ADVM, acoustic Doppler velocity meter; MHz, megahertz. **Abbreviations:** ton/d, ton per day; ton/yr, ton per year]

Site	Sediment surrogate	Period of analysis	Total sediment load (tons)	Average daily load (ton/d)	Average annual load (ton/yr)	Percent difference in average annual load between acoustic surrogate model and sediment transport curves (percent)
Clearwater River	3-MHz ADVM backscatter	May 8, 2008–	721,000	824	300,400	
	2008–10 sediment transport curve	September 30, 2010	944,000	1,079	394,000	27
	1970s sediment transport curve		742,000	848	309,000	3
Snake River	1.5-MHz ADVM backscatter	April 2, 2009–	2,580,000	4,720	1,720,000	
	2008–10 sediment transport curve	September 30, 2010	3,350,000	6,120	2,230,000	26
	1970s sediment transport curve		1,480,000	2,700	987,000	-54

Summary and Conclusions

The U.S. Geological Survey, in cooperation with the U.S. Army Corps of Engineers, evaluated the use of acoustic backscatter, turbidity, laser diffraction, and streamflow as surrogate technologies to estimate real-time suspended-sediment concentrations (SSC) and loads in the Clearwater and Snake Rivers during 2008–10. Acoustic backscatter, measured using acoustic Doppler velocity meters (ADVMs), had the best relation with measured SSC, was less affected by biological fouling, and could be measured in a larger part of the channel than the other evaluated surrogate technologies. As a result, ADVMs capture more of the cross-sectional variability that is represented in the physical sediment samples collected at the study sites. Although organic matter concentrations were low at both sites, they most likely contributed to model error at low SSC. Model error at high SSC may have been partially due to vertical stratification of sediment (particularly sand), which was not always well-represented in the fixed-depth, horizontal sampling volume of the ADVMs. Improved estimates of SSC when sand concentrations are high may be obtained by installing an ADVM lower in the water column to measure backscatter in zones where sand is likely transported.

Overall, a single frequency ADVM was adequate to estimate suspended sediment in most of the streamflow conditions at both study sites, and optimal frequency was dependent on sediment characteristics. Acoustic backscatter provides improved estimates of suspended sediment concentration and load over traditional sediment-transport curves based on streamflow over short (monthly and storm event) and long (annual) time scales when sediment load is highly variable. In addition, acoustic backscatter better represents sediment contributions from a combination of regulated and unregulated sources, which can be difficult to represent with a univariate sediment-transport curve.

Sediment-surrogate technologies can be a cost-effective component of a long-term fluvial sediment monitoring program. Once an initial regression model is developed between surrogate data and SSC, samples can be collected less frequently, thus reducing long-term operation and maintenance costs for a sediment monitoring station. Sediment surrogates also allow the estimation of sediment when it is unsafe to sample the stream, such as during flood events. Inspection of the sediment record, estimated using a surrogate model, may reveal significant episodic sediment-transport events that would be difficult to detect otherwise. Traditional suspended-sediment estimation techniques using streamflow alone may provide poor results over small time scales or in streams with partially regulated flow, episodic sediment sources, and non-equilibrium sediment transport, as is the case for the Clearwater and Snake Rivers. Sediment-surrogate technologies are an effective means to obtain continuous, accurate estimates of suspended sediment concentrations and loads for general monitoring and sediment-transport modeling. In the Clearwater and Snake Rivers, estimates of SSC using surrogate models will allow water managers and scientists to identify the timing, magnitude, and duration of high sediment load and to better monitor long-term basin response to sediment-management strategies.

Acknowledgments

The authors wish to thank USGS employees Joseph Bunt (retired), Peter Elliott, Justin Schultz, and Doug Ott for their assistance in establishing and operating the sediment surrogate instruments. Special thanks go to hydrologists and hydrologic technicians from the USGS Idaho Water Science Center's Boise and Post Falls Field Offices for assistance with sediment and streamflow data collection. The authors are grateful to fellow members of the USGS Sediment Acoustics Leadership Team for advancing and guiding the development of sediment surrogate techniques and providing valuable advice throughout the study.

References Cited

Agrawal, Y.C., Whitmire, Amanda, Mikkelsen, Ole A., and Pottsmith, H.C., 2008, Light scattering by random shaped particles and consequences on measuring suspended sediments by laser diffraction: Journal of Geophysical Research, v. 113, 11 p.

Chanson, H., Takeuchi, M., and Trevethan, M., 2008, Using turbidity and acoustic backscatter intensity as surrogate measures of suspended sediment concentration in a small subtropical estuary: Journal of Environmental Management, v. 88, 11 p.

Clark, G.M., Fosness, R.L., and Wood, M.S., in press, Sediment transport in the lower Snake and Clearwater River basins, Idaho and Washington, 2008–2011. U.S. Geological Survey Scientific Investigations Report 2013-5083, 56 p.

Deines, K.L., 1999, Backscatter estimation using broadband acoustic Doppler current profilers, *in* IEEE Sixth Working Conference on Current Measurement, March 11–13, 1999: San Diego, Calif., [Proceedings], p. 249–253.

Downing, A., Thorne, P.D., and Vincent, C.E., 1995, Backscattering from a suspension in the near field of a piston transducer: Journal of the Acoustical Society of America, v. 97, no. 3, p. 1614–1620.

Duan, N., 1983, Smearing estimate—A nonparametric retransformation method: Journal of the American Statistical Association, v. 78, p. 605–610.

Elci, S., Aydln, R., and Work, P.A., 2009, Estimation of suspended sediment concentration in rivers using acoustic methods: Environmental Monitoring and Assessment, v. 159, no. 1–4, p. 255–265.

Flammer, G.H., 1962, Ultrasonic measurement of suspended sediment: U.S. Geological Survey Bulletin 1141-A, 48 p.

Gartner, J.W., 2004, Estimating suspended solids concentrations from backscatter intensity measured by acoustic Doppler current profiler in San Francisco Bay, California: Marine Geology, v. 211, p. 169–187.

Gartner, J.W., and Gray, J.R., 2005, Summary of suspended-sediment technologies considered at the Interagency Workshop of Turbidity and Other Sediment Surrogates—Proceedings of the Federal Interagency Sediment Monitoring Instrument and Analysis Research Workshop, September 9–11, 2003, Flagstaff, Arizona: U.S. Geological Survey Circular 1276, p. 1–15.

Glysson, G.D., 1987, Sediment-transport curves: U.S. Geological Survey Open-File Report 87–218, 47 p. (Also available at http://pubs.er.usgs.gov/publication/ofr87218.)

Gray, J.R., and Gartner, J.W., 2010, Surrogate technologies for monitoring suspended-sediment transport in rivers, *in* Poleto, Cristiano, and Charlesworth, Susanne, eds., Sedimentology of Aqueous Systems: Wiley-Blackwell, London, chap. 1, p. 3–45.

Gray, J.R., and Simões, F.J.M., 2008, Estimating sediment discharge, *in* Garcia, M.H., ed., Sedimentation engineering—processes, measurements, modeling, and practice: American Society of Civil Engineers, Manual 110, p. 1,067–1088.

Helsel, D.R., and Hirsch, R.M., 2002, Statistical methods in water resources: U.S. Geological Survey Techniques of Water-Resources Investigations, book 4, chap. A3, 522 p. (Also available at http://pubs.usgs.gov/twri/twri4a3/.)

Jones, M.L., and Seitz, H.R., 1980, Sediment transport in the Snake and Clearwater Rivers in the vicinity of Lewiston, Idaho: U.S. Geological Survey Open-File Report 80–690, 179 p. (Also available at http://pubs.er.usgs.gov/publication/ofr80690.)

Lietz, A.C., and Debiak, E.A., 2005, Development of rating curve estimators for suspended-sediment concentration and transport in the C-51 canal based on surrogate technology, Palm Beach County, Florida, 2004–05: U.S. Geological Survey Open-File Report 2005–1394, 25 p. (Also available at http://pubs.usgs.gov/of/2005/1394/.)

Meral, R., 2008, Laboratory evaluation of acoustic backscatter and LISST methods for measurements of suspended sediments: Sensors, v. 8, no. 2, 16 p.

Nolan, K.M., Gray, J.R., and Glysson, G.D., 2005, Introduction to suspended-sediment sampling: U.S. Geological Survey Scientific Investigations Report 2005-5077, CD-ROM. (Also available at http://pubs.usgs.gov/sir/2005/5077/.)

Patino, Eduardo, and Byrne, M.J., 2004, Application of acoustic and optic methods for estimating suspended-solids concentrations in the St. Lucie River Estuary, Florida: U.S. Geological Survey Scientific Investigations Report 2004–5028, 23 p. (Also available at http://pubs.usgs.gov/sir/2004/5028/.)

Porterfield, G., 1972, Computation of fluvial-sediment discharge: U.S. Geological Survey Techniques of Water-Resources Investigations, book 3, chap. C3, 66 p. (Also available at http://pubs.usgs.gov/twri/twri3-c3/.)

Rasmussen, T.J., Ziegler, A.C., and Rasmussen, P.P., 2005, Estimation of constituent concentrations, densities, loads, and yields on lower Kansas River, northeast Kansas, using regression models and continuous water-quality modeling, January 2000 through December 2003: U.S. Geological Survey Scientific Investigations Report 2005–5165, 117 p. (Also available at http://pubs.usgs.gov/sir/2005/5165/.)

Reichel, G., and Nachtnebel, H.P., 1994, Suspended sediment monitoring in a fluvial environment: advantages and limitations applying an acoustic Doppler current profiler: Water Research, v. 28, no. 4, p. 751–761.

Runkel, R.L., Crawford, C.G., and Cohn, T.A., 2004, Load Estimator (LOADEST)—A FORTRAN program for estimating constituent loads in streams and rivers: U.S. Geological Survey Techniques and Methods, book 4, chap. A5, 69 p.

Schulkin, M., and Marsh, H.W., 1962, Sound absorption in sea water: Journal of the Acoustical Society of America, v. 34, no. 6, p. 864–865.

SonTek/Yellow Springs Instruments, 2007, Argonaut-SL system manual firmware version 11.8: San Diego, Calif., SonTek/YSI Inc., 314 p.

Teasdale, G.N., 2005, Satellite and aerial imaging in characterization, hydrologic analysis and modeling of inland watersheds and streams: Pullman, Wash., Washington State University, Department of Civil and Environmental Engineering, Ph.D. dissertation.

Teasdale, G.N., 2010, Sediment load, transport and accumulation in Lower Granite Reservoir on the Snake River—Proceedings of the 2nd Joint Federal Interagency Conference, Las Vegas, Nevada, June 27–July 1, 2010: Reston, Virginia, Advisory Committee on Water Information.

Thevenot, M.M., and Kraus, N.C., 1993, Comparison of acoustical and optical measurements of suspended material in the Chesapeake Estuary: Journal of Marine Environmental Engineering, v. 1, p. 65–79.

TIBCO Software Inc.®, 2008, TIBCO Spotfire S-+ 8.1 function guide, 148 p., accessed October 26, 2012, at www.msi.co.jp/splus/support/download/V81/functionguide.pdf.

Topping, D., Melis, T., Rubin, D., and Wright, S.A., 2004, High-resolution monitoring of suspended-sediment concentration and grain size in the Colorado River using laser-diffraction instruments and a three-frequency acoustic system, *in* Liu, Cheng, ed., Proceedings of the 9th International Symposium on River Sedimentation, October 18–21, 2004,Yichang, China: Tsinghua University Press, Beijing, China, p. 2,507–2,514.

Topping, D., Wright, S.A., Melis, T.S., and Rubin, D.M., 2006, High-resolution monitoring of suspended-sediment concentration and grain size in the Colorado River using laser-diffraction instruments and a three-frequency acoustic system—Proceedings of the 8th Federal Interagency Sedimentation Conference, April 2–6, 2006, Reno, Nevada: CD-ROM, ISBN 0-9779007-1-1, p. 539–546.

Uhrich, M.A., and Bragg, H.M., 2003, Monitoring instream turbidity to estimate continuous suspended-sediment loads and yields and clay-water volumes in the Upper North Santiam River Basin, Oregon, 1998–2000: U.S. Geological Survey Water-Resources Investigations Report 03-4098, 44 p. (Also available at http://pubs.er.usgs.gov/publication/wri034098.)

U.S. Army Corps of Engineers, 2002, Dredged material management plan and environmental impact statement, McNary Reservoir and Lower Snake River Reservoirs: U.S. Army Corps of Engineers, Walla Walla District, Hydrologic Analysis, appendix A, 27 p.

U.S. Geological Survey, 2006, Collection of water samples (ver. 2.0): U.S. Geological Survey Techniques of Water-Resources Investigations, book 9, chap. A4, accessed November 8, 2008, at http://pubs.water.usgs.gov/twri9A4/.

U.S. Geological Survey, 2012, Annual water data report for water year 2011: U.S. Geological Survey database, accessed November 8, 2012, at http://wdr.water.usgs.gov/wy2011/search.jsp.

Urick, R.J., 1975, Principles of Underwater Sound (2nd ed.): McGraw Hill, New York, 384 p.

Wagner, R.J., Boulger, R.W., Jr., Oblinger, C.J., and Smith, B.A., 2006, Guidelines and standard procedures for continuous water-quality monitors—Station operation, record computation, and data reporting: U.S. Geological Survey Techniques and Methods, book 1, chap. D3, 51 p. (Also available at http://pubs.usgs.gov/tm/2006/tm1D3/.)

Wall, G.R., Nystrom, E.A., and Litten, Simon, 2006, Use of an ADCP to compute suspended-sediment discharge in the tidal Hudson River, New York: U.S. Geological Survey Scientific Investigations Report 2006–5055, 16 p. (Also available at http://pubs.usgs.gov/sir/2006/5055/.)

Wood, M.S., 2010, Evaluation of sediment surrogates in rivers draining to Lower Granite Reservoir, ID and WA—Proceedings of the 2nd Joint Federal Interagency Conference on Sedimentation and Hydrologic Modeling, Las Vegas, Nevada, June 27–July 1, 2010: Reston, Virginia, Advisory Committee on Water Information, CD-ROM, 12 p.

Yellow Springs Instruments, 2011, 6-Series multiparameter water quality sondes user manual, rev. H: Yellow Springs Instruments, 377 p., accessed November 8, 2012, at http://www.ysi.com/media/pdfs/069300-YSI-6-Series-Manual-RevH.pdf.

This page left intentionally blank

Publishing support provided by the U.S. Geological Survey
Publishing Network, Tacoma Publishing Service Center

For more information concerning the research in this report, contact the
Director, Idaho Water Science Center
U.S. Geological Survey
230 Collins Road
Boise, Idaho 83702
http://id.water.usgs.gov

Wood and Teasdale—**Surrogate Technologies to Estimate Suspended Sediment, Clearwater River, Idaho, and Snake River, Wash., 2008–10**—Scientific Investigations Report 2013-5052

Lower Snake River Programmatic Sediment Management Plan Environmental Impact Statement

Appendix M

Sediment Transport in the Lower Snake and Clearwater River Basins, Idaho and Washington

Section 4. Sediment Transport in the Lower Snake and Clearwater River Basins, Idaho and Washington, 2008-11

U.S. Geological Survey

Prepared in Cooperation with the U.S. Army Corps of Engineers

Prepared in cooperation with the U.S. Army Corps of Engineers

Sediment Transport in the Lower Snake and Clearwater River Basins, Idaho and Washington, 2008–11

Scientific Investigations Report 2013–5083

U.S. Department of the Interior
U.S. Geological Survey

August 2014

Cover:
Background: Barge on Lower Granite Reservoir near Clarkston, Washington, transporting grain downstream to the Columbia River. Photograph by Rhonda Weakland, U.S. Geological Survey, February 1, 2010.

From left to right
Inset 1: Sampling sediment during high streamflow conditions on the Selway River, Idaho. Photograph by Doug Ott, U.S. Geological Survey, May 8, 2008.
Inset 2: Suspended-sediment sample collected from the Snake River near Anatone, Washington. Photograph by Greg Clark, U.S. Geological Survey, May 6, 2008.

Sediment Transport in the Lower Snake and Clearwater River Basins, Idaho and Washington, 2008–11

By Gregory M. Clark, Ryan L. Fosness, and Molly S. Wood

Prepared in cooperation with the U.S. Army Corps of Engineers

Scientific Investigation Report 2013–5083

U.S. Department of the Interior
U.S. Geological Survey

U.S. Department of the Interior
SALLY JEWELL, Secretary

U.S. Geological Survey
Suzette M. Kimball, Acting Director

U.S. Geological Survey, Reston, Virginia: 2013

Suggested citation:
Clark, G.M., Fosness, R.L., and Wood, M.S., 2013, Sediment transport in the lower Snake and Clearwater River Basins, Idaho and Washington, 2008–11: U.S. Geological Survey Scientific Investigations Report 2013-5083, 56 p.

Contents

Figures

Figures

Tables

Conversion Factors and Datums

Conversion Factors

Inch/Pound to SI

Multiply	By	To obtain
	Length	
inch (in.)	25.4	millimeter (mm)
foot (ft)	0.3048	meter (m)
mile (mi)	1.609	kilometer (km)
	Area	
square mile (mi^2)	2.590	square kilometer (km^2)
	Flow rate	
cubic foot per second (ft^3/s)	0.02832	cubic meter per second (m^3/s)
	Mass	
ton, short (2,000 lb)	0.9072	megagram (Mg)
ton per square mile per year [(ton/mi^2)/yr]	0.3502	megagram per square kilometer year [(Mg/km^2)/yr]
ton per day (ton/d)	0.9072	metric ton per day
ton per month (ton/m)	0.9072	metric ton per month
ton per year (ton/yr)	0.9072	metric ton per year

SI to Inch/Pound

Multiply	By	To obtain
	Length	
millimeter (mm)	0.03937	inch (in.)
	Volume	
liter (L)	0.2642	gallon (gal)
	Mass	
gram (g)	0.03527	ounce, avoirdupois (oz)
kilogram per day (kg/d)	2.205	pound per day (lb/d)

Concentrations of chemical constituents in water are given either in milligrams per liter (mg/L) or micrograms per liter (µg/L).

Datums

Vertical coordinate information is referenced to the North American Vertical Datum of 1988 (NADV 88).

Horizontal coordinate information is referenced to North American Datum of 1983 (NAD83).

Altitude, as used in this report, refers to distance above the vertical datum.

Sediment Transport in the Lower Snake and Clearwater River Basins, Idaho and Washington, 2008–11

By Gregory M. Clark, Ryan L. Fosness, and Molly S. Wood

Abstract

Sedimentation is an ongoing maintenance problem for reservoirs, limiting reservoir storage capacity and navigation. Because Lower Granite Reservoir in Washington is the most upstream of the four U.S. Army Corps of Engineers reservoirs on the lower Snake River, it receives and retains the largest amount of sediment. In 2008, in cooperation with the U.S. Army Corps of Engineers, the U.S. Geological Survey began a study to quantify sediment transport to Lower Granite Reservoir. Samples of suspended sediment and bedload were collected from streamgaging stations on the Snake River near Anatone, Washington, and the Clearwater River at Spalding, Idaho. Both streamgages were equipped with an acoustic Doppler velocity meter to evaluate the efficacy of acoustic backscatter for estimating suspended-sediment concentrations and transport. In 2009, sediment sampling was extended to 10 additional locations in tributary watersheds to help identify the dominant source areas for sediment delivery to Lower Granite Reservoir. Suspended-sediment samples were collected 9–15 times per year at each location to encompass a range of streamflow conditions and to capture significant hydrologic events such as peak snowmelt runoff and rain-on-snow. Bedload samples were collected at a subset of stations where the stream conditions were conducive for sampling, and when streamflow was sufficiently high for bedload transport.

At most sampling locations, the concentration of suspended sediment varied by 3–5 orders of magnitude with concentrations directly correlated to streamflow. The largest median concentrations of suspended sediment (100 and 94 mg/L) were in samples collected from stations on the Palouse River at Hooper, Washington, and the Salmon River at White Bird, Idaho, respectively. The smallest median concentrations were in samples collected from the Selway River near Lowell, Idaho (11 mg/L), the Lochsa River near Lowell, Idaho (11 mg/L), the Clearwater River at Orofino, Idaho (13 mg/L), and the Middle Fork Clearwater River at Kooskia, Idaho (15 mg/L). The largest measured concentrations of suspended sediment (3,300 and 1,400 mg/L) during a rain-on-snow event in January 2011 were from samples collected at the Potlatch River near Spalding, Idaho, and the Palouse River at Hooper, Washington, respectively. Generally, samples collected from agricultural watersheds had a high percentage of silt and clay-sized suspended sediment, whereas samples collected from forested watersheds had a high percentage of sand.

During water years 2009–11, Lower Granite Reservoir received about 10 million tons of suspended sediment from the combined loads of the Snake and Clearwater Rivers. The Snake River accounted for about 2.97 million tons per year (about 89 percent) of the total suspended sediment, 1.48 million tons per year (about 90 percent) of the suspended sand, and about 1.52 million tons per year (87 percent) of the suspended silt and clay. Of the suspended sediment transported to Lower Granite Reservoir, the Salmon River accounted for about 51 percent of the total suspended sediment, about 56 percent of the suspended sand, and about 44 percent of the suspended silt and clay. About 6.2 million tons (62 percent) of the sediment contributed to Lower Granite Reservoir during 2009–11 entered during water year 2011, which was characterized by an above average winter snowpack and sustained spring runoff.

A comparison of historical data collected from the Snake River near Anatone with data collected during this study indicates that concentrations of total suspended sediment and suspended sand in the Snake River were significantly smaller during water years 1972–79 than during 2008–11. Most of the increased sediment content in the Snake River is attributable to an increase of sand-size material. During 1972–79, sand accounted for an average of 28 percent of the suspended-sediment load; during 2008–11, sand accounted for an average of 48 percent. Historical data from the Clearwater River at Spalding indicates that the concentrations of total suspended sediment collected during 1972–79 were not significantly different from the concentrations measured during this study. However, the suspended-sand concentrations in the Clearwater River were significantly smaller during 1972–79 than during 2008–11. The increase in suspended-sand concentrations in the Snake and Clearwater Rivers are probably attributable to numerous severe forest fires that burned large areas of central Idaho from 1980–2010.

Acoustic backscatter from an acoustic Doppler velocity meter proved to be an effective method of estimating suspended-sediment concentration and load for most streamflow conditions in the Snake and Clearwater Rivers. Models based on acoustic backscatter were able to simulate most of the variability in suspended-sediment concentrations in the Clearwater River at Spalding (coefficient of determination [R^2]=0.93) and the Snake River near Anatone (R^2=0.92). Acoustic backscatter seems to be especially effective for estimating suspended-sediment concentration and load over short (monthly and single storm event) and long (annual) time scales when sediment load is highly variable. However, during high streamflow events acoustic surrogate tools may be unable to capture the contribution of suspended sand moving near the bottom of the water column and thus, underestimate the total load of suspended sediment.

At the stations where bedload was collected, the particle-size distribution at low streamflows typically was unimodal with sand comprising the dominant particle size. At higher streamflows and during peak bedload discharge, the particle size typically was bimodal and was comprised primarily of sand and coarse gravel. About 55,000 tons of bedload was discharged from the Snake River to Lower Granite Reservoir during water years 2009–11, about 0.62 percent of the total sediment load delivered by the Snake River. About 9,500 tons of bedload was discharged from the Clearwater River to Lower Granite Reservoir during 2009–11, about 0.83 percent of the total sediment load discharged by the Clearwater River during 2009–11.

Introduction

Since construction of the first dam on the lower Snake River, the U.S. Army Corps of Engineers (USACE) has recognized that managing sediment is an ongoing maintenance issue in the reservoirs on the lower Snake River. Historically, the USACE has used dredging to manage accumulated sediment and to maintain a sufficient navigational channel. Recently, however, the USACE determined that managing sediment in the upstream watersheds might be a more effective approach to reducing sediment accumulation in the reservoirs. Although the USACE does not have the authority to manage land outside of the reservoir project boundaries, they can identify and evaluate management strategies that could be implemented on non-USACE property to reduce sediment mobilization and transport (Tetra Tech, 2006).

Because Lower Granite Reservoir is the farthest upstream reservoir on the lower Snake River, it receives and retains the largest amount of sediment. Based on extensive sediment range surveys conducted by the USACE, Lower Granite Reservoir contains an estimated 75 million cubic yards of sediment, with average annual sediment inputs of about 2.3 million cubic yards since impoundment in 1975 (Teasdale, 2010). Because of the accumulated sediment, water depths in the navigation channel near the Ports of Lewiston, Idaho, and Clarkston, Washington, at times are less than the 14-ft authorized depth and in some places are as shallow as 8 ft. Because of this reduction in the depths of the channel and the port berthing areas, some port facilities have been forced to operate at reduced capacity. Sedimentation has caused increased safety risks for the shipping industry; increased risks of grounding and damage to equipment; and decreased efficiencies due to modified approach, loading, and unloading procedures (U.S. Army Corps of Engineers, 2005).

In addition to these navigation issues, deposition of sediment and reduced channel capacity at the confluence of the Snake and Clearwater Rivers have reduced the effectiveness of the levee system that protects the cities of Lewiston and Clarkston from flooding. If allowed to continue, sedimentation may reduce the flow capacity to a point that the Standard Project Flood, an estimated or hypothetical flood that may be expected from the most severe combination of weather and flow conditions that are considered reasonably characteristic of the geographical area, may overtop the levees in Lewiston (U.S. Army Corps of Engineers, 2002).

The USACE asked the U.S. Geological Survey (USGS) to measure sediment transport in the Snake and Clearwater Rivers during construction and following the completion of Lower Granite Dam in 1972. The USGS collected data from the Snake River near Anatone, Washington, and the Clearwater River at Spalding, Idaho, from 1972 through 1979. From these data, the USGS developed sediment rating curves to estimate potential sediment transport and deposition to Lower Granite Reservoir (Jones and Seitz, 1980). Suspended silt and sand dominated the sediment load entering the reservoir, whereas bedload accounted for only about 5 percent. Based on the calculations by Jones and Seitz (1980), the Snake River delivered, on average, about 1.8 million tons per year (80 percent) of the total sediment load entering Lower Granite Reservoir; the Clearwater River accounted for about 0.47 million tons per year (about 20 percent).

In 2005, the USACE published a Notice of Intent (U.S. Army Corps of Engineers, 2005) stating plans to prepare an Environmental Impact Statement for a Programmatic Sediment Management Plan (PSMP) to address sediment management within the four lower Snake River reservoirs. The intent of the PSMP was to identify ways to reduce the amount of sediment entering the reservoirs, how to manage the sediment once it enters the reservoirs, and possible changes to structures or operations that could reduce maintenance yet maintain navigational access to the ports of Lewiston and Clarkston. By using various sediment management measures, the PSMP will become a comprehensive, watershed-level framework for managing sediment movement and deposition while maintaining current uses such as commercial navigation, irrigation withdrawals, recreation, and flow conveyance.

In March 2008, as part of its PSMP, the USACE asked the USGS to start a second sediment-sampling program in the lower Snake and Clearwater River Basins (fig. 1) and to evaluate sediment depositional characteristics in Lower Granite Reservoir. In addition to conventional sampling for suspended sediment and bedload, the USGS equipped streamgages on the Snake River near Anatone, Washington (USGS streamgage 13334300), and the Clearwater River at Spalding, Idaho (streamgage 13342500) (fig. 2) with acoustic Doppler velocity meters (ADVMs) and other instruments to evaluate whether surrogate technologies for measuring suspended-sediment concentration could adequately estimate suspended-sediment transport to Lower Granite Reservoir. In addition to the data described in this report, the USACE also contracted the USGS to evaluate sediment deposition within Lower Granite Reservoir (Williams and others, 2012; Braun and others, 2012).

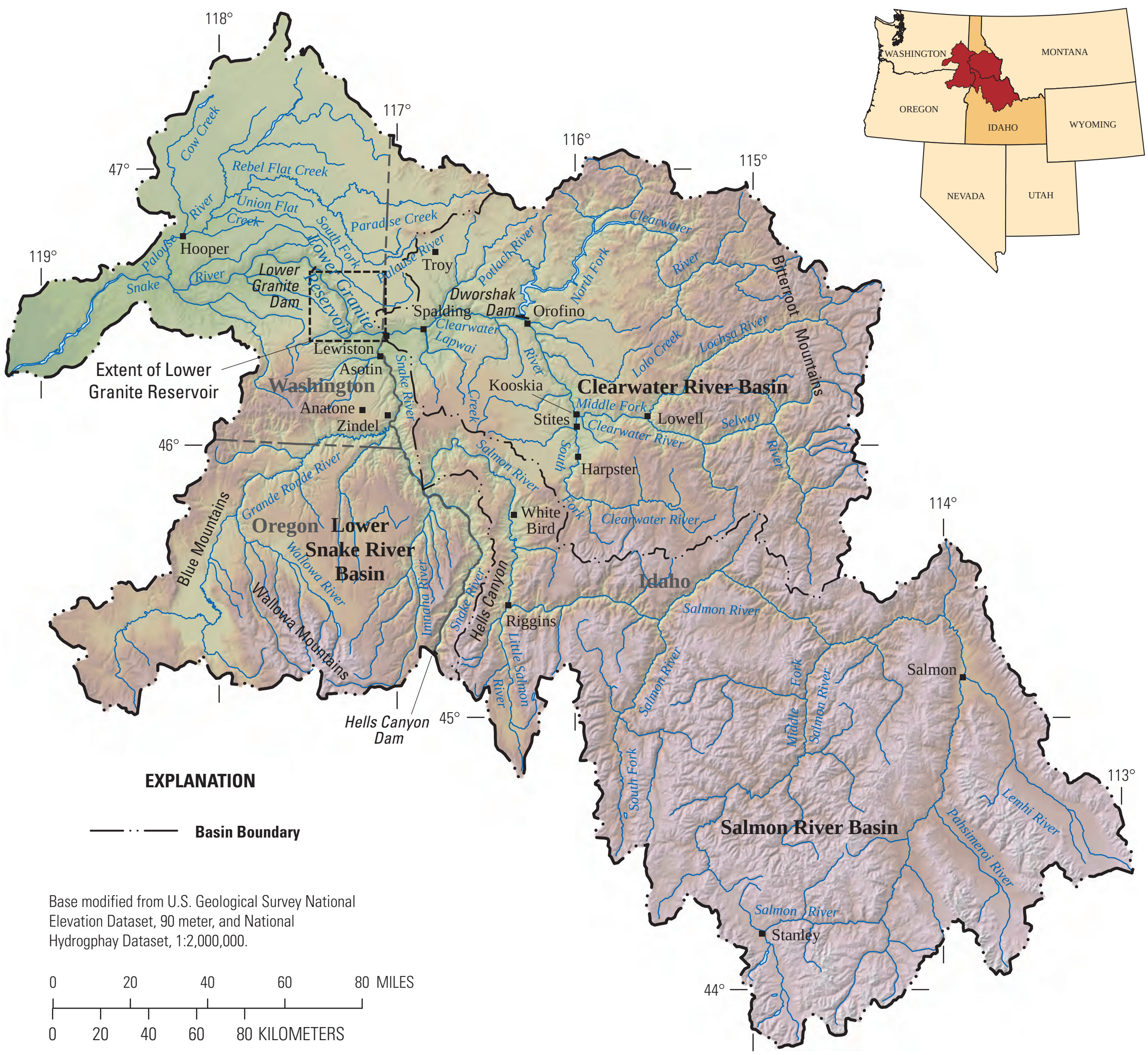

Figure 1. Lower Snake, Salmon, and Clearwater River Basins, Idaho, Oregon, and Washington.

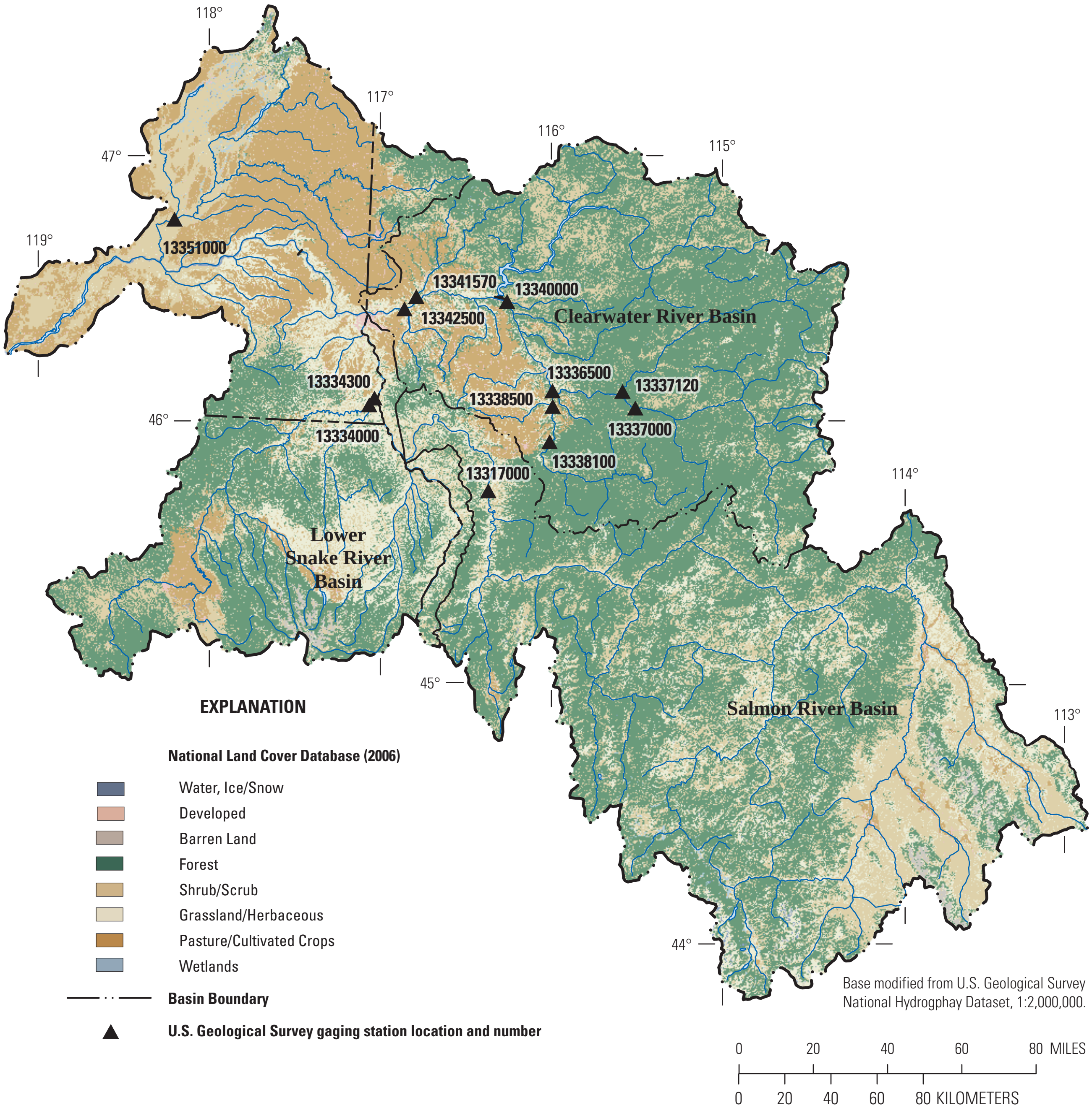

Figure 2. Land use and location of sediment-sampling stations in the lower Snake, Salmon, and Clearwater River Basins, Idaho, Oregon, and Washington, 2008–11.

Purpose and Scope

This report documents findings based on sediment data collected by the USGS in the lower Snake and Clearwater River Basins from 2008 through 2011. The purpose of this report is to provide information that improves the scientific understanding of the processes affecting sediment generation in the lower Snake and Clearwater River Basins and river hydrodynamics controlling sediment transport, deposition, and retention in Lower Granite Reservoir and downstream in the Snake River. The report provides suspended sediment and bedload data to (1) identify the dominant subbasins contributing sediment to Lower Granite Reservoir, (2) evaluate sediment transport in the Clearwater and lower Snake River Basins, and (3) quantify transport of sediment to Lower Granite Reservoir. Additionally, data collected using acoustic Doppler velocity meters (ADVMs) is summarized and compared with conventionally acquired sediment data to evaluate the efficacy of estimating suspended-sediment concentration (SSC) continuously by means of acoustic surrogates.

Description of Study Area

The drainage basin contributing sediment to Lower Granite Reservoir comprises an area of about 27,000 mi^2 that includes the Snake River Basin from Hells Canyon Dam downstream to the confluence with the Clearwater River and the Clearwater River Basin (fig. 1). The three dams constituting the Hells Canyon Complex (completed in 1967) on the Snake River effectively trap sediment transported from areas upstream of the dams (Parkinson and others, 2003), as does Dworshak Dam (completed in 1972) on the North Fork Clearwater River. The Hells Canyon Complex and Dworshak Dam effectively eliminate about 81 and 25 percent, respectively, of the total drainage basin in the Snake and Clearwater Rivers from contributing sediment to Lower Granite Reservoir. The Salmon River Basin (drainage area of about 14,000 mi^2) is about 71 percent of the remaining area in the Snake River Basin downstream of Hells Canyon Dam and about 52 percent of the total combined area of the Snake and Clearwater River Basins contributing sediment to Lower Granite Reservoir. Other contributing basins are the Clearwater (about 7,200 mi^2 or 27 percent of the total area), the Grande Ronde (about 3,950 mi^2 or 15 percent), and the Snake River Basin downstream of Hells Canyon Dam to Lower Granite Reservoir, but excluding the Salmon and Grande Ronde Basins (about 1,850 mi^2 or 7 percent). The Palouse River has a drainage basin of about 3,280 mi^2, and is a tributary to the Snake River about 48 mi downstream of Lower Granite Dam.

Salmon River Basin

The Salmon River is an unregulated, free-flowing river that originates in mountain ranges in Idaho and western Montana and flows about 410 mi through central Idaho to its confluence with the Snake River in lower Hells Canyon (fig. 1). The Salmon River derives its streamflow from several tributaries including the Lemhi, Pahsimeroi, Middle Fork Salmon, South Fork Salmon, and Little Salmon Rivers. Peak flows in the Salmon River generally occur in May and June during snowmelt runoff. Between 1975 and 2010, the Salmon River, on average, discharged about 10,700 ft^3/s to the Snake River. The Salmon River contributes about 32 percent of the mean streamflow measured at the Snake River near Anatone (streamgage 13334300 [fig. 2]) and about 22 percent of the combined streamflow entering Lower Granite Reservoir from the Snake and Clearwater Rivers (U.S. Geological Survey, 2013).

About 90 percent of the Salmon River Basin is comprised of Federal lands, about 77 percent national forest managed by the U.S. Forest Service, and 13 percent managed by the Bureau of Land Management. Nearly 80 percent of the land cover is forest in the Salmon River Basin (fig. 2); agricultural and urban areas combined account for less than 3 percent (Tetra Tech, 2006). Key geologic features in the Salmon River Basin are the Idaho Batholith and Challis volcanics that tend to produce coarse, sandy soils that are highly erodible when weathered (King and others, 2004). The erodible geology, steep topography, and lack of hydrologic control structures combine to mobilize large quantities of sediment from the Salmon River Basin to downstream waters. Numerous forest fires that burned large areas of the basin between 1980 and 2010 have further worsened the susceptibility of the Salmon River Basin to erosion.

Snake River Downstream of Hells Canyon Dam

The Snake River in the Hells Canyon reach incorporates drainages upstream of Lower Granite Reservoir and downstream of Hells Canyon Dam, exclusive of the Salmon and Grande Ronde River Basins (fig. 1). The supply of sediment to this reach of the Snake River is limited by upstream trapping in the Hells Canyon Complex of dams that was completed in 1967. Although sediment delivery to the Snake River in the Hells Canyon reach is limited, streamflow is generated from the entire 93,500-mi^2 drainage basin, including the area upstream of the Hells Canyon complex. In the 110-mi reach of the Snake River between Hells Canyon Dam and Lower Granite Reservoir, the Snake River flows primarily north, forming first the border between Idaho and Oregon, and then the border between Idaho and Washington.

The primary tributary in this reach, excluding the Salmon and the Grande Ronde Rivers, is the Imnaha River which enters from the west about 55 mi downstream of Hells Canyon Dam. Between Hells Canyon Dam and the Imnaha, the Snake River runs through a deep and narrow v-shaped valley entrenched in erosion-resistant basalt and metamorphic bedrock (Parkinson and others, 2003). About 22 percent of the 1,850 mi^2 area drained by the Snake River in the Hells Canyon reach is comprised of agricultural land, primarily in the lower parts of the drainage basin downstream of the confluence with the Imnaha. Forested land makes up about 47 percent of the drainage basin (fig. 2) (Tetra Tech, 2006). Sediment source studies in the Hells Canyon reach indicate that sediments transported in the Snake River are primarily coarse grained, gravel-sized materials derived from local landslides, talus slopes, and tributary inflows (Miller and others, 2003).

Grande Ronde River Basin

The Grande Ronde River flows about 180 mi in a northeasterly direction draining streams in the Blue and Wallowa Mountains of northeastern Oregon. Most of the Grande Ronde drainage basin is in Oregon with a small part in southeastern Washington. A major tributary to the Grande Ronde River is the Wallowa River. The Grande Ronde River flows into the Snake River about 23 mi upstream of the town of Asotin, Washington, and just upstream of the sampling location on the Snake River near Anatone (fig. 2). Because most of the drainage basin in the lower Grande Ronde is at an altitude less than 3,000 ft, runoff typically starts in April and lasts until late June when snowmelt occurs in higher elevation areas of the basin.

About 70 percent of the Grande Ronde Basin is forested and about 17 percent is agricultural land (fig. 2). About 50 percent of the basin is privately owned; most of these private lands lie within stream valleys along the Grande Ronde and Wallowa Rivers. Private lands primarily are used for agriculture, grazing, and forestry (Tetra Tech, 2006). The U.S. Forest Service manages about 47 percent of the land within the Grande Ronde Basin for multiple uses including timber production, livestock grazing, and recreation. The surface geology in the Grande Ronde Basin is primarily basalt from the Columbia River Group with a highly variable soil erosional capacity. In contrast to the Salmon River Basin, where most of the sediment is derived from natural processes, land-use practices probably account for a large part, if not most of the sediment production in the Grande Ronde Basin.

Clearwater River Basin

The Clearwater River originates in the Bitterroot Mountains at the border of Idaho and Montana and flows westward to its confluence with the Snake River at Lewiston, Idaho (fig. 1). Major tributaries to the Clearwater River include the Lochsa and Selway Rivers, the North and South Forks of the Clearwater River, and the Potlatch River. Dworshak Dam effectively traps most of the sediment transported from the North Fork Clearwater River drainage basin prior to reaching the main stem Clearwater River. From 1975 through 2010, the Clearwater River contributed about 30 percent of the streamflow (as measured at Spalding) entering Lower Granite Reservoir. Similar to the Salmon River, streamflow in the Clearwater River typically peaks in May and June in response to snowmelt runoff. Highly erosive igneous rocks underlay a large part of the Clearwater River Basin (King and others, 2004). As a result, much of the basin is highly susceptible to erosion and subsequent sediment transport. Overall, cropland and pastureland make up about 18 percent of the Clearwater River Basin (Tetra Tech, 2006). The intensity of agricultural activity generally increases in a downstream or westerly direction (fig. 2).

The Lochsa and Selway Rivers combined drain about 46 percent of the Clearwater River Basin, draining areas that are essentially 100 percent forested; the U.S Forest Service manages more than 95 percent of the land (Tetra Tech, 2006). Underlain by the Idaho Batholith, the Lochsa and Selway drainage basins are characterized by rock that weathers deeply to produce coarse, sandy soils with high erosion rates if disturbed (King and others, 2004).

The Potlatch River is the largest tributary (drainage basin of about 550 mi^2) to the lower Clearwater River Basin. The Potlatch River is a tributary to the Clearwater River about 15 mi upstream of Lower Granite Reservoir (fig. 1). About 57 percent of the Potlatch River drainage basin is forested, mostly in the northern upstream areas. Primary land-uses in the forested areas include timber harvest and other forest management practices. The downstream part of the drainage basin is predominantly agricultural (about 43 percent of the total basin area), used primarily for dryland agriculture and grazing (Latah Soil and Water Conservation District, 2007). Land-use activities in the drainage basin have resulted in changes in the vegetative cover, increases in soil compaction, and channel modifications that have resulted in a flashy hydrograph and rapid streamflow runoff (Latah Soil and Water Conservation District, 2007). Instantaneous streamflows of 8,000 ft^3/s in winter and early spring are not unusual.

Palouse River Basin

The Palouse River drains about 3,300 mi^2 of southeastern Washington and parts of the northern Idaho panhandle. The headwaters of the Palouse River originate in the forested mountains of northwestern Idaho; the river flows westward through farmland to its confluence with the Snake River about 48 mi downstream of Lower Granite Dam (fig. 1). Major tributaries to the Palouse River are the South Fork Palouse River and Paradise, Rebel Flat, Rock, Union Flat, and Cow Creeks. Activities that affect water quality in the Palouse River Basin include dryland agriculture (67 percent of the drainage basin), rangeland (26 percent), timber harvest, mining, and urban development (Washington State Department of Ecology, 2006). Irrigated farmland adjacent to the Palouse River and its tributaries comprises less than 1 percent of the land use. Forested land comprises about 6 percent of the drainage basin, primarily in the upland northern and eastern parts (fig. 2). Agricultural fields throughout the basin are highly susceptible to soil erosion from November through March when high intensity rainstorms can cause intensive runoff and soil erosion. These winter storms can deliver large quantities of sediment to streams throughout the Palouse River drainage basin (Ebbert and Roe, 1998).

Methods of Data Collection and Analysis

Data were collected for this study from March 2008 through September 2011 to evaluate sediment transport in the lower Snake and Clearwater River Basins and sediment deposition in Lower Granite Reservoir. Data collection included measurement of streamflow, conventional sampling for suspended sediment and bedload at 12 sampling stations in the lower Snake and Clearwater River Basins, and acoustic surrogate sampling at two USGS streamgages: the Snake River near Anatone, Washington and the Clearwater River at Spalding, Idaho (table 1). The methods and results of depositional surveys conducted in Lower Granite Reservoir are described in Williams and others (2012) and Braun and others (2012), respectively. This section of the report documents the methods used for data collection and analysis of streamflow and suspended sediment and bedload.

Table 1. U.S. Geological Survey streamgaging stations where sediment samples were collected, lower Snake and Clearwater River Basins, Washington and Idaho, water years 2008–11.

[Locations of stations are shown in figure 2. **Effective drainage area** does not include watershed area upstream of Dworshak and Hells Canyon Dams. **Abbreviations:** USGS, U.S. Geological Survey; mi^2, square mile]

USGS gaging station No.	Gaging station name	Effective drainage area (mi^2)	Sampling period	Type of streamflow record	Number of suspended-sediment samples	Number of bedload samples
13317000	Salmon River at White Bird, Idaho	13,500	03-2009–07-2011	Continuous	42	5
13334000	Grande Ronde River at Zindel, Washington	3,940	03-2009–07-2011	Indexed	38	0
13334300	Snake River near Anatone, Washington[1]	19,700	04-2008–07-2011	Continuous	39	16
13336500	Selway River near Lowell, Idaho	1,910	03-2009–07-2011	Continuous	37	11
13337000	Lochsa River near Lowell, Idaho	1,180	03-2009–07-2011	Continuous	36	3
13337120	Middle Fork Clearwater River at Kooskia, Idaho	5,490	03-2009–07-2011	Indexed	38	11
13338100	South Fork Clearwater River near Harpster, Idaho	865	03-2009–07-2011	Indexed	39	15
13338500	South Fork Clearwater River at Stites, Idaho	1,150	03-2009–07-2011	Continuous	41	14
13340000	Clearwater River at Orofino, Idaho	5,580	03-2009–07-2011	Continuous	36	7
13341570	Potlatch River below Little Potlatch Creek near Spalding, Idaho	583	03-2009–07-2011	Continuous	37	0
13342500	Clearwater River at Spalding, Idaho[1]	7,140	03-2008–07-2011	Continuous	40	11
13351000	Palouse River at Hooper, Washington	2,500	03-2009–07-2011	Continuous	33	0

[1] Station was equipped with suspended sediment surrogate technology.

Streamflow

Streamflow measurements at all of the sediment sampling stations were obtained using standard USGS methods (Mueller and Wagner, 2009; Turnipseed and Sauer, 2010). At 9 of the 12 sampling stations, streamflow was measured at an established streamgage using a continuous record of water stage calibrated to periodic onsite measurements of streamflow. For the three sampling stations without continuous streamflow record (table 1), streamflow was measured when sediment samples were collected, and then indexed to the streamflow at a nearby streamgage (or group of streamgages) with continuous data. The correlation between streamflow at the non-continuous sampling station and the continuous streamgage(s) was used to generate a daily mean streamflow record for the non-continuous sampling station over the period of this study. For example, instantaneous streamflow measurements made during sediment sample collection at the non-continuous sampling station on the South Fork Clearwater River near Harpster, Idaho (USGS station 13338100) from March 2009 through July 31, 2011, were indexed to the streamflow recorded simultaneously at the continuous streamgage on the South Fork Clearwater River at Stites, Idaho (USGS streamgage 13338500) ($R^2 = 0.996$). The resultant relation was used to estimate the daily mean streamflow at the South Fork Clearwater River near Harpster from the daily mean streamflow at South Fork Clearwater River at Stites for the period of study. The same methodology was used for two other non-continuous sampling stations; the Grande Ronde River at Zindel, Washington (USGS station 13334000) was indexed to an upstream streamgage with continuous record on the Grande Ronde River at Troy, Oregon ($R^2 = 0.976$), and the Middle Fork Clearwater River at Kooskia, Idaho (USGS station 13337120) was indexed to the combined streamflow from the continuous streamgage on the Selway River near Lowell, Idaho (USGS streamgage 13336500) and the Lochsa River near Lowell, Idaho (USGS streamgage 13337000) ($R^2 = 0.992$).

Suspended Sediment and Bedload

Streams transport sediment by carrying the finer particles in suspension with turbulent eddies and by rolling or skipping coarser particles along the streambed. The discharge of fine-grained particles typically is controlled by the available supply of fine-grained sediment. These fine-grained sediments generally move downstream in suspension at about the same velocity as the water. The sediment that moves on or near the stream bottom by sliding, rolling, or bouncing is bedload (Edwards and Glysson, 1999), which increases exponentially with increasing streamflow. The total sediment load in a stream is defined as the sum of the suspended-sediment load plus the bedload. Because the particle size distribution of the suspended load is a function of streamflow, substantial variation typically occurs in the concentration and grain-size characteristics of sediments both spatially at different locations in a stream and temporally with changes in the magnitude of streamflow.

For this study, suspended sediment and bedload sampling started in spring 2008 at the Snake River near Anatone and the Clearwater River at Spalding streamgages. In spring 2009, sample collection extended to 10 additional stations for suspended sediment and 7 stations for bedload to help quantify the sediment contributions from discrete subbasins in the lower Snake and Clearwater River Basins (table 1). Sample collection at all the stations continued through July 2011, following the end of the spring runoff. All sediment samples were collected using standard USGS methods, procedures, and equipment as documented by Edwards and Glysson (1999).

Suspended Sediment

Suspended-sediment samples were collected 9–15 times per year at each of the study stations to encompass a range of streamflow conditions (table 2). As illustrated in figure 3 at the Snake River near Anatone and the Clearwater River at Spalding, targeted suspended-sediment samples were collected during the ascending limb, the peak, and the descending limb of the snowmelt runoff hydrograph at each station to determine the effects of hysteresis on SSC. Significant hydrologic events such as a rain-on-snow event that occurred during January 2011 were targeted for additional sampling.

Suspended-sediment samples were collected using equal-width and depth-integrating techniques. Isokinetic D-96 collapsible-bag samplers were suspended from either a bridge or cableway to obtain the samples. Use of the D-96 allows for isokinetic sampling over a wide range of stream depths and velocities (Davis, 2005). For collection of suspended-sediment samples, the total stream width at each station was divided into 10 equal-width increments, and individual depth-integrated samples were collected at the centroid of each increment.

Table 2. Ranges of streamflow sampled and suspended-sediment concentrations in samples collected from the lower Snake and Clearwater River Basins, Washington and Idaho, water years 2008–11.

[Locations of stations are shown in figure 2. **Abbreviations:** USGS, U.S. Geological Survey; ft^3/s, cubic foot per second; mg/L, milligram per liter; µm, micrometer]

USGS gaging station No.	Gaging station name	Streamflow range when samples collected (ft^3/s)	Median suspended-sediment concentration (mg/L)	Range of suspended-sediment concentration (mg/L)	Median suspended-sediment fraction less than 62.5 µm (percent)	Range suspended-sediment concentration less than 62.5 µm (percent)
13317000	Salmon River at White Bird, Idaho	3,970–83,900	94	3.0–600	51	14–97
13334000	Grande Ronde River at Zindel, Washington	766–25,000	30	3.0–570	84	65–97
13334300	Snake River near Anatone, Washington	14,900–155,000	55	5.0–410	62	32–94
13336500	Selway River near Lowell, Idaho	651–32,500	11	1.0–180	42	15–89
13337000	Lochsa River near Lowell, Idaho	434–21,200	11	1.0–87	51	23–84
13337120	Middle Fork Clearwater River at Kooskia, Idaho	1,140–28,000	15	1.0–99	49	23–94
13338100	South Fork Clearwater River near Harpster, Idaho	194–11,000	26	1.0–200	61	28–90
13338500	South Fork Clearwater River at Stites, Idaho	213–12,400	24	2.0–530	62	39–94
13340000	Clearwater River at Orofino, Idaho	1,580–69,500	13	2.0–240	66	29–91
13341570	Potlatch River below Little Potlatch Creek near Spalding, Idaho	15.0–17,000	42	3.0–3,300	92	68–99
13342500	Clearwater River at Spalding, Idaho	3,390–78,900	21	3.0–210	70	30–96
13351000	Palouse River at Hooper, Washington	48.0–7,150	100	12–1,400	95	48–99

Individual samples from each centroid were composited in 3-L bottles until the entire cross section of the stream was sampled. Typically, two–three 3-L bottles were required for each suspended-sediment composite. Samples were sent to the USGS Cascade Volcano Observatory (CVO) sediment laboratory in Vancouver, Washington after collection where they were analyzed for total SSC and particle-size fraction less than 62.5 µm (Guy, 1969). In addition to the composited samples, selected suspended-sediment samples were collected at the Snake River near Anatone and Clearwater River at Spalding streamgages to document the river cross-sectional variability. For these samples, individual bottles were used to collect samples from each centroid in the cross section. The samples were then analyzed separately for sediment concentration and full-grain size analysis on the sediment size greater than a diameter of 62.5 µm.

The SSC in a stream generally varies in relation to streamflow. Because of this variability, summary statistics to characterize a stream, such as a mean concentration, may include bias resulting from variation in the sampling frequency and the timing of sampling over the stream hydrograph or a storm event. For this study, mean flow-weighted concentrations and suspended-sediment loads were simulated using LOADEST, a FORTRAN program for estimating constituent loads in streams and rivers (Runkel and others, 2004). LOADEST is based on a rating-curve method (Cohn and others, 1989, 1992; Crawford, 1991) that uses regression to estimate constituent load in relation to several predictor variables related to streamflow and time. This type of model has been used to estimate constituent concentrations for periods when sample data were not available (Gilroy and others, 1990), to estimate a basin flux of water-quality constituents (Goolsby and others, 1999), and to evaluate long-term trends in water-quality data (Smith and others, 1987).

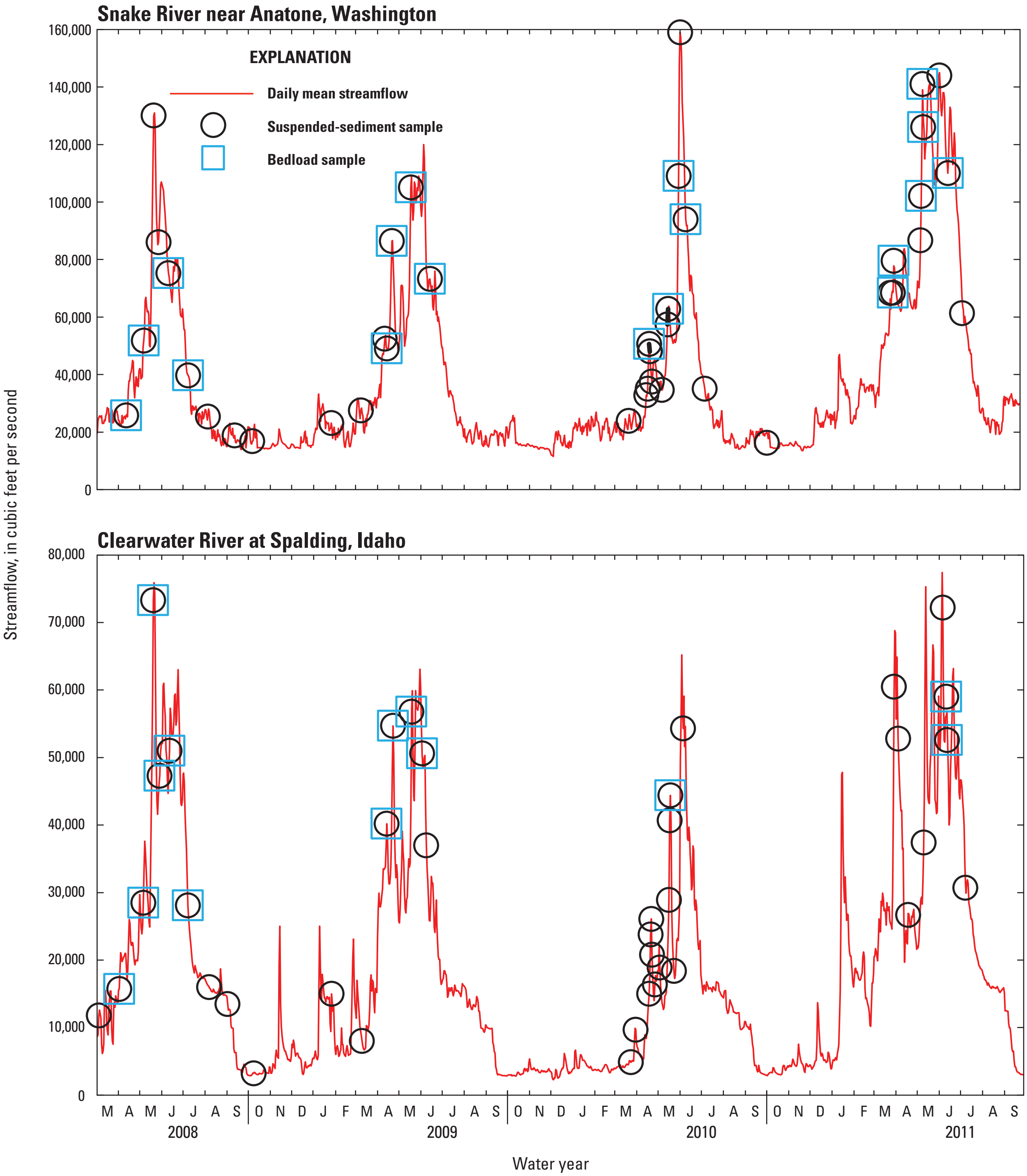

Figure 3. Streamflows at which suspended-sediment and bedload samples were collected from the Snake River near Anatone, Washington, and Clearwater River at Spalding, Idaho, water years 2008–11.

For this study, LOADEST was used to develop regression models for estimating the loads and flow-weighted concentrations of total suspended sediment (TSS) and the sand and fine-grained fractions of suspended sediment for each station for water years 2009 through 2011. For the streamgages on the Snake River near Anatone and the Clearwater River at Spalding, loads and concentrations were estimated for water years 2008 through 2011. The regression model used for the TSS and suspended-sediment size fractions was:

$$\ln L = I + a(\ln Q) + b(\ln Q^2) + c[\sin(2\pi T)] + d[\cos(2\pi T)] + \varepsilon \quad (1)$$

where

- L is the suspended-sediment load, in pounds per day;
- I is the regression intercept;
- Q is the centered streamflow, in cubic feet per second;
- T is the centered decimal time in years from the beginning of the calibration period;
- a, b, c, and d are regression coefficients that remain constant over time; and
- ε is unaccounted error associated with the regression model.

For each model, the predictor variables in the regression equation were selected on the basis of Aikaike Information Criteria (Aikaike, 1981; Judge and others, 1985). The criteria are designed to achieve a good compromise between using as many predictor variables as possible to explain the variance in load while minimizing the standard error of the resulting estimates. Estimates of the daily constituent load for each station were computed using the selected model (table 3) and daily mean streamflow. Bias introduced by conversion of the logarithm of load into estimates of actual load were corrected using the Bradu-Mundlak method (Bradu and Mundlak, 1970; Cohn and others, 1989; Crawford, 1991). A mean flow-weighted concentration for suspended sediment at each station was estimated as the TSS load over a given time period divided by the total streamflow at the station during the same period.

Suspended-Sediment Surrogates

The need to measure fluvial sediment has led to the development of sediment surrogate technologies, particularly in locations where streamflow alone may not be a good estimator of SSC because of regulated flow, hysteresis effect on sediment concentration, episodic sediment sources, and non-equilibrium sediment transport. An effective surrogate technology is low-maintenance and robust over a range of hydrologic conditions, and measured variables can be modeled to SSC, sediment load, and duration of elevated levels on a real-time and continuous basis. Although numerous surrogate technologies were tested during this study (including turbidity and laser diffraction), only acoustic backscatter measurements using ADVMs is described in this report. Wood and Teasdale (2013) present a detailed discussion for each of the surrogate technologies tested during this study, and compare and contrast the results.

Acoustic backscatter has been used successfully as a surrogate for SSC in the San Francisco Bay, California (Gartner, 2004), estuaries in Florida (Patino and Byrne, 2004), Colorado River (Topping and others, 2004), Hudson River, New York (Wall and others, 2006), the Aegean Region, Turkey (Elci and others, 2009), and subtropical estuaries in Australia (Chanson and others, 2008). For the acoustic backscatter method, a device is used that emits an acoustic pulse into the water. Theoretically, the strength of the reflected pulse, called backscatter, increases when more particles, in this case assumed to be sediment, are present in the water. Acoustic instruments have shown great promise in sediment surrogate studies because they are robust to biological fouling and measure profiles of backscatter across a sampling volume rather than at a single point in the stream (Gartner and Gray, 2005). Acoustic frequencies were selected for this study to maximize sensitivity of backscatter to dominant grain size (lower frequency for the sand fraction and higher frequency for the fines fraction) and to minimize errors due to changing grain-size distribution, as described in Gartner (2004) and Topping and others (2004). To estimate the concentrations of total suspended sediment, sands, and fines, acoustic backscatter data were corrected for (1) beam spreading, (2) transmission losses due to absorption by water, and (3) absorption or attenuation by sediment. In this study, the Clearwater River at Spalding and the Snake River near Anatone streamgages (table 1) were instrumented with surrogate technologies.

The equal-width-increment suspended-sediment samples collected at the lower Snake and Clearwater River gaging stations were used to develop the relation between SSC and ADVM backscatter. The sampling strategy targeted the ascending limb, the peak, and the descending limb of the snowmelt runoff hydrograph at each station. Forty suspended-sediment samples from the Clearwater River and 39 samples from the lower Snake River were collected during the study period March 2008 to July 2011. Samples submitted for analysis were a composite representative of the entire cross section. As mentioned previously, cross-sectional variability in SSC in the Clearwater and Snake Rivers was evaluated by individually analyzing 10 separate vertically integrated samples from the width of the river channel. Cross-section variability was analyzed for four sample sets collected from the Clearwater River and five sample sets collected from the Snake River. All suspended-sediment samples collected from the Snake River near Anatone and Clearwater River at Spalding streamgages were analyzed for organic content using a loss-on ignition analysis (Schumacher, 2002) to evaluate the effect of organic matter on errors in the surrogate analysis.

Table 3. Regression coefficients and coefficients of determination for models used to estimate concentrations and loads of total suspended sediment and suspended-sediment size fractions at stations in the lower Snake and Clearwater River Basins, Washington and Idaho.

[Locations of stations are shown in figure 2. The regression equation is $\ln L = I + a(\ln Q) + b(\ln Q^2) + c[\sin(2\pi T)] + d[\cos(2\pi T)] + \varepsilon$, where L is the sediment load in kilograms per day; I is the regression intercept; Q is the centered stream discharge in cubic feet per second; T is the centered decimal time in years from the beginning of the calibration period; a, b, c, and d, are regression coefficients that remain constant over time; ε is unaccounted error associated with the regression model; and R^2 (coefficient of determination) represents the amount of variance explained by the model. USGS, U.S. Geological Survey]

USGS gaging station No.	Gaging station name	*I*	Regression coefficient				R^2 (percent)
			a	*b*	*c*	*d*	
Total suspended sediment							
13317000	Salmon River at White Bird, Idaho	15.47	2.518	-0.079	-0.684	-0.790	89
13334000	Grande Ronde River at Zindel, Washington	11.84	2.236	0.575	-0.713	0.506	91
13334300	Snake River near Anatone, Washington	15.69	3.093	0.084	-0.540	0.160	95
13336500	Selway River near Lowell, Idaho	11.02	2.609	0.512	-0.923	-0.437	95
13337000	Lochsa River near Lowell, Idaho	10.38	2.193	0.402	-0.948	0.024	96
13337120	Middle Fork Clearwater River at Kooskia, Idaho	11.86	2.250	0.402	-0.947	-0.308	95
13338100	South Fork Clearwater River near Harpster, Idaho	12.04	2.714	0.030	-0.796	-1.610	96
13338500	South Fork Clearwater River at Stites, Idaho	11.04	2.463	0.328	-0.730	-0.442	95
13340000	Clearwater River at Orofino, Idaho	12.24	2.229	0.630	-0.831	-0.311	93
13341570	Potlatch River below Little Potlatch Creek near Spalding, Idaho	11.08	2.251	0.126	-0.143	-0.697	93
13342500	Clearwater River at Spalding, Idaho	12.57	2.047	0.590	0.461	-0.477	90
13351000	Palouse River at Hooper, Washington	12.64	1.655	0.021	-0.930	-0.210	87
Total suspended sands							
13317000	Salmon River at White Bird, Idaho	14.51	3.212	-0.197	-1.098	-0.816	95
13334000	Grande Ronde River at Zindel, Washington	9.97	2.797	0.847	-0.541	-0.134	92
13334300	Snake River near Anatone, Washington	14.70	3.993	-0.465	-0.490	-0.056	97
13336500	Selway River near Lowell, Idaho	9.32	2.798	0.659	-0.755	0.394	95
13337000	Lochsa River near Lowell, Idaho	9.84	2.588	0.414	-0.798	-0.582	96
13337120	Middle Fork Clearwater River at Kooskia, Idaho	10.95	2.696	0.490	-0.558	-0.670	96
13338100	South Fork Clearwater River near Harpster, Idaho	11.30	3.190	-0.114	-0.459	-1.867	96
13338500	South Fork Clearwater River at Stites, Idaho	9.95	2.889	0.396	-0.301	-0.709	97
13340000	Clearwater River at Orofino, Idaho	10.65	2.587	0.751	-0.607	-0.003	95
13341570	Potlatch River below Little Potlatch, near Spalding, Idaho	8.49	2.156	0.191	-0.327	-0.982	97
13342500	Clearwater River at Spalding, Idaho	10.83	2.525	0.694	0.242	-0.854	92
13351000	Palouse River at Hooper, Washington	9.54	1.376	0.068	-0.727	0.148	69
Total suspended fines							
13317000	Salmon River at White Bird, Idaho	15.20	2.349	-0.076	-0.831	-1.281	82
13334000	Grande Ronde River at Zindel, Washington	11.65	2.150	0.507	-0.709	0.607	90
13334300	Snake River near Anatone, Washington	15.12	2.717	0.225	-0.563	0.342	92
13336500	Selway River near Lowell, Idaho	10.89	2.377	0.321	-1.033	-0.933	92
13337000	Lochsa River near Lowell, Idaho	9.76	1.978	0.350	-1.099	0.148	93
13337120	Middle Fork Clearwater River at Kooskia, Idaho	11.28	1.981	0.353	-1.171	-0.236	91
13338100	South Fork Clearwater River near Harpster, Idaho	11.41	2.469	0.063	-0.977	-1.538	94
13338500	South Fork Clearwater River at Stites, Idaho	10.53	2.250	0.292	-0.857	-0.281	93
13340000	Clearwater River at Orofino, Idaho	11.92	1.991	0.545	-0.907	-0.376	90
13341570	Potlatch River below Little Potlatch, near Spalding, Idaho	10.95	2.270	0.120	-0.131	-0.658	92
13342500	Clearwater River at Spalding, Idaho	12.30	1.845	0.518	0.651	-0.358	86
13351000	Palouse River at Hooper, Washington	12.56	1.694	0.021	-0.928	-0.265	88

The ADVMs at the Clearwater River at Spalding were co-located with the streamgage and installed about 16 ft upstream of the streamgage. In May 2008, the station was equipped with a 0.5 megahertz (MHz) Sontek™ Argonaut-SL ADVM and 3 MHz Sontek™ Argonaut-SL ADVM with datalogger and satellite telemetry. The ADVMs were mounted on an aluminum slide track that could be raised and lowered as needed to service equipment. The 0.5 and 3 MHz ADVMs measured backscatter in five discrete, equally sized cells in a horizontal sampling volume, 5.0–100 ft and 3.3–12 ft from the instrument, respectively. The sampling volume for each ADVM was selected based on meter frequency, availability of suspended material to reflect the acoustic pulse, and any obstructions in the beam path. The ADVMs collected backscatter data 2 minutes of every 15 minutes.

In April 2009, the Snake River near Anatone streamgage was equipped with a 0.5 MHz Sontek Argonaut-SL ADVM and 1.5 MHz Argonaut-SL ADVM with datalogger and satellite telemetry. The station was located on the left streambank about 1,000 ft upstream of the streamgage and the sediment sampling location. The 0.5 and 1.5 MHz ADVMs were mounted on an aluminum slide track and were configured to measure backscatter in five discrete, equally sized cells in a horizontal sampling volume, 6.6–203 and 6.6–59 ft from the instrument, respectively. The ADVMs collected backscatter data 2 minutes of every 15 minutes.

Acoustic backscatter data must be corrected prior to relating the data to the mass concentration of suspended sediment in the water column. Factors affecting acoustic backscatter readings include transmission losses due to absorption by water, absorption or attenuation by sediment, and beam spreading. However, the methods for correcting backscatter data differ and can substantially alter estimates of SSC. Thus, selection of an appropriate method is important in the analysis of acoustic backscatter data. For this study, candidate methods for correcting the backscatter data were reviewed; methods selected for use with data collected at the Snake River and Clearwater River stations are documented in Wood and Teasdale (2013).

Following correction of the backscatter data, measurements were averaged over a 1-hour period bracketing the time that sediment samples were collected. This allowed concurrent measurements to relate backscatter data to the measured SSC at each station. Relations between backscatter and SSC were evaluated using ordinary least squares regression. All of the SSC data were log transformed prior to regression. Acoustic backscatter data are reported in a log-based scale and do not require a transformation. Regression models were selected based on statistical significance of explanatory variables (p-values) and various regression statistics such as coefficient of determination (R^2), standard error, Mallow's Cp (Ott and Longnecker, 2001), and prediction error sum of squares (PRESS) (Helsel and Hirsch, 1992) statistics. A nonparametric bias correction factor described in Duan (1983) was applied to each best-fit regression model to correct for low bias induced by log transformation and subsequent re-transformation of the dependent variable. The factor was used to correct each value of SSC as well as upper and lower 95 percent confidence intervals estimated by a regression model.

Bedload

Unlike suspended-sediment transport, bedload often is not detectable. When bedload transport does occur, it is often extremely variable both spatially within the stream channel and temporally during steady streamflow conditions (Hubbell, 1964). During this study, bedload was collected at most of the stations when streamflow was sufficiently high to initiate bedload transport. However, at some stations, the stream cross-section was not conducive for collecting bedload because of poor channel geometry, backwater conditions, extreme turbulence, or a combination of these factors. Bedload samples were collected at only two of the three stations in the Snake River drainage basin upstream of lower Granite Reservoir. The channel bottom at the Grande Ronde River at Zindel, Washington, sampling station is composed of uneven bedrock, making the site nearly impossible to sample with the Helley-Smith bedload sampler. In the Clearwater River Basin, 7 of the 8 stations were sampled at least 3 times for bedload, with the Lochsa River at Lowell limited to 3 samples because of backwater conditions from the Selway River. The Potlatch River was not sampled because of backwater conditions from the Clearwater River. Although bedload sampling was attempted on numerous occasions at the Palouse River station, bedload was never retained in the sampler. It is difficult to determine whether the lack of bedload in the Palouse River at Hooper was real or an artifact of a poor sampling location. The number of bedload samples collected at each station is listed in table 1. The timing of bedload sampling for the Snake River near Anatone and the Clearwater River at Spalding streamgages from March 2008 through July 2011 is shown in figure 3.

Most bedload samples were collected using a Helley-Smith type sampler with a 6- by 6-in. nozzle (Helley and Smith, 1971); a few samples were collected in 2011 using an Elwha style sampler with a 4- by 8-in. nozzle. An equal-width-increment sampling method as described by Edwards and Glysson (1999) was used to collect bedload. This method involves dividing and collecting samples in the stream channel at evenly spaced sections to represent bedload transport accurately across the entire channel. When possible, samples were collected at 20 equally spaced intervals with duration of 60 seconds on the stream bottom per interval. At some stations and at some streamflows, fewer than 20 sections were sampled because of extremely fast and turbulent stream conditions.

For analysis, all sectional samples were composited into one sample representing the entire cross section. Duplicates were collected during each sampling event and analyzed separately at the USGS CVO sediment laboratory. For analysis, the results for the duplicate samples are reported as an average. The bedload samples were analyzed for total mass and full phi (ϕ) particle size increments from $\phi = 4$ (62.5 μm) to $\phi = -7$ (128 mm).

Because of the large variability in the spatial and temporal pattern of bedload transport, curves relating bedload to streamflow generally have a larger degree of uncertainty than do curves for suspended-sediment transport. To estimate bedload for use in transport curves, the following equation (Edwards and Glysson, 1999), was used:

$$Qb = (k \times W \times M) \ / T \qquad (2)$$

where

- Qb is bedload discharge, in tons per day;
- k is a conversion factor specific to the sampler orifice (0.381 for the Helley Smith and 0.141 for the Elwha);
- W is the total stream width, in feet;
- M is the total mass of bedload sample, in grams and
- T is the total time the sampler was on the bed, in seconds.

The best-fit equation between streamflow and bedload discharge was used to estimate the total bedload discharge for the period of interest using either the continuous or indexed daily streamflow record. Because of the paucity of samples at some stations and the variability at most of the stations, the bedload discharge estimates obtained during this study have a wide range of associated error and should not be viewed as precise estimates.

The grain size and statistics software GRADISTAT (Blott and Pye, 2001) was used to classify the particle-size distribution data. Emmett (1976) described the particle size distribution as bimodal at the Snake River near Anatone and the Clearwater River at Spalding streamgages. Standard statistical measures such as the arithmetic (normal distribution) or geometric (log-normal) method of moments are not suitable for identifying the bimodal particle size distribution because of non-normality. Folk and Ward (1957) described a graphical geometric (log-normal) method to determine grain-size analysis statistics. Blott and Pye (2001) determined this method to be the most appropriate for parameter-based estimation of bimodal bedload transport. Parameters used to describe the particle-size distribution in this study included sample distribution (unimodal, bimodal), cumulative exceedence values (D_{10}, D_{50}, D_{90}), and cumulative percentage finer by weight. Standard deviation (sorting), skewness (positive or negative preference), and kurtosis (peakedness around the mean) were not used in this analysis as they were determined to be unreliable for bimodal bedload distributions.

Sediment Transport in the Lower Snake and Clearwater River Basins

Because sediment transport in streams varies in response to hydrologic conditions, information on streamflow in a historical context is critical for assessing sediment transport and deposition in the lower Snake and Clearwater River Basins. The magnitude and timing of streamflow in the lower Snake and Clearwater River Basins generally are determined by the amount of water derived from the winter snowpack and reservoir operations at Hells Canyon and Dworshak Reservoirs. As such, rivers and streams in the lower Snake and Clearwater River Basins typically reach peak flows in April, May, or June in association with spring snowmelt runoff. High streamflows occasionally occur in lower elevation basins in the autumn and winter in association with rain-on-snow events that can cause flooding and substantial transport of sediment. Generally, however, when precipitation and snowpack are below average, streamflow from runoff is lower than normal, and transport of sediment in streams is below average. In contrast, when precipitation, snowpack, and runoff are above average, sediment transport may be larger than normal. Generally, streamflows drop rapidly over the summer following the loss of the snowpack, and low flow typically is in September or October.

From March 2008 through September 2011, streamflow conditions in the lower Snake and Clearwater River Basins as represented by the streamgages on the Snake River near Anatone and the Clearwater River at Spalding were quite variable in relation to the most recent 30-year average (fig. 4). Streamflow in the Snake and Clearwater Rivers during water years 2008, 2009, and, in particular, 2011 generally exceeded the 30-year average during most of the year. During 2010, streamflow in the Snake and Clearwater Rivers was less than the 30-year average for most of the year, exceeding the average streamflow only during the brief period of snowmelt runoff from late May through early June. A pronounced rain-on-snow event occurred during January 2011 affecting streamflows and sediment transport in the Potlatch River below Little Potlatch near Spalding (USGS streamgage 13341570) and the Palouse River at Hooper (USGS streamgage 13351000). This event occurred across many of the lower-elevation drainage basins in the lower Snake and Clearwater River Basins and is evident in the hydrograph spike in late January 2011 for the Snake River near Anatone and in particular for the Clearwater River at Spalding (fig. 4).

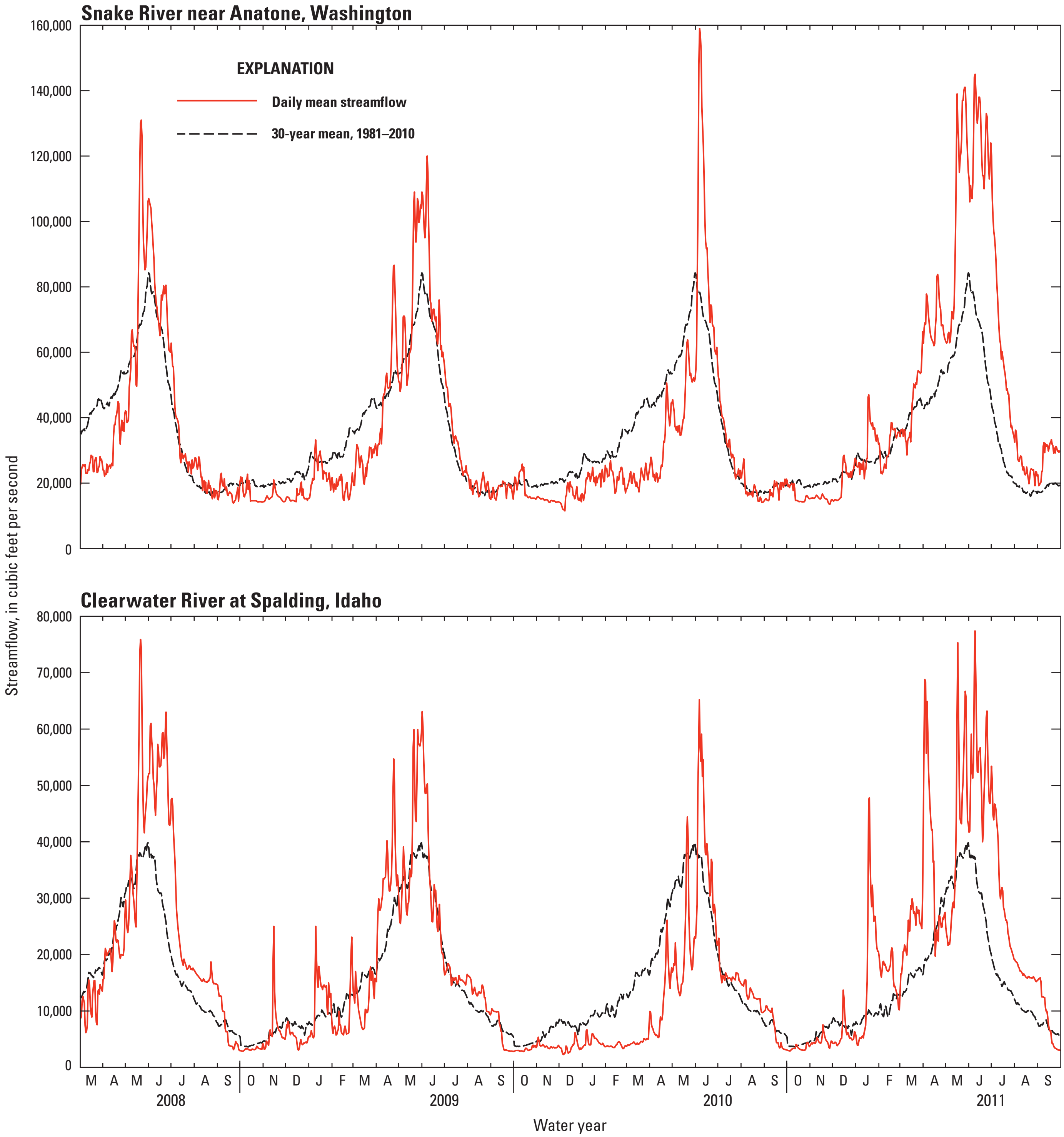

Figure 4. Daily mean streamflow in the Snake River near Anatone, Washington and the Clearwater River at Spalding, Idaho, 2008–11, compared with the 30-year mean for water years 1981–2010.

Suspended-Sediment Transport

The number of suspended-sediment samples collected varied from 33 to 42 per station during the sampling period (table 1). Fitted regression lines for a log-log power fit with associated R^2 values of TSS and streamflow for selected stations in the lower Snake and Clearwater River Basins are shown in figure 5. Because there is considerable scatter around the regression lines and the R^2 values at some stations were relatively low, a degree of uncertainty exists in the TSS load calculations based on streamflow. However, assuming that the streamflows in individual subbasins during 2009–11 are representative of normal conditions, their relative contributions to the overall sediment load delivered to Lower Granite Reservoir probably are accurate. Based on the hydrographs for 2009–11 compared to the 30-year mean for the Snake River near Anatone and the Clearwater River at Spalding (fig. 4), this assumption probably is valid.

The concentrations and load of suspended sediment transported in streams were variable, spanning 3–5 orders of magnitude during water years 2008–11 (fig. 6). The largest measured concentrations of suspended sediment were in samples collected from the Palouse and Potlatch Rivers during the rain-on-snow event in January 2011. Concentrations of TSS, which includes both the sand and fine-grained fractions, in the Potlatch River ranged more than 4 orders of magnitude during the study from a low of 3 mg/L during baseflow conditions to more than 3,000 mg/L in January 2011 during the rain-on-snow event (table 2). Samples collected from the Palouse River at Hooper had the largest median concentration of TSS (100 mg/L) and the largest suspended sediment fraction as fine-grained silt and clay less than 62.5 µm in diameter (median 95 percent). Other rivers with a large percentage of fine-grained suspended sediment were the Potlatch River (median 92 percent) and the Grand Ronde River (median 84 percent) (table 2). In contrast to the other stations sampled during this study, the Palouse and Potlatch Rivers and, to a lesser extent, the Grande Ronde River showed an increase in the fraction of fine-grained sediment with increasing streamflow. The Palouse, Potlatch, and Grande Ronde Rivers all drain basins with relatively large proportions of agricultural activity, which probably accounts for the relatively large percentage of fine-grained sediment.

The second largest median TSS concentration (94 mg/L) was measured in samples collected at Salmon River at White Bird, Idaho (USGS streamgage 13317000). However, as a percentage of the TSS, the fine-grained fraction (median of 51 percent) was smaller in samples collected in the Salmon River as compared with the Palouse, Potlatch, and Grande Ronde Rivers. The smallest TSS with median concentrations of 11, 11, 15, and 13 mg/L were measured in samples collected from the Selway and Lochsa Rivers, the Middle Fork Clearwater River at Kooskia, and the Clearwater River at Orofino (USGS streamgage 13340000), respectively. The TSS concentration in samples from the Lochsa River and the Middle Fork Clearwater River at Kooskia did not exceed 100 mg/L in any of the samples collected during this study (table 2).

Samples collected from the Selway River, Lochsa River, and the Middle Fork Clearwater River at Kooskia, and samples from the Salmon River at White Bird, had relatively small percentages of fine-grained sediment. The median silt and clay fractions at each of these stations were about 50 percent or less. All stations in the network, except the agriculturally affected Palouse, Potlatch, and Grande Ronde Rivers, exhibited an increase in the sand-size fraction of suspended sediment with an increase in streamflow. As a result, during the peak of spring snowmelt runoff, most of the suspended sediment transported in the lower Snake and Clearwater River Basins was sand-sized material larger than 62.5 µm.

Based on the transport curves (fig. 6*B*), the load of TSS in the Palouse River ranged from about 1 to more than 10,000 tons per day and in the Potlatch River ranged from less than 0.1 to more 40,000 tons per day. However, because the transport curves in figure 6*B* represent a best-fit line through the data for each station, during peak runoff the actual concentration and load of TSS is often much larger than the load estimated using the sediment-transport curves. This is evident in the stations shown in figure 5 where the best-fit regression line for each station underestimates the measured TSS concentration at high streamflow. For instance, multiple samples collected from the Palouse and Potlatch Rivers during the January 2011 rain-on-snow event indicate that the suspended-sediment transport far exceeded the estimates based on the transport curves shown in figure 6. For the Palouse River, four TSS samples collected January 17–18 at streamflows ranging from 5,670 to 7,150 ft^3/s had concentrations between 930 and 1,400 mg/L, about twice the amount estimated using the transport curve values of 490–600 mg/L, respectively. For the Potlatch River, five samples collected January 16–17 at streamflows ranging from 8,760 to 17,000 ft^3/s had TSS concentrations of between 1,400 and 3,300 mg/L, more than three times the estimated concentrations of 420 and 940 mg/L, respectively.

Because the LOADEST program uses multiple variables to predict SSC and load, simulation results from the model generally provide better estimates than those based on transport curves as shown in figure 6. LOADEST was therefore used to develop regression models (table 3) for each station to estimate the load of TSS, total suspended sand, and total suspended fines for water years 2009–11(table 4). To determine the annual load, the daily load for each constituent was estimated using the daily mean streamflow and summed to determine the annual load. Regression coefficients and coefficients of determination (R^2) for the LOADEST models at each station are given in table 3.

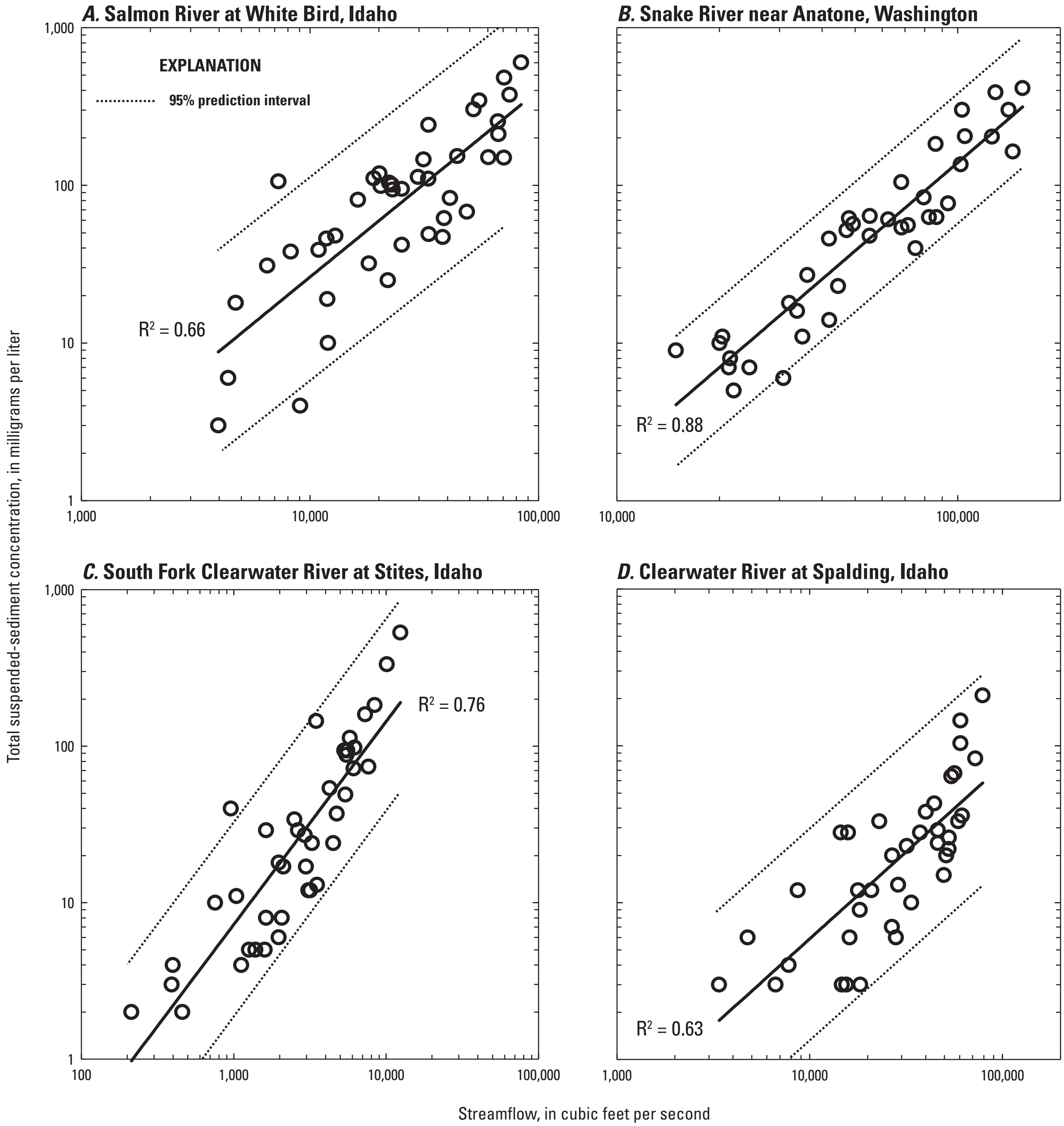

Figure 5. Suspended-sediment transport curves and 95-percent prediction intervals representing best-fit regression equations for a log-log power fit of total suspended sediment with streamflow in the (*A*) Salmon River at Whitebird, Idaho, (*B*) Snake River near Anatone, Washington, (*C*) South Fork Clearwater River at Stites, Idaho, and (*D*) Clearwater River at Spalding, Idaho.

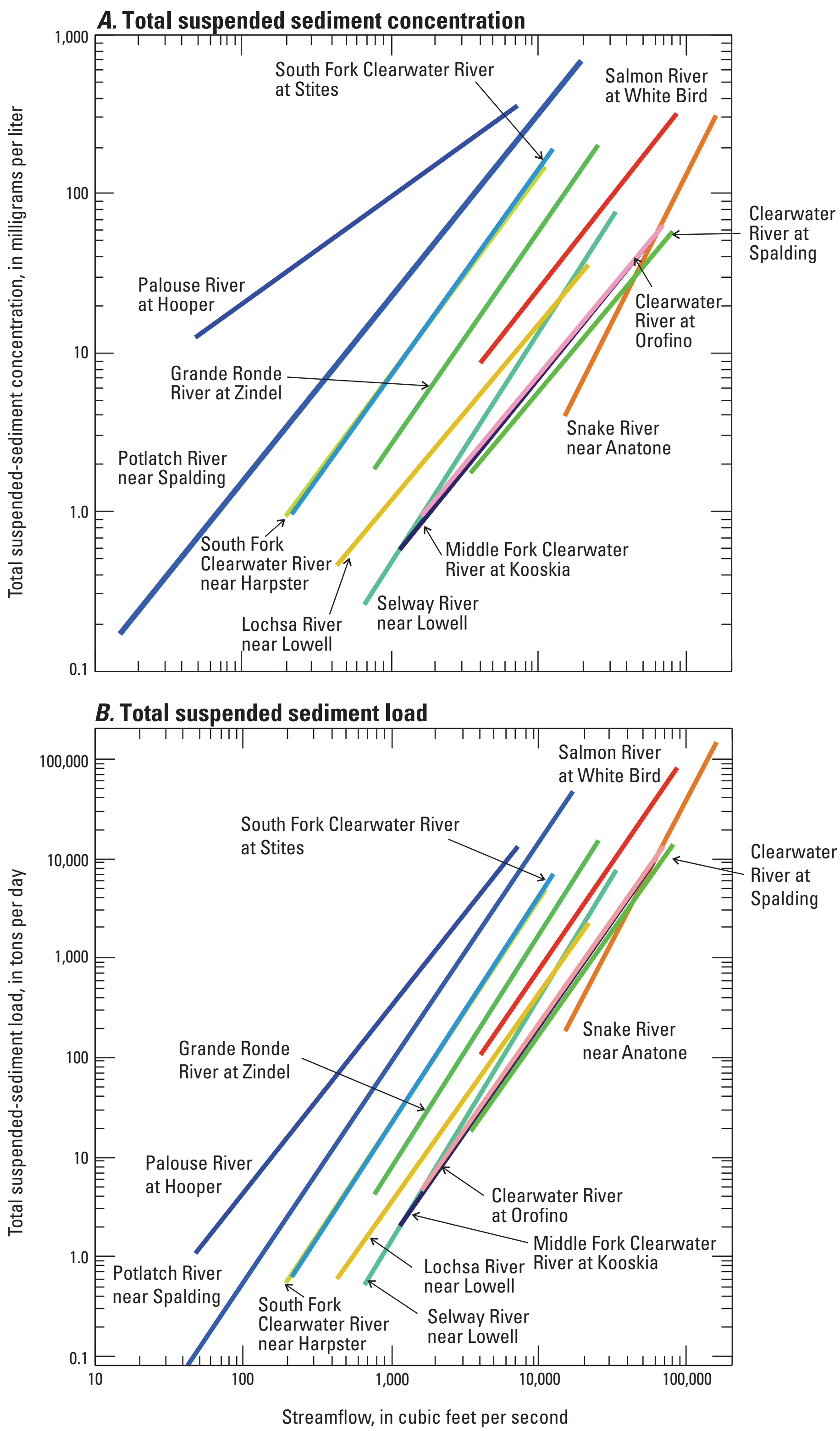

Figure 6. Suspended-sediment transport curves representing best-fit regression equations for (*A*) total suspended-sediment concentrations and (*B*) total suspended-sediment loads at sampling stations in the lower Snake and Clearwater River Basins, Washington and Idaho.

High R^2 values indicate that the LOADEST models did an excellent job of accounting for the variability in the suspended- sediment loads: 30 of the 36 models accounted for 90 percent or more of observed variability. The models account for less than 80 percent of the variability in the observed sediment load only for the Palouse River and only for the sand-size sediment fraction. Generally, the model simulation results showed the best fit (highest R^2) for the sand size fraction and the poorest fit for the fine-grained fraction. A notable exception was for the Palouse River, where the best-fit model occurred for total suspended fines ($R^2=0.88$) and the poorest fit occurred for the total suspended sands ($R^2=0.69$).

For each of the stations in the sampling network, the estimated loads of total suspended sediment (fig. 7), suspended sands, and suspended fines were largest during water year 2011 and smallest during water year 2010 (table 4). The difference in the TSS load for the Palouse and Potlatch Rivers during water years 2010 and 2011 was particularly notable. The TSS load in the Palouse River was about 8 times larger in 2011 than in 2010 and in the Potlatch River was more than 50 times larger in 2011 than in 2010. The large difference in the sediment load between 2011 and 2010 in the Palouse and Potlatch Rivers is attributable to the rain-on-snow event that occurred in these drainage basins during January 2011. In the Palouse River at Hooper, the TSS load during January 17–19, 2011, was about 64,600 tons, roughly 19 percent of the 2011 water year total of 335,000 tons and about 9 percent of the TSS load transported in the Palouse River during water years 2009–11 (table 4). During January 16–17, 2011, the estimated TSS load in the Potlatch River exceeded 110,000 tons, more than one-half of the total estimated load of 212,000 tons for the entire 2011 water year and about 40 percent of the total TSS load transported in the Potlatch River during water years 2009–11 (table 4).

Table 4. Estimated annual, total, and mean loads of suspended sediment, suspended sand, and suspended fines for stations in the lower Snake and Clearwater River Basins, Washington and Idaho, water years 2009–11.

[Locations of stations are shown in figure 2. **Abbreviations:** C.I., confidence interval; USGS, U.S. Geological Survey]

USGS gaging station No.	Gaging station name	Total suspended sediment (tons)			Total suspended sands (tons)			Total suspended fines (tons)		
		Estimated load	Lower 95 percent C.I.	Upper 95 percent C.I.	Estimated load	Lower 95 percent C.I.	Upper 95 percent C.I.	Estimated load	Lower 95 percent C.I.	Upper 95 percent C.I.
	Water year 2009									
13317000	Salmon River at White Bird, Idaho	1,660,000	962,000	2,720,000	952,000	590,000	1,450,000	744,000	387,000	1,330,000
13334000	Grande Ronde River at Zindel, Washington	278,000	174,000	425,000	52,200	29,500	86,900	224,000	138,000	347,000
13334300	Snake River near Anatone, Washington	1,820,000	1,340,000	2,420,000	848,000	631,000	1,110,000	998,000	687,000	1,410,000
13336500	Selway River near Lowell, Idaho	153,000	87,700	250,000	116,000	59,600	203,000	46,600	25,400	81,400
13337000	Lochsa River near Lowell, Idaho	42,300	29,000	60,700	24,500	15,300	38,200	18,700	12,000	28,500
13337120	Middle Fork Clearwater River at Kooskia, Idaho	194,000	127,000	289,000	115,000	72,500	175,000	86,000	50,300	141,000
13338100	South Fork Clearwater River near Harpster, Idaho	44,600	31,200	63,200	22,100	14,500	32,900	22,700	15,000	34,100
13338500	South Fork Clearwater River at Stites, Idaho	48,800	33,400	69,400	18,700	13,200	26,100	28,900	18,600	43,100
13340000	Clearwater River at Orofino, Idaho	300,000	182,000	475,000	154,000	89,200	249,000	150,000	85,500	252,000
13341570	Potlatch River below Little Potlatch Creek, near Spalding, Idaho	57,800	20,600	135,000	2,840	1,460	5,120	55,500	18,600	134,000
13342500	Clearwater River at Spalding, Idaho	335,000	215,000	501,000	137,000	81,600	215,000	199,000	122,000	310,000
13351000	Palouse River at Hooper, Washington	318,000	130,000	672,000	19,600	4,950	55,500	290,000	123,000	596,000

Table 4. Estimated annual, total, and mean loads of suspended sediment, suspended sand, and suspended fines for stations in the lower Snake and Clearwater River Basins, Washington and Idaho, water years 2009–11.—Continued

[Locations of stations are shown in figure 2. **Abbreviations:** C.I., confidence interval; USGS, U.S. Geological Survey]

USGS gaging station No.	Gaging station name	Total suspended sediment (tons)			Total suspended sands (tons)			Total suspended fines (tons)		
		Estimated load	Lower 95 percent C.I.	Upper 95 percent C.I.	Estimated load	Lower 95 percent C.I.	Upper 95 percent C.I.	Estimated load	Lower 95 percent C.I.	Upper 95 percent C.I.
Water Year 2010										
13317000	Salmon River at White Bird, Idaho	1,030,000	590,000	1,700,000	524,000	321,000	811,000	476,000	242,000	876,000
13334000	Grande Ronde River at Zindel, Washington	144,000	73,600	258,000	46,700	18,300	99,600	109,000	55,300	195,000
13334300	Snake River near Anatone, Washington	1,650,000	1,130,000	2,320,000	795,000	552,000	1,110,000	855,000	543,000	1,290,000
13336500	Selway River near Lowell, Idaho	60,700	32,500	104,000	44,800	20,400	86,000	19,400	10,300	33,600
13337000	Lochsa River near Lowell, Idaho	18,300	12,700	25,800	9,720	6,120	14,800	8,810	5,660	13,200
13337120	Middle Fork Clearwater River at Kooskia, Idaho	81,600	53,000	121,000	44,800	27,900	68,600	38,800	22,400	63,400
13338100	South Fork Clearwater River near Harpster, Idaho	14,200	9,860	19,900	7,440	4,800	11,000	7,260	4,730	10,800
13338500	South Fork Clearwater River at Stites, Idaho	16,200	10,700	23,500	6,360	4,340	8,990	9,850	6,120	15,100
13340000	Clearwater River at Orofino, Idaho	143,000	82,900	232,000	71,400	38,900	121,000	75,100	40,800	130,000
13341570	Potlatch River below Little Potlatch Creek near Spalding, Idaho	4,090	982	11,700	229	93	482	3,810	844	11,300
13342500	Clearwater River at Spalding, Idaho	152,000	92,200	237,000	58,900	33,500	96,700	91,200	52,200	150,000
13351000	Palouse River at Hooper, Washington	39,800	12,700	96,700	2,960	572	9,410	35,000	11,800	82,500

Table 4. Estimated annual, total, and mean loads of suspended sediment, suspended sand, and suspended fines for stations in the lower Snake and Clearwater River Basins, Washington and Idaho, water years 2009–11.—Continued

[Locations of stations are shown in figure 2. **Abbreviations:** C.I., confidence interval; USGS, U.S. Geological Survey]

USGS gaging station No.	Gaging station name	Total suspended sediment (tons)			Total suspended sands (tons)			Total suspended fines (tons)		
		Estimated load	Lower 95 percent C.I.	Upper 95 percent C.I.	Estimated load	Lower 95 percent C.I.	Upper 95 percent C.I.	Estimated load	Lower 95 percent C.I.	Upper 95 percent C.I.
					Water year 2011					
13317000	Salmon River at White Bird, Idaho	2,400,000	1,410,000	3,870,000	1,300,000	832,000	1,950,000	1,060,000	560,000	1,870,000
13334000	Grande Ronde River at Zindel, Washington	288,000	164,000	489,000	60,500	28,600	122,000	228,000	129,000	389,000
13334300	Snake River near Anatone, Washington	5,450,000	3,860,000	7,500,000	2,800,000	2,000,000	3,800,000	2,700,000	1,770,000	3,970,000
13336500	Selway River near Lowell, Idaho	154,000	91,500	247,000	109,000	58,500	186,000	50,500	28,200	86,300
13337000	Lochsa River near Lowell, Idaho	65,200	44,500	93,600	40,400	25,400	62,100	27,800	17,500	42,900
13337120	Middle Fork Clearwater River at Kooskia, Idaho	239,000	159,000	351,000	147,000	95,700	217,000	104,000	60,900	170,000
13338100	South Fork Clearwater River near Harpster, Idaho	87,100	53,300	142,000	46,500	26,500	79,300	41,700	23,800	72,800
13338500	South Fork Clearwater River at Stites, Idaho	101,000	60,600	159,000	51,300	31,000	80,900	52,900	30,200	87,200
13340000	Clearwater River at Orofino, Idaho	517,000	301,000	845,000	285,000	159,000	479,000	243,000	132,000	423,000
13341570	Potlatch River below Little Potlatch Creek near Spalding, Idaho	212,000	50,900	607,000	12,900	5,090	27,400	199,000	44,700	598,000
13342500	Clearwater River at Spalding, Idaho	662,000	394,000	1,050,000	297,000	164,000	498,000	372,000	210,000	618,000
13351000	Palouse River at Hooper, Washington	335,000	139,000	691,000	20,900	5,210	58,600	304,000	132,000	608,000

Table 4. Estimated annual, total, and mean loads of suspended sediment, suspended sand, and suspended fines for stations in the lower Snake and Clearwater River Basins, Washington and Idaho, water years 2009–11.—Continued

[Locations of stations are shown in figure 2. **Abbreviations:** C.I., confidence interval; USGS, U.S. Geological Survey]

USGS gaging station No.	Gaging station name	Total suspended sediment (tons)			Total suspended sands (tons)			Total suspended fines (tons)		
		Estimated load	Lower 95 percent C.I.	Upper 95 percent C.I.	Estimated load	Lower 95 percent C.I.	Upper 95 percent C.I.	Estimated load	Lower 95 percent C.I.	Upper 95 percent C.I.
Water years 2009–11										
13317000	Salmon River at White Bird, Idaho	5,090,000	2,960,000	8,290,000	2,780,000	1,740,000	4,210,000	2,280,000	1,190,000	4,080,000
13334000	Grande Ronde River at Zindel, Washington	710,000	412,000	1,170,000	159,400	76,400	308,000	561,000	322,000	931,000
13334300	Snake River near Anatone, Washington	8,920,000	6,330,000	12,200,000	4,440,000	3,180,000	6,020,000	4,550,000	3,000,000	6,670,000
13336500	Selway River near Lowell, Idaho	368,000	212,000	601,000	270,000	138,000	475,000	116,000	63,900	201,000
13337000	Lochsa River near Lowell, Idaho	126,000	86,200	180,000	74,600	46,800	115,000	55,300	35,200	84,600
13337120	Middle Fork Clearwater River at Kooskia, Idaho	515,000	339,000	761,000	307,000	196,000	461,000	229,000	134,000	374,000
13338100	South Fork Clearwater River near Harpster, Idaho	146,000	94,400	225,000	76,000	45,800	123,000	71,700	43,500	118,000
13338500	South Fork Clearwater River at Stites, Idaho	166,000	105,000	252,000	76,400	48,500	116,000	91,600	54,900	145,000
13340000	Clearwater River at Orofino, Idaho	960,000	566,000	1,550,000	510,000	287,000	849,000	468,000	258,000	805,000
13341570	Potlatch River below Little Potlatch Creek near Spalding, Idaho	274,000	72,500	754,000	16,000	6,640	33,000	258,000	64,100	743,000
13342500	Clearwater River at Spalding, Idaho	1,150,000	701,000	1,790,000	493,000	279,000	810,000	662,000	384,000	1,080,000
13351000	Palouse River at Hooper, Washington	693,000	282,000	1,460,000	43,500	10,700	124,000	629,000	267,000	1,290,000

Table 4. Estimated annual, total, and mean loads of suspended sediment, suspended sand, and suspended fines for stations in the lower Snake and Clearwater River Basins, Washington and Idaho, water years 2009–11.—Continued

[Locations of stations are shown in figure 2. **Abbreviations:** C.I., confidence interval; USGS, U.S. Geological Survey]

USGS gaging station No.	Gaging station name	Mean suspended sediment (tons)			Mean suspended sands (tons)			Mean total suspended fines (tons)		
		Estimated load	Lower 95 percent C.I.	Upper 95 percent C.I.	Estimated load	Lower 95 percent C.I.	Upper 95 percent C.I.	Estimated load	Lower 95 percent C.I.	Upper 95 percent C.I.
Water years 2009–11										
13317000	Salmon River at White Bird, Idaho	1,696,667	986,667	2,763,333	926,667	580,000	1,403,333	760,000	396,667	1,360,000
13334000	Grande Ronde River at Zindel, Washington	236,667	137,333	390,000	53,133	25,467	102,667	187,000	107,333	310,333
13334300	Snake River near Anatone, Washington	2,973,333	2,110,000	4,066,667	1,480,000	1,060,000	2,006,667	1,516,667	1,000,000	2,223,333
13336500	Selway River near Lowell, Idaho	122,667	70,667	200,333	90,000	46,000	158,333	38,667	21,300	67,000
13337000	Lochsa River near Lowell, Idaho	42,000	28,733	60,000	24,867	15,600	38,333	18,433	11,733	28,200
13337120	Middle Fork Clearwater River at Kooskia, Idaho	171,667	113,000	253,667	102,333	65,333	153,667	76,333	44,667	124,667
13338100	South Fork Clearwater River near Harpster, Idaho	48,667	31,467	75,000	25,333	15,267	41,000	23,900	14,500	39,333
13338500	South Fork Clearwater River at Stites, Idaho	55,333	35,000	84,000	25,467	16,167	38,667	30,533	18,300	48,333
13340000	Clearwater River at Orofino, Idaho	320,000	188,667	516,667	170,000	95,667	283,000	156,000	86,000	268,333
13341570	Potlatch River below Little Potlatch Creek near Spalding, Idaho	91,333	24,167	251,333	5,333	2,213	11,000	86,000	21,367	247,667
13342500	Clearwater River at Spalding, Idaho	383,333	233,667	596,667	164,333	93,000	270,000	220,667	128,000	360,000
13351000	Palouse River at Hooper, Washington	231,000	94,000	486,667	14,500	3,567	41,333	209,667	89,000	430,000

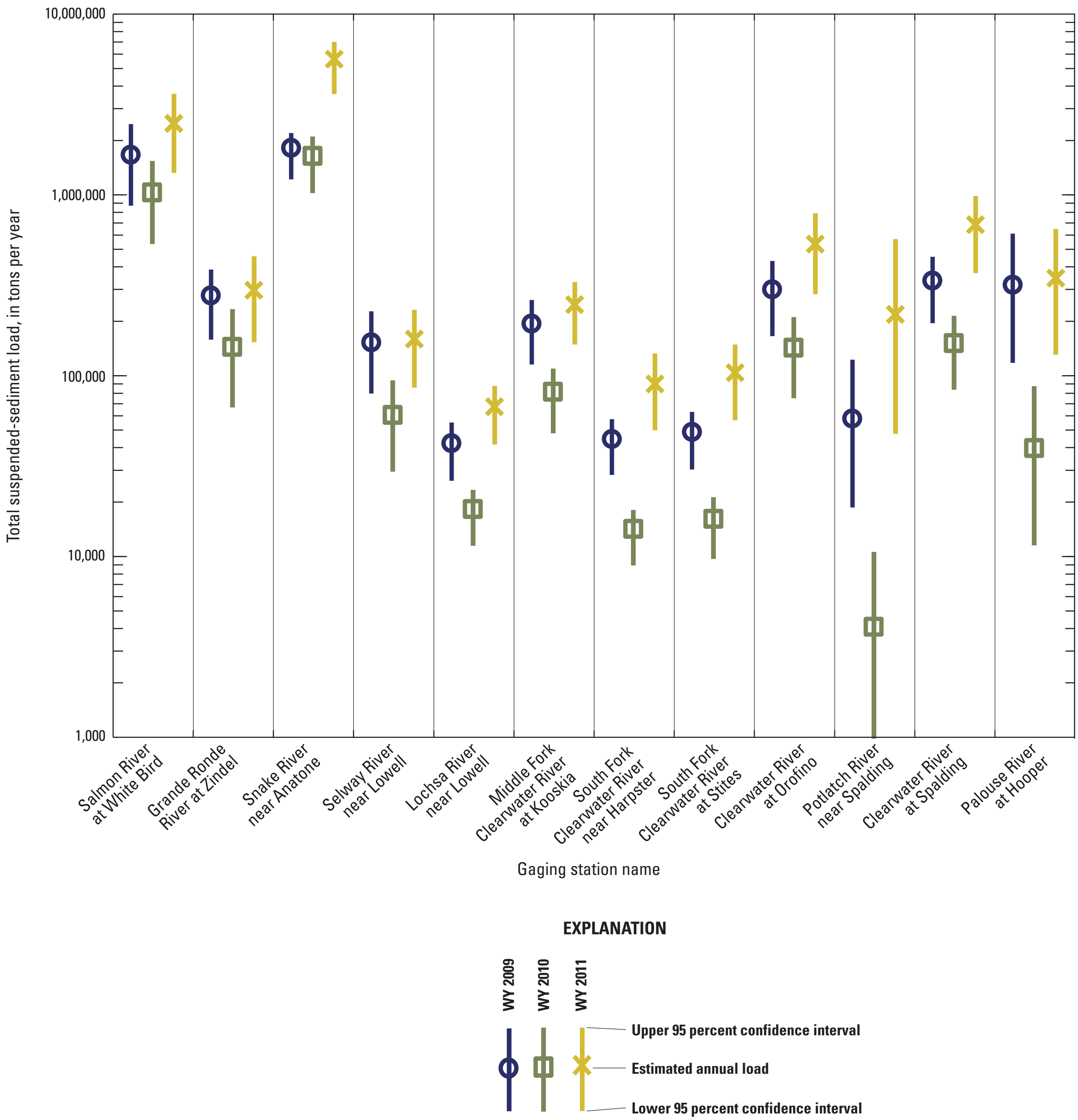

Figure 7. Estimated total suspended-sediment loads and 95-percent confidence intervals for stations in the lower Snake and Clearwater River Basins, Idaho and Washington, water years (WY) 2009–11.

The Salmon River as measured at White Bird contributed most of the TSS load in the Snake River as measured at the Anatone station and a large part of the TSS load entering Lower Granite Reservoir. However, the relative contribution of the Salmon River to the TSS load entering the reservoir varied annually during water years 2009, 2010, and 2011. During water year 2009, the Salmon River contributed an estimated 1.66 million tons of suspended sediment to the Snake River and accounted for more than 90 percent of the 1.82 million tons of suspended sediment entering Lower Granite Reservoir from the Snake River. During water years 2010 and 2011, the Salmon River contributed 1.03 million and 2.4 million tons, or about 62 and 44 percent, respectively, of the suspended sediment entering the reservoir from the Snake River drainage basin. The suspended-sediment yield from the Salmon River Basin, particularly the sand-sized fraction, was one of the largest of the basins evaluated (fig. 8). During the 3 years of sample collection, the mean annual yield of suspended sediment from the Salmon River Basin was about 125 tons per square mile per year [(tons/mi^2)/yr] of which about 55 percent was sand. Overall, during water years 2009–11, the Salmon River transported about 5.1 million tons of suspended sediment to the Snake River, equivalent to about 51 percent of the TSS, about 56 percent of the suspended sand, and about 44 percent of the suspended fine-grained load entering Lower Granite Reservoir from the combined Snake and Clearwater Rivers (fig. 9*A*–*C*).

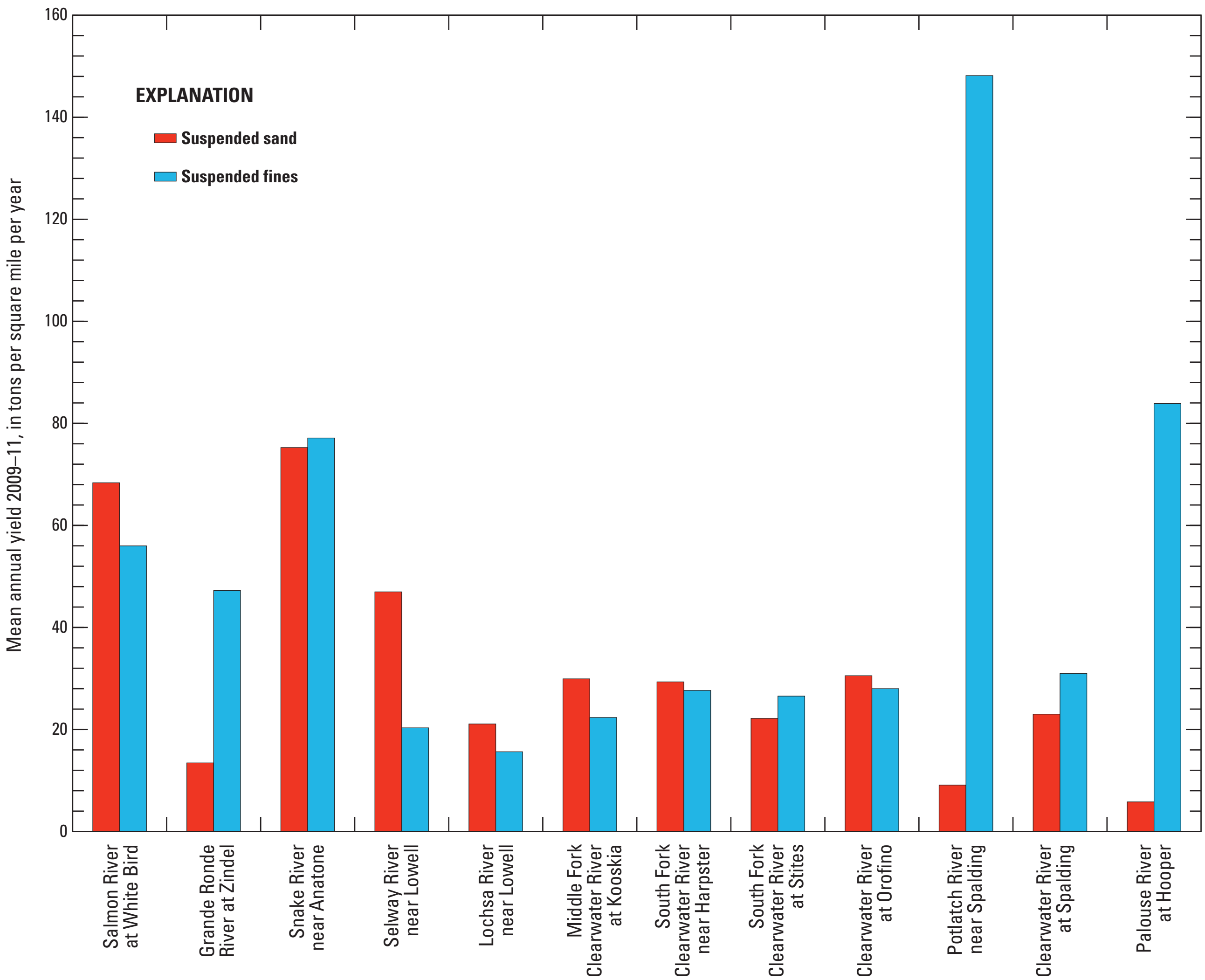

Figure 8. Mean annual yield of suspended sand and fines in the lower Snake and Clearwater River Basins, Washington and Idaho, water years 2009–11.

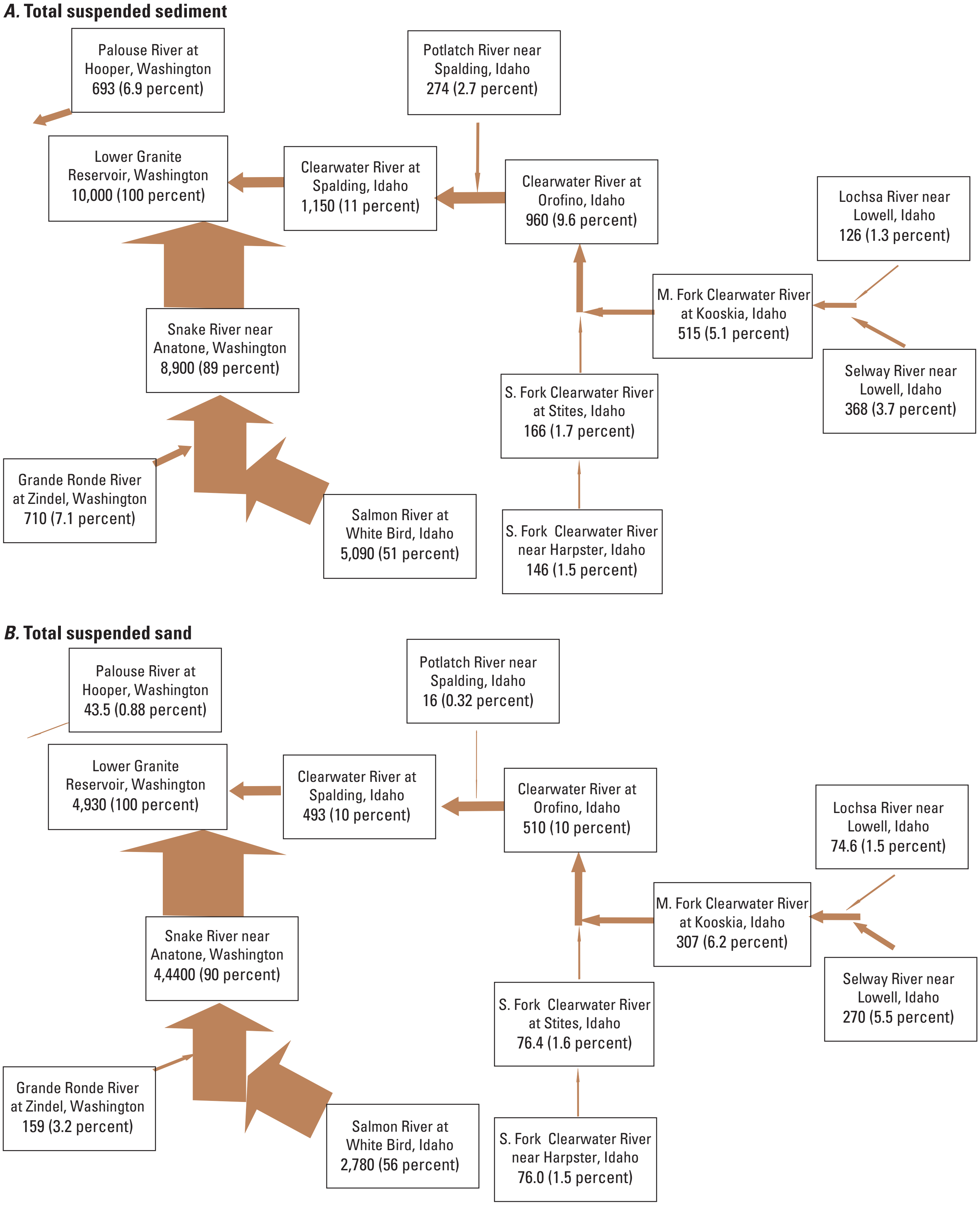

Figure 9. Estimated loads of (*A*) total suspended sediment, (*B*) total suspended sand, and (*C*) total suspended fines transported in the lower Snake and Clearwater River Basins, water years 2009–11. Values are in thousands of tons and percentage of total load entering Lower Granite Reservoir during water years 2009–11. Width of each arrow is proportional to the estimated suspended sediment load.

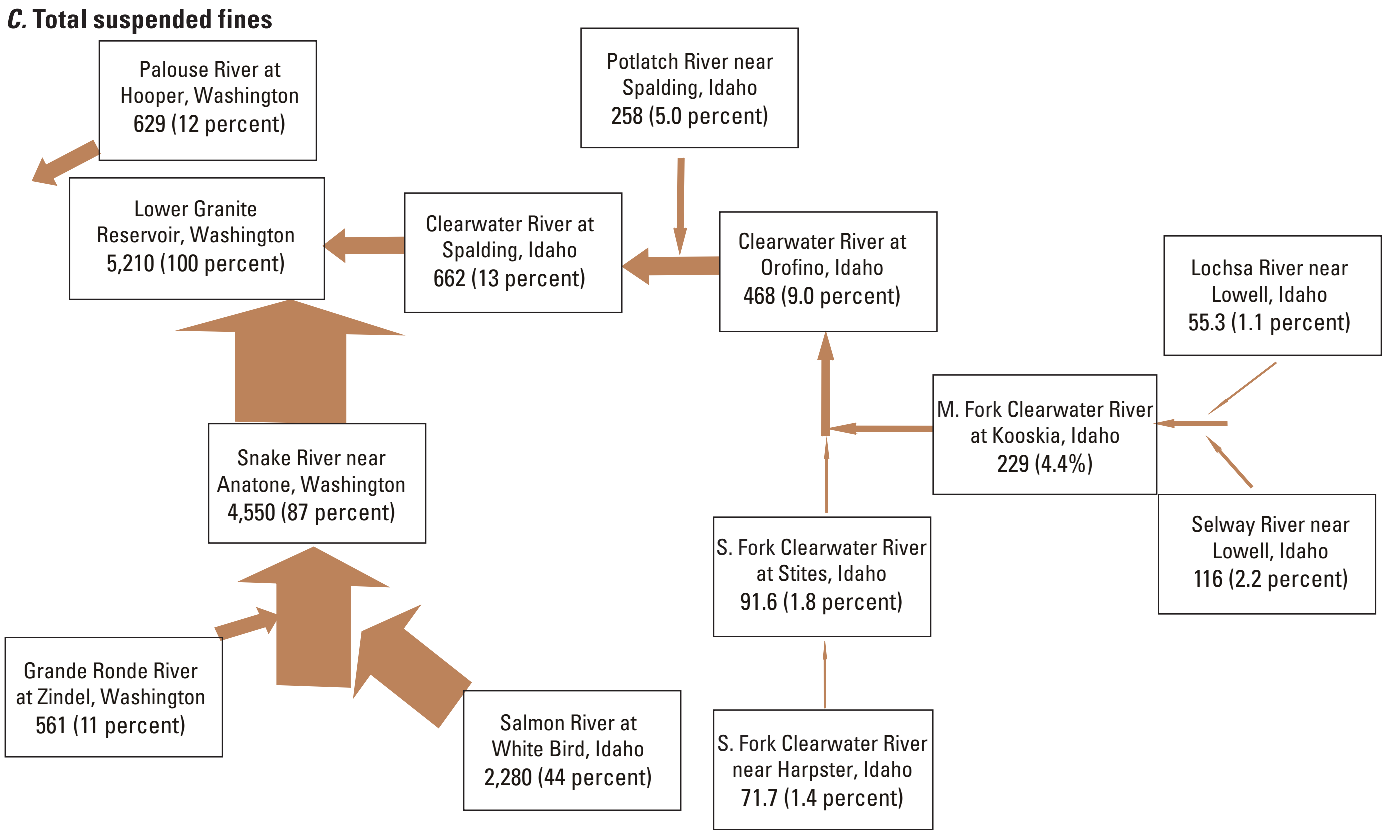

Figure 9.—Continued

The Grande Ronde River enters the Snake River just upstream of the Snake River near Anatone station (fig. 2). During water years 2009–11, the Grande Ronde River as measured at the Zindel station, contributed about 710,000 tons of suspended sediment to the Snake River (fig. 9*A*), about 79 percent of which was fine-grained sediment (table 4). The mean annual yield of suspended sediment from the Grande Ronde River Basin was about 60 (tons/mi^2)/yr, of which about 47 (tons/mi^2)/yr was fine-grained sediment (fig. 8). Overall, the TSS load in the Grande Ronde River was equivalent to about 7.1 percent of the suspended sediment, about 3.2 percent of the suspended sand, and about 11 percent of the suspended fines that entered Lower Granite Reservoir during water years 2009–11 (fig. 9*A*–*C*).

A primary contributor of TSS in the Clearwater drainage basin, particularly the sand-size fraction, is the Selway River, which discharged about 368,000 tons of TSS during water years 2009–11. The Selway River accounted for about 71 percent of the TSS and about 88 percent of the suspended sand as measured downstream in the Middle Fork Clearwater River at Kooskia. The Lochsa River contributed about 126,000 tons, or about 24 percent of the TSS in the Middle Fork Clearwater River at Kooskia. Of the TSS discharged from the Selway and Lochsa Rivers, about 73 and 59 percent, respectively, was sand-sized. The mean annual basin yields of suspended sediment from the Selway and Lochsa Rivers were 64 and 36 (tons/mi^2)/yr, respectively during 2009–11. Overall, the sediment load delivered from the Selway River drainage basin was equivalent to about 32 percent of the TSS and about 55 percent of the suspended sand discharged to Lower Granite Reservoir from the Clearwater River during water years 2009–11. The TSS load from the Lochsa River drainage basin was equivalent to about 11 percent of the TSS and about 15 percent of the suspended sand discharged from the Clearwater River Basin during water years 2009–11. As a percentage of the TSS load entering Lower Granite Reservoir from both the Snake and Clearwater Rivers, the Selway River accounted for only about 3.7 and 5.5 percent, and the Lochsa River only about 1.3 and 1.5 percent of the TSS and total suspended sand, respectively (fig. 9*A* and 9*B*).

Combined, the Middle Fork Clearwater River (as measured at Kooskia, Idaho) and the South Fork Clearwater River (as measured at Stites, Idaho) discharged about 681,000 tons of suspended sediment during water years 2009–11 (fig. 9*A*). Of this total, about 76 percent, or 515,000 tons was from the Middle Fork Clearwater River, equivalent to about 45 percent of the TSS and 62 percent of the suspended sand entering Lower Granite Reservoir from the Clearwater River. TSS discharged from the South Fork Clearwater River was equivalent to about 14 percent of the TSS and 16 percent of the suspended sand entering Lower Granite Reservoir from the Clearwater River during water years 2009–11.

From the confluence of the South Fork Clearwater River at Stites and the Middle Fork Clearwater River at Kooskia downstream to the station at Orofino, the Clearwater River accrued about 279,000 tons of suspended sediment during water years 2009–11 (fig. 9*A*). Of this accrual, about 54 percent was fine-grained sediment. The Potlatch River contributed an additional 274,000 tons of suspended sediment to the Clearwater River. About 94 percent of the suspended sediment discharged from the Potlatch River was fine-grained sediment. The mean annual yield of TSS (156 [tons/mi^2]/yr) and of fine-grained suspended sediment (148 [tons/mi^2]/yr) from the Potlatch River Basin were the largest of all the stations monitored during water years 2009–11 (fig. 8). During water year 2011, the yield of TSS and fine-grained sediment from the Potlatch River Basin were about 362 and 343 (tons/mi^2)/yr, respectively. Although the TSS load from the Potlatch River was equivalent to about 24 percent of the TSS load entering Lower Granite Reservoir from the Clearwater River during water years 2009–11, the fine-grained sediment discharged from the Potlatch River was equivalent to about 39 percent of the fine-grained load entering the reservoir from the Clearwater River. During water year 2011, the load from the Potlatch River was equivalent to about 32 percent of the TSS and 53 percent of the fine-grained suspended sediment as measured in the Clearwater River at Spalding. During water year 2011, streamflow in the Potlatch River accounted for less than 1 percent of the total combined streamflow entering Lower Granite Reservoir from the Snake and Clearwater Basins. However, the TSS load and the fine-grained suspended-sediment load from the Potlatch River were equivalent to about 3.5 and 6.5 percent, respectively of the total transported to Lower Granite Reservoir, most of which was generated during the rain-on-snow event in mid-January.

The mean annual yield of TSS in the Palouse River as measured at Hooper, Washington, was about 92 (tons/mi^2)/yr during water years 2009–11. More than 90 percent of the sediment transported in the Palouse River was fine-grained sediment. Although the Palouse River discharges to the Snake River downstream of Lower Granite Reservoir, the load of suspended sediment transported in the Palouse River during water years 2009–11 was about 693,000 tons, equivalent to about 6.9 percent of the total discharged to Lower Granite Reservoir during water years 2009–11 (fig. 9*A*). The load of fine-grained sediment transported in the Palouse River during the same period was about 629,000 tons, equivalent to about 95 percent of the 662,000 tons of fine-grained sediment transported from the Clearwater River to Lower Granite Reservoir (fig. 9*C*).

Suspended Sediment Delivery to Lower Granite Reservoir

Combined, the Snake and Clearwater Rivers discharged about 10 million tons of suspended sediment to Lower Granite Reservoir during water years 2009–11 (table 4; fig. 9*A*). However, the delivery of sediment to Lower Granite Reservoir varied annually. About 60 percent of the 3-year total was discharged to the reservoir during water year 2011, which was characterized by a large winter snowpack, a sustained spring runoff, and high TSS loads in the Snake and Clearwater Rivers through most of the summer (fig. 10). During water years 2009–11, the Snake River accounted for about 89 percent of the TSS, about 90 percent of the suspended sand, and about 87 percent of the suspended fines entering Lower Granite Reservoir (figs. 9*A*–*C*). Only during water year 2010 did the Clearwater River account for more than 15 percent of the TSS load entering Lower Granite Reservoir.

Comparison with 1972–79 Study

Comparing data from this study with data collected during water years 1972–79 as described in Jones and Seitz (1980) indicate that, on average, the Clearwater River contributed a larger percentage of the TSS load entering Lower Granite Reservoir during 1972–79 than during 2008–11. Jones and Seitz (1980) used sediment transport curves to estimate loads, and they reported that, on an average annual basis, the Snake River accounted for about 80 percent and the Clearwater River about 20 percent of the TSS load entering Lower Granite Reservoir during 1972–79. To evaluate differences in the sediment transport characteristics between the data collected by Jones and Seitz and the data collected during this study, sediment transport curves for both study periods were compared (fig. 11). For the Snake River near Anatone (fig. 11*A*), the transport curves for TSS show larger concentrations and loads over the entire range of streamflow during 2008–11 as compared to 1972–79. An Analysis of Covariance (ANCOVA) (Helsel and Hirsch, 1992) indicates that the difference in concentrations of TSS ($p=0.006$, fig. 11*A*) and suspended sands ($p<0.001$, fig. 12*B*) were significantly larger ($\alpha=0.05$) during 2008–11 as compared to 1972–79. However, the concentrations of suspended fines ($p=0.193$) were not significantly different (fig. 12*A*). The best-fit lines on figure 11*B* for the Clearwater River at Spalding indicate that the concentrations and load of suspended sediment in relation to streamflow was similar during 1972–79 as compared to 2008–11. An ANCOVA

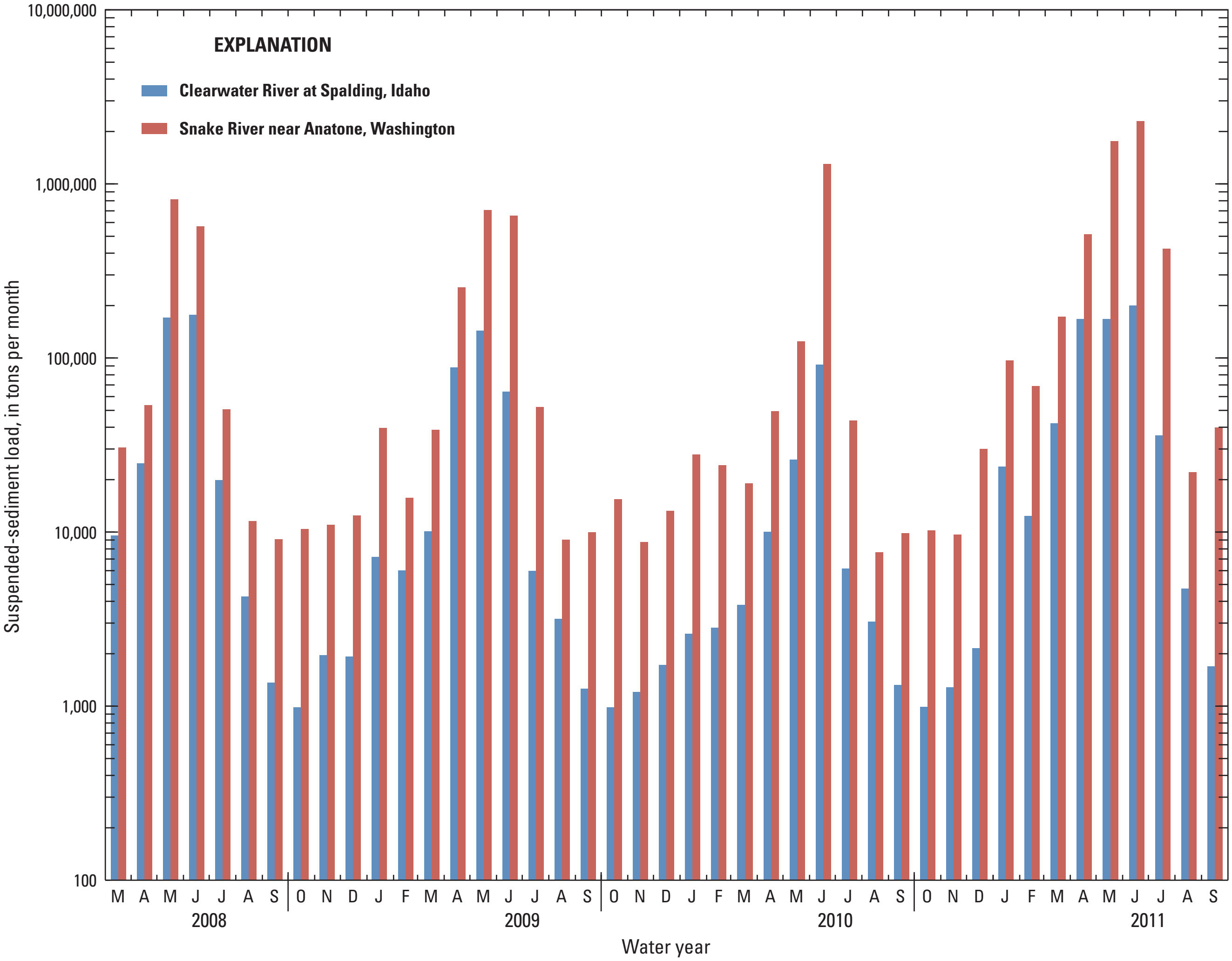

Figure 10. Suspended-sediment loads delivered monthly to Lower Granite Reservoir from the Snake and Clearwater Rivers, Washington and Idaho, March 2008–September 2011.

indicates that the difference in concentrations of TSS ($p=0.853$) and suspended fines ($p=0.666$) in the Clearwater River were not statistically significant between the two periods. However, the suspended-sand concentration in the Clearwater River at Spalding was significantly larger ($p=0.011$) during 2008–11 as compared to 1972–79.

Using continuous streamflow records and suspended-sediment data collected during 1972–79, loads for suspended sand and suspended fines were estimated for the Snake River near Anatone and the Clearwater River at Spalding using the LOADEST model. The suspended sand and suspended fines were analyzed separately for the 1970s data to estimate the fractional loads during each year for 1972–79 and 2009–11 (fig. 13). The results indicate that the TSS load entering Lower Granite Reservoir from the Snake River increased from an annual average of about 71 percent of the total in water years 1972–79 to 89 percent in water years 2009–11. Conversely, the load from the Clearwater River decreased from 29 percent during 1972–79 to 11 percent during 2009–11.

As a proportion of the TSS load entering Lower Granite Reservoir from the combined Snake and Clearwater Rivers, the sand fraction increased from an annual average of about 30 percent during 1972–79 to 48 percent during 2009–11. Most of the increase in the sand load was attributable to the Snake River. In the Snake River near Anatone, the sand fraction increased from an average of 28 percent of the TSS load during 1972–79 to an average of 48 percent during 2009–11 (fig. 13). Data for the Salmon River are not sufficient to estimate suspended-sediment loads for 1972–79.

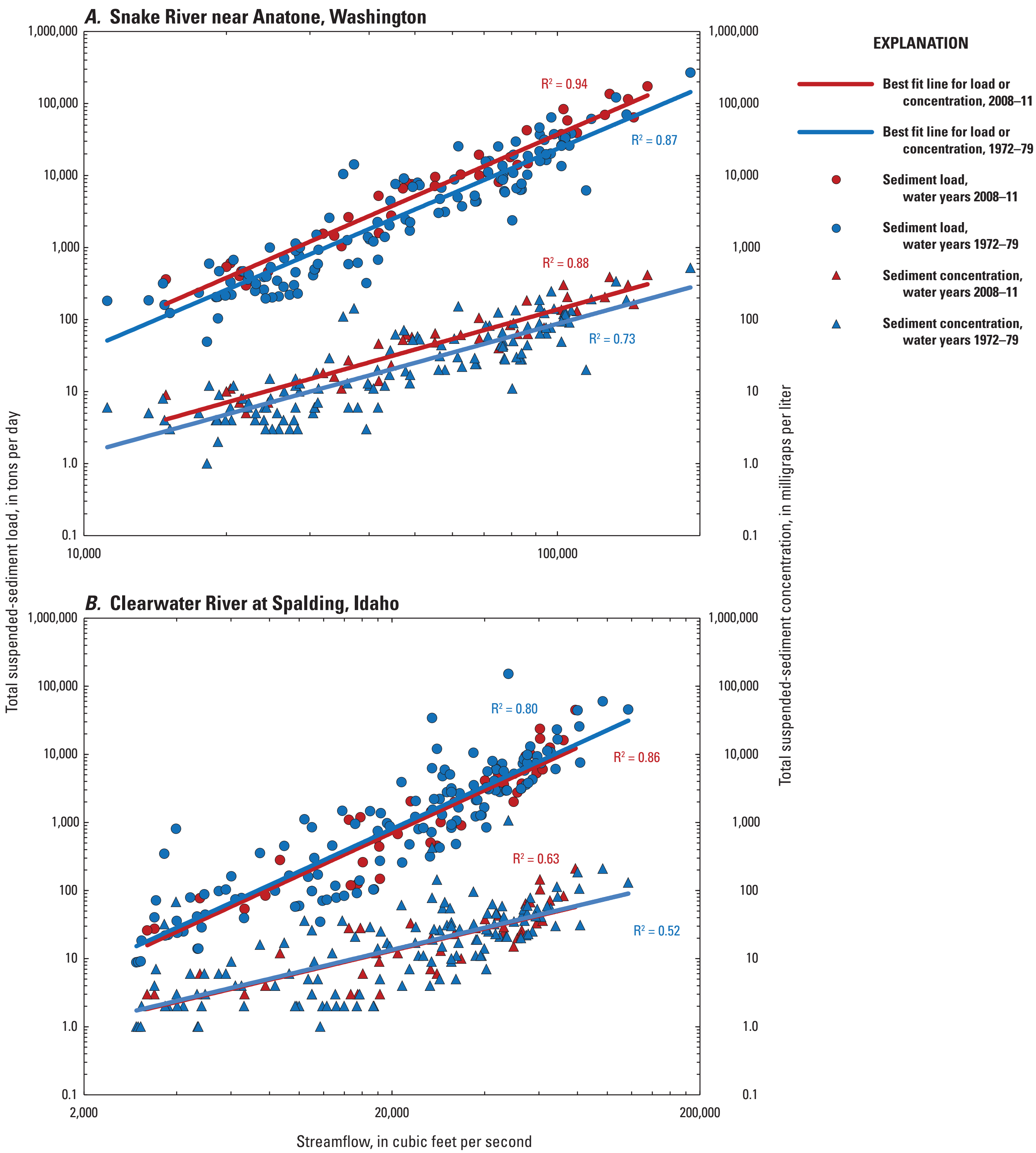

Figure 11. Suspended-sediment transport curves for concentrations and loads in the (*A*) Snake River near Anatone, Washington, and (*B*) Clearwater River at Spalding, Idaho, for data collected during water years 1972–79 and 2008–11.

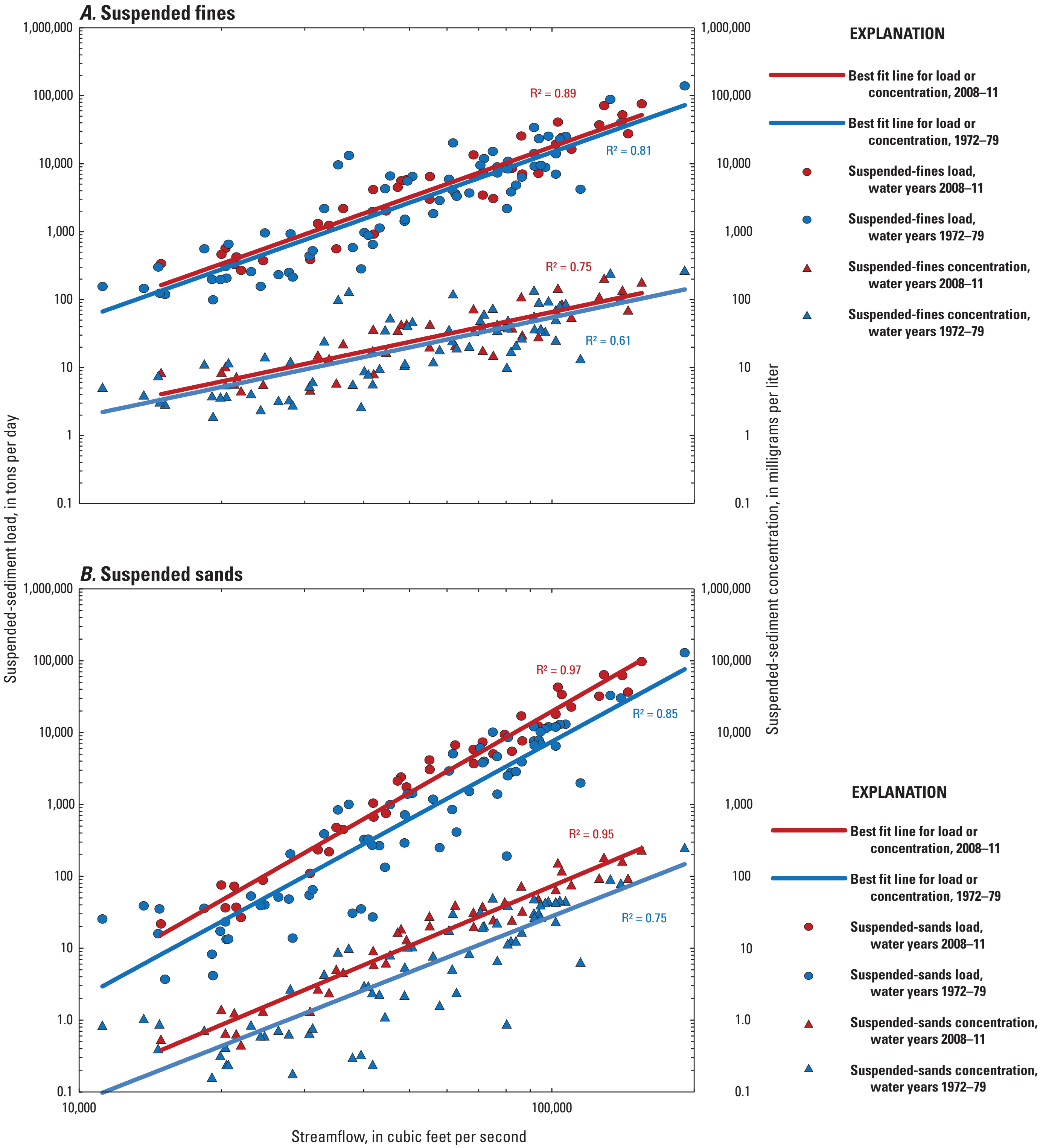

Figure 12. Suspended-sediment transport curves for concentrations and loads for (*A*) suspended fines and (*B*) suspended sands, Snake River near Anatone, Washington, water years 1972–79 and 2008–11.

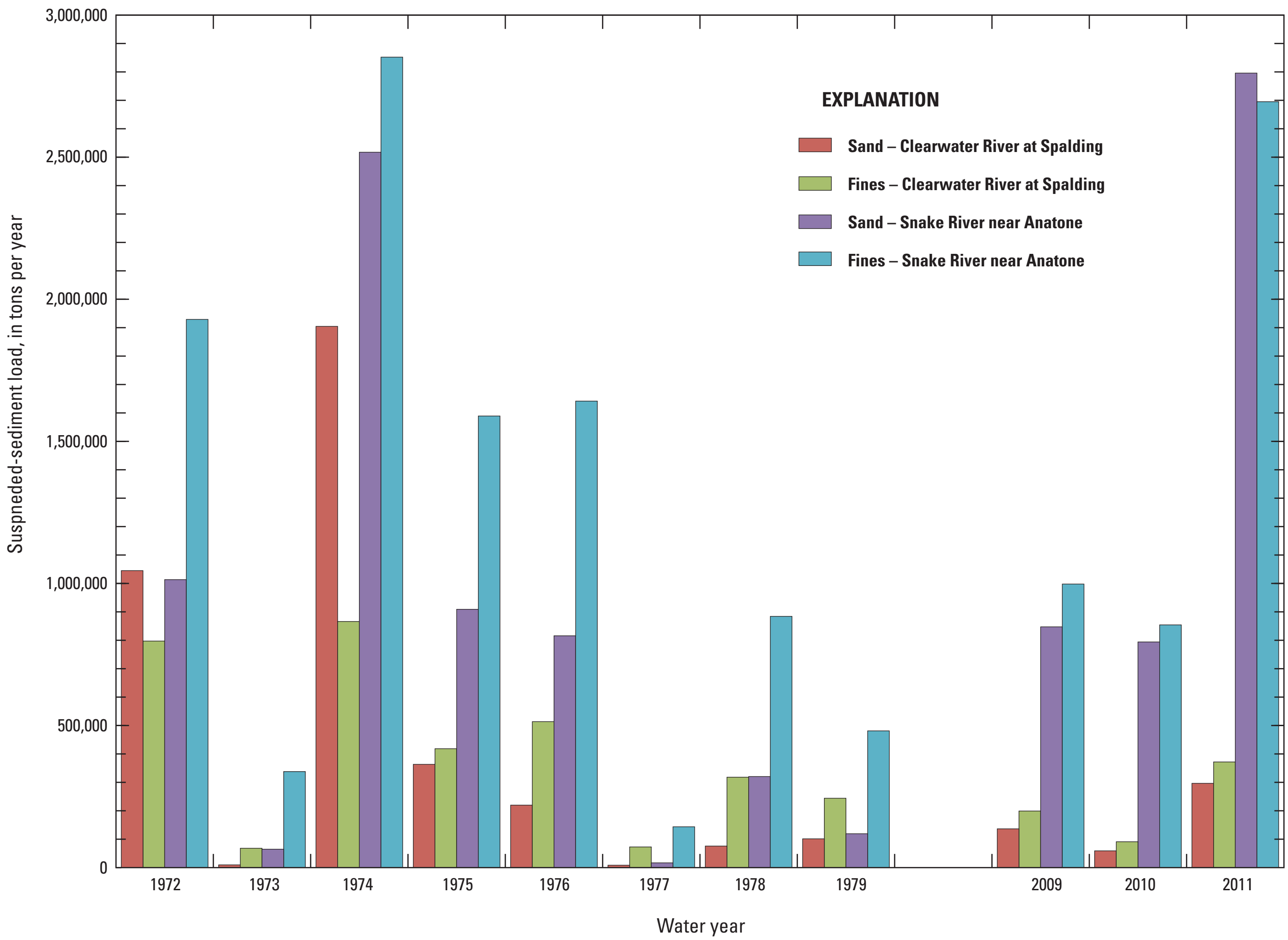

Figure 13. Estimated annual suspended sand and fine loads, Snake River near Anatone, Washington, and Clearwater River at Spalding, Idaho, water years 1972–79 and 2009–11.

However, the increase in the suspended-sand load noted in the Snake River near Anatone probably is attributable to the Salmon River. A century of fire suppression and other forest-management practices resulted in an increase in the number and severity of forest fires in central Idaho during the last quarter of the 20th century (Burton, 2005) and the first decade of the 21st century. The effect of wild fires on sediment mobility can be particularly dramatic in the Salmon River Basin and other areas of central Idaho where disturbance of steep drainage basins with highly erosive soils can mobilize large quantities of sand and gravel to streams (King and others, 2004). Although it is beyond the scope of this study, it would be insightful to obtain fluvial sediment data from select locations within the Salmon River Basin to identify critical subbasins and to quantify the magnitude of sediment delivery to discrete reaches of the Salmon River, the lower Snake River, and ultimately to Lower Granite Reservoir.

Suspended-Sediment Surrogates

Surrogate models were developed using suspended sediment and acoustic backscatter data collected during water year 2010, and data from water year 2011 were used to validate the models. The best surrogate models based on the highest R^2 were developed using the 1.5MHz ADVM at the streamgage on the Snake River near Anatone and the 3MHz ADVM at the streamgage on the Clearwater River at Spalding (table 5; fig. 14). Separate models were developed for each streamgage to estimate overall SSC as well as concentrations of sand and fines (table 5). SSC results from water year 2011 matched the acoustic surrogate models, on average, -8.3 percent at the Snake River station and +9.8 percent at the Clearwater River station. Major deviations from the models were not evident in water year 2011 except for one sample with a low sediment concentration at the Clearwater River gaging station (fig. 14).

Table 5. Summary of acoustic surrogate and LOADEST models used to evaluate suspended-sediment concentrations at the Snake River near Anatone, Washington, and Clearwater River at Spalding, Idaho.

[Locations of stations are shown in figure 2. **Abbreviations:** R^2, coefficient of determination; RPD, relative percent difference between sample and model results; BCF, Duan's bias correction factor; MHz, megahertz; ABScorr, acoustic backscatter corrected for beam spreading and attenuation by water and sediment (dB, decibel); ln, natural log; SSC, suspended-sediment concentration (milligrams per liter); *Q*, streamflow (cubic feet per second); *T*, is the centered decimal time in years from the beginning of the calibration period]

Gaging station name	Model	Number of samples used for regression; validation	Model	R^2	Average RPD (percent)	Standard error	BCF
Snake River near Anatone	1.5MHz_ABS_{corr}	22; 9	SSC = $10^{[(0.0756\times 1.5MHz\_ABScorr)-4.676]}\times 1.048$	0.92	+10	1.39	1.048
			Sand concentration = $10^{[(0.105\times 1.5MHz\_ABScorr)-7.636]}\times 1.129$	0.89	+24	1.73	1.129
			Fines concentration = $10^{[(0.0615\times 1.5MHz\_ABScorr)-3.730]}\times 1.084$	0.81	+19	1.54	1.084
	LOADEST	38	ln SSC = 3.96 + 2.09(ln$Q$) + 0.08(lnQ^2) - 0.54[sin(2πT)] + 0.16[cos(2πT)]	0.90			
			ln sand conc = 2.97 + 2.99(ln$Q$) - 0.46(lnQ^2) - 0.49[sin(2πT)] - 0.06[cos(2πT)]	0.95			
			ln fines conc = 3.38 + 1.72(ln$Q$) + 0.22(lnQ^2) - 0.56[sin(2πT)] + 0.34[cos(2πT)]	0.80			
Clearwater River at Spalding	3MHz_ABS_{corr}	30; 11	SSC = $10^{[(0.0557*3MHz\_ABScorr)-2.431]}\times 1.040$	0.93	+8.6	1.34	1.040
			Sand concentration = $10^{[(0.0743\times 3MHz\_ABScorr)-4.147)]}\times 1.146$	0.87	+34	1.71	1.146
			Fines concentration = $10^{[(0.0461\times 3MHz\_ABScorr)-2.030]}\times 1.097$	0.78	+19	1.58	1.097
	LOADEST	38	ln SSC = 1.79 + 1.05(ln$Q$) + 0.59(lnQ^2) + 0.46[sin(2πT)] - 0.48[cos(2πT)]	0.74			
			ln sand conc = 0.05 + 1.53(ln$Q$) + 0.69(lnQ^2) + 0.24[sin(2πT)] - 0.85[cos(2πT)]	0.84			
			ln fines conc = 1.53 + 0.85(ln$Q$) + 0.52(lnQ^2) + 0.65[sin(2πT)] - 0.36[cos(2πT)]	0.62			

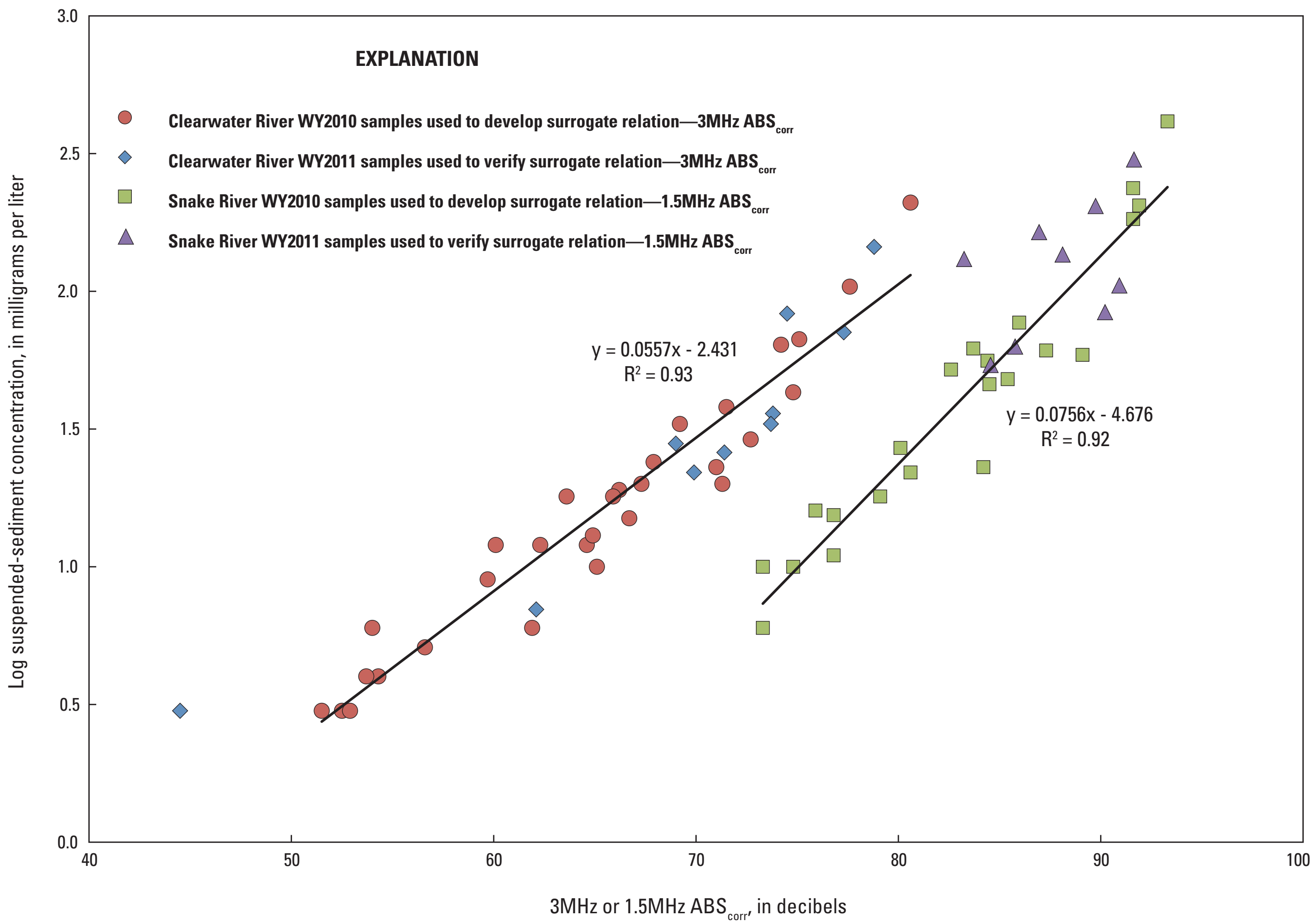

Figure 14. Best-fit surrogate models for the Snake River near Anatone, Washington, using the 1.5MHz acoustic Doppler velocity meter (ADVM) and the Clearwater River at Spalding, Idaho, using the 3MHz ADVM, water years 2010–11.

Suspended-sediment loads computed using the acoustic surrogate models for the Snake and Clearwater Rivers were compared to the loads calculated using LOADEST. The acoustic surrogate models were developed for concentration only, and loads were calculated by multiplying concentration estimates by daily streamflow as measured at each streamgage. Performance of the models was compared by first evaluating the coefficient of determination (R^2) of the acoustic surrogate and LOADEST concentration (not load) models. The acoustic surrogate models had a better correlation than the LOADEST concentration models at both stations for SSC and suspended fines and for suspended sand at the Clearwater River station (table 5). The LOADEST concentration model had a better correlation than the acoustic surrogate models for suspended sands at the Snake River station (table 5).

Load results for the Snake River using LOADEST and acoustic surrogate models were markedly different. The largest difference occurred in water year 2011, when the suspended-sediment load calculated using the LOADEST model was more than three times higher than the load calculated using the acoustic surrogate model (table 6). The total monthly sediment loads were substantially higher using the LOADEST model as compared to the acoustic surrogate model, particularly during May and June (fig. 15*A*). Generally, SSC at the Snake River station were underestimated by the acoustic surrogate model when concentrations were high (greater than 200 mg/L) and had a high percentage of sand. The unregulated Salmon River contributed an average 59 percent of the streamflow passing the Snake River at Anatone streamgage during these sampling events, but there was no clear relation between the percentage

Table 6. Comparison of suspended-sediment loads estimated using acoustic backscatter and LOADEST models in the Snake River near Anatone, Washington, and Clearwater River at Spalding, Idaho.

[Locations of stations are shown in figure 2. **Total suspended-sediment load** may not equal total sand load plus total fines load due to errors in individual models. **Abbreviations:** MHz, megahertz; ABS_{corr}, acoustic backscatter corrected for beam spreading and attenuation by water and sediment (dB, decibel); *Q*, streamflow]

Gaging station name	Water year	Model	Total suspended-sediment load (tons)	Total suspended-sand load (tons)	Total suspended-fines load (tons)
Snake River near Anatone	2009	$1.5MHz\_ABS_{corr}$ [1]	1,460,000	709,000	789,000
		LOADEST (Q, Q^2, seasonality)	1,820,000	848,000	998,000
	2010	$1.5MHz\_ABS_{corr}$	1,120,000	589,000	606,000
		LOADEST (Q, Q^2, seasonality)	1,650,000	795,000	855,000
	2011	$1.5MHz\_ABS_{corr}$	1,740,000	701,000	1,030,000
		LOADEST (Q, Q^2, seasonality)	5,450,000	2,800,000	2,700,000
	Overall	$1.5MHz\_ABS_{corr}$	4,320,000	2,000,000	2,430,000
		LOADEST (Q, Q^2, seasonality)	8,920,000	4,440,000	4,550,000
Clearwater River at Spalding	2009	$3MHz\_ABS_{corr}$	315,000	138,000	180,000
		LOADEST (Q, Q^2, seasonality)	335,000	137,000	199,000
	2010	$3MHz\_ABS_{corr}$	169,000	73,900	98,200
		LOADEST (Q, Q^2, seasonality)	152,000	59,000	91,200
	2011	$3MHz\_ABS_{corr}$	645,000	329,000	342,000
		LOADEST (Q, Q^2, seasonality)	662,000	297,000	372,000
	Overall	3MHz_ABScorr	1,130,000	541,000	620,000
		LOADEST (Q, Q^2, seasonality)	1,150,000	493,000	662,000

[1]Loads presented for the $1.5MHz\_ABS_{corr}$ in water year 2009 are for April–September only.

of unregulated streamflow passing the station and percent error in the estimated SSCs. There also was no clear relation between percent organic matter and percent error in the estimations. Some of the error in the acoustic surrogate model at high sand concentrations may be due to the placement of the ADVM in the water column. If the sand particles were not well-mixed in the water column during specific events or were transported in a layer close to the streambed, the ADVM would not have detected those particles because it is mounted approximately mid-depth in the water column. This scenario is likely, particularly in water year 2011, because of the large amount of sand transport measured in the Salmon River and contributed to the Snake River upstream of the surrogate monitoring station at Anatone.

Further examination of estimated SSCs in water year 2011 shows that the LOADEST model produces much higher estimated concentrations than the sediment surrogate model on the descending limb of the hydrograph (fig. 16). The acoustic surrogate model should be a more direct measurement of sediment concentrations as compared to the LOADEST model (which is based on flow, time, and seasonality terms), at least during storm events. The pattern over the ascending and descending limbs of the hydrograph show that the LOADEST model is affected by hysteresis, but perhaps less so than a traditional transport curve based on a single streamflow term (Wood and Teasdale, 2013). Generally, the acoustic surrogate model matched more closely with the measured SSCs in samples collected at the Snake River near Anatone than the LOADEST model, except during high streamflow in May and June 2011 (fig. 16). Neither the acoustic or the LOADEST model performed well during this period, especially during June when the sample results were between the concentrations estimated by the two models.

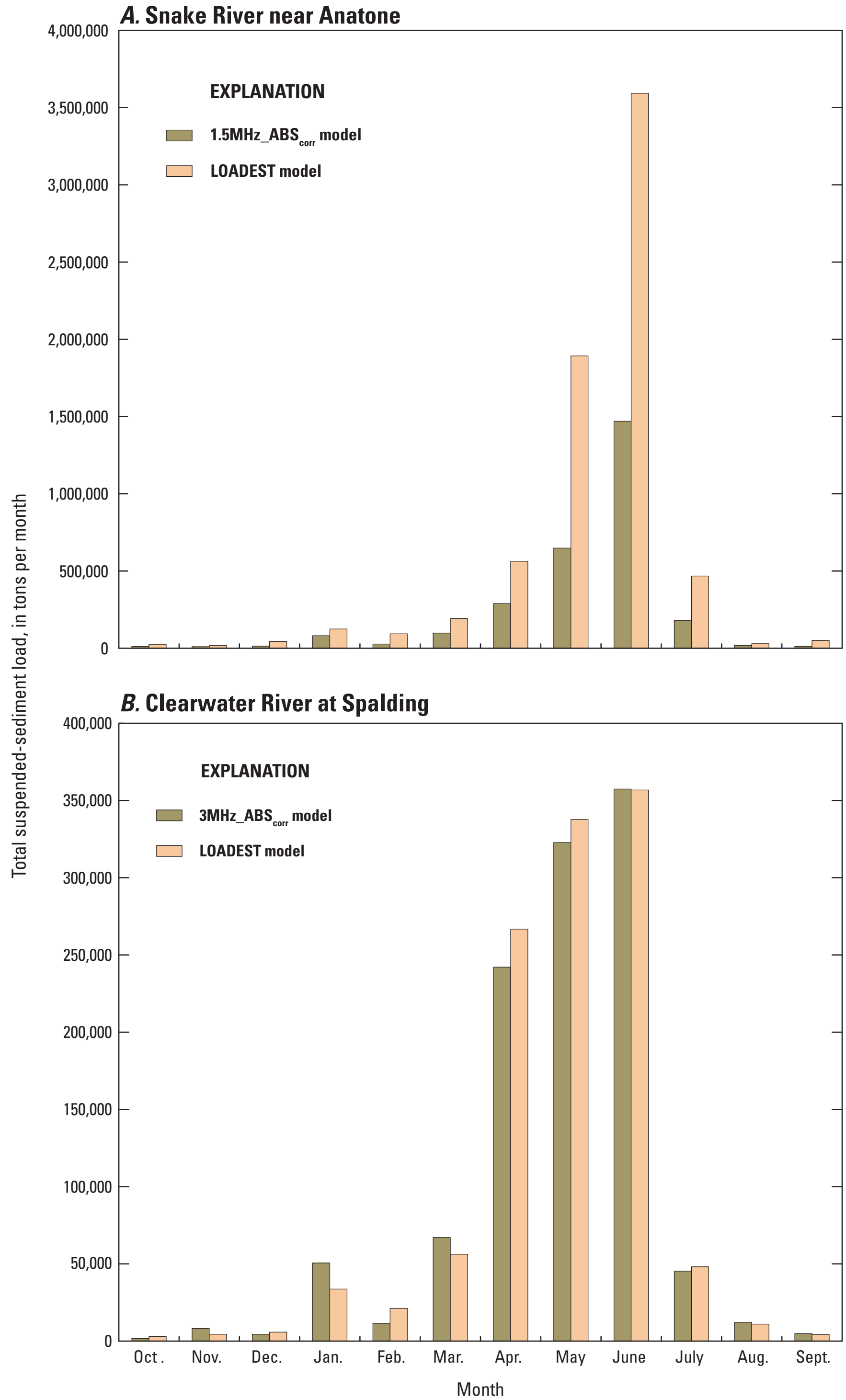

Figure 15. Comparison of total monthly sediment load estimated using acoustic backscatter and LOADEST models in the (*A*) Snake River near Anatone, Washington, and (*B*) Clearwater River at Spalding, Idaho, water years 2009–11.

NOTE: Each month represents the total load that occurred during that month within the study period. For example, the total load for May in the Clearwater River is the sum of loads in May 2009, May 2010, and May 2011.

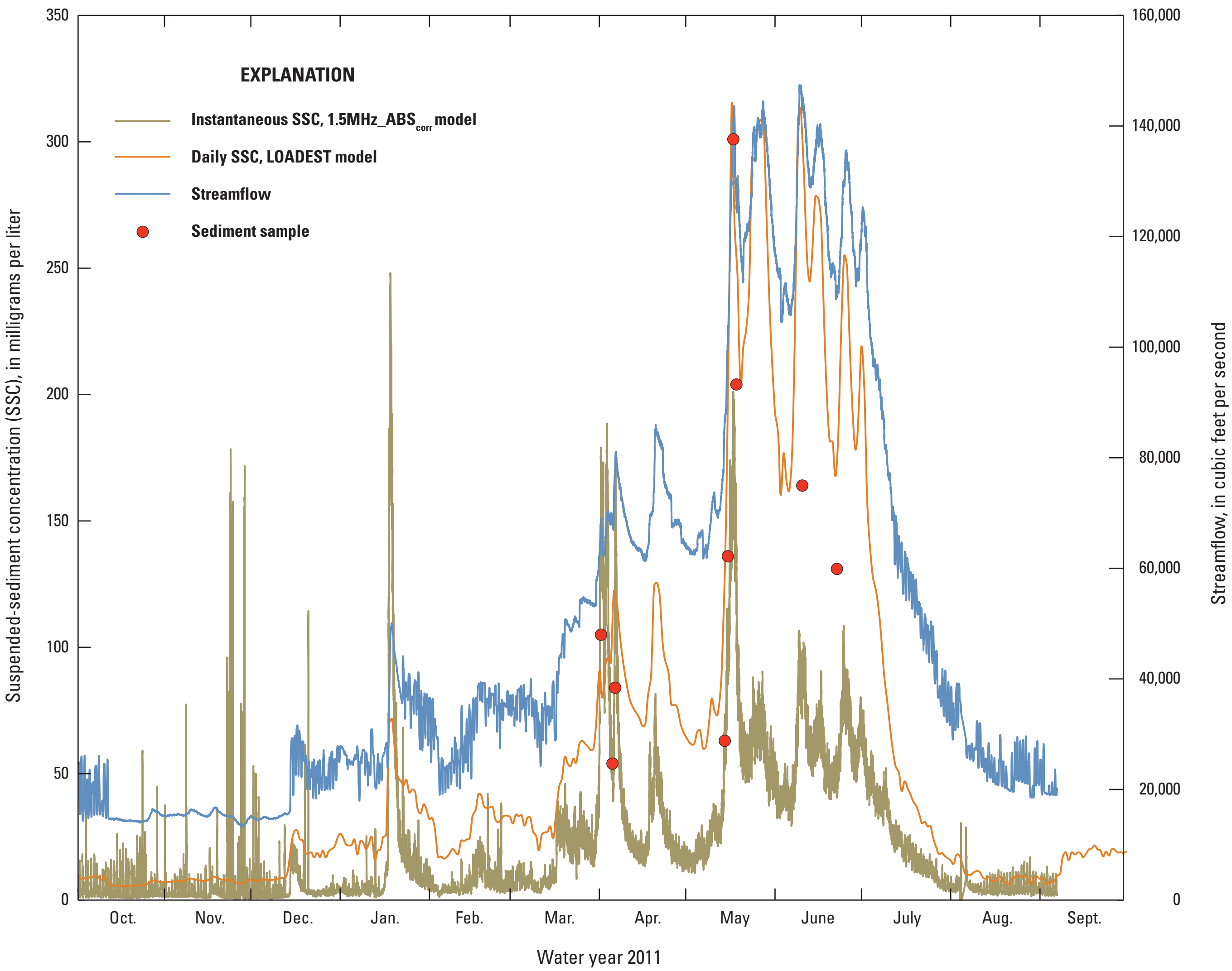

Figure 16. Comparison of suspended-sediment concentrations estimated using acoustic backscatter and a LOADEST model, Snake River near Anatone, Washington, water year 2011.

Model simulation results for load compared well for the Clearwater River station. Suspended-sediment loads at the Clearwater River computed by the acoustic surrogate and LOADEST models matched within 3–11 percent on an annual basis and within 2 percent over the entire study period (table 6). The percent differences in the Clearwater River were slightly higher for total suspended-sand load, from 1–22 percent on an annual basis. Overall, however, the model results compared well. The acoustic surrogate model, in general, produced sand load estimates using the 1.5 MHz ADVM that were slightly higher than the estimates generated using the LOADEST model (9 percent higher for the entire study period). Suspended fines loads, which were estimated using the higher frequency 3.0 MHz ADVM, compared within 7–10 percent on an annual basis between the two models, and within 7 percent for the entire study period. The monthly average suspended-sediment loads for 2010–11 for the Clearwater River also compared well between the acoustic surrogate and LOADEST models (fig. 15*B*).

For storm events, the acoustic surrogate models provide a more direct measure of sediment concentrations as compared to LOADEST or traditional transport curves that are based only on streamflow. Thus, the acoustic surrogates probably are a more accurate method for estimating suspended-sediment loads over a short period or when real-time response is needed. Additionally, LOADEST models cannot be used to provide real-time, instantaneous load estimates because of post-processing requirements. Differences in load estimates between the acoustic surrogate and LOADEST models were further examined by summing estimated loads over the ascending and descending limbs of the hydrograph for several well-defined hydrologic events during the study period: seven events for the Snake River near Anatone and eight events for the Clearwater River at Spalding (table 7). Loads calculated using the acoustic surrogate model were higher on the ascending limb (negative percent difference) and lower on the descending limb (positive percent difference) as compared to loads calculated using the LOADEST model in all cases except for one event at the Snake River station (ascending limb) and two events at the Clearwater River station (one on the ascending limb, one on the descending limb). For all events combined, loads calculated using the acoustic surrogate model were 11–14 percent higher on the ascending limb and 24–65 percent lower on the descending limb as compared to loads calculated using the LOADEST model. The highest calculated and measured SSC typically were higher on the ascending limb (especially for acoustics), but total calculated loads often were higher on the descending limb than the ascending limb due to a prolonged recession in the streamflow.

During the June 2010 spring snowmelt runoff, multiple suspended-sediment samples were collected and compared to the acoustic surrogate results to validate the relative performance as compared to LOADEST models. In the Snake and Salmon River Basins, a large pulse of sediment-laden water was delivered from the Salmon River to the Snake River during this snowmelt runoff event. This sediment pulse was captured in the acoustic surrogate model as a spike in the acoustic backscatter on June 3 (fig. 17*A*), but not by the LOADEST model, which is primarily based on changes in streamflow. Samples were not collected on June 3, 2010 to verify either model. The acoustic surrogate model showed a rapid decrease in SSC directly following the peak of the hydrograph on June 3, whereas the LOADEST model showed elevated SSC until well after the peak. The sample with high SSC collected on June 6 does not match estimates from either model, but the samples collected on June 4 and June 14 match well with the estimated SSC from the acoustic surrogate model. The acoustic surrogate model estimated sand concentrations close to all three of the sand concentrations in the samples collected from the Snake River (fig. 17*B*). The largest difference between model estimates and the June 6 simulation results was for the fines concentration (fig. 17*C*), which was better represented by the LOADEST model. During the April 2010 hydrologic event on the Clearwater River (fig. 18), the sample SSC results match the acoustic surrogate model estimates closely, whereas the LOADEST model underestimates most concentrations and loads throughout the event (fig. 18, table 7).

Table 7. Comparison of suspended-sediment loads during selected hydrologic events calculated using acoustic backscatter and a LOADEST model in the Snake River near Anatone, Washington, and Clearwater River at Spalding, Idaho.

[Locations of stations are shown in figure 2. **ABS_{corr}:** Acoustic backscatter corrected for beam spreading and attenuation by water and sediment (dB, decibel). **LOADEST:** Load Estimator. Percentages in parentheses indicate negative difference. **Abbreviation:** NA, not applicable]

Gaging station name	Event No.	Dates of event	Suspended-sediment load over ascending limb of hydrograph (tons)			Suspended-sediment load over descending limb of hydrograph (tons)		
			ABScorr	LOADEST	Percent difference	ABS_{corr}	LOADEST	Percent difference
Snake River near Anatone	NA	NA–All seven events combined	729,000	632,000	(14)	862,000	1,700,000	65
	1	April 18–May 3, 2009	122,000	85,900	(35)	89,600	115,000	25
	2	May 5–11, 2009	48,600	37,400	(26)	24,400	37,800	43
	3	May 18–24, 2009	98,400	86,700	(13)	106,000	159,000	40
	4	April 20–27, 2010	15,700	13,000	(19)	12,100	13,100	8
	5	May 16–30, 2010	33,000	26,100	(23)	48,400	59,900	21
	6	June 2–19, 2010	267,000	214,000	(22)	481,000	953,000	66
	7	May 11–19, 2011	144,000	169,000	16	100,000	357,000	112
Clearwater River at Spalding	NA	NA–All eight events combined	274,000	245,000	(11)	225,000	287,000	24
	1	May 13–24, 2008	59,400	94,500	46	13,000	22,200	52
	2	April 21–May 1, 2009	13,000	10,700	(19)	17,700	32,600	59
	3	April 16–27, 2010	5,740	2,990	(63)	3,700	3,260	(13)
	4	May 14–26, 2010	14,700	6,880	(72)	7,370	10,700	37
	5	June 2–July 5, 2010	70,600	55,600	(24)	34,900	37,300	7
	6	January 15–February 2, 2011	17,600	5,520	(104)	17,800	18,600	4
	7	March 29–April 15, 2011	55,500	45,300	(20)	93,900	113,000	18
	8	May 11–20, 2011	37,400	23,400	(46)	36,200	49,600	31

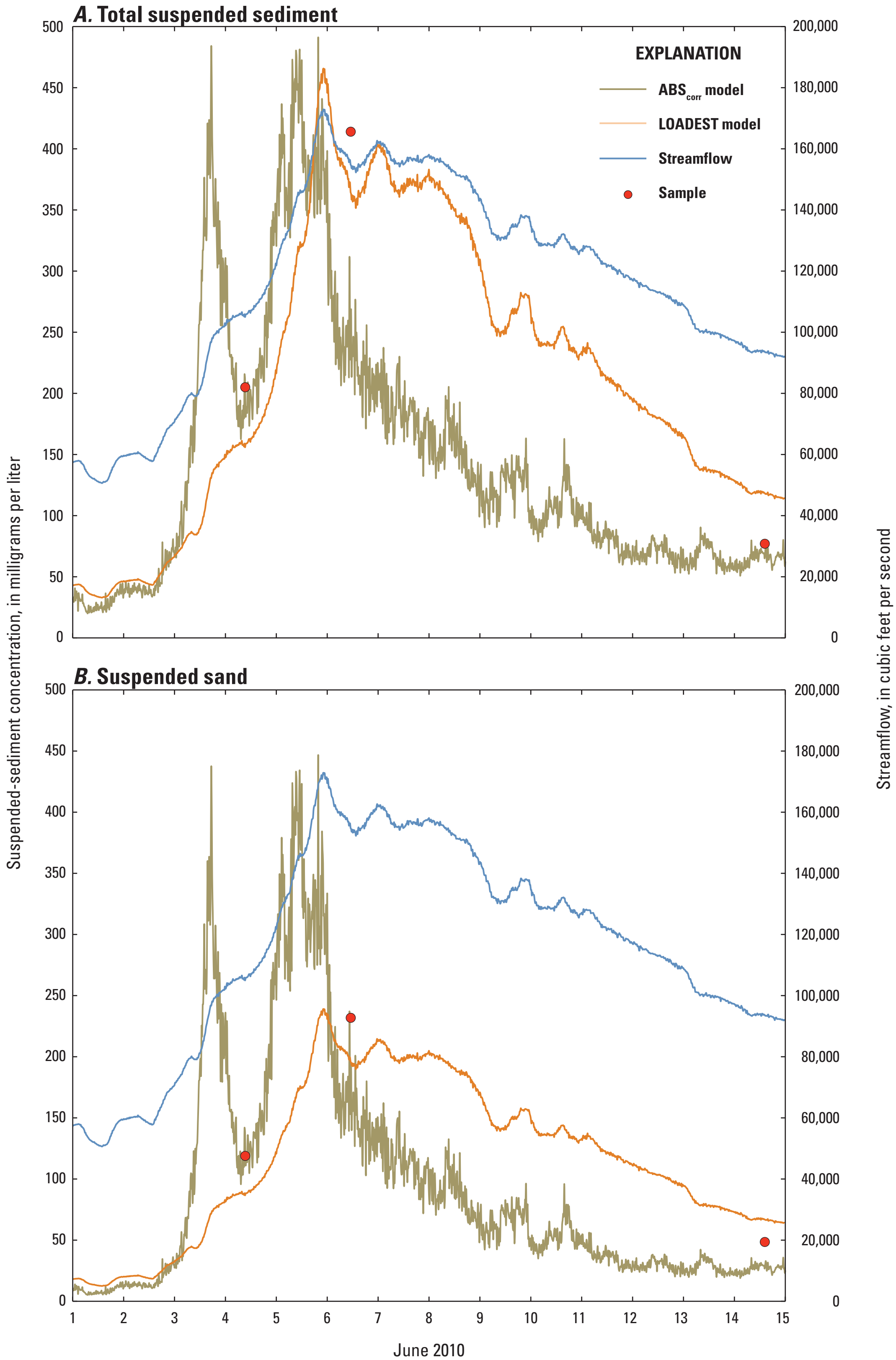

Figure 17. Comparison of (*A*) total suspended sediment, (*B*) suspended sand, and (*C*) suspended fine concentrations estimated using acoustic backscatter and a LOADEST model during spring snowmelt runoff at Snake River near Anatone, Washington, June 2010.

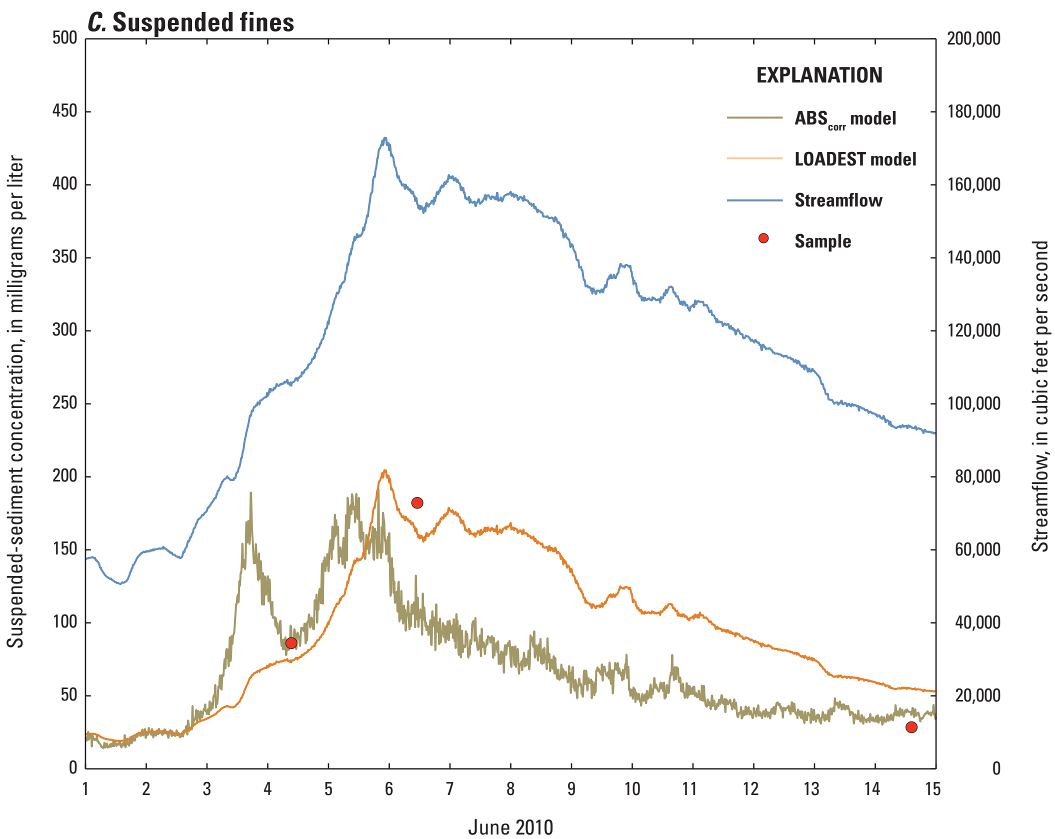

Figure 17.—Continued

Overall, in the Snake River near Anatone and the Clearwater River at Spalding, acoustic backscatter appeared to better estimate the SSC and suspended-sediment load than the LOADEST model over short periods. This is primarily because acoustic backscatter (1) is not affected by hysteresis; (2) provides a more direct, in-situ measurement of suspended sediment; and (3) is better able to represent sediment sources from a combination of regulated and unregulated sources, which can be poorly represented by a model based primarily on changes in streamflow. However, on a monthly and (or) annual basis, the acoustic surrogate and LOADEST models produced similar sediment load estimates for the Clearwater River at Spalding. Which model produced better estimates of monthly and annual sediment loads for the Snake River near Anatone is inconclusive. Much of the difference between the model simulation results is represented on the falling limb of the hydrograph and at mid-range streamflows during which few samples were collected. However, during high streamflow events such as the snowmelt runoff in the Snake River during 2011, acoustic surrogate tools may be unable to capture the contribution of suspended sand moving near the bottom of the water column and thus, may underestimate the total load of suspended sediment.

It is useful to show the acoustic surrogate model simulation results for comparison with LOADEST models as a demonstration that the most desirable method for estimating sediment load depends on the period of interest, the type of sediment being transported, and the degree of mixing and (or) stratification of the sediment in the stream. On an annual basis, both the LOADEST and surrogate models appear to provide a good estimate of suspended-sediment loads in the Snake and Clearwater Rivers. However, because surrogate methods for estimating loads were not available in all the tributary basins evaluated during this study, the LOADEST simulation results were used for the basin-wide sediment budgets to provide a consistent method for comparison.

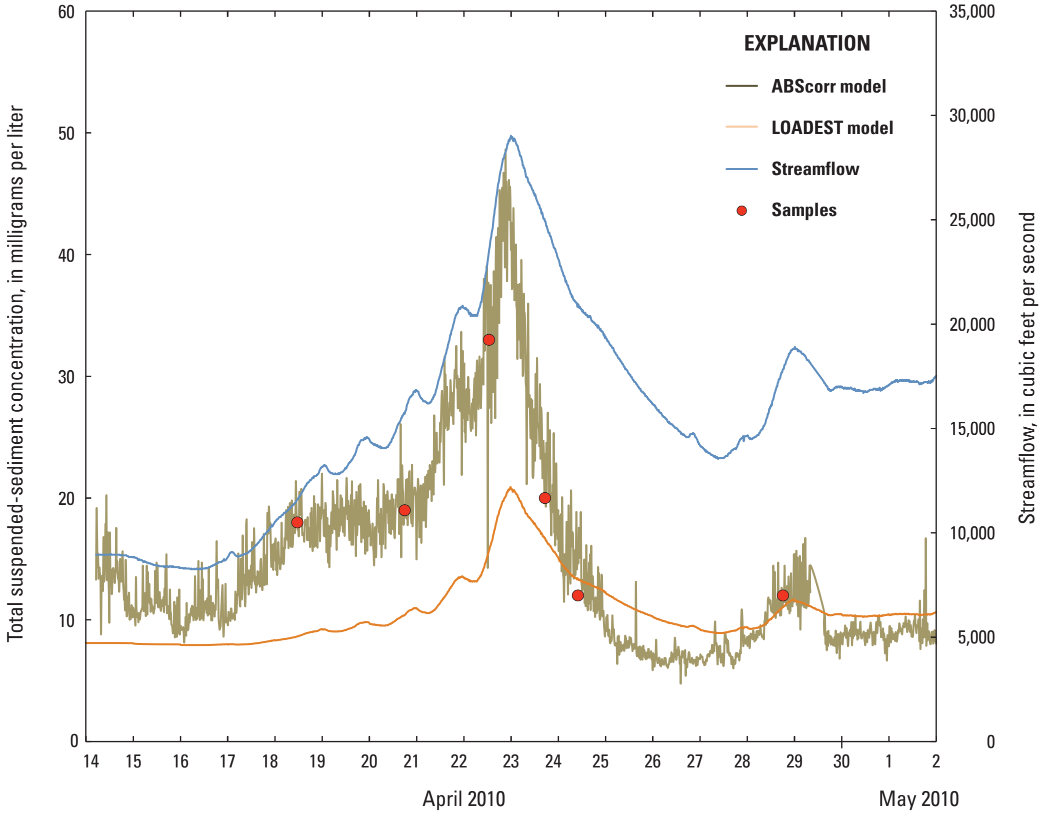

Figure 18. Comparison of total suspended-sediment concentrations estimated using acoustic backscatter and a LOADEST model during a hydrologic event at Clearwater River at Spalding, Idaho, April and May 2010.

Bedload

Bedload was highly variable throughout the Snake and Clearwater River Basins and at each station where samples were collected (table 8). Measured bedload ranged from zero during base flow conditions at all stations to a maximum of 4,140 ton/d in the Salmon River at White Bird at a streamflow of 70,800 ft^3/s (table 8). Stations located in upstream areas of a drainage basin generally had a larger percentage of the total sediment load as bedload (fig. 19) and a stronger correlation (higher R^2) between streamflow and bedload discharge as compared to stations located downstream (table 9). High stream gradients and high stream velocities at upstream stations probably account for the higher percentage of bedload. Best-fit regression equations and coefficients of determination (R^2) for the stations where bedload was collected are presented in table 9. Bedload transport curves are shown in figure 20. At most of the stations with measureable bedload, the particle size distribution (table 10) typically was unimodal at lower streamflows, with sand being the dominant particle size. At higher streamflows and during peak bedload discharge, the particle size was typically bimodal, with sand and coarse gravel composing the predominant particle size.

In the Snake River Basin, the measured bedload at the Salmon River at White Bird ranged from 25.9 to 4,140 ton/d (table 8). However, only five bedload samples were collected from the Salmon River during this study, and the correlation between streamflow and bedload was relatively poor ($R^2 = 0.46$; table 9). Three of the five samples collected from the Salmon River were unimodal, with 99 percent of the bedload composed of sand. The two other bedload samples from the Salmon River were bimodal and consisted of 35–45 percent gravel (2–64 mm diameter) and 55–65 percent sand (0.063–2 mm diameter) (table 10). Based on the best-fit regression equation (table 9), the total bedload discharge in the Salmon River was about 66,000 tons during water years 2009–11; about 1.3 percent of the total sediment load transported in the Salmon River at White Bird (fig. 19).

Table 8. Bedload data from sampling stations in the lower Snake and Clearwater River Basins, Washington and Idaho, water years 2008–11.

[Locations of stations are shown in figure 2. **Sampler type:** HS, Helley Smith. **Abbreviations:** ft, foot; ft^3/s, cubic foot per second; ton/d, ton per day]

Date	Mean sample time	Channel width (ft)	Streamflow, instantaneous (ft^3/s)	Number of sampling points	Rest time on bottom (seconds)	Sampler type	Bedload discharge (ton/d)
Salmon River at White Bird, Idaho (13317000)							
04-24-09	1030	370	32,400	10	60	HS	188
05-20-09	1332	460	70,800	10	60	HS	4,140
06-03-09	1535	445	60,400	10	60	HS	189
06-11-09	0821	400	41,000	10	60	HS	25.9
05-15-11	1245	430	55,300	7	60	HS	545
Snake River near Anatone, Washington (13334300)							
05-06-08	1600	560	49,800	20	60	HS	110
06-10-08	1145	597	73,200	10	60	HS	271
07-08-08	0920	550	40,900	10	60	HS	14.2
04-16-09	0915	570	46,600	20	60	HS	16
04-23-09	1230	590	83,000	10	60	HS	214
05-20-09	1330	630	105,000	20	60	HS	89.8
06-16-09	1750	600	72,100	20	60	HS	165
05-20-10	0916	580	62,500	8	60	HS	176
06-04-10	1425	617	105,000	20	60	HS	195
06-14-10	1518	622	93,700	20	60	HS	170
04-04-11	1519	570	68,000	20	60	HS	406
04-05-11	1310	570	79,900	20	60	HS	317
05-14-11	1555	589	102,000	14	60	HS	20.4
05-16-11	1335	608	142,000	14	60	HS	346
05-17-11	1550	608	125,000	13	60	HS	183
06-21-11	1248	590	110,000	15	60	HS	491
Selway River near Lowell, Idaho (13336500)							
04-22-09	1045	270	14,000	20	60	HS	17.5
05-18-09	1500	300	18,500	20	60	HS	234
05-19-09	1040	315	27,300	20	60	HS	463
05-21-09	1123	310	20,300	20	60	HS	75.2
06-09-09	1231	303	13,800	20	60	HS	72.1
05-19-10	1110	306	16,400	20	60	HS	24.9
06-04-10	1350	308	21,800	20	60	HS	440
06-15-10	1318	300	14,200	20	60	HS	29.4
05-17-11	1025	305	19,400	20	60	HS	151
05-24-11	1730	308	22,000	20	60	HS	92
06-10-11	0816	305	20,600	20	30	HS	86.1
Lochsa River near Lowell, Idaho (13337000)							
05-18-11	0815	276	12,600	20	60	HS	132
06-07-11	0905	275	21,200	20	60	HS	329
06-10-11	1036	280	14,800	20	60	HS	26.0

Table 8. Bedload data from sampling stations in the lower Snake and Clearwater River Basins, Washington and Idaho, water years 2008–11.—Continued

[Locations of stations are shown in figure 2. **Sampler type:** HS, Helley Smith. **Abbreviations:** ft, foot; ft^3/s, cubic foot per second; ton/d, ton per day]

Date	Mean sample time	Channel width (ft)	Streamflow, instantaneous (ft^3/s)	Number of sampling points	Rest time on bottom (seconds)	Sampler type	Bedload discharge (ton/d)
Middle Fork Clearwater River at Kooskia, Idaho (13337120)							
04-22-09	1500	465	25,600	20	60	HS	23.6
05-18-09	1523	455	34,000	20	60	HS	336
05-19-09	1530	490	46,000	14	60	HS	222
05-21-09	1653	460	35,000	20	60	HS	258
06-09-09	1600	460	24,000	20	60	HS	13.9
05-21-10	1607	457	22,700	20	60	HS	13.5
06-04-10	1500	495	44,100	20	60	HS	163
06-16-10	1011	455	23,400	20	60	HS	33.7
05-17-11	1600	470	37,000	20	60	HS	163
05-26-11	0830	500	46,700	20	60	HS	146
06-08-11	1044	508	57,000	20	60	HS	592
South Fork Clearwater River near Harpster, Idaho (13338100)							
04-08-09	1021	72	1,410	20	60	HS	0.6
04-14-09	1252	66	2,340	20	60	HS	10.3
04-22-09	0937	80	5,540	20	60	HS	16.7
05-07-09	0930	82	6,340	6	60	HS	79
05-13-09	1230	76	4,000	20	60	HS	5.8
05-21-09	1145	80	6,070	12	60	HS	103
06-10-09	1414	63	3,190	17	60	HS	19.2
04-22-10	1507	71	2,450	20	60	HS	11.4
05-19-10	1525	72	2,830	20	60	HS	10.8
05-20-10	1216	70	2,820	20	60	HS	12.3
06-06-10	0840	80	4,650	20	60	HS	21.4
06-14-10	1328	76	3,270	20	60	HS	18.2
05-10-11	1057	75	3,900	20	60	HS	12
06-11-11	1000	82	6,750	18	60	HS	29
06-28-11	0903	71	3,470	17	60	Elwha	12.9
South Fork Clearwater River at Stites, Idaho (13338500)							
04-14-09	1646	150	2,930	20	60	HS	4.4
04-22-09	1402	154	5,310	20	60	HS	30.6
05-07-09	1430	144	6,720	20	60	HS	190
05-13-09	1630	154	4,020	20	60	HS	32.6
05-21-09	1430	160	5,470	20	60	HS	155
06-10-09	0833	153	3,260	20	60	HS	18.8
04-22-10	1925	151	2,450	20	60	HS	10.2
05-19-10	1822	150	2,640	20	60	HS	10.1
05-20-10	0847	150	3,480	20	60	HS	18.4
06-05-10	1425	158	6,110	20	60	HS	208
06-15-10	1803	150	3,090	20	60	HS	31.2
05-10-11	1545	155	4,220	20	60	HS	12.8
06-10-11	1555	161	7,490	20	60	HS	603
06-28-11	1210	147	3,480	20	60	Elwha	31.2

Table 8. Bedload data from sampling stations in the lower Snake and Clearwater River Basins, Washington and Idaho, water years 2008–11.—Continued

[Locations of stations are shown in figure 2. **Sampler type:** HS, Helley Smith. **Abbreviations:** ft, foot; ft^3/s, cubic foot per second; ton/d, ton per day]

Date	Mean sample time	Channel width (ft)	Streamflow, instantaneous (ft^3/s)	Number of sampling points	Rest time on bottom (seconds)	Sampler type	Bedload discharge (ton/d)
Clearwater River at Orofino, Idaho (13340000)							
04-23-09	0953	360	38,500	20	60	HS	2.64
05-19-09	1612	375	57,700	20	60	HS	44.4
06-02-09	1809	372	46,000	20	60	HS	378
06-04-10	0948	375	49,900	20	60	HS	381
06-10-10	0917	373	45,800	20	60	HS	217
06-06-11	1428	380	49,300	20	60	HS	754
06-28-11	1518	365	37,400	20	60	Elwha	23.9
Clearwater River at Spalding, Idaho (13342500)							
05-05-08	1500	440	29,300	20	60	HS	11.9
05-19-08	1430	460	78,900	9	30	HS	841
05-28-08	1015	450	46,700	20	60	HS	149
06-11-08	1345	440	49,700	20	60	HS	155
07-07-08	1345	440	28,000	20	60	HS	6.0
04-15-09	1145	440	37,700	20	60	HS	15.2
04-23-09	1545	450	56,300	20	60	HS	43.3
05-19-09	0955	450	60,600	20	60	HS	12
06-03-09	0949	450	51,100	20	60	HS	383
05-20-10	1532	444	46,200	20	60	HS	126
06-15-11	1015	432	54,500	10	30	Elwha	21
Palouse River at Hooper, Washington (13351000)							
03-24-09	1133	142	4,240	20	60	HS	36.8
01-17-11	1121	145	5,670	20	60	HS	5.1
01-18-11	1035	148	7,150	20	60	HS	2.5

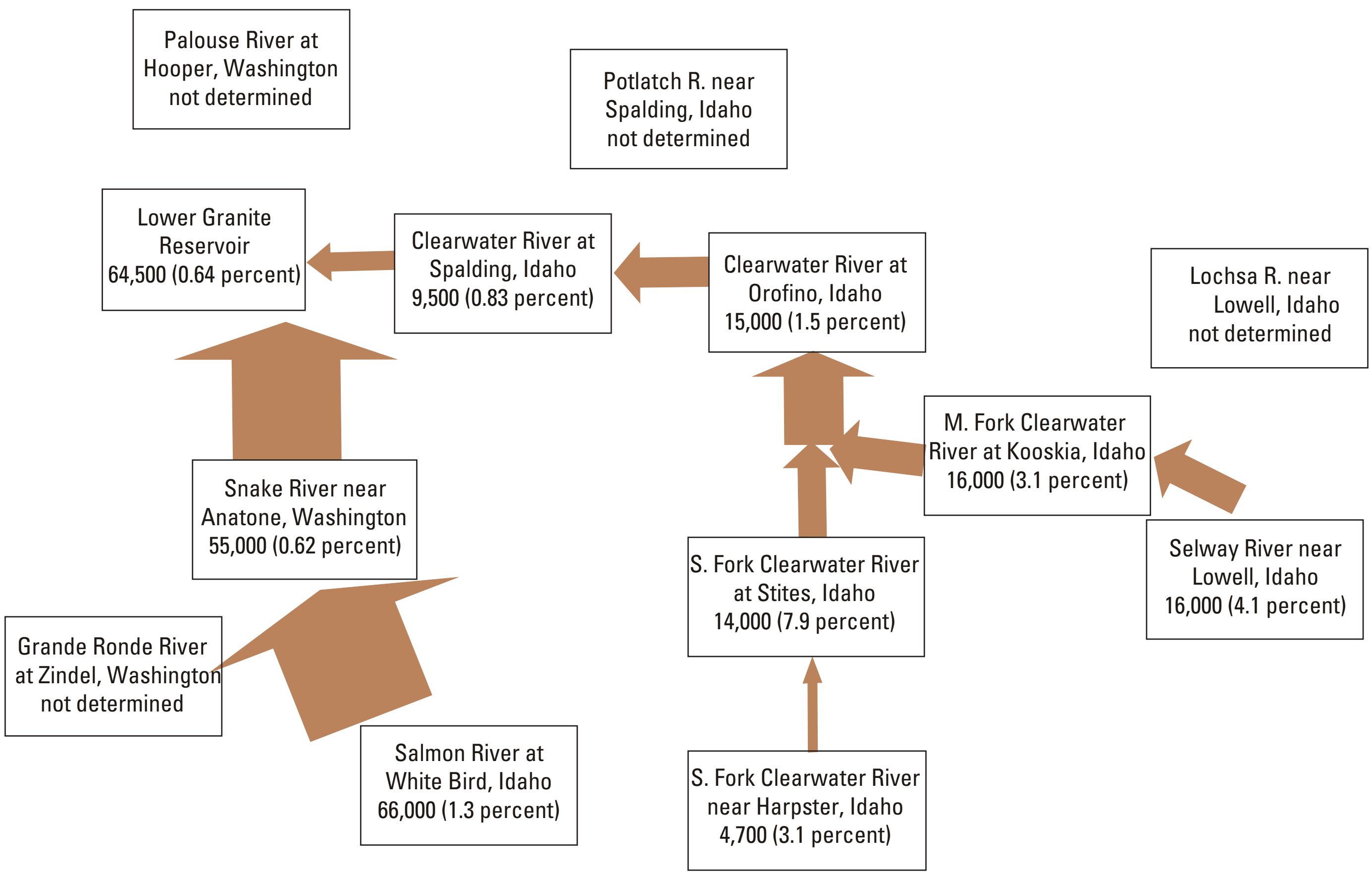

Figure 19. Estimated bedload transported in the lower Snake and Clearwater River Basins, Washington and Idaho, water years 2009–11. Values are in tons and percentage of total sediment load (suspended and bedload) transported during water years 2009–11. Width of each arrow is proportional to the estimated bedload.

Table 9. Best-fit regression equations for bedload from sampling stations in the lower Snake and Clearwater River Basins, Washington and Idaho, water years 2008–11.

[Locations of stations are shown in figure 2. Only stations with at least five samples are shown. $\mathbf{R^2}$: coefficient of determination. **Abbreviations:** USGS, U.S. Geological Survey; *BS*, bedload discharge, in tons per day; *Q*, streamflow, in cubic feet per second]

USGS gaging station No.	Gaging station name	Best-fit regression equation	R^2
13317000	Salmon River at White Bird, Idaho	$\log BS = 5.033\times10^{-17}Q^{3.992}$	0.46
13334300	Snake River near Anatone, Washington	$\log BS = 1.842\times10^{-06}Q^{1.603}$	0.26
13336500	Selway River near Lowell, Idaho	$\log BS = 1.732\times10^{-15}Q^{3.919}$	0.61
13337120	Middle Fork Clearwater River at Kooskia, Idaho	$\log BS = 8.220\times10^{-10}Q^{2.644}$	0.30
13338100	South Fork Clearwater River near Harpster, Idaho	$\log BS = 2.639\times10^{-15}Q^{3.652}$	0.77
13338500	South Fork Clearwater River at Stites, Idaho	$\log BS = 1.081\times10^{-11}Q^{3.470}$	0.79
13340000	Clearwater River at Orofino, Idaho	$\log BS = 7.707\times10^{-33}Q^{7.312}$	0.30
13342500	Clearwater River at Spalding, Idaho	$\log BS = 6.767\times10^{-15}Q^{3.403}$	0.42

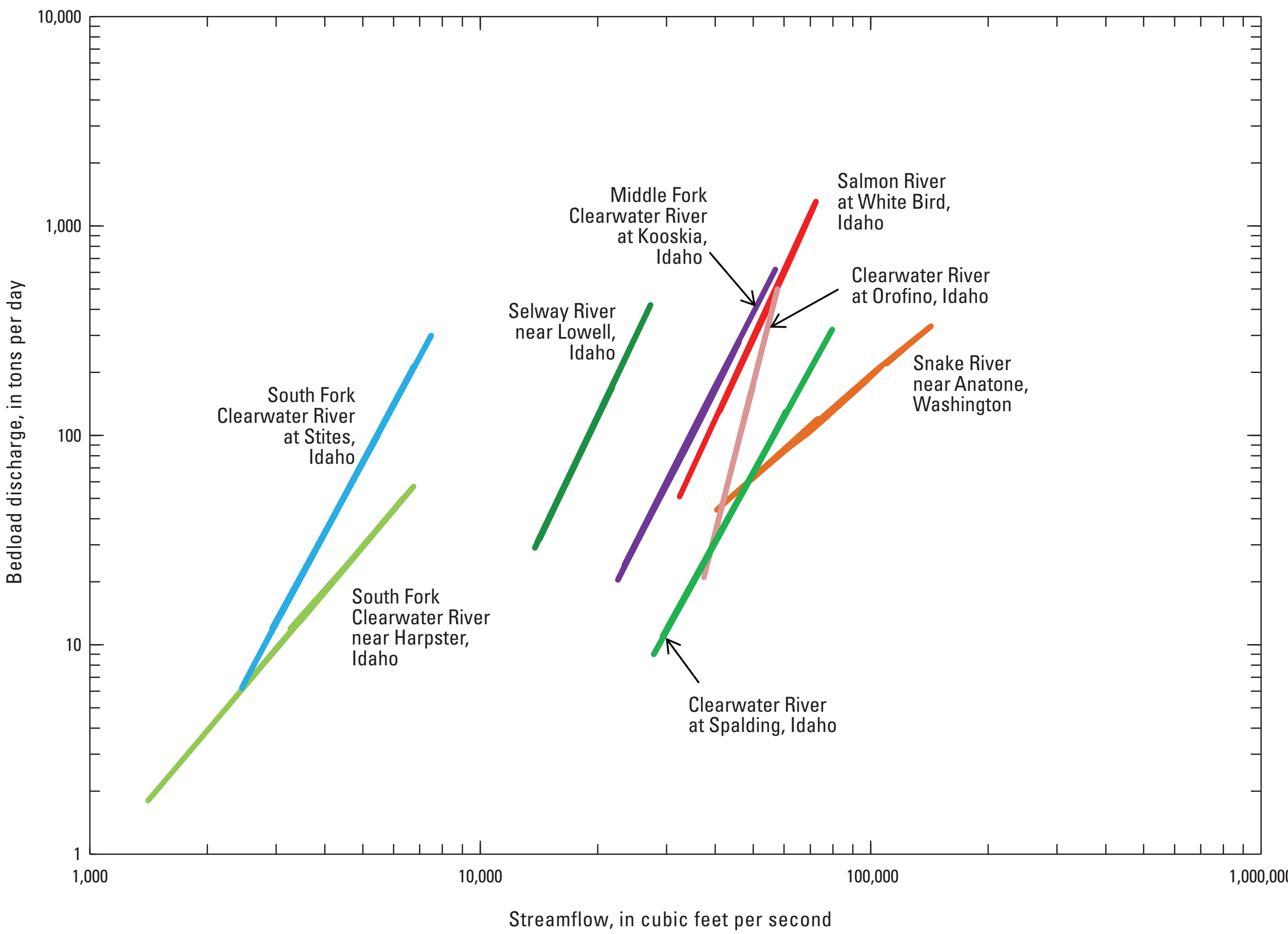

Figure 20. Bedload transport curves representing best-fit regression equations for selected stations in the lower Snake and Clearwater River Basins, Washington and Idaho.

Table 10. Particle-size distribution for bedload samples collected from stations in the lower Snake and Clearwater River Basins, Washington and Idaho, water years 2008–11.

[Locations of stations are shown in figure 2. **Abbreviations:** <, less than; mm, millimeter]

Date	Mean sample time	< 128 mm (percent)	< 63.0 mm (percent)	< 31.5 mm (percent)	< 16.0 mm (percent)	< 8.0 mm (percent)	< 4.0 mm (percent)	< 2.0 mm (percent)	< 1.0 mm (percent)	< 0.50 mm (percent)	< 0.25 mm (percent)	< 0.125 mm (percent)	< 0.063 mm (percent)
Salmon River at White Bird, Idaho (13317000)													
04-24-09	1030	100	100	100	100	100	100	99	94	23	1	0	0
05-20-09	1332	100	96	84	67	61	57	55	52	18	2	0	0
06-03-09	1535	100	100	83	74	69	66	65	61	12	3	0	0
06-11-09	0821	100	100	100	100	100	99	98	94	7	0	0	0
05-15-11	1245	100	100	100	100	100	100	99	97	55	5	1	0
Snake River near Anatone, Washington (13334300)													
05-06-08	1600	100	100	66	54	53	53	52	50	36	1	0	0
06-10-08	1145	100	100	88	83	69	64	63	60	45	1	0	0
07-08-08	0920	100	100	100	100	100	100	99	96	73	4	0	0
04-16-09	0915	100	100	100	98	90	82	75	63	3	0	0	0
04-23-09	1230	100	81	32	28	27	26	24	21	2	0	0	0
05-20-09	1330	100	100	100	100	100	99	96	88	46	6	1	0
06-16-09	1750	100	100	90	71	56	46	40	32	6	0	0	0
05-20-10	0916	100	100	78	71	67	63	59	54	4	0	0	0
06-04-10	1425	100	100	82	74	63	59	57	52	26	3	0	0
06-14-10	1518	100	82	82	76	71	67	63	58	4	0	0	0
04-04-11	1519	100	69	34	15	10	9	8	7	1	0	0	0
04-05-11	1310	100	60	29	11	4	3	3	2	0	0	0	0
05-14-11	1555	100	100	17	17	14	13	13	12	10	1	0	0
05-16-11	1335	100	100	89	60	35	22	17	13	6	0	0	0
05-17-11	1550	100	77	34	29	19	12	8	6	0	0	0	0
06-21-11	1248	100	90	29	9	5	2	0	0	0	0	0	0
Selway River near Lowell, Idaho (13336500)													
04-22-09	1045	100	100	100	90	88	87	85	70	3	0	0	0
05-18-09	1500	100	100	100	98	98	97	96	68	3	0	0	0
05-19-09	1040	100	86	71	63	61	59	57	38	4	0	0	0
05-21-09	1123	100	83	66	48	38	34	33	26	1	0	0	0
06-09-09	1231	100	100	100	99	92	85	76	35	0	0	0	0
05-19-10	1110	100	100	100	100	100	100	98	82	7	0	0	0
06-04-10	1350	100	91	83	81	80	78	75	48	2	0	0	0
06-15-10	1318	100	100	92	89	88	86	84	53	1	0	0	0
05-17-11	1025	100	100	100	94	89	85	80	50	14	1	0	0
05-24-11	1730	100	100	86	82	80	78	75	49	14	0	0	0
06-10-11	0816	100	100	56	51	50	49	46	29	1	0	0	0
Lochsa River near Lowell, Idaho (13337000)													
05-18-11	0815	100	82	66	56	45	38	33	20	6	1	0	0
06-07-11	0905	100	82	81	79	76	74	70	45	4	0	0	0
06-10-11	1036	100	100	82	54	43	38	33	20	6	0	0	0
Middle Fork Clearwater River at Kooskia, Idaho (13337120)													
04-22-09	1500	100	100	100	100	100	99	97	79	3	0	0	0
05-18-09	1523	100	73	25	16	15	14	14	11	1	0	0	0
05-19-09	1530	100	100	57	49	48	47	45	37	15	1	0	0
05-21-09	1653	100	100	99	95	91	87	84	65	3	0	0	0
06-09-09	1600	100	100	100	100	97	92	86	59	2	0	0	0
05-21-10	1607	100	100	100	100	97	91	88	68	4	0	0	0
06-04-10	1500	100	100	99	97	95	93	90	74	10	0	0	0
06-16-10	1011	100	100	100	99	95	90	86	59	1	0	0	0
05-17-11	1600	100	72	55	44	40	37	36	33	13	1	0	0
05-26-11	0830	100	100	82	78	71	66	63	58	28	2	0	0
06-08-11	1044	100	73	65	63	61	57	54	46	5	0	0	0

Table 10. Particle-size distribution for bedload samples collected from stations in the lower Snake and Clearwater River Basins, Washington and Idaho, water years 2008–11.—Continued

[Locations of stations are shown in figure 2. **Abbreviations:** <, less than; mm, millimeter]

Date	Mean sample time	< 128 mm (percent)	< 63.0 mm (percent)	< 31.5 mm (percent)	< 16.0 mm (percent)	< 8.0 mm (percent)	< 4.0 mm (percent)	< 2.0 mm (percent)	< 1.0 mm (percent)	< 0.50 mm (percent)	< 0.25 mm (percent)	< 0.125 mm (percent)	< 0.063 mm (percent)
South Fork Clearwater River near Harpster, Idaho (13338100)													
04-08-09	1021	100	100	100	100	100	99	95	83	34	5	0	0
04-14-09	1252	100	100	100	96	92	89	85	62	2	0	0	0
04-22-09	0937	100	100	80	78	75	70	66	44	2	0	0	0
05-07-09	0930	100	100	100	96	93	89	83	58	6	1	0	0
05-13-09	1230	100	100	100	98	87	81	76	57	13	1	0	0
05-21-09	1145	100	100	98	95	89	83	72	43	1	0	0	0
06-10-09	1414	100	100	86	82	80	75	68	39	1	0	0	0
04-22-10	1507	100	100	100	100	100	98	96	71	2	0	0	0
05-19-10	1525	100	100	100	100	99	96	89	50	2	0	0	0
05-20-10	1216	100	100	100	96	91	87	82	53	2	0	0	0
06-06-10	0840	100	100	100	99	95	87	73	37	1	0	0	0
06-14-10	1328	100	100	100	94	87	78	69	42	1	0	0	0
05-10-11	1057	100	100	100	100	100	99	96	81	53	10	0	0
06-11-11	1000	100	100	93	88	84	80	73	51	2	0	0	0
06-28-11	0903	100	100	100	100	98	94	85	49	1	0	0	0
South Fork Clearwater River at Stites, Idaho (13338500)													
04-14-09	1646	100	100	90	90	90	90	86	64	6	1	0	0
04-22-09	1402	100	100	81	71	70	68	66	53	5	0	0	0
05-07-09	1430	100	97	71	56	45	36	33	22	1	0	0	0
05-13-09	1630	100	100	100	90	79	71	65	45	1	0	0	0
05-21-09	1430	100	100	94	80	70	61	53	35	1	0	0	0
06-10-09	0833	100	100	90	70	53	40	31	17	1	0	0	0
04-22-10	1925	100	100	100	64	56	52	48	34	1	0	0	0
05-19-10	1822	100	100	100	86	75	68	63	45	2	0	0	0
05-20-10	0847	100	100	83	79	78	76	72	57	3	0	0	0
06-05-10	1425	100	91	74	60	52	45	40	29	1	0	0	0
06-15-10	1803	100	94	94	83	69	61	53	31	1	0	0	0
05-10-11	1545	100	100	100	92	87	84	82	72	40	4	0	0
06-10-11	1555	100	74	52	39	31	24	19	13	5	0	0	0
06-28-11	1210	100	100	77	58	52	46	39	19	0	0	0	0
Clearwater River at Orofino, Idaho (13340000)													
04-23-09	0953	100	100	100	86	78	74	72	62	5	1	0	0
05-19-09	1612	100	100	21	12	11	11	11	10	1	0	0	0
06-02-09	1809	100	94	49	23	12	10	10	9	0	0	0	0
06-04-10	0948	100	86	51	40	34	31	29	25	2	0	0	0
06-10-10	0917	100	91	52	37	31	25	22	18	0	0	0	0
06-06-11	1428	100	66	36	25	18	12	10	9	1	0	0	0
06-28-11	1518	100	100	77	74	70	65	61	57	2	0	0	0
Clearwater River at Spalding, Idaho (13342500)													
05-05-08	1500	100	100	100	100	99	99	98	98	74	3	1	1
05-19-08	1430	100	38	33	33	33	33	33	32	26	3	0	0
05-28-08	1015	100	100	97	95	95	94	93	91	51	1	0	0
06-11-08	1345	100	100	49	31	29	28	28	27	18	0	0	0
07-07-08	1345	100	100	100	100	100	100	99	96	76	2	0	0
04-15-09	1145	100	100	100	88	87	86	85	82	1	0	0	0
04-23-09	1545	100	100	67	43	41	41	40	37	17	2	0	0
05-19-09	0955	100	100	100	86	85	85	83	76	15	2	0	0
06-03-09	0949	100	47	14	6	5	5	5	5	0	0	0	0
05-20-10	1532	100	49	29	27	27	26	26	25	2	0	0	0
06-15-11	1015	100	100	100	100	100	100	100	99	78	7	0	0

The measured bedload discharge in the Snake River near Anatone ranged from 14.2 to 491 ton/d based on 16 samples collected during 2008–11 (table 8). Based on a composite sample of all bedload sediment collected at Anatone, and using the GRADISTAT statistical software (Blott and Pye, 2001), the particle-size distribution was bimodal, with coarse gravel (16–31.5 mm) accounting for 25.7 percent of the bedload material and medium sand (0.25–0.50 mm) making up 22.0 percent (table 10). Notably absent in the bedload collected from the Snake River near Anatone was small gravel. Applying the best-fit relation between streamflow and bedload discharge (table 9) to determine the transport in the Snake River for water years 2009–11 indicates about 55,000 tons of bedload, or about 0.62 percent of the total amount of sediment discharged from the Snake River to Lower Granite Reservoir (fig. 19).

In the Clearwater River Basin, bedload samples were collected from the Lochsa and Selway Rivers 3 and 11 times, respectively. At both stations, the particle-size distribution was bimodal, with medium sand and course gravel being the two dominant sizes (table 10). A comparison of the bedload data collected during this study from the Lochsa and Selway Rivers with data collected during 1994–97 by the U.S. Forest Service at the same sampling locations (King and others, 2004) is shown in figure 21.

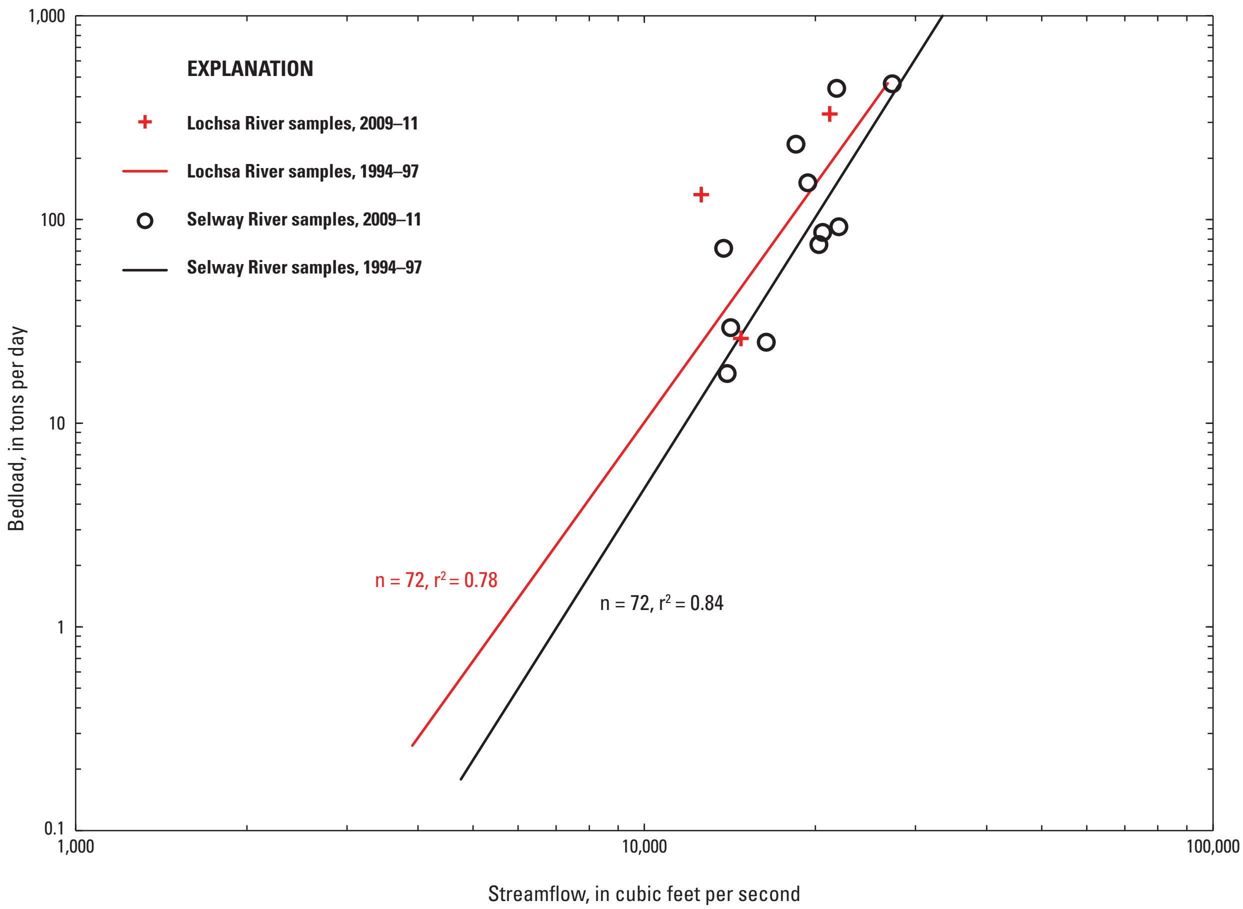

Figure 21. Bedload transport curves based on samples collected from the Lochsa and Selway Rivers near Lowell, Idaho, during water years 2009–11, and during 1994–97 by King and others (2004).

Although the range in streamflow at which bedload samples were collected was larger during the 1994–97 study, at streamflows of similar magnitude, the bedload data collected during 2009–11 corresponded well with the 1994–97 data. King and others (2004) determined that bedload discharge constituted less than 4 percent of the total sediment discharged from the Lochsa and Selway Rivers. Bedload was not estimated for the Lochsa River during 2009–11 because of the paucity of samples collected during this study. However, using the best-fit regression for the data collected from the Selway River during 2009–11, bedload constituted about 4 percent of the total sediment discharge from the Selway River (fig. 19).

Bedload samples were collected at the South Fork Clearwater River near Harpster, and South Fork Clearwater River at Stites 15 and 14 times, respectively during 2009–11 (table 10). Streamflows at Harpster ranged from 1,410 to 6,750 ft^3/s, and bedload discharge ranged from 0.6 to 103 ton/d. At the Stites station, instantaneous streamflows ranged from 2,450 to 7,490 ft^3/s and bedload ranged from 4.4 to more than 600 ton/d (table 8). Based on these data, it is apparent that although the South Fork Clearwater River at Stites is only 15 mi downstream of the Harpster station, at high streamflow the bedload transported at Stites is about one order of magnitude larger than at Harpster (fig. 20). The particle-size distribution of the bedload at both South Fork Clearwater River stations was bimodal, with the dominant size classes being medium-sized sand and medium-sized gravel. Using the equations from table 9, the bedload at Harpster constituted about 3.1 percent of the total sediment discharge during water years 2009–11, whereas at Stites the bedload constituted about 7.9 percent (figure 19).

Bedload samples were collected in the middle and lower sections of the Clearwater River at the Middle Fork Clearwater River at Kooskia, Clearwater River at Orofino, and Clearwater River at Spalding stations. Bedload discharge and bedload as a percentage of the total sediment load decreased from upstream to downstream through this reach of the Clearwater River (fig. 19) in response to a decrease in the stream gradient. The Middle Fork Clearwater River at Kooskia was sampled 11 times during 2009–11 at streamflows ranging from 22,700 to 57,000 ft^3/s (table 8). Bedload at Kooskia ranged from 13.5 to 592 ton/d, with an estimated bedload transport of 16,000 tons during water years 2009–11, approximately equivalent to the bedload discharge from the Selway River (fig. 19). The composited particle size distribution at Kooskia was bimodal, with medium sand (45 percent) and coarse gravel (12 percent) being the two dominant sizes. Bedload at the Kooskia station constituted about 3.1 percent of the total sediment load discharged from the Middle Fork Clearwater River as measured at Kooskia (fig. 19).

Bedload samples were collected seven times during 2009–11 at Clearwater River at Orofino at streamflows ranging from 37,400 to 57,700 ft^3/s. Bedload at Orofino ranged from 2.64 to 754 tons/d (table 8). The total calculated transport at Orofino was about 15,000 tons during water years 2009–11, about one-half of the combined bedload discharged from the South Fork and Middle Fork Clearwater Rivers (fig. 19). Downstream of Orofino at the Clearwater River at Spalding station, the total bedload during water years 2009–11 was about 9,500 tons, less than 1 percent of the total sediment transport at the station during that period. The reach of the Clearwater River from Orofino to Spalding probably transports less sediment (both suspended load and bedload) than it did historically because of the construction of Dworshak Reservoir, which essentially negates sediment delivery to the main stem Clearwater River from the North Fork Clearwater River. The total bedload for 2009–11 in the Clearwater River at Spalding was about 9,500 tons, about 15 percent of the total bedload discharged to Lower Granite Reservoir from the combined Clearwater and Snake Rivers. Overall, bedload accounted for only about 0.64 percent of the total sediment load entering Lower Granite Reservoir during water years 2009–11 (fig. 19).

Bedload data collected from the Snake River near Anatone and the Clearwater River at Spalding during 1972–79 (Jones and Seitz, 1980) indicated that historically, bedload was larger and comprised a larger part of the overall sediment load. Based on 63 samples collected during 1972–79 from the Snake River near Anatone at streamflows ranging from 27,500 to 161,000 ft^3/s, the mean bedload was about 450 ton/d and ranged from less than 1.0 to about 5,600 ton/d. In comparison, the mean bedload based on 16 samples collected at Anatone during this study was about 130 ton/d and ranged from 14.2 to 491 ton/d (table 8). Although the magnitude of streamflows sampled during both study periods were similar, the mean bedload was about 3.5 times higher during 1972–79. Jones and Seitz (1980) reported that bedload comprised about 4 percent of the overall sediment load transported in the Snake River during 1972–79, whereas results from this study indicate that bedload comprised less than 1 percent of the sediment load. Although the relation between streamflow and bedload was relatively poor for the 1972–79 ($R^2=0.44$) and 2008–11 data ($R^2=0.26$), there is an apparent shift in the bedload transport curve, indicating less bedload in the Snake River near Anatone during 2008–11 (fig. 22). The reason for this apparent shift is difficult to determine given the increase in the transport of suspended sand during 2008–11. Additional bedload data collected during 2008-11 from the Snake River near Anatone would be helpful to verify the apparent decrease in bedload in the Snake River.

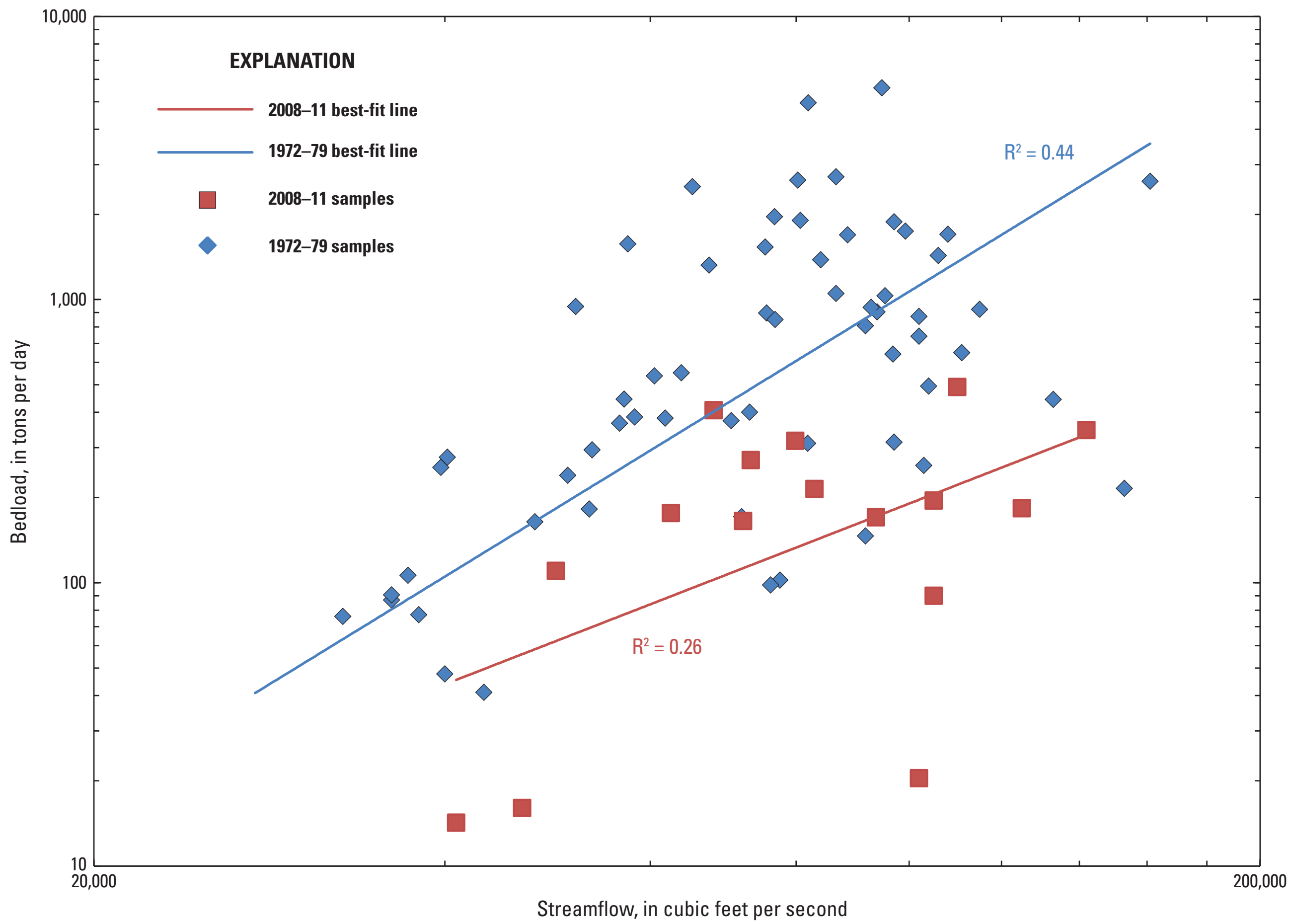

Figure 22. Bedload transport curves comparing data collected at Snake River near Anatone, Washington, during water years 1972–79 and 2008–11.

Similarly, a comparison of data from 1972–79 and 2008–11 indicated a decrease in bedload in the Clearwater River at Spalding (fig. 23). The mean bedload during 1972–79 based on 78 samples collected at the Spalding station was about 120 ton/d, ranging from less than 1.0 to about 3,700 ton/d. The mean bedload based on 11 samples collected during 2008–11 was about 54 ton/d, ranging from about 6.0 to 840 ton/d (table 8). Based on this comparison, bedload in the Clearwater River during 1972–79 was markedly larger (mean of about 2.2 times) at roughly equivalent stream discharge. Jones and Seitz (1980) reported that, similar to the Snake River, during 1972–79 bedload comprised about 4 percent of the total sediment load in the Clearwater River. The 2008–11 data indicate that bedload was less than 1 percent of the sediment load in the Clearwater River at Spalding. The relation between streamflow and bedload was better (higher R^2) for the Clearwater River than the Snake River for both sampling periods (figs. 22 and 23).

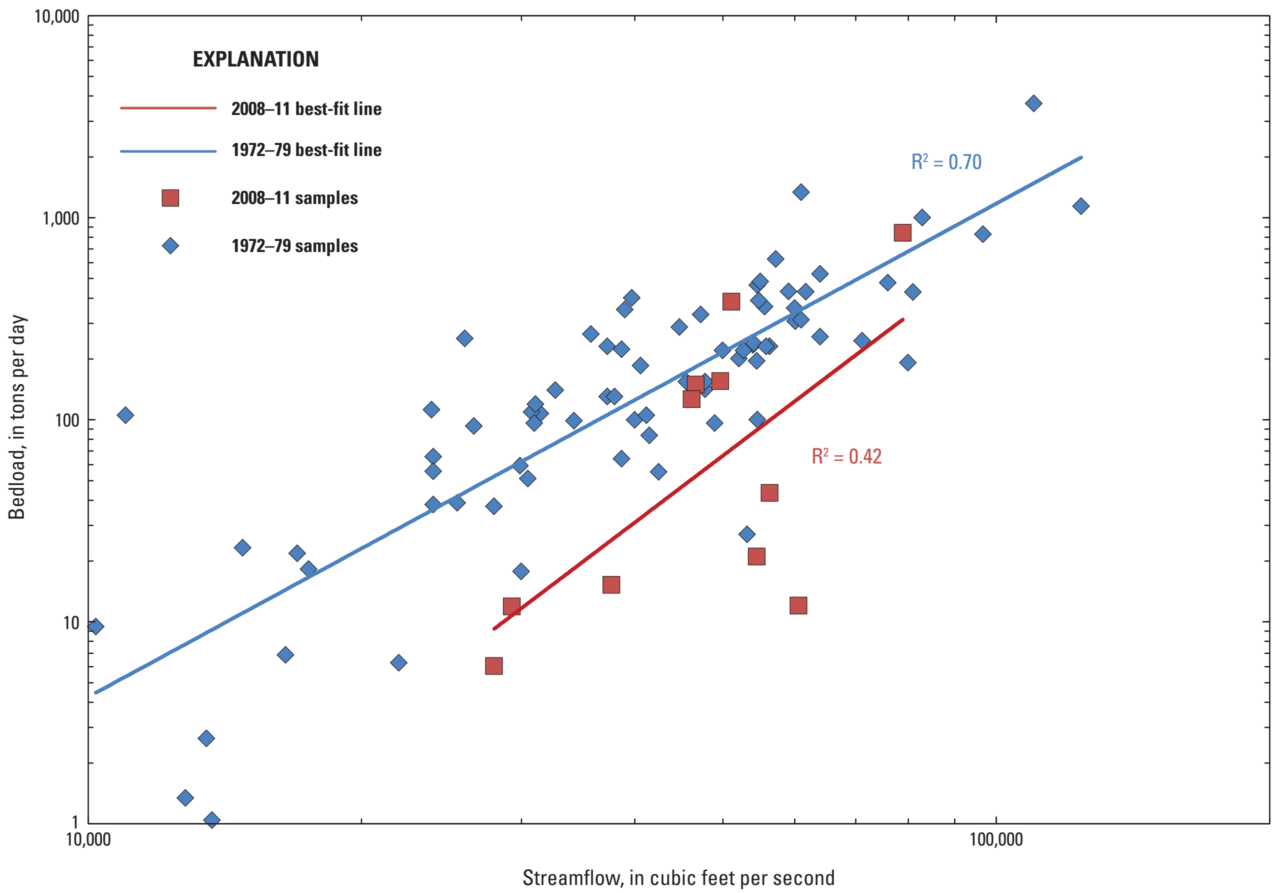

Figure 23. Bedload transport curves comparing data collected at Clearwater River at Spalding, Idaho, water years 1972–79 and 2008–11.

Summary

Since Lower Granite Dam was completed in 1975, about 75 million cubic yards of sediment have accumulated in Lower Granite Reservoir, an average annual accumulation of about 2.3 million cubic yards through 2008. In 2008, the U.S. Geological Survey (USGS), in cooperation with the U.S. Army Corps of Engineers (USACE), conducted sediment sampling in the Snake River near Anatone, Washington, and the Clearwater River at Spalding, Idaho, to quantify sediment loading to Lower Granite Reservoir and to evaluate sediment depositional characteristics in the reservoir. In 2009, sediment sampling was extended to 10 additional sampling stations in the lower Snake and Clearwater River basins to help identify the subbasins contributing most of the sediment being delivered to Lower Granite Reservoir.

Of the stations sampled during 2009–11, the largest measured total suspended sediment (TSS) concentrations were in samples collected from the Potlatch (3,300 mg/L) and Palouse (1,400 mg/L) Rivers during a rain-on-snow event that occurred in January 2011. The largest median concentration of TSS (100 mg/L) and the largest suspended sediment fraction as fine-grained silt and clay (median of 95 percent) were in samples collected from the Palouse River. Other rivers with a large percentage of fine-grained suspended sediment were the Potlatch (median of 92 percent) and the Grand Ronde (median of 84 percent) Rivers. The Palouse, Potlatch, and Grande Ronde Rivers all drain basins with relatively large proportions of agricultural activity. The Selway and Lochsa Rivers, the Middle Fork Clearwater River at Kooskia, and the Clearwater River at Orofino generally had small concentrations of TSS with medians of 11, 11, 15, and 13 mg/L, respectively.

During water years 2009–11, Lower Granite Reservoir received about 10 million tons of suspended sediment from the combined loads of the Snake and Clearwater Rivers. About 60 percent of sediment entering the reservoir during 2009–11 occurred during water year 2011, which was characterized by a large winter snowpack followed by sustained spring runoff and high suspended-sediment transport during most of the summer. Of the sediment load entering the reservoir, the Snake River accounted for about 89 percent of the TSS, about 90 percent of the suspended sand, and about 87 percent of the suspended fines. The Salmon River contributed about 51 percent of the TSS, about 56 percent of the suspended sand, and about 44 percent of the suspended fines transported to Lower Granite Reservoir.

A comparison of historical sediment data collected from the Snake River with data collected during this study indicated that concentrations of TSS and suspended sand were significantly larger during 2008–11 compared to 1972–79, whereas the concentrations of suspended fines were not. In the Snake River, the sand fraction increased from an average of 28 percent of the TSS load during 1972–79 to an average of 48 percent during 2009–11. The increase in the suspended-sand load in the Snake River is probably attributable to numerous severe forest fires that burned large areas of central Idaho from 1980–2010. Additional fluvial-sediment monitoring in the Salmon River Basin would be helpful to identify source areas and to quantify the magnitude of sediment delivery to discrete reaches of the Salmon River, the lower Snake River, and Lower Granite Reservoir.

In the Clearwater River, data collected during this study indicated that the TSS and suspended fines concentrations during 1972–79 were not significantly different from the concentrations during 2008–11. However, the concentrations of suspended sand in the Clearwater River were significantly larger during 2008–11. The increase in the sand load in the Clearwater River may also be attributable to forest fire activity in areas of the basin with highly erodible soils.

Suspended-sediment surrogate models developed using acoustic Doppler velocity meters (ADVMs) effectively estimated suspended-sediment concentrations (SSCs) and loads for most streamflow conditions in the lower Snake and Clearwater Rivers. At both stations (lower Snake River near Anatone and Clearwater River at Spalding) instrumented with ADVMs, surrogate models developed using acoustic backscatter had a better correlation than LOADEST models for SSC and suspended fines. Surrogate models also had a better correlation for suspended sands at the Spalding station on the lower Clearwater River. Over short (monthly and storm event) and long (annual) time scales when sediment concentrations and loads are highly variable, acoustic backscatter appears to provide better estimates of sediment concentration and load than do traditional sediment transport curves based solely on streamflow. Because acoustic backscatter is not affected by hysteresis, it provides a direct, in-situ measurement of suspended sediment, and is effective in representing sediment sources from a combination of regulated and unregulated sources. On a monthly and (or) annual basis, the acoustic surrogate and LOADEST models appear to produce similar sediment load estimates for the Clearwater River at Spalding. However, estimates of SSCs and loads in the Snake River differed substantially between the acoustic surrogate and LOADEST models. The largest difference occurred in water year 2011, when the suspended-sediment load calculated using the LOADEST model was more than three times higher than the suspended-sediment load calculated using the acoustic surrogate model. The largest discrepancies between the LOADEST and acoustic surrogate models occur primarily during high streamflow, when the SSC and the suspended sand fraction are large. This discrepancy may be a result of acoustic surrogate tools being unable to capture the contribution of suspended sand moving near the bottom of the water column.

Bedload accounted for less than 1 percent of the total sediment load entering Lower Granite Reservoir from the Snake and Clearwater Rivers. The estimated bedload in the Salmon River at White Bird during 2009–11 was about 66,000 tons, the largest amount of the stations sampled. The lower Snake River basin, which includes the Salmon River, had the second largest measured bedload with a total of 55,000 tons during 2009–11, about 0.62 percent of the total sediment load entering Lower Granite Reservoir from the Snake River. The estimated bedload in the Clearwater River at Spalding was only about 9,500 tons, roughly 0.83 percent of the total sediment load transported to Lower Granite Reservoir from the Clearwater River.

Acknowledgments

The USGS wishes to thank the U.S. Army Corps of Engineers, Walla Walla District for providing funding for this project. Special thanks go to USGS field personnel from the Idaho Water Science Center Boise and Post Falls Field Offices who were responsible for most of the data collection.

References Cited

Aikaike, Hirotugu, 1981, Likelihood of a model and information criteria: Journal of Econometrics, v. 16, no. 1, p. 3–14.

Blott, S.J., and Pye, Kenneth, 2001, GRADISTAT—A grain size distribution and statistics package for the analysis of unconsolidated sediments: Earth Surface Processes and Landforms, v. 26, p. 1237–1248.

Bradu, Dan, and Mundlak, Yair, 1970, Estimation in lognormal linear models: Journal of the American Statistical Association, v. 65, no. 329, p. 198–211.

Braun, C.L., Wilson, J.T., Van Metre, P.C., Weakland, R.J., Fosness, R.L., and Williams, M.L, 2012, Grain-size distribution and selected major and trace element concentrations in bed-sediment cores from Lower Granite Reservoir and Snake and Clearwater Rivers, eastern Washington and northern Idaho, 2010: U.S. Geological Survey Scientific Investigations Report 2012-5219, 81 p.

Burton, T.A., 2005, Fish and stream habitat risks from uncharacteristic wildfire—Observations from 17 years of fire-related disturbances on the Boise National Forest, Idaho: Forest Ecology and Management, v. 211, p. 140–149.

Chanson, Hubert, Takeuchi, Maiko, and Trevethan, Mark, 2008, Using turbidity and acoustic backscatter intensity as surrogate measures of suspended sediment concentration in a small subtropical estuary: Journal of Environmental Management, v. 88, p. 1406–1416.

Cohn, T.A., Caulder, D.L., Gilroy, E.J., Zynjuk, L.D., and Summers, R.M., 1992, The validity of a simple statistical model for estimating fluvial constituent loads—An empirical study involving nutrient loads entering Chesapeake Bay: Water Resources Research, v. 28, no. 9, p. 2353–2363.

Cohn, T.A., Delong, L.L, Gilroy, E.J., Hirsch, R.M., and Wells, D.K., 1989, Estimating constituent loads: Water Resources Research, v. 25, no. 5, p. 937–942.

Crawford, C.G., 1991, Estimation of suspended-sediment rating curves and mean suspended-sediment loads: Journal of Hydrology, v. 129, p. 331–348.

Davis, B.E., 2005, A guide to the proper selection and use of federally approved sediment and water-quality samplers: U.S. Geological Survey Open-File Report 2005-1087, 20 p. (Also available at http://pubs.er.usgs.gov/publication/ofr20051087.)

Duan, N.,1983, Smearing estimate: A nonparametric retransformation method: Journal of the American Statistical Association, v.78, no. 383, p. 605–610.

Ebbert, J.C., and Roe, R.D., 1998, Soil erosion in the Palouse River Basin—Indications of improvement: U.S. Geological Survey Fact Sheet 069-98. (Also available at http://wa.water.usgs.gov/pubs/fs/fs069-98/.)

Edwards, T.K., and Glysson, G.D., 1999, Field methods for measurement of fluvial sediment: U.S. Geological Survey Techniques of Water-Resources Investigations, book 3, chap. C2, 89 p. (Also available at http://pubs.usgs.gov/twri/twri3-c2/.)

Elci, S., Aydln, R., and Work, P.A., 2009, Estimation of suspended sediment concentration in rivers using acoustic methods: Environmental Monitoring and Assessment, v 59, p. 255–265.

Emmett, W.W., 1976, Bedload transport in two large, gravel-bed rivers, Idaho and Washington: Proceedings, Third Federal Inter-Agency Sedimentation Conference, Denver, Colo., p. 4-101–4-114.

Folk, R.L., and Ward, W.C., 1957, Brazos River bar—A study in the significance of grain size parameters: Journal of Sedimentary Petrology, v. 27, p. 3–26.

Gartner, J.W., 2004, Estimating suspended solids concentrations from backscatter intensity measured by acoustic Doppler current profiler in San Francisco Bay, California: Marine Geology, v. 211, p. 169–187.

Gartner, J.W., and Gray, J.R., 2005, Summary of suspended-sediment technologies considered at the Interagency Workshop on Turbidity and Other Sediment Surrogates, in Gray, J.R., ed., Proceedings of the Federal Interagency Sediment Monitoring Instrument and Analysis Research Workshop, September 9–11, 2003, Flagstaff, Arizona: U.S. Geological Survey Circular 1276, 9 p. (Also available at http://pubs.er.usgs.gov/publication/cir1276.)

Gilroy, E.J., Hirsch, R.M., and Cohn, T.A., 1990, Mean square error of regression-based constituent transport estimates: Water Resources Research, v. 26, p. 2069–2088.

Goolsby, D.A., Battaglin, W.A., Lawrence, G.B., Artz, R.S., Aulenbach, B.T., Hooper, R.P., Keeney, D.R., and Stensland, G.J., 1999, Flux and sources of nutrients in the Mississippi-Atchafalaya River Basin—Topic 3 Report for the Integrated Assessment on Hypoxia in the Gulf of Mexico: Silver Spring, Md., National Oceanic and Atmospheric Administration Coastal Ocean Program Decision Analysis Series No. 17, 130 p.

Guy, H.P., 1969, Laboratory theory and methods for sediment analysis: U.S. Geological Survey Techniques of Water-Resources Investigations, book 5, chap. C1, 58 p. (Also available at http://pubs.usgs.gov/twri/twri5c1/.)

Helley, E.J., and Smith, Winchell, 1971, Development and calibration of a pressure-difference bedload sampler: U.S. Geological Survey Open-File Report, 18 p.

Helsel, D.R., and Hirsch, R.M., 1992, Statistical methods in water resources: New York, Elsevier, 522 p.

Hubbell, D.W., 1964, Apparatus and techniques for measuring bedload: U.S. Geological Survey Water-Supply Paper 1748, 74 p. (Also available online at http://pubs.er.usgs.gov/publication/wsp1748.)

Jones, M.L., and Seitz, H.R., 1980, Sediment transport in the Snake and Clearwater Rivers in the vicinity of Lewiston, Idaho: U.S. Geological Survey Open-File Report 80-690, 179 p.

Judge, C.G., Griffiths, W.E., Hill, R.C., Lutkepohl, H., and Lee, T.C., 1985, The theory and practice of econometrics: New York, John Wiley and Sons, p. 870–873.

King, J.G., Emmett, W.W., Whiting, P.J., Kenworthy, R.P., and Barry, J.J., 2004, Sediment transport data and related information for selected coarse-bed streams and rivers in Idaho: Fort Collins, Colo., U.S. Department of Agriculture, Forest Service, Rocky Mountain Research Station, Gen. Tech. Rep. RMRS-GTR-131, 26 p.

Latah Soil and Water Conservation District, 2007, Potlatch River Watershed Management Plan: Latah Soil and Water Conservation District Web site, accessed February 7, 2013, at http://latahsoil.org/id50.html.

Miller, S., Glanzman, R., Doran, S., Parkinson, S.K., Buffington, J., and Milligan, J., 2003, Geomorphology of the Hells Canyon Reach of the Snake River, in Technical appendices for Hells Canyon Hydroelectric Project: Boise, Id., Idaho Power Technical Report E.1-2.

Mueller, D.S., and Wagner, C.R., 2009, Measuring discharge with acoustic Doppler current profilers from a moving boat: U.S. Geological Survey Techniques and Methods, book 3, chap. A22, 72 p.

Ott, Lyman, and Longnecker, Michael, 2001, An introduction to statistical methods and data analysis, (5th ed.): Pacific Grove, California, Duxbury, 1152 p.

Parkinson, S., Anderson, K., Conner, J., and Milligan J., 2003, Sediment transport, supply and stability in the Hells Canyon reach of the Snake River: Idaho Power Technical Report for FERC No. 1971, 140 p.

Patino, E., and Byrne, M.J., 2004, Application of acoustic and optic methods for estimating suspended-solids concentrations in the St. Lucie River Estuary, Florida: U.S. Geological Survey Scientific Investigations Report 2004-5028, 23 p. (Also available at http://pubs.usgs.gov/sir/2004/5028/.)

Runkel, R.L., Crawford, C.G., and Cohn, T.A., 2004, Load Estimator (LOADEST)—A FORTRAN program for estimating constituent loads in streams and rivers: U.S. Geological Survey Techniques and Methods, book 4, chap. A5, 69 p. (Also available at http://pubs.er.usgs.gov/publication/tm4A5.)

Schumacher, B.A., 2002, Methods for the determination of total organic carbon (TOC) in soils and sediments: U.S. Environmental Protection Agency publication NCEA-C-1282, 23 p.

Smith, R.A., Alexander, R.B., and Wolman, M.G., 1987, Water-quality trends in the Nation’s rivers: Science, v. 235, p. 1607–1615.

Teasdale, G.N., 2010, Sediment load, transport and accumulation in Lower Granite Reservoir on the Snake River: 2nd Joint Federal Interagency Conference, Las Vegas, Nevada, June 27–July 1, 2010.

Tetra Tech, 2006, Investigation of sediment source and yield, management, and restoration opportunities within the lower Snake River Basin: Submitted to Walla Walla District, U.S. Army Corps of Engineers, Delivery Order No. 7, Contract W912EF-05-D-002.

Topping, D., Melis, T., Rubin, D., and Wright, S.A. ,2004, High-resolution monitoring of suspended-sediment concentration and grain size in the Colorado River using laser-diffraction instruments and a three-frequency acoustic system, in Cheng Liu, ed., Proceedings of the 9th International Symposium on River Sedimentation, October 18–21, 2004: Yichang, China, International Sediment Initiative, p. 2507–2514.

Turnipseed, D.P., and Sauer, V.B., 2010, Discharge measurements at gaging stations: U.S. Geological Survey Techniques and Methods book 3, chap. A8, 87 p. (Also available at http://pubs.er.usgs.gov/publication/tm3A7.)

U.S. Army Corps of Engineers, 2002, Dredged Material Management Plan and Environmental Impact Statement, McNary Reservoir and Lower Snake River Reservoirs, appendix A—Hydrologic Analysis: U.S. Army Corps of Engineers, 27 p.

U.S. Army Corps of Engineers, 2005, Intent to prepare a draft Environmental Impact Statement, Programmatic Sediment Management Plan, lower Snake River reservoirs, in the states of Washington and Idaho: Federal Register, v. 70, no. 190, p. 57569–57570.

U.S. Geological Survey, 2013, USGS surface-water data for Idaho: U.S. Geological Survey database, accessed February 7, 2013, at http://waterdata.usgs.gov/id/nwis/sw.

Wall, G.R., Nystrom, E.A., and Litten, Simon, 2006, Use of an ADCP to compute suspended-sediment discharge in the tidal Hudson River, New York: U.S. Geological Survey Scientific Investigations Report 2006-5055, 16 p. (Also available at http://pubs.er.usgs.gov/publication/sir20065055.)

Washington State Department of Ecology, 2006, Palouse River Watershed: Washington State Department of Ecology Focus Sheet 06-10-002, 2 p.

Williams, M.L., Fosness, R.L., and Weakland, R.J., 2012, Bathymetric and underwater video survey of Lower Granite Reservoir and vicinity, Washington and Idaho, 2009–10: U.S. Geological Survey Scientific Investigations Report 2012-5089, 22 p. (Also available at http://pubs.er.usgs.gov/publication/sir20125089.)

Wood, M.S., and Teasdale, G.N., 2013, Use of surrogate technologies to estimate suspended sediment in the Clearwater River, Idaho, and Snake River, Washington, 2008–10: U.S. Geological Survey Scientific Investigations Report 2013-5052, 30 p. (Also available at http://pubs.usgs.gov/sir/2013/5052/.)

Publishing support provided by the U.S. Geological Survey
Publishing Network, Tacoma Publishing Service Center

For more information concerning the research in this report, contact the
Director, Idaho Water Science Center
U.S. Geological Survey
230 Collins Road
Boise, Idaho 83702
http://id.water.usgs.gov

Clark and others—**Sediment Transport in the Lower Snake and Clearwater River Basins, Idaho and Washington**—Scientific Investigations Report 2013–5083